

ANATOMICAL, BIOMECHANICAL AND BEHAVIOURAL CHARACTERISTICS
OF THE HUMAN MASSETER MUSCLE

by

MÔNICA DE LORENZO TONNDORF

D.D.S., Federal University of Rio de Janeiro, 1986

A THESIS SUBMITTED IN PARTIAL FULFILLMENT OF
THE REQUIREMENTS FOR THE DEGREE OF
DOCTOR OF PHILOSOPHY

in

THE FACULTY OF GRADUATE STUDIES
(Department of Oral Biology)

We accept this thesis as conforming
to the required standard

THE UNIVERSITY OF BRITISH COLUMBIA

October 1993

©Mônica L. Tonndorf, 1993

In presenting this thesis in partial fulfilment of the requirements for an advanced degree at the University of British Columbia, I agree that the Library shall make it freely available for reference and study. I further agree that permission for extensive copying of this thesis for scholarly purposes may be granted by the head of my department or by his or her representatives. It is understood that copying or publication of this thesis for financial gain shall not be allowed without my written permission.

(Signature)

Department of Oral Biology

The University of British Columbia
Vancouver, Canada

Date November 8, 1993

ABSTRACT

There is little information on the anatomical and functional organization of the human jaw muscles, despite their importance to the masticatory system and disorders which affect it. The current studies examined the anatomical, biomechanical and functional characteristics in the multipennate human masseter muscle as a model for understanding function in the human jaw.

Masseter anatomy was investigated in fetuses, adult cadavers, and living subjects by histology, gross anatomical dissection and Magnetic-Resonance (MR) imaging. Nerve pathways and muscle-fibre arrangements suggested that both fetal and adult muscles could be divided into at least four neuromuscular compartments. Although some fetal specimens had developed pennation, internal aponeuroses were seldom present. Structural variations were also found in the cadaveric material and living subjects. As the number of aponeuroses increased with development, and their thickness varied between individuals, individualized contraction strategies are likely to occur during function.

Movements of masseter insertion sites during jaw function were modelled in dry skulls. Muscle origins and insertions were measured three-dimensionally at different gapes and simulated masticatory positions. Their movements varied with craniofacial dimensions and their locations on the mandible. For some parts of the muscle, the balancing-side and the incisal-contact positions provided the most advantageous lines of muscle fibre action, while for others, the working-side task was most favourable. Separate portions of the muscle are thus uniquely placed to perform specific tasks.

Movements of four insertion sites were also recorded in four living subjects. Insertion areas were identified on MR-derived reconstructions, and movements recorded with a jaw-tracking device. Ranges of insertion displacement were similar to these estimated for dry skulls, and varied between individuals.

Interference electromyography, and single-motor-unit (MU) techniques were used to study physiological responses in eight subjects. The behaviour of low-threshold MUs was investigated relative to changes in bite side and experimental paradigm while subjects were biting on a force transducer. For each unit, the recruitment threshold, sustained-bite forces, the rate and regularity of sustained firing, and the coefficient of variation, were measured. Assessments were also made of the accuracy with which the target rates were attained, and of the contribution of each MU's firing rate to bite force. These measures of behaviour frequently differed between tasks, but not reproducibly. The highest reproducibility and firing-rate accuracy were achieved when visual and auditory MU feedback was provided. A tendency for increased firing rate, and decreased discharge variability was found when subjects had no feedback. As approximately 50% of the units did not show reproducible behavioural characteristics, it seems that differences in intramuscular activation, differential activation of other muscles, and the inherent variability seen in low-threshold MU studies generally make quantitative comparisons of focal activity in the masseter implausible.

Finally, a method was developed for locating the positions of moving needle electrodes relative to internal aponeuroses. It combined scanning electromyography, optical tracking of electrodes, MR imaging, and three-dimensional reconstruction. The

territorial sizes of 162 MUs were then assessed in the muscles of four subjects. Their mean width was 3.7 ± 2.3 mm. Most MU territories were confined between tendons, although 10% of the units clearly extended across at least one tendon. This focal dispersion of most territories provides a firm anatomical basis for selective activation of the muscle.

The findings collectively indicate an anatomical, biomechanical and physiological basis for differential motor control of at least four neuromuscular compartments in the human masseter muscle. The extent to which the central nervous system selectively activates these compartments, or coactivates them, remains to be demonstrated under functional conditions.

TABLE OF CONTENTS

	PAGE
ABSTRACT	ii
TABLE OF CONTENTS	v
LIST OF FIGURES	xi
LIST OF TABLES	xvi
ACKNOWLEDGEMENTS	xviii
1. INTRODUCTION	1
1.0 Introduction to the Thesis	1
Review of the Literature	
1.1 Skeletal Muscle Development	2
1.2 Muscle Architecture and Mechanics	10
1.3 Motor-Unit Organization	18
1.3.1 Motor-Unit Arrangement	18
1.3.2 Fibre Characteristics	19
1.4 Motor-Unit Activity	20
1.4.1 Recruitment	21
1.4.2 Firing Rate	21
1.4.3 Behaviour	22
1.4.4 Summary	25
1.5 Partitioning	25

1.6	Jaw Muscle Organization	28
1.6.1	Structure	29
1.6.2	Fibre Composition	33
1.6.3	Jaw Biomechanics	35
1.6.4	Summary	36
1.7	Anatomical Design of the Masseter	38
1.7.1	Muscle Organization	39
1.7.2	Innervation Pattern	43
1.7.3	Muscle Fibre Characteristics	45
1.7.4	Spindle Distribution	46
1.7.5	Summary	47
1.8	Functional Design of the Masseter	47
1.8.1	Motor-unit Territory	47
1.8.2	Functional Differentiation	49
1.8.3	Motor-unit Activity	52
1.8.3	Conclusion	54
2.	STATEMENT OF THE PROBLEM	56
3.	STUDIES	60
3.1	Masseter Morphology	61
3.1.1	Exploratory Experiments on Fetal Masseter Anatomy	61
3.1.1.1	Materials and Methods	62
3.1.1.1.1	Nerve Staining	65

3.1.1.1.2	Connective-Tissue and Muscle-Fibre Staining .	68
3.1.1.1.3	Muscle-Fibre Staining and Orientation Assessment	68
3.1.1.1.4	Muscle Reconstruction	68
3.1.1.2	Results	74
3.1.1.2.1	Nerve Distribution	74
3.1.1.2.2	Connective-Tissue Development	76
3.1.1.2.3	Muscle-Fibre Orientation	76
3.1.1.3	Discussion	83
3.1.2	Adult Masseter Anatomy	87
3.1.2.1	Materials and Methods	88
3.1.2.1.1	Gross Anatomical Dissection	88
3.1.2.1.2	Chemical Dissection	89
3.1.2.2	Results	90
3.1.2.3	Discussion	98
3.1.3	Morphological Reconstruction in Living Subjects	101
3.1.3.1	Methods	101
3.1.3.1.1	Magnetic-Resonance Imaging	101
3.1.3.1.2	Imaging	103
3.1.3.1.3	Reconstruction	107
3.1.3.1.4	Error of Method	111
3.1.3.2	Results	111

3.1.3.3	Discussion	117
3.2	Movement of Masseter Insertions at different Jaw Positions	125
3.2.1	Simulated Function in Dry Skulls	126
3.2.1.1	Methods	126
3.2.1.2	Results	133
3.2.1.2.1	Cephalometric Analysis of the Skull Sample ..	133
3.2.1.2.2	Sample Variation in Insertion Site Location during Dental Intercuspatation	136
3.2.1.2.3	Effect of Jaw Position on Insertion Site Location	136
3.2.1.2.4	Differences within Putative Muscle Layers ...	141
3.2.1.2.5	Differences between Putative Muscle Layers .	143
3.2.1.2.6	Orientation of Masseter Insertion relative to Origin	145
3.2.1.2.7	Discussion	147
3.2.2	Function in Living Subjects	157
3.2.2.1	Methods	158
3.2.2.2	Results	163
3.2.2.3	Discussion	169
3.3	Evaluation of the Masseter's Functional Performance	175
3.3.1	Electromyographic Recording Techniques	175
3.3.2	Preliminary Experiments using Single-Wire EMG Recording	

Technique	176
3.3.2.1 Materials and Methods	177
3.3.2.2 Results	183
3.3.2.3 Discussion	187
3.3.3 Motor-Unit Behaviour	192
3.3.3.1 General Methods	192
3.3.3.1.1 Motor-Unit Recording	192
3.3.3.1.2 Bite-Force Measurement	196
3.3.3.1.3 Sampling and Data Analysis	201
3.3.3.2 Effect of Bite Side on MU Behaviour	202
3.3.3.2.1 Methods	204
3.3.3.2.2 Results	208
3.3.3.2.3 Discussion	217
3.3.3.3 Effect of Experimental Paradigm	222
3.3.3.3.1 Methods	222
3.3.3.3.2 Results	224
3.3.3.3.3 Discussion	227
3.4 Motor-Unit Territory Relative to the Masseter's Internal Architecture .	230
3.4.1 Methods	232
3.4.1.1 Stereotactic Location of EMG Needle Electrode Scans	232
3.4.1.1.1 Morphologic Reconstruction	232
3.4.1.1.2 Motor-Unit Recording	233

3.4.1.1.3 Needle Location	234
3.4.1.1.4 Scan Location	236
3.4.1.1.5 Methodological Errors	239
3.4.1.2 Motor-Unit Territory	243
3.4.2 Results	245
3.4.3 Discussion	250
4. GENERAL DISCUSSION AND CONCLUSIONS	260
5. FUTURE DIRECTIONS	265
6. BIBLIOGRAPHY	269
7. APPENDIX	299

LIST OF FIGURES

	PAGE
Figure 1 Fetal peripheral-nerve staining	66
Figure 2 Fetal connective-tissue staining	69
Figure 3 Cross-sectional optical scan (Z-scan) through a 10- μ m fetal-muscle section	72
Figure 4 Superimposition of two horizontal optical sections situated at both extremes of a 10- μ m-thick fetal muscle section	73
Figure 5 Masseteric nerve pathway in the human fetal masseter	75
Figure 6 Development of aponeurotic layers in the fetal masseter and medial pterygoid muscles	77
Figure 7 Masseter muscle fibres in the 18 weeks old human fetus	78
Figure 8 Characteristics of fetal muscle tissues	79
Figure 9 Parasagittal sections from two 18-week human fetuses showing fibre orientation complexity	80
Figure 10 Masseter-muscle dissection showing the superficial and intermediate muscle layers	92
Figure 11 Masseter-muscle dissection showing its layered arrangement posteriorly and the ascending attachment sites of muscle fibres as the layers become deeper	93
Figure 12 Masseter-muscle cross-section showing its internal aponeuroses ...	95

Figure 13	Masseter-muscle fibre endings	96
Figure 14	Reference L-shaped grid attached to a plastic eyeglass frame	105
Figure 15	Coronal spin-echo Magnetic Resonance image	106
Figure 16	Antero-lateral view of the sectional outlines of a reference grid and right masseter muscle with its internal tendons.	109
Figure 17	Three-dimensional reconstruction of the reference grid, masseter muscle and internal tendons	110
Figure 18	Linear and angular measures used to compare the reconstructed against the true reference grid	112
Figure 19	MR coronal sections of two subjects showing differences in internal muscle architecture	115
Figure 20	Computer reconstruction of interstitial tissues in the right masseter muscle, viewed frontally	116
Figure 21	Schematic illustration of MR data acquisition	122
Figure 22	Masseter attachment points represented by six origin and twelve insertion points	128
Figure 23	Orientation of the three planes of the skull's coordinate system . . .	130
Figure 24	Illustration of the seven representative jaw positions	132
Figure 25	Mean displacements of the twelve insertion points at six different jaw positions	142
Figure 26	Mean functional displacements of four putative muscle attachment sites in the human masseter	146

Figure 27	Orientation of origin and insertion sites	148
Figure 28	Orientation of origin and insertion sites at three jaw positions	150
Figure 29	Anterior view of the sectional outlines of a reference grid, right mandibular ramus and condyle, and selected right-masseter-tendinous insertions	159
Figure 30	Schematic illustration of the global setup for a jaw tracking run . . .	161
Figure 31	Diagram illustrating the displacement trajectories of insertions of aponeuroses II and IV in living subjects	168
Figure 32	Rectified, digitized data from three muscle sites, obtained during a vertically oriented maximum tooth clench	180
Figure 33	Illustration of the right masseter muscle in the lateral and frontal views, showing wire electrode location	182
Figure 34	Rectified, digitized data from three electrode sites	184
Figure 35	Smoothed, normalized data from three electrode sites plotted against each other for three representative tasks	185
Figure 36	Raw data from four muscle sites, obtained during different clenching tasks	186
Figure 37	Raw data from four muscle sites, obtained during two distinct grinding movements	188
Figure 38	Motor-unit recording technique in the masseter muscle	193
Figure 39	Effects of different bandpass-filters on a single MU waveform shape	195
Figure 40	Sagittal and frontal profiles of the skull showing location and	

	orientation of bite force measurements	197
Figure 41	Calibration of the force transducer.	199
Figure 42	Illustration of the Bite Force Transducer in situ	200
Figure 43	Recruitment and firing pattern of a masseter MU at different bite force levels	205
Figure 44	Distribution of recruitment thresholds by task.	209
Figure 45	Recruitment thresholds arranged according to task for 10 MUs from five subjects	210
Figure 46	Changes in bite force when attempted MU firing at 10 Hz is increased to 15 Hz	212
Figure 47	Distribution of Coefficients of Variation arranged by task for attempted MU firing rates of 10 Hz and 15 Hz	213
Figure 48	Two-dimensional plot of the ISI standard deviations of the first against the second right-sided biting task, and against the left side	214
Figure 49	Distribution of "Accuracy Indices" arranged by task for attempts at two different rates of MU firing	216
Figure 50	Schematic illustration of the global setup for a needle tracking run	235
Figure 51	Schematic representation of the merge of the three datasets	237
Figure 52	Right antero-lateral view of the final reconstruction	238
Figure 53	Typical EMG records obtained during two separate needle scans . .	240
Figure 54	Coronal view of the 3D reconstruction of part of the right masseter muscle	241

Figure 55	Needle movement velocity during two separate needle scans	247
Figure 56	Distribution histogram of the territorial widths of 162 single MUs in the right masseter muscle	248
Figure 57	Relative sizes and frequencies of confined and extended MU territories	249
Figure 58	Distribution of MU territories with widths greater than 3 mm, according to muscle region	251

LIST OF TABLES

	PAGE
Table I Orientation of muscle-fibre subgroups relative to the mandibular ramus on the horizontal plane (Angle I) and relative to the plane of cut (Angle II)	82
Table II Linear and angular dimensions measured from homologous points on the reference grids of six subjects and their reconstructed counterparts	113
Table III Facial dimensions of female and male skulls	134
Table IV Craniometric measurements in fourteen skulls	135
Table V Mean location of putative muscle insertion sites for 14 skulls	137
Table VI Effect of jaw position on displacement of insertions expressed by mean orthogonal distances	138
Table VII Effect of jaw position on displacement of insertions expressed by mean linear distances	144
Table VIII Linear regression analyses for points representing attachment sites	149
Table IX Anteroposterior dimensions of the mandibular insertions of Aponeuroses II and IV in four subjects	164
Table X Displacements of one insertion point of one subject at different jaw positions	165
Table XI Mean displacements and standard deviations of four insertion points	

	of four subjects at different jaw positions	166
Table XII	Mean displacements and standard deviations of four insertions of four subjects during right-sided chewing	170
Table XIII	Mean displacements and standard deviations of four subjects during left-sided chewing	171
Table XIV	Discharge patterns and sustained-bite force levels of MUs activated during four tasks	226
Table XV	Muscle width and mediolateral territorial dimensions from MUs in the right masseter muscle of four subjects	252
Table XVI	Displacements of four insertion points of subject I at different jaw positions	300
Table XVII	Displacements of four insertion points of subject II at different jaw positions	301
Table XVIII	Displacements of four insertion points of subject III at different jaw positions	302
Table XIX	Displacements of four insertion points of subject IV at different jaw positions	303

ACKNOWLEDGEMENTS

I wish to express my gratitude to my supervisor Dr Alan G Hannam, whose scientific guidance and enthusiasm made this project possible.

I would like to thank Drs JM Gosline, JA Pearson and VM Diewert for their invaluable comments, suggestions and encouragement throughout the development of this thesis; Mr JP Sweeney, Ms B Tait, L Weston, C Vadgama and J Scott for their technical advice and assistance, Ms C Louie for the grammatical corrections of the manuscript, Mr B McCaughey for the photography, and Mr P Ma for his statistical advice. I am indebted to Dr K Sasaki for his guidance in the early stages of this work, Dr C Price who enabled my access to the Magnetic Resonance Unit, and Dr T Koriath who introduced and guided me through the I-DEAS™ package. Special thanks for all my friends and experimental subjects for their continuous support and enthusiasm.

I am especially grateful to Drs JD Waterfield and DM Brunette for their continuous support and advice, which enabled the fulfilment of this thesis.

This thesis is dedicated to my husband, Emilio, and parents, Maria Lucia, Manfred and Nilo. Their unfailing support, love and strength gave me the endurance to overcome these difficult years and to accomplish this project.

1. INTRODUCTION

1.0 Introduction to the Thesis

The human masseter is a powerful muscle, consisting of several muscle layers and interleaving internal aponeuroses arranged in a multipennate pattern, which becomes more complex with the development of function. Together with other masticatory muscles, it displaces the mandible, creates interocclusal and articular forces, and induces stress in the mandible and cranium. Contraction of the masticatory muscles affects craniofacial development, is commonly associated with craniomandibular disorders, and can interfere with clinical, orthodontic corrections made to the craniofacial skeleton.

Although this multipennate arrangement of the masseter provides an anatomical substrate for complex internal muscle mechanics, little is known on how it contracts. In most jaw models, its function is represented as a simple force vector, when in fact muscle tension acts over a broad attachment area with diverse regional magnitudes of force.

Contrary to the early assumption that the masseter is composed of a homogeneous, whole-muscle motoneuron pool, recent studies have revealed that MUs are activated in separate task-groups. In some occasions, task-groups can be inactive, depending on the performed jaw effort, however most often they are active throughout various tasks, showing only changes in their patterns of behaviour. Whether these separate motoneuron pools are related to internal muscle architecture, however, remains

uncertain.

It is necessary to develop new experimental techniques for use in living human subjects which can record both the internal muscle architecture and the three-dimensional location of the jaw during various tasks, and which can also stereotactically locate muscle-activity recording electrodes. Only when such techniques are developed will the structural, biomechanical and functional interactions within the muscle be better understood.

Review of the Literature

1.1 Skeletal Muscle Development

The craniofacial muscles are the first to develop in the body, in keeping with the cephalocaudal sequence of fetal development (Sperber, 1989; Noden, 1991). These muscles develop from paraxial mesoderm that condenses rostrally as incompletely segmented somitomeres and fully-segmented somites. The myomeres of the somitomeres and of the somites form primitive mononucleated myogenic cells, termed myoblasts; these undergo repeated mitotic division and subsequently fuse with each other to form multinucleated myotubes. Once this has occurred further nuclear division ceases, and thus myocytes (muscle fibres) are formed (Sperber, 1989; Mastaglia, 1981). Few myotubes remain after the 20th week, at which time most fibres are packed with myofibrils and have peripheral nuclei (Fenichel, 1966). Myotubes showing degenerative changes have been found in muscles of 10-16 week old human fetuses, and it has been

suggested that cell death is part of the normal process of myogenesis during intrauterine life (Webb, 1977).

While the formation of primary myotubes is well known, there is still uncertainty about the source of subsequent generations of myotubes and the mechanism whereby the number of muscle fibres increases during late fetal development (Mastaglia, 1981). Initially, it was suggested that fibre numbers increase by a process of budding or by longitudinal splitting of the first-formed fibres (Cuajunco, 1942). Later, a more likely alternative view was provided: that secondary and subsequent generations of myotubes develop from a persisting population of undifferentiated mononucleated cells lying in close proximity to the primary myotubes (Kelly and Zacks, 1969; Ontell, 1977). A proportion of these undifferentiated "fibroblast-like" cells are thought to remain in this condition as satellite cells which are seen in muscle fibres in late fetal (Ishikawa, 1966) and early adult life (Mauro, 1961).

Whereas the myogenic lineages of the masticatory muscles are traceable to paraxial mesoderm, the connective tissues associated with these muscles originate from the neural crest (Noden, 1991). During formation, the myoblast populations destined to form branchial-arch skeletal muscles move from the paraxial mesoderm into the neural crest, which provides their surrounding connective tissue: epimysium, perimysium and endomysium (Sperber, 1989). Initially, most of the myoblast populations are compact and morphologically homogeneous, but as they near their terminal locations the myogenic cells become interspersed with the nonmyogenic cells (Noden, 1991).

During the embryonic period, a definitive architecture for each muscle

emerges as tendons and connective tissue septa become distinct and muscle fibres become arranged in specific configurations. This arrangement of individual muscles follows distinct scenarios (McClearn and Noden, 1988; Noden, 1991). In the simplest case, a myogenic condensation forms within a single somitomere and then shifts to its terminal site giving rise to a single muscle. In other cases, a common premuscle mass will give rise to several muscles. Individual muscles may segregate from the original condensation either prior to or following the appearance of primary myotubes. Subsequently, the developing myofibres elongate and align in precise orientations that precede and predict the later segregation of individual muscles. Although the actual orientation of muscle fibres often changes during later stages of craniofacial growth, these initial differences in alignment between compartments remain constant. All these events occur prior to the formation of definitive attachments, suggesting that cues for myofibre orientation are present in the mesenchymal environment of the fusing myoblasts prior to differentiation of connective tissues (McClearn and Noden, 1988).

This notion that myogenic cells have little role in regulating gross spatial patterning in voluntary muscles has been confirmed by experiments involving transplantation of trunk somites into the head, with subsequent formation of typical masticatory muscles (Noden, 1986). Hence, myoblast populations are not preprogrammed with respect to the geometry of the tissue they will form; rather, after migration, they participate in muscle development according to the dictates of the local environment. In contrast, the connective tissue precursors are known to contain detailed instructions regarding their ultimate shape and relation to other elements (Noden, 1991).

The stage at which attachments with skeletal connective tissues form is unique for each muscle and is independent of the other aspects of muscle maturation. Differential growth of individual muscles and gross changes in head morphology cause the relations both among muscles and between muscles and skeletal elements to change dramatically (Noden, 1991). The masticatory muscles differentiate as individual entities from first-arch mesenchyme, migrate, and gain attachment to bone some time after their differentiation. The migration of muscles and ligaments relative to their bony attachments is a consequence of periosteal growth. The masseter has little distance to migrate, but its growth and attachment are closely associated with the mandibular ramus, which undergoes remodelling throughout the early, active growth period. As a consequence, these muscles must continually readjust their insertions and, to a much lesser extent, their sites of origin (Sperber, 1989; Herring *et al*, 1993; Covell and Herring, 1993).

Although the actual orientation of muscle fibres often changes during later stages of craniofacial growth, the initial orientation of myotubes presages the adult patterns (Noden, 1991). This is also observed in the fetal pig masseter, in which the basic arrangement of internal tendons and disposition of muscle fibres is already present (Herring and Wineski, 1986). The relative size of tendons, however, varies between fetal and adult specimens. With age, the length of fasciculi decreases relative to muscle weight, while the variance in length among different parts of the muscle increases (Herring and Wineski, 1986). Likewise, a discrepancy between the growth velocities of the entire muscle and the muscle fibres is found in the rabbit, where the origin-insertion

length increases relatively more quickly than the fibre length (Langenbach and Weijs, 1990).

During the formation of the trigeminal nervous system, an increase in motor neuron production occurs in focal zones known as rhombomeres (Källen, 1956, 1962). Nuclei of the trigeminal (Vth) cranial nerve are found to span two rhombomeres (Keynes and Lumsden, 1990), and the generation of this efferent population often involves several waves of neuron production across the intervening inter-rhombomeric boundary (Altman and Bayer, 1982; Covell and Noden, 1989). In contrast, neurons of the cranial sensory ganglia derive from the neural crest and from neurogenic placodes, which are focal thickenings of the embryonic surface ectoderm (Hamburger, 1961; Johnston and Hazelton, 1972; D'Amico-Martel and Noden, 1983).

Whereas the early stages of myogenesis may proceed normally in the absence of a nerve supply, the process of innervation enhances muscle development and is important for the complete differentiation of the muscle fibre (Mastaglia, 1981). The histogenesis and morphogenesis of muscles and nerves influence each other as the muscle masses form and the nerve and blood supply to them differentiates. Motor nerves establish contact with the myocytes, stimulating their activity and further growth by hypertrophy; failure of nerve contact or activity results in muscle atrophy. Nerve and vascular connections, established at this time, persist even after the muscles have migrated from their site of origin. This explains the long and sometimes tortuous paths that nerves and arteries may follow in adult anatomy (Sperber, 1989).

In the m. biceps brachii of the human fetus primitive nerve branches ramify

among the developing muscle cells during the 10th week, and myoneural junctions begin to form during the 11th week of intrauterine life (Cuajunco, 1942). At the same time, the myoblasts show more abundant and better-developed myofibrils, and at the periphery of most of these cells, all the characteristic striations of adult human voluntary muscle fibres may be distinguished. The earliest stage of the neuromuscular spindle formation is also found in this period (Cuajunco, 1940), and at 15 weeks, contacts between axons and muscle cells are seen frequently (Gamble, Fenton and Allsopp, 1978).

Since myoneural junctions have formed in the limb muscles by the 10th week of fetal life, they must have formed earlier in the head and neck, following the cephalocaudal sequence. Indirect evidence for this is that the earliest reflex movement elicitable in the human fetus occurs at 7½ weeks' menstrual age¹ (Hamilton, Boyd & Mossman, 1962), when some neck muscles contract in response to cutaneous stimuli applied to the lips. This indicates that the trigeminal nerve is the first cranial nerve to become active. Soon after the initial reflex muscle activity, spontaneous muscle movements can also be identified. These are believed to begin at 9½ weeks' menstrual age, followed by active mouth closure at 11 weeks, and intrauterine thumb sucking as early as 18 weeks. Swallowing occurs at 12 weeks, as the fetus starts drinking amniotic fluid (Humphrey, 1970; Sperber, 1989). At the same time, myelination, which is an indicator of nerve activity, appears first in the trigeminal nerve but is not complete until the age of 1-2 years (Sperber, 1989).

¹ Development events are commonly dated from the last menstrual period. Therefore, the *menstrual age* of the developing human is 2 weeks greater than the true age (i.e. when fertilization occurs) of the fetus (Moore, 1983).

During the early stages of development, several motor axons with different thresholds innervate a single muscle fibre ("polyneural innervation"). Studies at different postnatal ages show that the elimination of the redundant axon terminals occurs gradually, the mature one-on-one pattern being established a few weeks after birth in most muscles (Purves and Lichtman, 1980; Redfern, 1970; Bagust *et al*, 1973). The elimination of some of these initial connections results from a competitive withdrawal of axonal branches, and the course of this competitive rearrangement is influenced by activity (Lichtman and Purves, 1983). It has been postulated that this selective loss of certain axon branches is in order to refine the topographic projection of the neurons giving rise to these axons (Tolbert, 1987). Another possible role for this process of synapse elimination is that it could shape the adult innervation territory in a complex muscle from a less precise innervation pattern (Brown and Booth, 1983; Bennett and Lavidis, 1984). In a recent study however, it has been shown that, at least for the rat lateral gastrocnemius muscle, this is not true. This muscle is innervated in a compartment-specific manner at birth, and postnatal synapse elimination generally does not serve to establish "neuromuscular compartments"². Essentially, these are established by a process occurring before the time of birth; the innervation pattern being fully consistent with the infrastructures of the muscles (Donahue and English, 1989). Subsequently, as the muscle gradually develops, a denser innervation forms without modifying the basic structure of the original pattern (Schumacher, 1989).

² Each *neuromuscular compartment* is defined as the innervation territory of a single naturally occurring primary muscle nerve branch and has been shown to be composed of an aggregation of single motor units (English and Weeks, 1984; Janun and English, 1986).

All muscles undergo a period of secondary myogenesis that begins late in fetal life (Donahue *et al*, 1991). This process is nearly complete at birth in some muscles, so that most muscle fibres increase in size but not in number early in infancy (Ontell and Dunn, 1978). Secondary myogenesis continues postnatally in other muscles, increasing the number of muscle fibres up to 60% (Donahue *et al*, 1991). Satellite cells are believed to play a role in this postnatal growth (Mastaglia, 1981); moreover the discontinuous and gradual increase in muscle fibre size can be accounted for mainly by an increase in the myofibrillar material within the fibre (Goldspink, 1980). With age there is a change in the proportions of the fibre types (Sjöström *et al*, 1992), and with exercise, hypertrophy of the individual fibres is observed. The converse, muscle disuse, results in fibre atrophy. Although it is commonly assumed that there is no increase in the number of fibres with age or training, it was recently reported that the mean number of fibres in a muscle fascicle increases from childhood to adult age, and thereafter (middle and old age) reduces (Sjöström *et al*, 1992). In addition to hypertrophy, muscle fibres also increase in length during postnatal growth. This increase in length is associated with an increase in the number of sarcomeres in series along the myofibrils, and hence along the length of the fibres (Goldspink, 1980).

At birth, the suckling muscles of the lips and cheeks are relatively more developed than the muscles of mastication (Gasser, 1967). Indeed, at birth, mobility of the face is limited. Later, a more rapid growth of the muscles of mastication is observed, as there is a conversion from suckling toward mastication, and later into adult mastication. Hence, the facial muscles increase fourfold in weight and the muscles of

mastication increase sevenfold, between birth and adulthood (Sperber, 1989).

In summary, there is no definite ontological data regarding the fetal development of the jaw muscles in humans, but the available evidence suggest that most major structural elements are formed at an early stage. The rate of growth of jaw muscles and their attachments have been studied in humans, sub-human primates, rats, goats, capybara and rabbits, as increasing demands (such as dietary changes) are made on masticatory function. A common theme is the increase in the diversity of fibre directions, pennation and whole-muscle orientations. In humans, qualitative data imply that although the muscle attachments migrate with growth, their number and relative disposition remain fairly constant from birth (Gaspard, 1987). And with the exception of Schumacher's (1962) account of the increased pennation complexity from newborn to old age cadavers, there are no detailed studies on aponeuroses and muscle fibre lengths, angulation and attachment location according to fetal age.

1.2 Muscle Architecture and Mechanics

Many muscle fibres are grouped into bundles (fascicles) of varying size and pattern, each of which is surrounded by "perimysium", and several of which form an individual muscle. Fascicles vary in length from a few millimetres to many centimetres (15-30 cm in sartorius; Williams *et al*, 1989), and may be composed of multiple fibres in series (Loeb *et al*, 1987). For example, in the semitendinosus muscle in goats, fascicles are 16 cm long, and are composed of short fibres, which overlap each other by at least 30% of their length, and are arranged into groups of narrow bands that run end-to-end.

In separate parts of the muscle, bands are composed of a different number of overlapping fibres. These fibres also vary in length according to region (Gans *et al*, 1989; Thomson *et al*, 1991). In addition, muscle fibres are not uniform in type and diameter (ranging from 10-60 μm), and may vary between whole muscles, sometimes between muscle subvolumes or even within a single subvolume (Williams *et al*, 1989; Hopf, 1934).

Their attachment to bone can be either "musculous", in which case the fibres attach directly to periosteum, or "aponeurotic", in which case the attachment is through an intervening collagenous structure, which can be a fascia, tendon or aponeurosis. In addition, there are two categories for an aponeurotic attachment: internal where muscle fibres insert into both sides, or external where fibres insert into one side only (Dullemeijer, 1974; Van der Klaauw, 1963).

To understand the mechanics of a muscle, it is important to know the fascicular orientation, which may be parallel or oblique relative to the muscle's direction of pull. Muscles which have their fascicles arranged parallel to their line of traction are referred to as parallel-fibred muscles. These produce translational motion exclusively. Muscles with obliquely arranged fascicles may be triangular (fan-shaped) or pennate (feather-like) in construction, and this enables the fibres to rotate about their origins, increasing the angle of pennation as they shorten (Gans, 1982), while the insertion translates along the desired direction (Otten, 1988). Pennate muscles may vary in their complexity and can be classified as unipennate, bipennate or multipennate structures (Gans and Bock, 1965; Williams *et al*, 1989).

When compared against pennate structures, parallel-fibred muscles have the

largest number of sarcomeres in series. Consequently, during contraction their insertions have the greatest excursions and achieve higher movement velocities, while their sarcomeres simultaneously maintain an advantageous position on the length-tension curve, which is broader in parallel-fibred muscles. The role of this type of muscle is to enable large and rapid movements (Gans and Bock, 1965; Gans, 1982).

In contrast, pennate-muscle fibres run roughly parallel to each other, but at an angle towards their insertion along which the muscle force is exerted. Here, individual fibres are shorter, and the range of excursion (in which maximum tension can be produced) is reduced. The absolute distance that individual fibres can act is smaller, even though the resultant movement of the tendon is slightly more than that of any fibre. The advantage of pennation is that it allows more fibres to be packed into available spaces, increasing the muscle's cross-sectional area and therefore overall force production. Another advantage is that it provides a structural basis for the nervous system to control portions of a muscle independently, perhaps to produce force vectors in various directions. Similarly, if activated differentially, fibres may move their insertion laterally as well as toward its origin (Gans, 1982).

Theoretical models of pennate muscles are generally drafted with fibres attached to parallel tendinous insertions at both ends. In many of these muscles, the aponeuroses are unconstrained and may show local deformation (such as bent ends), as a unilateral contraction induces moments near the attachment site (Gans and Gaunt, 1991). That is, fibres induce couples, which are a pair of forces of the same magnitude, with parallel lines of action (along the origin and insertion tendons) and opposite

directions. The sum of the components of these two forces cancel each other, and the equivalent rotational moments will tend to twist the set of muscles inward, toward the line of action. In such cases, only mechanical stops, such as bones, fascia and other active muscles can keep the lines of origin and insertion from rotating towards the same plane (Gans, 1982). Provided that this rotation is avoided, the resultant vector of the force generated by the fibres will then contribute to translation of the tendinous insertions, that will slide past each other, maintaining the distance between them and the muscle volume unchanged (Benninghoff and Rollhäuser, 1952; Gans and Bock, 1965; Gans, 1982; Hatze, 1978; Otten, 1988). Since muscle fibres are angled relative to the tendon, some of the force will be lost in the static condition. In the dynamic condition, however, an increased excursion of the central tendon is achieved which partially compensates for some of this force loss (Muhl, 1982; Gans and de Vree, 1987).

Other designs were proposed for different types of muscle architecture. One example was introduced by Woittiez and colleagues (1984), in which the distance between tendinous sheets decreases upon muscle contraction, due to their initial non-parallel arrangement (Woittiez *et al*, 1984); and another example (Benninghoff and Rollhäuser, 1952; Otten, 1988), in which muscle fibres have slightly different orientations and therefore different pennation angles relative to their insertion. Here, provided that the aponeuroses move parallel to their original orientations, these fibres must consequently shorten by different amounts.

Most often, investigators have dealt with unipennate muscles, which have a bony attachment at their origin, and a parallel tendinous sheet at their insertion. As

noted earlier, a rotational moment can be maintained at the bony insertion, and the force of muscle pull transmitted along the aponeurosis (Otten, 1988). In some muscles, however, two tendinous sheets are arranged at an angle relative to the point-like attachments to bone or external tendons. In this case, no moment can be sustained at the transition of aponeurosis to external tendon; therefore, the most likely direction of muscle pull is a straight line through the external tendons (Huijing and Woittiez, 1984; Woittiez *et al*, 1984; Otten, 1988; Heslinga and Huijing, 1990; Scott and Winter, 1991). This difference in design affects the magnitude of the resultant force and the tendon displacement. Relative to the former case, the amount of shortening and volume decreases in the latter system, indicating that this type of muscle should have bulging of curved fibres (Otten, 1988).

The force generated by a muscle fibre depends on its physiological cross-section (Weber, 1846; Weijs and Hillen, 1985; Gans and de Vree, 1987) and its physiological characteristics. The latter will be reviewed in subsequent sections. In addition, the force production is affected by the position of the fibres' sarcomeres on the length-tension curve, by a change of length during isometric contraction (shortening produces less force; lengthening, produces greater forces), and by the overlap of actin and myosin filaments (Gans, 1982). Since force generation is also affected by the distance and velocity of the myofibre displacement, the positions of its attachment sites are critical (Gans and Gaunt, 1991).

It is commonly believed that the force generated by a whole muscle is the scaled-up version of the force generated by a single motor unit, which in turn is a scaled-

up version of the force generated by a single muscle fibre. This assumption seemed plausible for simple, parallel-fibred muscles, in which fibres extend the entire length of the fascicles, from origin to insertion. However, this assumption was found not to be true for muscles with more complex architecture, such as the anterior sartorius muscle of cats (Scott *et al*, 1992). The anterior sartorius is a parallel-fibred muscle composed of short, in series fibres, arranged into separate neuromuscular compartments (Thomson *et al*, 1991). When these fibres are independently stimulated, it causes the muscle to shorten at the end closest to the nerve branch and lengthen at the neighbouring site. At short, whole-muscle lengths, stimulation of one compartment generates only a small fraction of the total muscle-force output, while at increased whole-muscle lengths, an increased fraction of total muscle force can be generated. This relationship between active and passive muscle subvolumes allows complex modulation of whole-muscle force production (Scott *et al*, 1992). Moreover, it could be suggested that differential hypertrophy of muscle fibres occurs within a muscle as a consequence of intramuscular force heterogeneity. Hence, it is possible that fibre angulation may change differently in separate regions of a muscle.

Hypertrophy is responsible for the increase in length of pennate muscles during exercise and especially growth (e.g. gastrocnemius medialis; Woittiez *et al*, 1986; 1989; Heslinga and Huijing, 1990), while it has been suggested that hypertrophy plays a minor role in the increase of the length of parallel-fibred muscles (e.g. semitendinosus lateralis; Willems and Huijing, 1992). The latter type of muscle increases its length by increasing the number of sarcomeres within the fibres. There are functional differences

between the two types of muscles; parallel-fibred muscles maintain a greater range of length in which active force can be generated, while pennate muscles have this range reduced. For both types of muscle, the increase in muscle fibre diameter is accommodated by an increase in length of the aponeurosis and muscle fibres and by the enlargement of the bony attachment area. Although the fibre angles relative to the bony attachment remain constant, changes of the aponeurosis angle with the line of pull can be observed and may differ within different regions of a muscle (Willems and Huijing, 1992).

Consequently, non-homogeneous behaviour of separate muscle portions introduces new difficulties for understanding the design of muscles, especially muscles with complex structures. Differential contraction of distinct muscle subvolumes may cause internal shearing forces and regional changes in intramuscular pressure, affecting overall muscle behaviour in complex ways. In addition, fibres which attach on one side to tendinous sheets and on the other to bony surfaces may intrinsically shorten by different amounts and over different angles due to changes in the length of the attachment tendon (Otten, 1988).

Finally, we can note that the architectural design of a muscle has a significant effect on its mechanical action. The arrangement of both muscle fibre and connective tissue influences muscle function and can introduce differences in compliance³ (Borg and Caulfield, 1980). Within a muscle, connective tissue is present in the sarcolemma, between fibres, and as tendinous inscriptions, aponeuroses and attachment tendons

³ *Compliance* is the ratio of change in length to change in force.

(Partridge and Benton, 1981), each of which has inherent elastic properties. They operate in conjunction with the contractile muscle components (Hill, 1950; Partridge and Benton, 1981; Zajac, 1989), and are of importance in the generation of muscle stiffness⁴, especially in muscles with long tendons. For instance, increased tendon stiffness will limit the stretch of the tendon, therefore allowing the muscle fibres to remain in the desired portion of the length tension range (Peterson *et al*, 1982, 1984). Because of the difficulty in linking the physiology of single muscle fibres with that of whole bone-muscle-connective tissue structures, models have been commonly used to offer functional and mechanical explanations of muscle design. One way of producing such a model is to incorporate detailed structural and functional properties of a particular muscle to produce a realistic mechanical result. Once these models are tested against measurable functional characteristics, they can be used to assess functional properties which are difficult to measure *in vivo*. Additionally, it is clear that individual muscles have their own characteristics, making it necessary to match function to the structural system that it belongs to (Otten, 1988). However, this is a formidable undertaking for pennate muscles, and it has not yet been achieved for any complex muscle in a proper manner (Hannam and McMillan, 1993).

⁴ *Stiffness* is the ratio of change in force and the change of length causing the force.

1.3 Motor-Unit Organization

1.3.1 Motor-Unit Arrangement

Several skeletal muscle fibres are innervated by a single alpha motoneuron; together they form a "motor-unit" (MU), which is the basic functional unit of the motor system (Sherrington, 1929). It has been commonly assumed that all fibres of a MU are of the same histochemical type (Henneman and Olson, 1965; Brandstater and Lambert, 1973), although recent studies have questioned this (Larsson, 1992). There is both histochemical and electrophysiological evidence that muscle fibres of a single MU are diffusely scattered within the MU's territory and intermingled with fibres of other units (Ekstedt, 1964; Edström and Kugelberg, 1968; Stålberg *et al*, 1976; Buchthal and Schmalbruch, 1980). This wide distribution with extensive MU overlap is partly responsible for the evenness and smoothness obtained during light voluntary muscle contraction, resulting in a more or less uniform tension at the muscle tendon, even when very few motor units are active (Buchthal and Schmalbruch, 1970).

Both the number of MUs and the number of muscle fibres belonging to a MU vary greatly within a particular muscle and especially between different muscles. For example, muscles which are used in high-precision tasks show considerably fewer fibres per MU (Stålberg *et al*, 1986). It has been estimated that for the human extra-ocular muscles there are 2970 MUs and 9 fibres per MU (Feinstein *et al*, 1955), while for the masseter muscle there are 1452 MUs and 640 fibres per unit (Carlsöö, 1958).

1.3.2 Fibre Characteristics

Identification of fibre types was originally achieved by the differentiation of the metabolic characteristics of the muscle fibres. These were analysed by histochemical staining procedures to reveal the activity of their metabolic enzymes. In one of the early studies, Ranvier (1873) related differences in muscle function to colour, classifying muscles as red or white. Later, the scale for rating the fibre's oxidative potentials was further expanded to include intermediate staining intensities. In recent years, more sensitive immunocytochemical techniques have been developed for use with both fluorescence and electron microscopy to reveal muscle fibre's structural proteins (Gollnick and Hodgson, 1986; Miller, 1991).

Although histochemical methods yield valuable information concerning the properties of muscle fibres, ultimately the most important aspect of the typing of fibres relates to what role the fibres play during muscle contraction. To study this, physiological techniques have been developed to activate MUs independently (Burke, 1981; Buchthal and Schmalbruch, 1980). With the advancement of these techniques, the initial classification of red, intermediate and white became synonymous with slow-contracting (S), fast-contracting fatigue-resistant (FR), and fast-contracting fatigue-susceptible muscles (FF), respectively (Burke *et al*, 1971; Gollnick and Hodgson, 1986). Subsequently, other nomenclatures have been introduced to characterize fibre types (as reviewed by Close, 1973; Burke, 1981; and Mao *et al*, 1992); type I, IIA, IIB fibres (Brooke and Kaiser, 1970); slow twitch oxidative (SO), fast twitch oxidative glycolytic (FOG), and fast twitch glycolytic (FG) fibres (Barnard *et al*, 1971); and B, C, A fibres

(Henneman and Olson, 1965). Historically, this diversity of nomenclature created great confusion, making comparisons of data from different studies difficult. The histochemical properties of types of muscle fibre differ between muscles (Luschei and Goldberg, 1981; Taylor *et al*, 1973) and between species (Gollnick and Hodgson, 1986); they can also change with age (Sjöström *et al*, 1992) and gender (Miller, 1991).

Muscle fibre diameter is frequently related to the histochemical fibre type. In many mammalian muscles, the diameters of type IIB fibres are larger than those of IIA fibres, which in turn are larger than those of type I fibres (Burke, 1981). However, exceptions to this pattern are found in some human muscles, where type I fibres are larger than type II fibres. This inconsistency might be the result of fibre size changes following exercise or inactivity, and again different types of fibres may be affected differently. Training increases the cross-sectional muscle fibre area, while inactivity decreases it (MacDougall *et al*, 1980; Salmons and Henriksson, 1981). Furthermore, it has been conclusively demonstrated that muscle fibres adapt to increased demands for endurance by changing their metabolic profile. This is brought about by increasing their oxidative potential (Edström and Grimby, 1986).

1.4 Motor-Unit Activity

Given the arrangement of MUs described above, a description of how muscular force is attained by the nervous system is appropriate. The nervous system produces graded increases in force in two primary ways: (1) Through the progressive "recruitment" of MUs, it increases the number of active MUs. (2) Through "rate coding",

it modulates the firing frequency of individual motor neurons (Henneman, 1979; Freund, 1983; De Luca, 1985; Carew and Ghez, 1985). A brief description follows.

1.4.1 Recruitment

During a graded skeletal muscle contraction, MUs are normally activated in an orderly sequence, which is related to the size of their innervating motoneurons (reviewed in Burke, 1981). Neurons with the smallest cell bodies are the first to be activated, and as the synaptic input increases in strength, larger motoneurons are progressively recruited. This recruitment order is known as the "size principle" (Henneman, 1981).

Human motor-unit recruitment thresholds (RTs), i.e. the forces at which units are first activated for a given task, are generally reproducible under controlled conditions but they can vary (Tanji and Kato, 1973a; Freund *et al*, 1975; Miles *et al*, 1986). RTs depend on the rate of isometric contraction of the muscles involved, decreasing the unit's threshold dramatically when ballistic contractions are used (Büdingen and Freund, 1976), and upon muscle length (Miles *et al*, 1986). In addition, RTs of biceps-brachii MUs were also found to be reduced by successive voluntary isometric contractions (Suzuki *et al*, 1990).

1.4.2 Firing Rate

It is well-known that small units are the first to be activated, and as their firing rates increase, muscle force output increases proportionally (Freund *et al*, 1975; Tanji

and Kato, 1973b; Monster and Chan, 1977; Milner-Brown *et al*, 1973; De Luca, 1985). Small, low-threshold units discharge regularly and with a far more pronounced firing rate modulation than units recruited at higher muscle forces (Freund *et al*, 1975). The lowest possible firing rate of a unit does not seem to differ significantly between MUs recruited at different thresholds or between muscles (for review see Freund, 1983), and this firing rate is characterized by an irregular pattern of discharge (Kranz and Baumgartner, 1974; Person and Kudina, 1972) which becomes more regular as the firing rate increases above a critical level.

Thus, the interaction of progressive MU recruitment and the modulation of MU firing rates is responsible for the transition from a series of motor-unit twitches to a tetanic contraction, with consequent smooth increase in muscle force (Buchthal and Schmalbruch, 1980; Burke, 1981; Clamann, 1970; De Luca, 1985).

1.4.3 Behaviour

Most evidence on the patterns of motor control has been obtained from animal studies, in which global electromyographic activity is commonly recorded with implanted electrodes in awake animals, and single MU characteristics sampled during highly-invasive surgical procedures. While the latter type of experimental approach is well controlled, the observed behaviour of MU activity is however stereotyped, and the effect of decerebration on the pattern of motor control is uncertain (Burke, 1981). In turn, the use of human subjects offers many advantages in MU behaviour studies, due to their ability to perform highly-skilled, voluntary motor tasks (Freund, 1983; Miles *et*

al, 1986; Hannam and McMillan, 1993).

A consistent pattern of MU behaviour has been conventionally reported for several limb muscles. Small units are recruited at low thresholds. They have high resistance to fatigue, long contraction time (Edström and Grimby, 1986), and their lower firing rate limit is maintained between 5 and 8 Hz, producing lower twitch tensions than larger units. However, this lower rate limit is not precisely fixed and seems to vary for functionally different muscles (Tanji and Kato, 1981; Person and Kudina, 1972).

In addition, there has been abundant documentation of the fact that during slow ramp contractions, consistent ordering of MU recruitment is generally found within a particular collection of units belonging to a single anatomically defined muscle which is known as a motor pool (Desmedt, 1980; Burke, 1981; Schmidt and Thomas, 1981; Thomas *et al*, 1978; 1987). These findings introduced the idea that the RT of a unit, within the spectrum of thresholds in a motor pool, is a stable property, and that the threshold level remains unchanged in different motor acts (Henneman *et al*, 1974; Burke, 1981). Contrary to this classical concept, it has been occasionally observed that unit RTs may vary significantly during the performance of a given movement (Petajan, 1981). When repeated, movements may appear to be identical, but can be accomplished by various strategies (Freund, 1983), such as by varying degrees of muscle contraction depending on the level of coactivation of antagonistic muscles (Carew and Ghez, 1985; Petajan, 1981). The recruitment order can be also altered under different postures (Person, 1974), or by contracting multifunctional muscles in different directions (Thomas *et al*, 1978; Desmedt and Godaux, 1981; ter Haar Romeny *et al*, 1982). This alteration

in MU recruitment order has been generally observed between units with similar thresholds (Tanji and Kato, 1973b), and slight changes in synaptic efficiency or the activation of sensory afferents with an uneven distribution of the terminals to the motoneuron pool have been implicated in RT reversals (Kanda *et al*, 1977; Lüscher *et al*, 1979). It has been also observed in a multi-functional muscle that as the muscle changes the direction of effort, the resultant muscle force produced also changes. However, when the ratios of RT relative to muscle force for the different tasks are compared, they apparently remain identical (Thomas, Ross and Stein, 1986). This area remains quite controversial (Enoka and Stuart, 1984), however evidence suggests that at least in a single function muscle, the recruitment pattern is highly stereotyped, with little chance for flexibility in MU recruitment order (Schmidt and Thomas, 1981).

Generally, in the past, investigators analysed randomly distributed MUs activated by simple, whole-muscle contractions. As seen earlier, however, in some muscles a MU may perform multiple tasks (ter Haar Romeny *et al*, 1982), and in other muscles distinct tasks may recruit separate parts of the classically defined motoneuron pool, that is separate groups of MUs. This has been observed for the human biceps brachii (ter Haar Romeny *et al*, 1982) and extensor digitorum communis (Thomas *et al*, 1978; Riek and Bawa, 1992). In the latter muscle, the overlapping subpopulations of motoneurons were reported to maintain an orderly recruitment pattern, despite of changes in task (Riek and Bawa, 1992).

1.4.4 Summary

The MU represents the functional quantum by which the nervous system regulates the development of muscle force. This regulation occurs by concurrent variation in the number of active MUs and their rate of firing. The relationship between MU recruitment and firing rate modulation varies between muscles, but the result is always an ability to finely grade muscle force.

The strategy by which the nervous system controls MUs to generate and modulate muscle force is, however, not fully understood. It is believed that there is uniform behaviour of recruitment and firing rates of a collection of MUs belonging to a motoneuron pool; this property is termed the "common drive". However, the behaviour of a motoneuron pool can be altered depending on the task performed by the muscle. For example, a motoneuron pool may or may not be activated, or alternatively it may have its properties altered upon task change.

The concept of "task group" was therefore proposed, in which within a muscle separate functional groups of motor and sensory neurons are differentially activated to achieve optimal control over restricted parts of a movement.

1.5 Partitioning

"Neuromuscular partitioning" refers to features of neuromuscular organization that provide a morphological basis for subdividing a muscle into recognizable subdivisions (Windhorst *et al*, 1989). A number of recent studies have shown that mammalian muscles are partitioned with respect to both their motor and sensory

innervation. These partitions are organized about the primary branches of the respective muscle nerves and are known as "neuromuscular compartments" (English and Letbetter, 1982a). As each primary branch of a nerve enters a muscle it innervates fibres in a discrete subvolume of the muscle and contains an unique group of motor axons. That is, branches of individual motor axons course exclusively in only one primary muscle nerve branch (English and Weeks, 1984; Janun and English, 1986; English, 1990), although in one single case in a newborn animal an axon branched in two directions at a nerve branch point (English, 1990). In the adult these innervation territories do not overlap (English and Weeks, 1984; English, 1990).

In some muscles, the neuromuscular compartments may be partially separated by internal tendon sheets (English and Letbetter, 1982a; Richmond *et al*, 1985; Armstrong *et al*, 1988). These were thought to either act as physical barriers to axon growth or to serve as axon guidance cues during development, resulting in the restriction of axons to a particular compartment. In the gluteus maximus of the rat, however, no such tendons are found, although the muscle is compartmentalized by the primary branches of both muscle nerves. This finding suggests that the neonatal compartment-specific pattern of innervation for this muscle must be established independently of the arrangements of tendons (English, 1990). The same has been observed in the rat anterior digastric, which, despite its simple muscle architecture, consists of three neuromuscular compartments (English and Timmis, 1991).

These compartments may differ in both their composition of muscle fibre types (English and Letbetter, 1982b; Bennett *et al*, 1988) and fibre architecture. Within

each neuromuscular compartment of the pig masseter, fibre type is relatively homogeneous, but there are marked differences between them (Herring *et al*, 1979). MUs are also generally confined to small volumes within a single compartment (English and Weeks, 1984). This pattern was confirmed in the pig masseter, and territories were found to be smaller than those in most limb muscles. This may be due to the length of masseter fibres, which are shorter than these in limb (Herring *et al*, 1989).

Afferent axons supplying muscle spindles within a single intramuscular compartment are found in the same nerve branches as the motor axons innervating the surrounding extrafusal muscle fibres (Farina and Letbetter, 1977). When these motor axons are stimulated, a more potent response of muscle receptors is observed within their own intramuscular compartment than in adjacent and more distant regions of the muscle (Cameron *et al*, 1981). This preferential response of muscle receptors to localized perturbations within a muscle is known as "sensory partitioning", and has been demonstrated in both cat (Binder and Stuart, 1980) and human subjects (McKeon and Burke, 1983).

Analysis of the anatomical organization of motor nuclei has shown that spinal motoneurons that supply a neuromuscular compartment can be organized into groups forming a "compartment nucleus". That is, a motor nucleus can be arranged topographically (Weeks and English, 1985). In addition, different compartment nuclei contain motoneurons of different sizes, which are highly correlated with the types of muscle fibres they innervate (Weeks and English, 1987). Similar topographic organization has been observed for afferent axons that project to the spinal cord within a relatively

discrete portion of the muscle's afferent entry zone (Cameron *et al*, 1981). This partitioning of segmental connections within a nucleus is known as "central partitioning" (Windhorst *et al*, 1989).

Collectively, it appears that the role of partitioning is to provide a basis for the nervous system to control structurally complex muscles differentially. On the one hand, partitioning may moderate the effects of mechanical heterogeneity. In some complex muscles, variations have been found in the fibre length and in the angle of pennation. In this type of muscle, differential motor control may enable distinct regions to undergo different relative amounts of lengthening and shortening, in order to contribute uniformly to motion at the muscle's common tendon. On the other hand, partitioning may provide the substrate for differential control of muscular regions that are specialized for diverse functional capabilities (Windhorst *et al*, 1989). The latter postulate has been confirmed in some complex limb muscles, where compartments could be activated independently of other compartmental subdivisions within the muscle during controlled activity (English, 1984; English and Weeks, 1987).

1.6 Jaw Muscle Organization

The masticatory system comprises five muscles: temporalis, medial pterygoid and masseter, which are jaw-closing muscles, and digastric and lateral pterygoid. Each of these latter two muscles are formed by two heads: the anterior and posterior bellies of the digastric, and the superior and inferior heads of the lateral pterygoid. Although these muscles have multiple functions, they are normally classified as jaw openers

(Miller, 1991).

As stated earlier, a muscle may be classified as parallel-fibred, unipennate, bipennate or multipennate, depending on the complexity of its structure. In the jaw muscles, examples of all four types of structure can be found.

1.6.1 Structure

The digastric muscle consists of two parallel-fibred bellies separated by an intermediate tendon, which is attached to the hyoid bone. The posterior belly arises from the digastric notch on the mastoid process, projects anteriorly and inferiorly, connecting with the anterior belly which projects anteriorly and superiorly to the mandible (Williams *et al*, 1989; Miller, 1991; Hannam and McMillan, 1993).

Traditionally, it has been thought that both bellies contract simultaneously to achieve jaw opening, retrusion or hyoid elevation. The posterior and anterior bellies are, however, innervated separately by trigeminal and facial motoneurons and, at least in rats, are divided into separate neuromuscular compartments (English and Timmis, 1991). This structure offers a basis for differential activation strategies. Non-synchronous activity has been occasionally observed (Munro, 1974; Widmalm *et al*, 1987a), nevertheless electromyographic data suggest that most often there is synchronized activity in the two bellies during all mandibular movements, including chewing and swallowing (Munro, 1972; 1974; Yemm, 1977).

Conventionally, the lateral pterygoid muscle is considered to be one muscle, consisting of two heads which have different orientations. The superior head originates

from the infratemporal crest and roof of the infratemporal fossa and converges posteriorly, laterally and caudally, while the almost three times larger inferior head originates from the lateral surface of the lateral pterygoid plate of the sphenoid bone and converges laterally and posteriorly towards the neck of the condyle. Both fan-like muscle heads converge towards the fovea of the mandibular condyle and attach to fovea, articular capsule, and articular disc. Despite several intramuscular tendons at origin and insertion, the lateral pterygoid has a very simple anatomy (Schumacher, 1961c; Widmalm *et al*, 1987b; Wilkinson, 1988; Meyenberg *et al*, 1986; Carpentier *et al*, 1988; Miller, 1991; Hannam and McMillan, 1993).

The lateral pterygoid's two bellies are believed to function mostly independently; the inferior head is more efficient in jaw opening, and the superior head more inclined to facilitate jaw closing and tooth clenching (Miller, 1991). An alternative view is that all fibres act as one muscle, with varying amounts of activity that could gradually change the whole-muscle line of pull according to the biomechanical demands of the task (Widmalm *et al*, 1987b). Although there is no direct evidence for this postulate, it is consistent with previous observations that fibres belonging to the inferior head are very active during tooth-clenching in eccentric jaw positions, even though they are normally considered to be active only in the balancing side during jaw laterotrusion (Wood *et al*, 1986) and in mandibular retrusion (Widmalm *et al*, 1987b; Hannam and McMillan, 1993).

When viewed from the lateral aspect, the temporalis muscle is a broad fan-shaped muscle originating from the temporal fossa and converging into a flat, also fan-

shaped tendon that inserts onto the anterior, medial and posterior surfaces of the coronoid process, as well as the anterior border of the ascending mandibular ramus. The insertion tendon extends upwards as an internal aponeuroses, separating the muscle into two layers. When viewed frontally, the anterior part of the muscle has a typical bipennate structure, with the fibres diverging from the central aponeurosis at increasing pennation angles in the infero-superior direction. Seen from the lateral view, fibres run vertically in the anterior part of the muscle, radiating to become almost horizontal posteriorly. At this level, the muscle is thinner mediolaterally and has no obvious bipennate arrangement (Schumacher, 1961c; Hannam and McMillan, 1993).

Anatomically, the more complex structure of the temporalis suggest that groups of fibres may be separately activated, depending on mechanical demand. It has been known for some time that graded, task-sensitive activation can occur in the anterior, middle and posterior fibres, during the elevation, retrusion and lateral displacement of the jaw (Møller, 1966; Miller, 1991; Blanksma and van Eijden, 1990; Hannam and McMillan, 1993). Mediolaterally, the superficial and deep muscle layers on either side of the central aponeurosis can be also selectively activated (Wood, 1986). Together, this behavioural flexibility and structural composition of regions of the muscle, which have different cross-sectional areas (anteriorly the muscle has a much larger cross-section than posteriorly), implies not only differential muscle usage, but also that the development of tensions throughout the muscle is not homogeneous (Blanksma and van Eijden, 1990; Hannam and McMillan, 1993).

The medial pterygoid is a rectangular, bulky muscle situated on the medial

side of the mandibular ramus, running downwards, backwards and outwards from its origin in the pterygoid fossa to insert onto a triangular area on the inside of the mandibular angle. The internal structure is multipennate, consisting from six to eight interleaving aponeuroses, which can extend about two thirds of the way into the muscle, attaching to bone above and below in an alternating fashion (Schumacher, 1961c). In the frontal view, the orientation and closeness of the interleaving aponeuroses offer little geometry with which to vary the line of muscle pull. When viewed laterally, the muscle fibres have a slightly fanned arrangement. When fibres located anteriorly are compared against the others located posteriorly, their alignment is more vertical, (i.e. they are oriented upwards, inwards, but with a lesser forward angulation (Hannam and McMillan, 1993).

Electromyographic studies in the medial pterygoid have shown that this muscle is highly active during intercuspal clenching, protrusion and contralateral laterotrusion (Gibbs *et al*, 1984; Møller, 1966; Vitti and Basmajian, 1977). During clenching in the intercuspal position, the level of muscle activity can be modulated by varying the bite force direction (Wood, 1986), suggesting that a task-dependent gradation of different muscle regions is possible. Information on differential contraction, however, is difficult to obtain, partly because of the difficult physical access to the muscle for electrical recordings and partly because individual subjects use the muscles differently (Hannam and Wood, 1981; Hannam and McMillan, 1993).

The masseter is a rectangular-shaped, multipennate muscle, which has the second largest cross-sectional area of all masticatory muscles (Weijs and Hillen, 1985;

Hannam and Wood, 1989). It can be divided anatomically into two or three partially separate layers, which originate from the zygomatic arch and extend downwards, backwards and inwards to attach to the lateral surface of the mandibular ramus. Like the medial pterygoid, internally it consists of three to five interleaving and alternating aponeuroses, which extend into the muscle by approximately two thirds of the whole-muscle length (Ebert, 1939; Schumacher, 1961c).

The overall role of this muscle is to elevate, protrude and move the mandible laterally, however, increasing evidence that different parts of this muscle contract differentially depending on the jaw task indicates that this muscle can also produce fine-skilled movements (Greenfield and Wyke, 1956; Belser and Hannam, 1986; Blanksma *et al*, 1992).

1.6.2 Fibre Composition

In general, the fibre-type properties of intrafusal fibres in the masseter of rat, guinea-pig, rabbit, cat and macaque monkey resemble those in limb muscle spindles (Rowlerson *et al*, 1988), but there are significant differences between jaw and limb extrafusal muscle fibre types. Firstly, larger fibre diameters can be found in limbs (Eriksson and Thornell, 1983) where different types of fibres are distributed in a mosaic-like pattern. In contrast, jaw muscles contain many fibres of the same histochemical type (Stålberg *et al*, 1986). Based on this histological appearance of densely-packed fibres of the same type, the speculation of fibre-clumping was raised (Eriksson and Thornell, 1983). This appearance would be considered pathological if present in the limb or trunk,

where it would indicate denervation and reinnervation (Schwartz *et al*, 1976). To address this, the fibre concentration (i.e. the mean number of fibres per MU within the small uptake area of the single-fibre electrode, Stålberg and Thiele, 1975) of the masseter was compared against that of the first dorsal interosseus. The fibre concentration in both muscles was found to be similar; thus, the masseter does not show any sign of grouping of fibres from the same MU (Stålberg *et al*, 1986).

In addition, large numbers of ATPase intermediate (IM) fibres and type IIC fibres are found in the jaws, but they are scarce in the limbs (Ringqvist *et al*, 1982). The composition of myosin isozymes is different between jaw and limb muscles. The human masseter contains neonatal myosin heavy chains and embryonic myosin light chains that are characteristic of developing muscles (Butler-Browne *et al*, 1988), and cardiac-specific myosin-heavy-chain is also exclusively found in skeletal muscles which originate from the cranial part of the embryo (Bredman *et al*, 1991). These differences between jaw and limb muscles suggest that finer gradation of contraction speeds in jaw muscle fibres could be possible.

In the jaw muscles, regions are composed of different histochemical fibre types in varying proportions, implying a functionally-related distribution. In all muscles, type I fibres predominate, especially in the anterior and deeper regions, while there is a trend towards equal proportions of type I and II fibres posteriorly and superficially (Miller, 1991; Hannam and McMillan, 1993). A similar pattern is observed for jaw muscles in pigs and primates (Herring *et al*, 1979; Clark and Luschei, 1981). Here, MUs are confined to regions, which were previously defined histochemically.

1.6.3 Jaw Biomechanics

During mastication, a complex contraction pattern of the masticatory muscles induces spatial rotations and translations of the mandible, simultaneously producing forces to the food bolus and articular joints. While these forces should ideally be measured directly from individual subjects, this is not always feasible, and instead mathematical models have been used to calculate them.

In this approach, it has been commonly assumed that the mandible is a rigid beam which behaves according to static equilibrium principles. Here, muscle force vectors are applied at their appropriate two or three-dimensional sites, and bite forces and joint reaction forces are then derived (Osborn and Baragar, 1985; Throckmorton and Throckmorton, 1985; Nelson, 1986; Smith *et al*, 1986; Faulkner *et al*, 1987; Koolstra *et al*, 1988a; Koriath and Hannam, 1990). The orientation of these muscle lines of action (including the point of application and direction of muscle force) are generally determined by dissection (Smith *et al*, 1986; Koolstra *et al*, 1988a), estimated from dried bone (Baron and Debussy, 1979) or radiographs (Throckmorton and Throckmorton, 1985), or by defining a line through the centroids of contiguous muscle slices (An *et al*, 1984; Koolstra *et al*, 1989; Hannam and Wood, 1989). The maximum magnitude that an individual muscle force can reach is determined by its physiological cross-sectional area (Weijs and Hillen, 1984a; Hannam and Wood, 1989), while its degree of activation contributing to a particular jaw task is determined electromyographically (Møller, 1966; MacDonald and Hannam, 1984a,b).

From these models, it was found that the resultant forces produced at the

teeth and joints depend on several factors. Firstly, they depend on the bite point location (Pruim *et al*, 1980; Nelson, 1986), on mandibular position (Koolstra *et al*, 1988a) and on the orientation of the jaw muscle vectors, rather than only on the muscle's intrinsic strengths (Throckmorton and Throckmorton, 1985). In addition, depending on the muscles contraction patterns, bite and joint forces can be developed in a wide range of directions (Nelson, 1986), in which the vectors together form a force envelope (Koolstra *et al*, 1988a). The shape of these envelopes, in turn, is influenced by changes in the direction of masticatory muscle vectors, especially vectors of the masseter muscle (Koolstra *et al*, 1988b).

While useful, these models have several limitations. Aside from the fact that they are based on static and rigid beam theories, interactions between the structure and function of the jaw muscles are normally limited by the incorporation of muscle properties which are unmatched to the morphology of the model under study, and restricted by simple, single vector muscle representation. Consequently, in recent years a different modelling approach, involving finite-element modelling, has been used to reveal internal structural stresses, as well as local deformations (Korioth *et al*, 1992). So far, this method has been successfully used to study deformations within a human mandible upon simulated static tooth-clenching, utilizing, however, average physiological data which was not specific to the morphology under investigation.

1.6.4 Summary

Despite the importance of masticatory muscles to craniofacial growth and

mastication, our understanding of their design, functional characteristics and biomechanics is limited. In this system, examples of both parallel-fibred and multipennate arrangements can be found, each of which has its unique characteristics. And, as the result of their coordinated contractions, they induce complex dental, articular and cranial tensions, as well as movements of the mandible.

The diverse arrangement of muscle fascicles, coupled with the regional distribution of different biochemical fibre types, offers a substantial anatomical basis for differential contraction. This may subsequently produce heterogeneous tensions throughout the muscle, and therefore produce resultant force vectors in a variety of directions, which are known to affect reaction forces at the condyles and bite points.

Among the masticatory muscles, the masseter is the most complex and powerful, with the potential of influencing the bite force envelope most extensively. It is an important muscle during the power stroke in chewing, it is multipennate, and it has complex histochemical properties. In addition, its peripheral and central connectivities are better understood than most jaw muscles, possibly because it is easily accessible for electromyographic recordings.

In humans, the masseter is commonly involved in disorders of the orofacial area. Despite a universal structural principle of the same muscles among different species, muscle properties are unique to the species. Therefore, a better understanding of the characteristics of the human masseter's contraction is desirable, since they are directly applicable to the understanding of the structural and functional organization of human masticatory apparatus.

There are considerable advantages and disadvantages of using human subjects. Human subjects, unlike animals, are able to comply with complex instructions. The disadvantages, however, include the technical restrictions imposed by handling living tissues, as opposed to more invasive methods (including post mortem material) which are possible in animal experiments. Despite the limited kind of experiments in humans, promising techniques are presently being developed, which could be applied to the jaw muscles.

Based on the above outlined characteristics, the human masseter muscle is a good study model to further understand the contraction patterns of the masticatory system. Therefore, a more detailed description of the masseter's anatomical and functional design will be introduced in the next sections.

1.7 Anatomical Design of the Masseter

Mammalian masseter muscles arise from the lower border of the zygomatic arch as far anteriorly as the zygomatic process, and extend downwards and backwards to insert over a wide area of the mandibular ramus, extending from the mandibular angle to the level of the coronoid process. The masseter incorporates a complex system of internal aponeuroses (tendinous sheets) which divide the muscle into subvolumes with differing fibre orientations and pennation angles. In each subvolume, muscle fibres run continuously from one aponeurosis to the other, and at least in the rat masseter, no tendinous inscriptions between the muscle fibres occur (Matsumoto and Katsura, 1985). Common to all mammals is the size of the aponeuroses which cover large areas of each

muscle layer antero-posteriorly. In contrast, the orientation and position of the aponeuroses vary between species, due to their individual functional needs. Since internal architecture is important for the motor performance of a muscle, a detailed description of the masseter muscle anatomy will be presented and compared against other mammals in the following sections.

1.7.1 Muscle Organization

The rat masseter muscle has been described as having anywhere from two to four parts (Romer, 1939; Becht, 1954). In order to reconcile this lack of descriptive consistency, Hiiemae (1967) proposed that the separation of a muscle into distinct parts where no clear anatomical division exists (as occurs in the masseter) is justified only when there are large differences in fibre orientation and position, enabling the inference that the parts so defined have a different action. On this functional basis, Hiiemae and Houston (1971) divided the rat (*Rattus norvegicus* L.) masseter into four: one superficial, unipennate part (essentially regarded as a separate muscle), and three deep portions. In a more recent report by Matsumoto and Katsura (1985), the masseter muscle was further subdivided. Eleven compartments were described on the basis of fibre architecture alone. However, potential errors may arise using this classification, which may divide the muscle into too many compartments. It is possible to separate the muscle into different putative parts erroneously, influenced solely by the gradual changes in orientation that the fibres undergo from the muscle's origin to insertion. Nevertheless, irrespective of the quantity of separate muscle portions, dissections by Schumacher (1961a) revealed a system of

three interleaving aponeuroses.

In contrast, Herring and Scapino (1973) were unable to describe discrete, anatomically separate divisions in the masseter muscles of the pig (*Sus Scrofa* dom.). Macroscopic examination of this muscle (Herring *et al*, 1979) revealed gradual changes in fibre angulation dorso-ventrally at its surface. These observations lead Herring *et al* (1989) to the conclusion that it was not possible to identify strict anatomical compartments in the muscle on the basis of fibre orientation alone since the angulation of fibres was not constant through the same muscle layer. Also dissimilar to the rat, Schumacher (1961b) identified four internal aponeuroses. In the anterior part of the muscle, the aponeuroses are obliquely oriented, interdigitating septa, while in the posterior part they become broad and parasagittal. Among them, the fasciculi are long and vertical (relative to the tooth row) anteriorly, while the posterior fasciculi are short and near-horizontal, extending antero-posteriorly (Herring, 1980).

A number of detailed accounts on the human masseter anatomy are available in the literature. However, reports are inconsistent, describing the human masseter as consisting of two to eight portions of muscle. The simplest description divides the muscle into two parts, one "superficial" and one "deep" (Sicher, 1960; Schumacher, 1961c; DuBrul, 1980). In agreement with Sicher's original definition, Last (1966), Mosolov (1972), Gaspard *et al* (1973), and Williams *et al* (1989) also reported superficial and deep portions, but expanded the description by adding a third "intermediate" portion. In contrast, Ebert (1939) identified a third, "anterior" portion, situated laterally and separately from the superficial portion. This author's rationale was that although this

small portion was difficult to identify initially, it deserved to be described as separate, due to its simple parallel-fibred arrangement. Additional anatomical subdivisions were later introduced by Gaspard *et al* (1973), who separated the superficial part into two subsidiary layers, the "lamina prima et secunda". To further confuse the issue, Yoshikawa and Suzuki (1962) divided the masseter into eight parts. In their report, the superficial masseter is divided into two layers (lamina prima et secunda), consistent with Gaspard's anatomical account. They also identified one intermediate and three deep portions. The anterior deep has a simple structure, while the deep posterior portion is divided into four parts arranged medio-laterally, the deepest of which constitutes a separate portion called the M. maxillo-mandibularis. Despite the lack of agreement among previous reports, all above mentioned authors agree that irrespective of the number of muscle portions or layers, the various muscle portions are fused together on the zygomatic arch. The various portions also fuse anteriorly at their insertions on the mandible, but they diverge from each other posteriorly to allow passage of the masseteric artery and nerve.

Dissections performed by Ebert (1939) and Schumacher (1961c) revealed several internal aponeuroses which extend into the muscle body, alternating from the zygomatic arch and the lateral surface of the mandibular ramus. These reports however differed with respect to the number of aponeuroses. At least four of them could be visualized by magnetic resonance imaging in living subjects (Lam *et al*, 1991). In concurrence with Schumacher's (1961c) nomenclature, Aponeurosis I was the most lateral of the four and anchored to the zygomatic arch. Aponeurosis II attached to the mandibular ramus and extended superiorly into the muscle. Aponeurosis III attached to

the zygomatic arch and extended inferiorly into the muscle, more medial than aponeurosis II. The most medial aponeurosis, IV, was located on the deep surface of the muscle. Each aponeurosis had an unique three-dimensional orientation determined by the relative orientations of the zygomatic arch and mandibular ramus, both of which varied with craniofacial morphology (Lam *et al*, 1991). Because of morphological variations, widths between adjacent aponeurosis varied among subjects, and it was suggested that muscle fibre orientations between aponeuroses may result in unequal pennation angles at each end of the fibres (Lam *et al*, 1991).

Besides these differently-graded angles of pennation, the muscle fibres also differ in length, averaging 26 mm, but ranging from 14 to 39 mm (Schumacher, 1961c; Van Eijden and Raadsheer, 1992). In the muscle, these differences in length occur anteroposteriorly. Anteriorly they range from 24-30 mm; in the middle of the muscle they range from 19-26 mm and posteriorly from 14-19 mm. In the coronal view, the muscle fibres are arranged in various orientations between the contiguous aponeuroses. Whereas their angles of pennation vary between 12° and 14° in the anterior portion of the muscle (decreasing posteriorly to average 11° in the main, superficial portion), muscle fibres have identical lengths throughout a given coronal section (Ebert, 1939).

The masseter's origin and insertion has consistently been described as consisting of mixed musculous and aponeurotic attachments (Ebert, 1939; Schumacher, 1961c; Gaspard, 1987). Dissections and osteological studies revealed that besides the main aponeuroses, there are other, possibly smaller, tendinous attachments inserting into the lateral surface of the mandibular ramus (Baron and Debussy, 1979; Gaspard, 1987).

Collectively, this muscle has a highly complex architecture, which varies among species, among individuals, and with functional demand. Its multipennate arrangement allows more fibres to be packed into a small volume, resulting in a large physiological cross-sectional area, which may also vary significantly in humans depending on the individual's craniofacial type, being greatest in subjects with brachiocephalic skulls, short facial heights and small gonial angles (Weijs and Hillen, 1984b). In addition, the fibre orientation, relative to the functional occlusal plane, allows this muscle to produce large forces at the teeth (Hannam and Wood, 1989).

1.7.2 Innervation Pattern

The masseter muscle is innervated by a branch of the mandibular division of the trigeminal nerve. This branch, termed the masseteric nerve, enters the muscle at its medial and posterior aspect, after passing through the mandibular notch (Williams *et al*, 1989). Immediately before entering the muscle, the nerve divides into different trunks, which then diverge rostrally, ventrally and caudally (Lau, 1972; Xiguang *et al*, 1986) to ramify into the muscle layers situated between the aponeuroses (Schumacher, 1989).

In pigs, three separate nerve branches enter the masseter and distribute around the internal aponeuroses. Two rostral branches, which also supply the zygomatico-mandibularis, are small nerves and supply the dorsorostral aspect of the masseter. A third, more caudal main branch, divides into four terminal nerves with variable distributions. It innervates all of the muscle including at least part of the dorsorostral corner (Herring *et al*, 1989). In dogs and sheep however, only two separate

branches of the masseteric nerve enter the muscle (Lau, 1972). One supplies the proximal third of the muscle and the zygomatico-mandibularis, being equivalent to the first branch found in the pig. The second branch innervates a large portion of the muscle, extending across the muscle's medial and distal thirds. Despite the fact that these differences in innervation patterns between species were observed, they were considered to be minor and not fundamental (Schumacher, 1989).

In humans, the masseteric nerve may divide into two (Lau, 1972) or three (Xiguang *et al*, 1986) main branches just before entering the muscle. The first runs just inferiorly and along the zygomatic arch innervating the proximal, deep part of the muscle. The second runs on an oblique trajectory across the entire muscle and supplies its medial and distal thirds. In a few cases the second main branch splits into two trunks just before entering the muscle (Xiguang *et al*, 1986). The first trunk runs its conventional oblique trajectory, while the second trunk runs straight downwards, towards the angle of the mandible, innervating the posterior aspect of the superficial masseter. Further ramifications of the first branch also innervate a muscle portion situated between the masseter and temporalis. This portion is commonly described in the pig and rat, as well as in other mammals, as the zygomatico-mandibularis muscle (Eisler, 1912; Lau, 1972). In humans, this portion of the muscle was classified as the maxillo-mandibularis muscle by Yoshikawa and Suzuki (1962), a surprising nomenclature given the muscle's zygomatic origin.

1.7.3 Muscle Fibre Characteristics

With the exception of the posterior superficial part where there are approximately equal proportions of type I and II fibres (mostly type IIB), the adult human masseter consist mainly of type I fibres, which make up 62-72% of the muscle's total fibre content (Eriksson and Thornell, 1983; Vignon *et al*, 1980). Type I fibres occupy 88% of the cross-sectional area of the muscle's anterior deep part, but only 70% of the posterior superficial part. In contrast, type IIB fibres constitute only 7-21% of these subdivisions. Most of the type IIB fibres are found in the posterior superficial part (20.5%), and posterior deep part (15.2%). ATPase IM and type IIC fibres represent only about 9% of the total fibre population. Most type I fibres are larger than the type IIB fibres except in the intermediate part of the muscle (Eriksson and Thornell, 1983), and muscle fibre diameter differs between muscle subvolumes. In the superficial portion, diameters are larger than in the deep portion (Hopf, 1934). The significance of this is unclear, but like the distribution of fibre types, it implies that some kind of functional differentiation may occur. The masseter's type I fibres contain slow myosin, and its type II fibres contain mainly fast myosin, similar to the limb muscles (Thornell *et al*, 1984). However, the adult masseter also contains a neonatal myosin heavy chain (MHC) isozyme which has not been described in normal limb muscles (Butler-Browne *et al*, 1988). This neonatal MHC is expressed in ATPase IM and IIC fibres. In addition an embryonic isoform of myosin light chain (Butler-Browne *et al*, 1988; Soussi-Yanicostas *et al*, 1990) and a cardiac-specific myosin heavy chain have been found in the adult masseter, although its location is uncertain at present (Bredman *et al*, 1991).

1.7.4 Spindle Distribution

To further elucidate mechanisms in mandibular motor control, Eriksson and Thornell (1987) examined the muscle-spindle density and size in relation to extrafusal fibre-type composition in different portions of the human masseter by enzyme histochemistry. In contrast to findings by Kubota and Masegi (1977) who found similar spindle concentrations throughout the muscle of a new-born, Eriksson and Thornell (1987) found that spindles were distributed non-uniformly in the adult masseter muscle. In all subjects, spindle density had intramuscular differences. Most spindles were located in the deep portion, and no difference within this portion (antero-posteriorly) was found. The spindles in the deep portion were distinctive in that they contained the largest number of intrafusal fibres and had the largest diameters. Seventy-two percent of the intrafusal muscle fibres were contained in the spindles occupying the deep portion. Seventy-four percent of spindles were in the deep portion which is predominantly composed of type I fibres. These results are in concordance with Freimann's (1954) and Rowlerson and colleagues' (1988) findings that spindle density is greater in the deep masseter than in the superficial. Voss (1935) and Freimann (1954) also observed especially large spindles in the deep masseter. As in the case of fibre-typing studies, these findings also imply that individual portions of the masseter have specialized functions. In general, there are more spindles in anti-gravity, postural muscles, and in muscles controlling finely-graded movements, than in those used for coarse movements (Cooper and Daniel, 1963; Voss, 1971). Based on this knowledge, Eriksson and Thornell (1987) suggested considerable capacity for segmental proprioceptive reflexes in the adult

human masseter, especially in its deep portion.

1.7.5 Summary

Although muscle organization seems to be based on mechanical demands and efficiency, quantification of fibre orientation, the spatial location of muscle fibres, intramuscular septa and attachment sites, is rare. Although jaw muscle attachment sites in adult skulls have been described for one mandibular position, the large areas of attachment of many jaw muscles and the trajectories of functional jaw movements mean that various parts of these muscle's insertions must move differently; yet there are no data regarding such displacements as have been described in the rabbit (Weijs *et al*, 1989a,b).

1.8 Functional Design of the Masseter

1.8.1 Motor-unit Territory

Motor-unit territories have been investigated extensively in animal models (Burke, 1981), but are often analysed as a two-dimensional map, when in reality it is a three-dimensional volume. In addition, the total number of fibres in a MU is not represented in a single cross-section (Burke and Tsairis, 1973), therefore multiple sections along the muscle are necessary to reconstruct MU territory properly (Hannam and McMillan, 1993). In humans, where histological techniques are not possible, electrophysiological techniques are used to determine the volume in which fibres of a MU are distributed (Buchthal and Schmalbruch, 1970; Stålberg *et al*, 1976; McMillan

and Hannam, 1989a). Using this technique, MU territories have been estimated in the human masseter to be focal, spherically-shaped, and 3.7 mm long (Stålberg and Eriksson, 1987), although a small number of units reached 9.1-12.5 mm and were thought to extend over the whole muscle cross-section. In a different approach, measuring the linear distance between paired recording sites for the same MU, McMillan and Hannam (1991) reported average MU territory size of 8.8 mm for the masseter. These authors reported the territories as elliptical, oriented in an anteroposterior direction, and apparently arranged in layers throughout the muscle. These studies, nevertheless, have not been able to reveal the location of the MU territories relative to the intramuscular aponeuroses.

From studies on experimental animals, it is known that in at least some complex muscles, the innervation of primary branches divide the muscle into neuromuscular compartments (English and Letbetter, 1982a; English and Weeks, 1984), that may be defined by an internal tendinous network, and that muscle fibres pertaining to a single MU are contained within the boundaries of one of the compartments (English and Weeks, 1984). In this case, an individual motor axon may branch either distally to the primary branching of the muscle nerve, or proximally with all branches entering a single primary branch.

Alternatively, the possibility that the muscle fibres in a single MU are distributed over more than one neuromuscular compartment still exists for other muscles. Such a situation could arise if branching of individual motor axons occur proximally to the primary muscle nerve branch point, and the branches do not all enter a single

primary branch. Herring *et al* (1989) believes that this alternative innervation pattern is unlikely for the masseter muscle in pig, although in their study two or more widely separated regions in several instances, showed glycogen depletion. The authors' argument for rejecting this alternative explanation was that first, very few axons seemed to have proximal branching points, second, that multiple-area MUs have never been reported within any other muscle, and third, that multiple-area MUs would obscure any pattern of differential muscle activity, which are distinguished in the pig masseter (Herring *et al*, 1979).

It was then concluded that MU territories in the pig masseter are confined to muscle fascicles, and that the spatial separation of depleted regions were the result of stimulating nerve filaments containing adjacent nerve axons which supply different parts of the muscle. This was supported by their findings that, in contrast to other muscles, the nerve trunk in the pig masseter is not ordered somatotopically (Herring *et al*, 1989). Similar lack of organization was found for the facial nerve, although both the motor nuclei and the extratemporal portion of the nerve do show a somatotopic arrangement (Radpour and Gacek, 1985).

1.8.2 Functional Differentiation

The question of functional heterogeneity, that is whether the masseter always contracts as a unit or whether regional differences occur, has been posed for the pig (Herring *et al*, 1979), rabbit (Weijs and Dantuma, 1981) and man (Greenfield and Wyke, 1956). In pig, the electromyographic evidence shows that the different parts of the

masseter sometimes contract simultaneously with similar amplitude, during crushing on the balancing side and the power stroke on the working side, but more often there are regional differences (Herring *et al*, 1979). Seven to eight functional compartments with different electromyographic patterns could be described, but these compartments do not lie within strict anatomical boundaries, nor do they have any particular fibre orientation (Herring *et al*, 1989).

In the rabbit, on the other hand, differences in firing patterns of the anterior and posterior parts of the superficial masseter are negligible, while the well marked anterior and posterior portions of the deep masseter show slightly different firing patterns. Mediolaterally, five different compartments situated between aponeuroses fire at different times during chewing. On the balancing side, the superficial portions start firing, followed in a gradual transition by the deeper portions. The reversed firing sequence is observed in the working side muscle (Weijs and Dantuma, 1981). These authors suggested that because of the continuity of the firing pattern any grouping of compartments is arbitrary.

As reviewed earlier, anatomically the human masseter consists of at least two portions (superficial and deep). With respect to the Frankfort horizontal plane⁵, the deep muscle fibres run almost vertically downward, differentiating from those of the superficial muscle portion which are directed downward and posteriorly. Consequently, Carlsöö (1952) concluded that the deep portion of the masseter muscle could have

⁵ The *Frankfort horizontal plane* is defined by three points: the centre of the external auditory meatus on both sides, and the lowest point on the right infraorbital notch.

closing and retractive functions.

Many studies have attempted to separate the human masseter into separate portions on a functional basis. With surface electrodes, Greenfield and Wyke (1956) demonstrated differences in muscle activity between the superficial and deep portions of the human masseter, reporting greater activity in the deep portion during jaw retrusion and ipsilateral clenching. Conversely, the superficial portion was more active during protrusion, contralateral molar and incisor biting, and during protrusion without tooth contact. Belser and Hannam (1986), did not demonstrate any significant difference in electromyographic activity between surface and fine-wire electrodes when recording from the deep masseter, and decided to use the noninvasive surface electrodes for further investigation. In accordance with Greenfield and Wyke (1956), the authors found distinct separation of activity when intercuspal clenching was directed retrusively, and when subjects were clenching on the ipsilateral side. During these tasks, the deep portion of the muscle was more active. Their results indicated that for most clenching tasks, the masseter contracts differentially, nevertheless both parts of the muscle are active, even during incisal clenching. This led them to the speculation that despite some differential contraction, the muscle has normally a relatively restricted range of action because so much of it appears to contract so much of the time (Belser and Hannam, 1986).

In a more recent study, six fine-wire electrodes were used in the masseter; three in the deep and three in the superficial portions (Blanksma *et al*, 1992). Although no statistically significant differences between different muscle regions were found, a significant interaction between region and bite-force direction was present. By far the

largest deviation from the rest of the muscle was found for the deep posterior region; that is, its activity was the highest during postero-ipsilateral bites and lowest in oppositely directed efforts. The same pattern, although less striking and more variable, was found for the posterior superficial masseter. In the deep muscle, the activity pattern of the anterior and middle portions were very similar, but differed with higher activity from the deep posterior part during anteriorly- and anteromedially- directed bites. During these efforts, differential contraction was nearly absent but became more obvious during other directed tasks, unveiling a functional partitioning of the masseter in at least three parts: anterior deep, posterior deep and superficial.

Similar to the rabbit, in humans during chewing cycles, the masseter on the working-side was always more active than the masseter on the balancing-side; and maximum activity appeared earlier at the balancing side than at the working side. In addition, mediolateral differences within the muscle were found. On the balancing side, the peak muscular activity shifted from the superficial to the deep portion; the pattern is inversed on the working side (Van Eijden *et al*, 1993). On this latter side, the deep fibres of the masseter muscle contribute with relatively more activity to the final phase of the chewing stroke than does the superficial portion of the muscle, even though both are active bilaterally (Belser and Hannam, 1986).

1.8.3 Motor-unit Activity

Similar to what occurs in limbs, an orderly recruitment pattern of MUs has been reported in the jaw muscles of human and non-human primates (Desmedt and

Godaux, 1975, 1979; Goldberg and Derfler, 1977; Yemm, 1977; Clark *et al*, 1978), with only rare occurrences of activation order reversals (Desmedt and Godaux, 1979). In the masseter, recruitment threshold (RT) and force output of MUs are also correlated throughout force development (Goldberg and Derfler, 1977; Nordstrom and Miles, 1990; Yemm, 1977), although RTs could vary depending on task, prolonged muscle contraction (Nordstrom and Miles, 1991b), and with jaw opening (Miles *et al*, 1986). On the latter case, as the jaw gape increases, the RT also increases.

In earlier studies in the jaw muscles, MUs were assumed to belong to a homogeneous, whole-muscle motoneuron pool. The human masseter and temporalis muscles are, however, complex muscles, and are composed of a mixture of uni- and multifunctional units (Eriksson *et al*, 1984), the latter showing regional differences in behaviour (McMillan and Hannam, 1992). That is, most units located in the posterior, superficial region of the masseter contribute to tasks involving tooth contact, whereas in the anterior, inferior and superficial portion MUs were active in non-dental tasks, apparently contributing to jaw posture (McMillan and Hannam, 1992). In addition, masseter MUs were found to have their RTs changed with the direction of bite force; their "preferred" direction of effort was reflected in their RTs (Hattori *et al*, 1991). These observations infer that the masseter is organized into separate motoneuron task groups, which may be arranged to discrete regions at the motor nucleus and restricted to anatomical subvolumes at the periphery.

Contrary to large limb muscles in which MUs are continuously recruited until at least 90% of the maximum voluntary contraction (MVC) is reached (De Luca, 1985),

smaller muscles (such as the temporalis and masseter) recruit 50% of their MUs within 10-20% of MVC. To further increase their force output between 20-100% MVC, these muscles rely predominately on firing rate modulation (Clark *et al*, 1978; Derfler and Goldberg, 1978).

In the jaw muscles, the majority of MUs increase their mean firing rate with increases in bite force, and although spike train characteristics are similar to those recorded in limb muscles (Derfler and Goldberg, 1978), the lowest sustainable firing frequency (LSFF) of jaw muscles (10 Hz; Nordstrom *et al*, 1989) appear to be higher than in limb (6 Hz; Petajan, 1981). In the masseter and temporalis, this LSFF also depends on the jaw task performed (Eriksson *et al*, 1984; McMillan and Hannam, 1992), and on the anatomical site (McMillan and Hannam, 1992).

1.8.3 Conclusion

The localization of MUs to anatomical subvolumes offers the potential for more specific motor control rather than simple contraction of the muscle as a whole. It could permit the activation of muscle regions relatively independently of one another as needed, with the regional interactions dependent on the particular task and movement strategy involved (English, 1985). In the human masseter, MU territories are mostly small, and therefore appear to be restricted to muscle fascicles just as MU territories are in the pig masseter (Herring *et al*, 1989). However, the wide distribution of some MU territories (Stålberg and Eriksson, 1987) and the continuity in firing pattern observed during chewing (Van Eijden *et al*, 1993) suggests that in humans at least, muscle

compartments may not be defined entirely by internal muscle boundaries, and it is possible that functional distinct regions in the masseter may be fewer than those inferred by muscle architecture alone.

2. STATEMENT OF THE PROBLEM

The jaw muscles are responsible for the generation of forces within dental, articular and cranial tissues. Their functions promote jaw movements, have important implications in craniofacial growth and bone stresses, and can also be involved in disorders of the musculoskeletal system. Despite their importance in peripheral motor control, the structural, biomechanical and functional organization of the masticatory muscles are not well understood. It is known that each muscle has unique characteristics, including complex structural and histochemical properties, but we still cannot adequately explain how these muscles contract.

Little is known about human orofacial muscle development other than differentiation times and changes in size or weight. While the morphology and biomechanics of adult jaw muscles have received attention, there is virtually no information regarding their fetal counterparts, and although muscle organization seems to be based on mechanical and functional demands, quantification of intramuscular tendon sheets and attachment sites is scarce. Attachment sites in adult skulls have been described as extending into large bone areas, which suggest that during functional jaw movements different parts of these muscles' insertions must move differently; yet there are no data regarding such displacements. In addition, muscle activity appears to vary according to muscle region and task, suggesting that the human jaw muscles are partitioned in a manner roughly similar to the divisions of the same muscles in rabbits, rats and pigs. However, little is known on how reproducible are the firing characteristics of MUs, or how these are arranged relative to internal tendinous structures. The human

masseter muscle would be a good model to further basic knowledge in this area, because it exemplifies a complex muscular structure, its peripheral and central connectivities are better understood than most jaw muscles, and its location facilitates functional investigation.

To study muscle biomechanics and function relative to internal architecture in living humans, the following requirements should be met:

- a. Anatomical and biomechanical investigations of muscle structures should preferably be made in living subjects, instead of relying solely on gross anatomical and histological studies of cadaver material, which may have different dispositions of internal structures. In addition, non-invasive methods enable the evaluation of muscle mechanics during natural tasks.
- b. Appropriate intramuscular EMG recording techniques must be used to measure focal muscle activity with minimum discomfort to the subject.
- c. The reproducibility of activation in a muscle subvolume should be ascertained when the activity of a focal muscle region is to be analysed according to task, or if different muscle regions are to be compared.
- d. EMG recording-site locations should be related to internal muscle structures if the biomechanical role of muscle subvolumes is to be evaluated.

In this thesis, the following specific hypotheses and objectives are proposed:

- 1) It is hypothesized that in the masseter, the major structural boundaries that separate groups of muscle fibres with different orientations, are already present at an early fetal stage. Confirmation of this hypothesis would determine whether development of the human masseter is consistent with current views of muscle development in general, and add insight to our understanding of the formation of its structural muscle compartments. The aim would be to compare the internal structures of the fetal masseter muscle against their adult analogues.
- 2) It is hypothesized that portions of the masseter's insertion have different displacement characteristics, depending on the jaw movement performed, and that these differences reflect local biomechanical demands. Information regarding attachment displacement would be needed for any model of muscle mechanics, and could be useful for evaluating the muscle's length-tension characteristics under functional conditions. The goal would be to investigate spatial changes imposed upon the masseter's insertions as a result of the rotational and translatory movements of the human jaw.
- 3) It is hypothesized that the human masseter is divided into separate muscle portions which are activated differentially, depending on the task performed. Confirmation of this hypothesis would clarify our understanding of peripheral motor control in the masseter. The hypothesis could be examined by testing regional electrical muscle activity. The aim would be to assess the functional performance of a sample of MUs in one specific region of the masseter muscle, by testing both the effect of task on

MU activity and its reproducibility.

- 4) It is hypothesized that MU territories in the masseter are small and confined by tendinous boundaries. Confirmation of this hypothesis would signify that an anatomical basis for differential muscle contraction is possible in the human masseter, possibly enabling the generation of internal force vectors with different directions. The aim would be to combine imaging of the muscle with three-dimensional verification of MU territories revealed by MU recordings in the masseter.

Collectively, these experiments could be used to refine biomechanical models of the masticatory musculoskeletal system. They could provide new and fundamental insights into interactions between neuromuscular compartments and they could also advance the understanding of skeletal muscle function, so important in the etiology of muscular disorders.

3. STUDIES

In order to test the proposed hypotheses, experiments were carried out involving both structural and physiological studies as well as a combination of these types of investigations.

Anatomical studies were performed with different methodologies, including histological serial sectioning, conventional gross anatomical dissections, and Magnetic Resonance (MR) derived reconstructions of the masseter muscle. The use of histological sections of human fetal material was a practical means (due to its smaller size) of developing a methodology to study internal muscle architecture in the adult. The gross anatomical dissections were conducted to enhance familiarization with the muscle's anatomy for better interpretation of the MR images.

Experiments designed to study muscle activity were initially conducted exclusively with physiological methods, but in later projects both anatomical and physiological methodologies were used in conjunction. Here, new technical approaches had to be developed, i.e. a method for imaging the masseter internal architecture, a focal EMG recording technique, and a stereotactic method for locating the needle electrode recording site.

In this chapter, each experiment is presented in a separate section, which contains that study's specific material and methods, its related results, and their discussion.

3.1 Masseter Morphology

3.1.1 Exploratory Experiments on Fetal Masseter Anatomy

During post-natal development, from suckling to chewing, the masticatory apparatus undergoes dramatic conversion in function (Herring, 1985). Masticatory behaviour changes are gradual and occur during the transition through the deciduous, mixed and permanent dentitions. Concomitant and considerable changes in human masticatory movement patterns can be observed (Wickwire *et al*, 1981). While suckling mainly requires strenuous activity of the facial and lingual muscles, mastication involves strong activity in the jaw-closing muscles.

Whereas the early stages of myogenesis may proceed normally in the absence of a nerve supply (Mastaglia, 1981), the process of innervation enhances muscle development. Myoneural junctions begin to form in the human limb during the 11th week of intrauterine life (Cuajunco, 1942), a time in which jaw closure commences (Humphrey, 1971). Considerable mandibular development and muscular differentiation take place at this time (Furstman, 1963; Diewert *et al*, 1991). Of particular interest are the nature and destination of major nerve divisions, and the extent to which a pattern of connectivity is established at this early fetal age.

Considerable work has been performed in non-human animals with respect to the growth of the jaw muscles (Zey, 1939; Gagnot *et al*, 1977; Cachel, 1984; Herring and Wineski, 1986; Weijs *et al*, 1987; Hurov *et al*, 1988; Dechow and Carlson, 1990; Langenbach, 1992). Despite a marked change in skull shape, and concurrent change in the jaw muscles, the basic arrangement of muscle fibres and tendinous aponeuroses

seems to be relatively constant for pigs (Herring and Wineski, 1986) and rabbits (Weijs *et al*, 1987). Generally, the rabbit masseter has a positive allometric growth and its contribution to total muscle weight increases strongly (Langenbach and Weijs, 1990). The ratio of muscle-fibre to muscle-length decreases and a higher variance in length in different parts of the masseter muscle are observed during its development (Weijs *et al*, 1987; Herring and Wineski, 1986). It is also believed that pennation in the rabbit masseter increases with growth (Langenbach and Weijs, 1990).

Besides some data regarding attachment sites (Gaspard, 1987) and aponeuroses (Schumacher, 1962), in neonatal and adolescent human masseter muscle there is little research on human masticatory muscle development. Knowledge of the internal architecture from the fetal to the adult stages is desirable for a better understanding of the relationship between structure and changing function of the muscle.

In this section of the thesis, it is hypothesized that in the human masseter muscle major structural boundaries are found early in fetal life, and that these form the basis for later regional organization in the more complex adult muscle. In addition, it is speculated that fibre collections and major intramuscular tissue boundaries seen in the fetus have morphological and functional analogues in the adult. Thus the specific aim of this study was to divide the muscle into anatomical portions, and compare its organization with that of the adult muscle.

3.1.1.1 Materials and Methods

Six intact formalin-fixed fetal masseter muscles were obtained from human

specimens at 17-20 weeks. These fetal stages were selected on the basis of muscle tissue development. Based on previous reports, it was expected that both muscle fibres and myotubes would be present in fetuses older than 15 weeks (Mastaglia 1981; Gamble *et al*, 1978). In addition, the relationship between fibre orientation, aponeuroses and the ramus of the mandible are relatively constant throughout the peak human fetal growth period (Burdi and Spyropoulos, 1978).

The heads were obtained from the collection of the Department of Clinical Dental Sciences, University of British Columbia. They were hemisected, and individual masseter muscles were removed by cutting through the zygomatic arch anteriorly and posteriorly to the muscle's origin, through the body of the mandible anteriorly to the muscle's insertion, and through the tissue posterior to the mandibular ramus and condyle. In addition, horizontal cuts were made superior to the zygomatic arch and below the inferior border of the mandible. Because the developing skeletal elements of fetuses of this age are partly calcified, decalcification with 5% formic acid was undertaken over a period of two weeks. The specimens were placed in the decalcification medium, which was subjected to constant motion on a histokinette at room temperature, and the solution was changed every other day to prevent calcium build-up. Radiographs were taken at the end of each week to monitor the decalcification process. After decalcification was completed, the specimens were washed in running tap water for 24 hours.

To reconstruct three-dimensional (3D) shapes of tissues obtained from two-dimensional serial sections, external reference markers have been commonly used

(Gaunt, 1971; Meyer and Domanico, 1988). These markers can be natural objects (e.g. chives, thread or piece of paper) introduced into the embedding material along with the specimen, or tissue fiducials which can be either small holes drilled through the plastic embedding block peripheral to the biological specimen, or paint brushed along the block's sides (Brändle, 1989; Meyer and Domanico, 1988). The advantage of using natural objects as external markers is that they can be embedded in paraffin and can be easily sectioned, while artificial markers require the use of plastic embedding materials. The disadvantages of the use of natural markers, however, are that the introduced objects do not lie exactly perpendicular to the plane of section, and that they could theoretically undergo considerable distortion. If artificial reference markers are utilized, deformations caused by compression or stretching during sectioning can be corrected mathematically by the determination of correction factors. That is, if it is assumed that the deformation of a histological section is linear, affecting all points of that section equally, then all coordinate points of all reference markers and contour points should be shifted in the x and y directions by the same factors relative to their original locations. By calculating the distances between fiducial points and the angles formed between these points and by determining the change in positions of the reference markers relative to the reference system, distortions can be subsequently corrected.

Since the masseter muscles are fairly large (approximately 6 x 8 mm) at 17 weeks, they present a technical difficulty in terms of size. Cutting knives commonly used in sectioning plastic blocks have short edges, meant for sectioning smaller tissues. In addition, only thin sections can be obtained from plastic blocks. Stain infiltration into the

tissues embedded in plastic can also be reduced. To accommodate the large sample dimensions, and to obtain thicker sections of the tissue for silver staining techniques, paraffin was chosen as the embedding material. Natural markers (earthworms) were used as external references, which were useful as a coarse guide for matching the consecutive serial sections. After embedding, specimens were sectioned at 10 μm and sampled serially every 100 μm through the entire length of each block. The six specimens were divided into three groups, which were sectioned in the transverse, parasagittal and axial planes. Alternate sections were stained for nerve, connective tissue and muscle fibres (where present), with a modified Bielshowsky's silver impregnation method, picrosirius connective tissue stain, and haematoxylin and eosin, respectively.

3.1.1.1.1 Nerve Staining

Numerous impregnation methods for the demonstration of nerves in paraffin sections have been described (Samuel, 1953a,b; Peters, 1955a,b; Rowles, 1960). In the present study, three different techniques which can be applied to paraffin sections and peripheral nerve fibres were used: Bielschowsky (Culling, 1963), a modification of Palmgren's (Goshgarian, 1977), and the Marsland, Glees and Erikson's (Drury and Wallington, 1980) silver impregnation methods. However, none of the methods was specific, showing impregnation of nuclei and of connective tissue in addition to nerves. The specificity of silver impregnation depends largely upon an interrelationship between pH, time, temperature and silver concentration of the impregnating solution (Fernhead and Linder, 1956). The methods of fixation and tissue preparation, type of silver

Figure 1 Fetal peripheral-nerve staining. Histological feature of peripheral nerve showing neurofilament immunohistochemical reactivity on the axons. The calibration bar represents 30 μm .



compound used, buffer type, incubation time and the characteristics of the developing solution also play important roles in the specificity, reliability and reproducibility of silver impregnation (Linder, 1978). Although most of these variables could be carefully controlled during staining of the fetal specimens, the fixation process could not, because it had been carried out earlier, prior to the obtainment of the fetal material. If tissues are not fixed thoroughly immediately after the specimens are initially sampled, it would be expected that the nerve fibres would show a reduced affinity for silver, possibly due to loss of lipid, and that the finer nerve fibres and nerve endings could remain unstained (Linder, 1978). Apparently this was the case with the specimens used in this study, since in the attempt to stain nerve bundles, sections were developed beyond the ideal time when a high contrast between nervous and non-nervous tissue is expected. At longer development periods, the intensity of the background started to increase because connective tissue started to take up silver, thus compromising staining for nerve specificity.

Immunohistochemistry staining of the nerve fibres was therefore performed as an alternative method. The technique was identical to that described by McGeer *et al* (1989), in which specimens were processed with anti-human neurofilament antibody. Figure 1 shows the results of this technique in a peripheral nerve in a fetal masseter. Successful staining of the axons was obtained, while the surrounding tissues were stained only very weakly.

3.1.1.1.2 Connective-Tissue and Muscle-Fibre Staining

The combination of picrosirius (sirius red) staining (Junqueira *et al*, 1979a,b) and polarization microscopy allows the specific detection of collagen (Figure 2). It is known that Sirius Red stains collagen by reacting via the dye's sulphonic acid groups with the basic groups present in the collagen molecule. In addition, it is believed that the birefringency enhancement is achieved by the attachment of the elongated dye molecules to the collagen fibre so that the axes of both collagen and dye are parallel (Junqueira *et al*, 1979b).

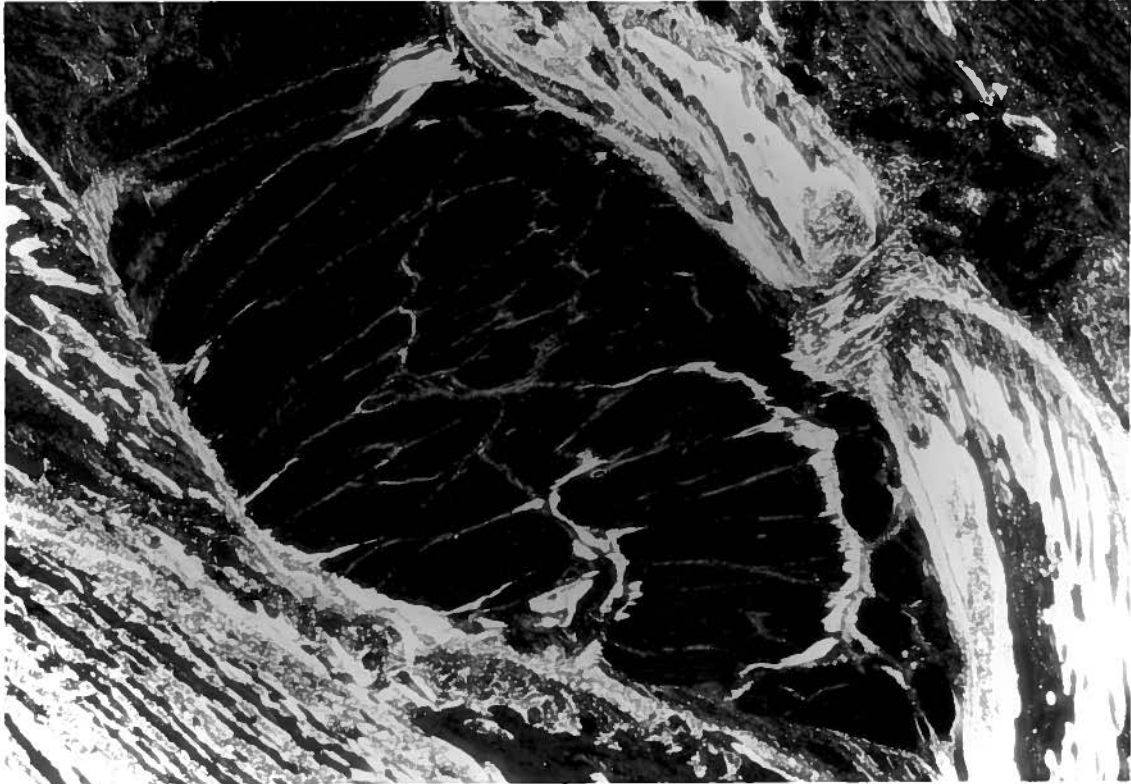
3.1.1.1.3 Muscle-Fibre Staining and Orientation Assessment

Haematoxylin and eosin staining (Culling, 1963) is commonly used to reveal the histological structure of tissues. A further advantage of eosin is that it fluoresces, enabling the detection of stained structures with confocal microscopy examinations employing Argon 488 laser beams.

3.1.1.1.4 Muscle Reconstruction

To reconstruct the fetal muscles, individual histological sections were photographed at low magnification. Since the specimens were large, each section was photographed over several fields. Negatives were printed and several of them were used to form a montage of each histological section. Major tissue boundaries, that is, tendinous sheets and connective-tissue outlines separating muscle fibres with marked differences in fibre orientation (Hiemae, 1967; Matsumoto and Katsura, 1987) were

Figure 2 **Fetal connective-tissue staining.** Polarized light micrograph of a tissue section of human fetal masseter muscle cut in the parasagittal plane. The tissue was stained by the picosirius method. Tendon and connective tissue are seen as white structures within the black muscle. The front of the muscle is oriented towards the upper left corner of the picture. The zygomatic arch and the mandibular ramus are seen above and below the muscle. The calibration bar represents 1 mm.



then traced from the montages. The initial goal was to code major muscle subdivisions as outlines, by measuring muscle-fibre orientation by the method described by Matsumoto and Katsura (1987). Essentially this consisted of measuring the axial ratios (minimum/maximum) of ten randomly chosen sectioned fibres of each homogeneous group, then using these ratios to classify fibre cross-sectional profiles into various classes (i.e. 0.21-0.30; 0.31-0.40, etc). Neighbouring outlines with ratios that fell within the same range were merged, and those with ratios that belonged to different classes were coded as separate muscle subdivisions. These were numbered 1-5, starting from the most anterior region of the muscle and progressing posteriorly. Therefore, neighbouring outlines always consisted of muscle fibres with distinct orientations, but it was possible that distant outlines were composed of fibres with similar axial ratios. Coded outlines were then digitized and assembled into profile stacks.

An extension of this technique was to measure the angle of the long axis of ten representative muscle fibres belonging to each group. To achieve this reproducibly, each histological slice was oriented on the microscope stage by aligning the lateral surface of the mandibular ramus with an eyepiece grid. In one specimen, the angles were measured relative to a common reference line (lateral surface of the mandibular ramus) in the plane of section (horizontal section) using a confocal microscope (Laser Scan Microscope, Carl Zeiss Inc, Oberkochen, Germany). The mandibular ramus was used as the plane of reference because it was found that the measurement of fibre angulation was more reproducible than when fibres were measured relative to the median plane.

In addition, the angle which the muscle fibres made to the plane of section

were measured. Again, each histological slice was kept oriented on the microscope stage aligned to the lateral surface of the mandibular ramus. A perpendicular optical scan was performed on the area of interest (Figure 3). The orientation of a given muscle fibre was then measured with the available confocal software by measuring the angle of the line extending between the centroids of both fibre endings relative to the plane of cut. Since the muscle-fibre extremes were often imaged as diffuse endings, this method did not prove to be reproducible. An alternative, more reliable method of measuring this angle was therefore pursued. It consisted of optically sectioning the specimen at two horizontal depth levels and subsequently calculating the fibre-orientation angle from depth and shift measurements. Each ten- μm -thick section was optically sectioned every 0.5 μm . At both depth extremes, the first optical section which resulted in sharp images were selected as the topmost and inferiormost levels. These were colour-coded and stored in the microcomputer. Sections were then superimposed, and the distance between the centroid of a single muscle fibre at one level was measured relative to the centroid of the same muscle fibre at the second level (Figure 4). The angle was then calculated as the arctangent of the ratio of the distance between centroids over the distance between the two levels. Ideally, these measurements should have been performed in thicker tissues; however, technically it proved too difficult to obtain paraffin sections which were thick enough (40 μm).

The two angles, that is fibre angulation relative to mandibular ramus and fibre angulation relative to the plane of the section, were then used to assign 3D orientations to the different fibre collections. The 3D orientation of each representative fibre

Figure 3 Cross-sectional optical scan (Z-scan) through a 10- μm fetal-muscle section. Confocal-microscope scan of a horizontal section through a fetal masseter muscle. The tissue was stained with haematoxylin and eosin and the muscle fibres were cut obliquely to the cross section (below). The white horizontal line represents the XY location at which the cross-sectional optical scan was performed. The tissue thickness is shown above. Two cursors (crosses) were placed at the centres of both ends of a selected muscle fibre, and the angle relative to the plane of cut was measured. In this example, the muscle fibre was oriented at 77° to the plane of cut.

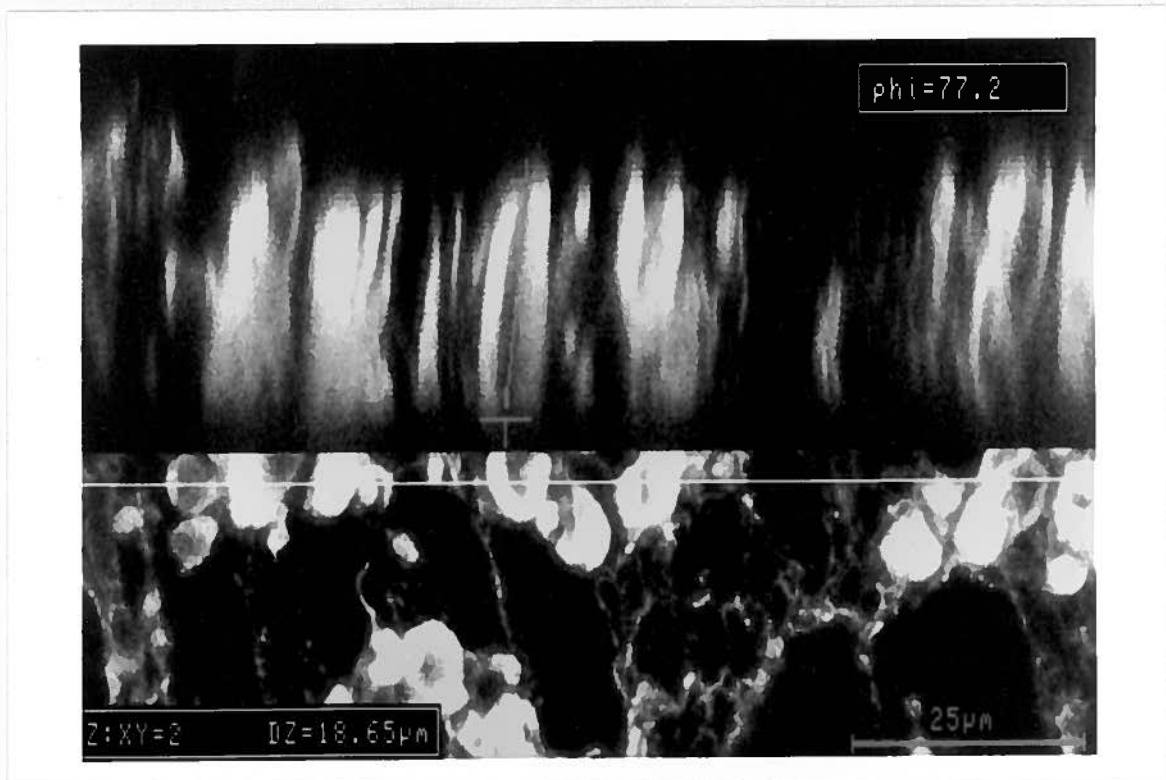
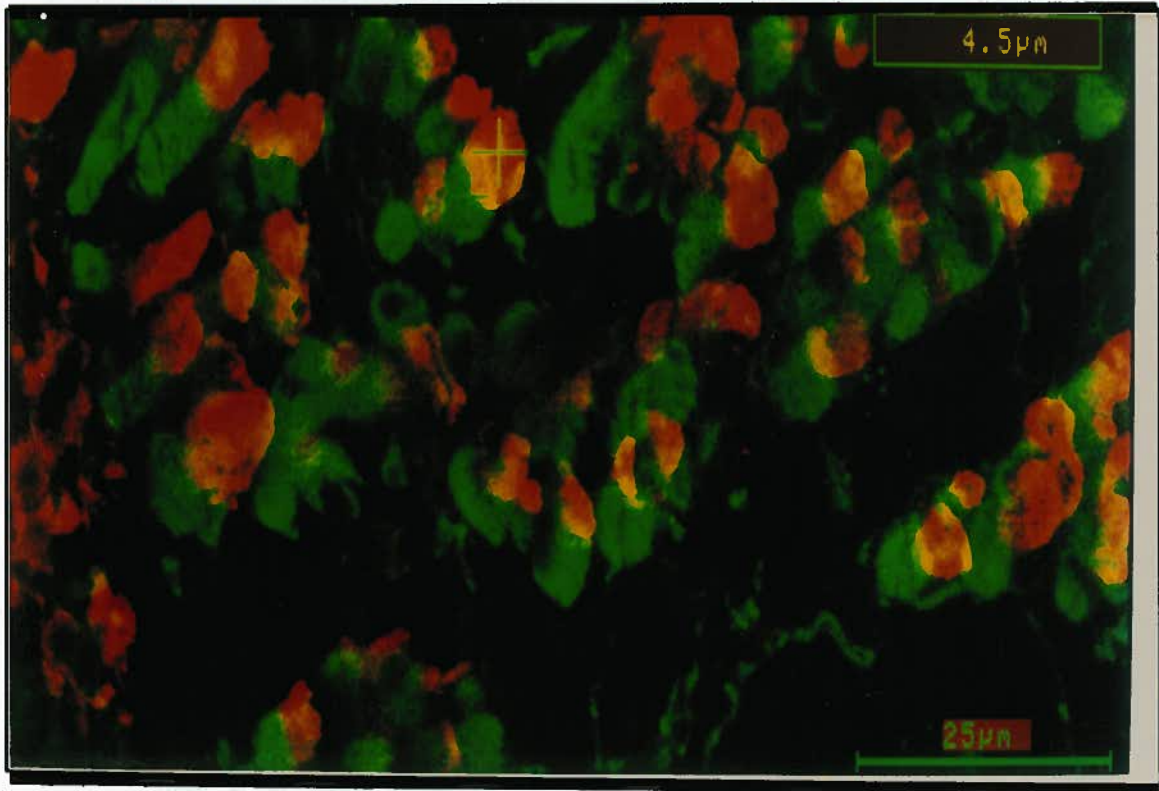


Figure 4 Superimposition of two horizontal optical sections situated at both extremes of a 10- μm -thick fetal muscle section. Confocal-microscope scan of a horizontal section through a fetal masseter muscle. The tissue was stained with haematoxylin and eosin and as before, the muscle fibres were cut obliquely to the cross section. The top section is colour-coded with red, while the bottom section with green. Cursors (crosses) are placed on the centroids of the muscle-fibre cross-section. Distance between the cursors is measured on the XY-plane and is 4.5 μm long.



measured was then displayed graphically as a constant length vector passing through the section profile at the respective location of measurement. By stacking section profiles, and with the aid of graphics rotation, it was possible to visualize changes in fibre orientation within groups as the level of section changed, and to do so in relationship to major septal divisions.

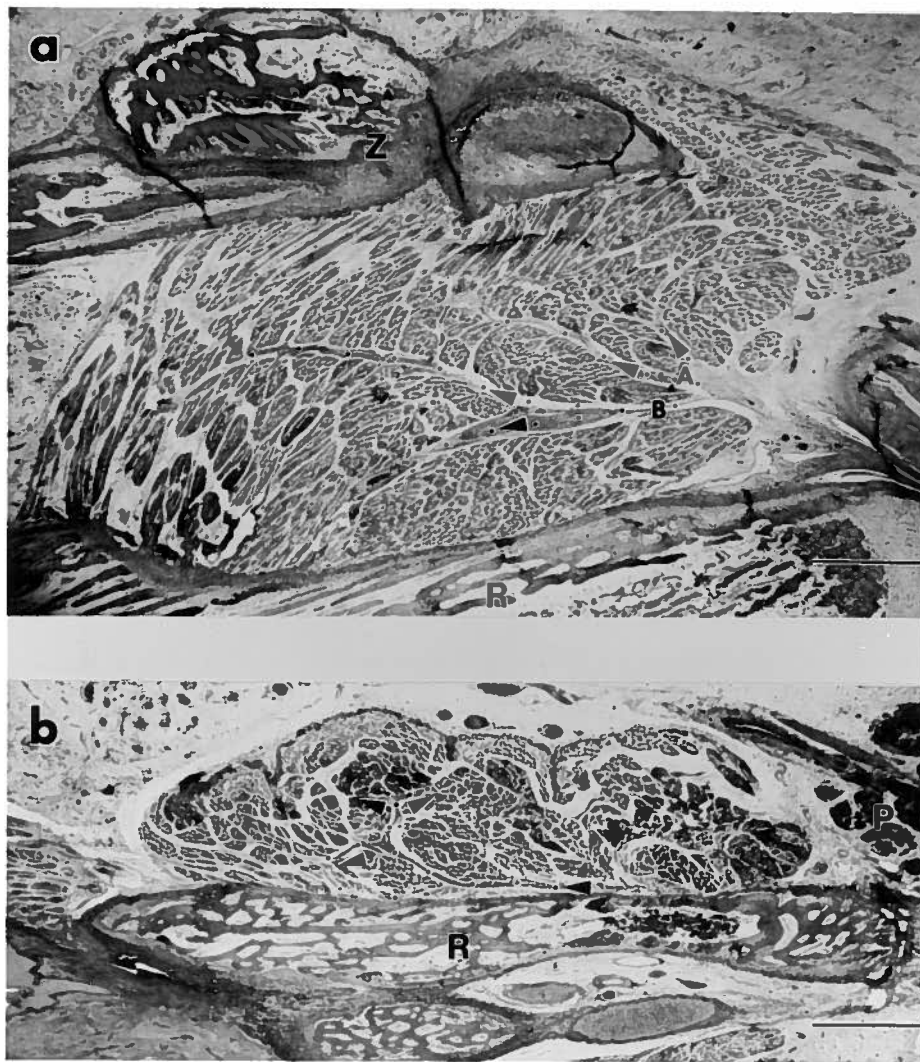
The angles of muscle fibre orientation relative to the mandibular ramus and relative to the plane of section were measured in one fetal masseter muscle sectioned in the horizontal plane. Five sections 400 μm apart were chosen for this analysis. In addition, two sets of two sections 100 μm apart were also measured to control for the accuracy of the method. Each muscle section was divided into muscle subportions defined according to fibre minimum/maximum ratios, as described above. Fibre angles were measured for a sample of ten fibres within each subgroup. Mean and standard deviation values were calculated for each group in each selected section.

3.1.1.2 Results

3.1.1.2.1 Nerve Distribution

As in the adult masseter muscle (Lau, 1972; Xiguang *et al*, 1986), in four fetal specimens the masseteric nerve was found to branch into two trunks before entering the muscle (Figure 5A). As previously described, trunk A divided into two main branches, which supply the posterior portion of the deep masseter. Trunk B divided into two main branches in the posterior third (Figure 5A) and in the middle (Figure 5B) of the muscle. These innervated the anterior and posterior portions of the superficial masseter, as well

Figure 5 Masseteric nerve pathway in the human fetal masseter. Tissues were stained with haematoxylin and eosin. (a) Medial parasagittal section of a masseter muscle. The nerve enters the muscle in two separate branches (A and B) from the medio-posterior aspect. Branch A innervates the deep posterior muscle portion. Branch B innervates the anterior and superficial muscle portions. (b) Horizontal section of a masseter muscle half-way through the muscle's longitudinal axis. The masseteric nerve runs parallel to the mandibular ramus forward and splits into two branches. One branch innervates the anterior deep portion. The second branch divides again into two; the first of which innervates the anterior superficial, while the second supplies the posterior superficial muscle portion (dots and arrows). Anterior is to the left. The calibration bar represents 1 mm. (P) Parotid gland; (R) Mandibular ramus; (Z) Zygomatic arch.



as the anterior portion of the deep masseter.

3.1.1.2.2 Connective-Tissue Development

Dense regular connective tissue was found in all specimens, and formed the fetal analogue of Aponeurosis I. With the exception of one specimen in which the primordial of Aponeuroses II and III (Figure 2) were also seen, other major aponeuroses in the masseter muscle were not reliably identifiable at this fetal stage, and clear separation of the masseter muscle into recognizable compartments by the identification of collagenous boundaries proved difficult in all investigated specimens. In contrast however, the medial pterygoid muscle showed well-formed dense connective-tissue layers in all sectioned specimens (Figure 6).

3.1.1.2.3 Muscle-Fibre Orientation

As expected, human fetuses at 17-20 weeks menstrual age comprised both myotubes and muscle fibres in mixed proportions (Figure 7). The embryonic muscle fibres consisted of centrally placed nuclei and peripherally disposed myofibrils (Figure 8). An increased number of blood cells was also commonly observed in specimens at this fetal age (Figure 8B).

Although the pennation pattern was not expected to be fully developed, the relationship between masseter muscle-fibre orientation and the ramus of the mandible, and also with occlusal plane, has been shown to be relatively constant throughout the peak human fetal growth period (Burdi and Spyropoulus, 1978). In the present study,

Figure 6 Development of aponeurotic layers in the fetal masseter and medial pterygoid muscles. Tissue was stained with Sirius Red and visualized with light microscopy. Note that only Aponeurosis I (arrows) is well formed in the masseter muscle. In contrast, in the medial pterygoid muscle several aponeuroses are already present (arrows). Anterior is to the left. (M) Masseter muscle; (MPt) Medial Pterygoid; (R) Mandibular ramus.



Figure 7 Masseter muscle fibres in the 18 weeks old human fetus. Muscle fibres are arranged within abundant loose connective tissue. Note the striation pattern already present at this developmental stage. Tissue was stained with haematoxylin and eosin and visualized with the confocal microscope.

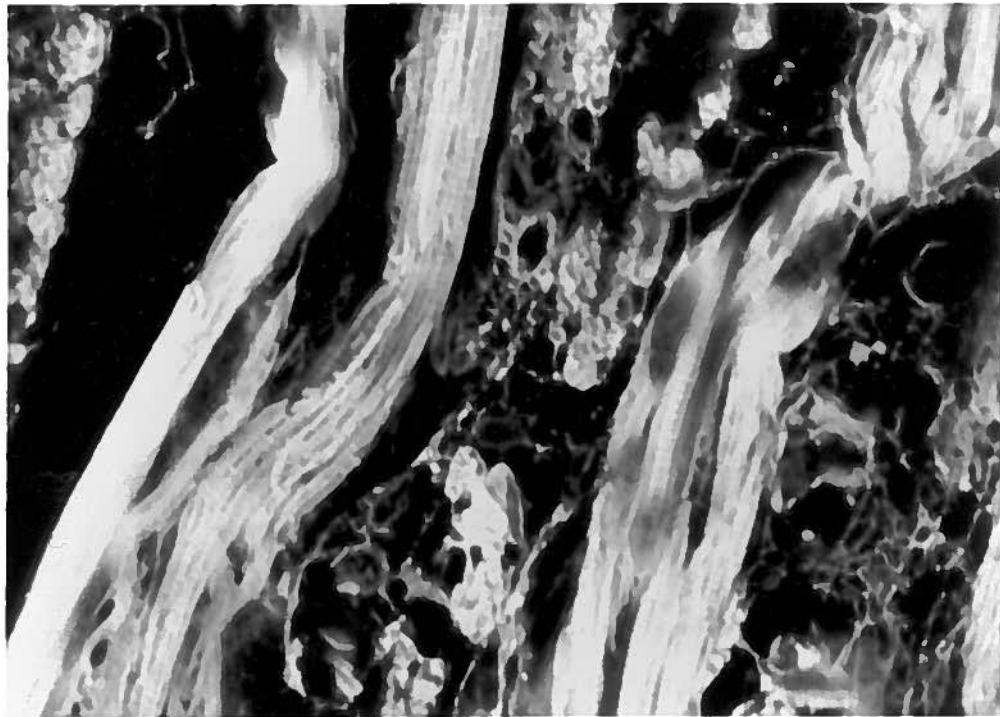


Figure 8 **Characteristics of fetal muscle tissues.** Both figures are different segments of the same histological section of masseter cut along the horizontal plane and stained with haematoxylin and eosin. Above, muscle fibres are cross-sectioned and are arranged in fascicles between loose connective tissue. The nuclei are centrally placed and at this stage myoblast fusions are still expected. Below, muscle fibres were cut obliquely. This region is also rich in blood cells. The calibration bar represents 25 μm .

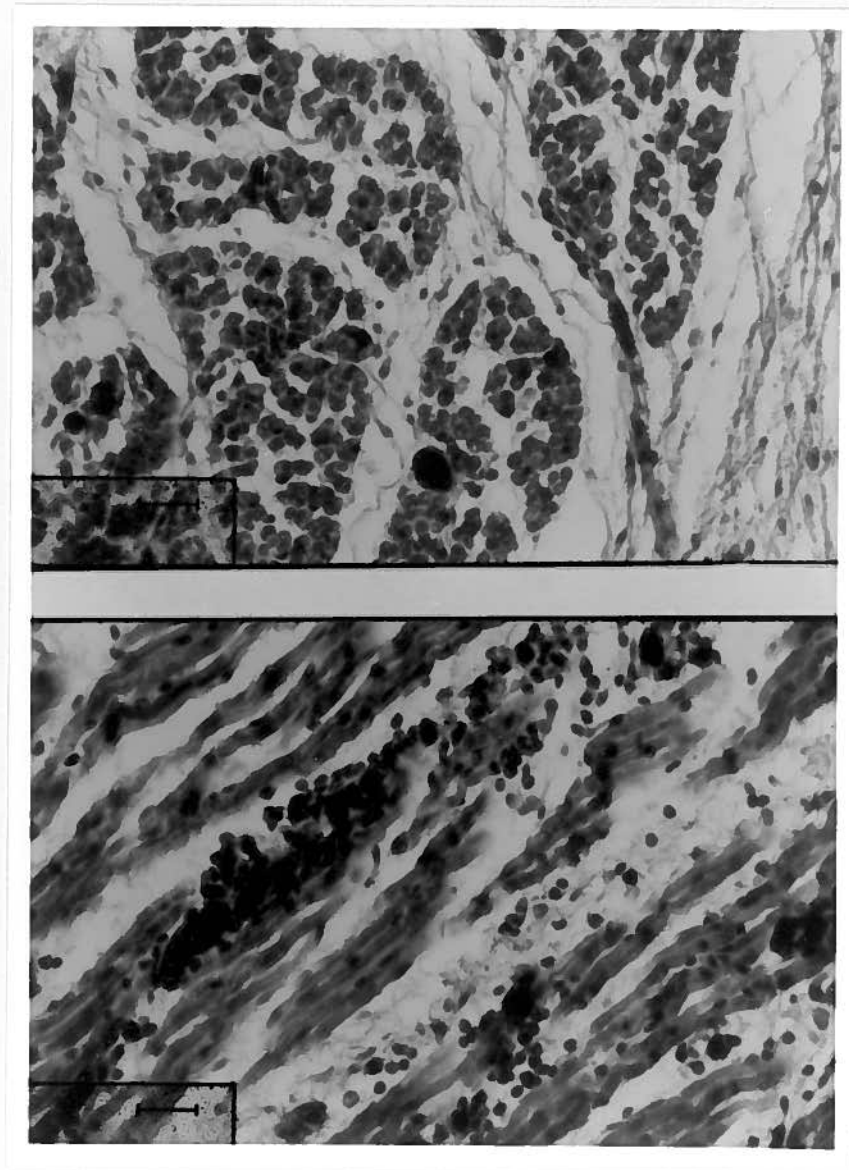
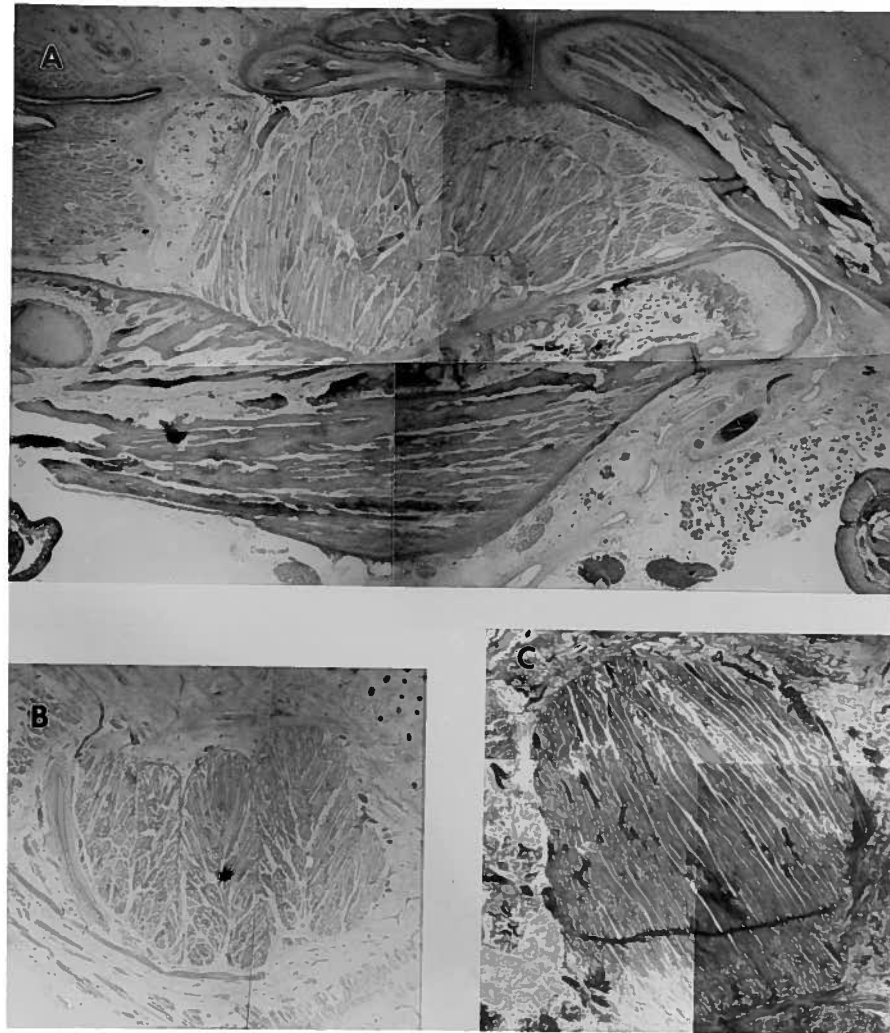


Figure 9 Parasagittal sections from two 18-week human fetuses showing fibre orientation complexity. (A) Medial section through the deep masseter region; (B) and (C) lateral sections through two different the superficial masseters. [A and B are obtained from the same specimen.] Note the different morphological pattern between B and C. Anterior is to the left.



pennation varied in complexity between specimens. Muscle fibres could run parallel in one case, while they formed arcades in similar regions of a different specimen (Figure 9). These differences in appearance could not be accounted for by differences in the planes of section.

Table I shows the muscle subdivisions per section, which were classified according to Matsumoto and Katsura's (1987) method of measuring muscle fibre cross-sectional minimum/maximum ratio (e.g. 0.21-0.30; 0.31-0.40, etc). In this horizontally sectioned specimen, muscle subdivision 1 is situated in the most anterior portion of each muscle slice, while the other subdivisions were progressively assigned towards the posterior muscle portion. Mean and standard deviation values for both angles, that is, fibre direction relative to the mandibular ramus (Angle I) and fibre direction relative to the plane of section (Angle II) were measured with confocal microscopy and are listed under the various muscle-section subdivisions. No consistent number of subdivisions were found when different sections were compared, and muscle fibre angulation did not follow a constant pattern for subsequent sections. Since the methods used were based partly on an already-established approach, and partly upon confocal microscopy which is known to have a higher resolution, these results were unexpected. They could be explained by the fact that either the muscle at this age was poorly organized, consisting of myotubes and/or short immature fibres aligned in various directions, or that there were flaws in the methodology used.

To confirm whether the methodological approach was reliable, the technical error of the measurement (Knapp, 1992) was evaluated by calculating the difference in

Table I Orientation of muscle-fibre subgroups relative to the mandibular ramus on the horizontal plane (Angle I) and relative to the plane of cut (Angle II). Muscle subdivisions per section were defined relative to the minimum/maximum ratio of the muscle fibres. Mean and standard deviation values are expressed in degrees. The values for the technical error of the measurement are shown in brackets where applicable.

ANGLE I

Section #	Muscle Subdivisions				
	1	2	3	4	5
80	22 ± 5	-25 ± 7	44 ± 10		
120	72 ± 13	46 ± 8	54 ± 2	23 ± 2	45 ± 14
160	-42 ± 33	45 ± 5			
190	58 ± 17	64 ± 13	26 ± 11	-31 ± 16	86 ± 17
200	55 ± 14 [1.5]	78 ± 6 [7]	48 ± 6 [11]	80 ± 16 [56]	
240	-23 ± 14	-41 ± 17	76 ± 6	-80 ± 3	55 ± 12
250	25 ± 4 [24]	longitudinal	transversal	57 ± 8 [69]	109 ± 7 [27]

ANGLE II

Section #	Muscle Subdivisions				
	1	2	3	4	5
80	19 ± 2	37 ± 4	58 ± 17		
120	33 ± 7	25 ± 6	29 ± 8	22 ± 3	49 ± 10
160	30 ± 8	61 ± 2			
190	33 ± 15	65 ± 8	-57 ± 20	-20 ± 5	-17 ± 4
200	26 ± 6 [3.5]	42 ± 7 [12]	56 ± 26 [57]	20 ± 48 [20]	
240	-15 ± 5	-21 ± 5	-39 ± 11	-70 ± 34	-27 ± 7
250	-63 ± 20 [24]	longitudinal	transversal	-51 ± 9 [10]	-41 ± 8 [7]

angulation of muscle fibres belonging to the equivalent subdivision in two consecutive sections 100 μm apart, (see Methods). The squared value of the difference was then divided by $2n$ (n is the sample size). The square root of the ratio resulted in the estimate of the technical error of the method. This was estimated for all muscle subdivisions (when applicable) for two pairs of sections (i.e. section 190 and 200; 240 and 250), and it was found that it varied from 1.5 to 69, suggesting that the approach was unreliable at this stage of fibre maturation.

3.1.1.3 Discussion

A primary muscle nerve branch has been defined as one of the branches of a muscle nerve as it enters the muscle at its hilus (English and Weeks, 1984). Glycogen-depletion studies have demonstrated that the primary branches of muscle nerves supply discrete subvolumes of the muscle (English, 1985) in a fascicle-specific pattern (Herring *et al*, 1989). Muscle fibres supplied by primary muscle nerve branches form neuromuscular compartments which have been postulated as the anatomical substrate for motor control (English and Weeks, 1984; English and Letbetter, 1982a). These compartments are known to be established before birth (Donahue and English, 1989). In the present study, two primary nerve branches were found, innervating the deep and superficial masseter. One of the main branches divided into three terminal branches intramuscularly, supplying the anterior deep, and anterior and posterior superficial muscle portions. Therefore, based upon its fetal development, it is possible that the human masseter muscle is divided into at least four neuromuscular compartments, each

of which could theoretically be activated differentially according to need.

Studies of postnatal muscle growth indicate that the weight of the masseter muscle has a positive allometric growth in rats (Hurov *et al*, 1988) and rabbits (Langenbach and Weijs, 1990), while it is isometric in primates (Cachel, 1984). Since masseter growth in rabbits is characterized by an overall increase of muscle length which is much smaller than the increase in muscle weight, the predominant muscle growth likely occurs by the increase of tendinous material and by the increase in muscle protein (actin and myosin). Increase in tendinous material was confirmed in the rat masseter muscle, in which tendon cross-sectional areas showed an isometric growth pattern relative to that of the muscle weight (Hurov *et al*, 1988). While the relative size of the surface area of the aponeurosis in the pig masseter remained unchanged during growth, the thickness increased disproportionately faster than the muscle mass growth (Richter and Herring, 1993). Since no clearly defined internal aponeuroses were found in the 20-week-old human masseter muscles, it seems that the connective tissue pattern present at this fetal stage evolves into tendinous sheets, in a similar fashion to the development of the muscle in rats and pigs. The formation of a dense collagen network would be stimulated by functional demand, increasing predominantly in thickness rather than in length. This proposition is partially supported by Schumacher's (1962) findings on the masseter muscles from the neonatal to old age. In contrast, the medial pterygoid has well developed internal tendinous sheets, at least as early as at 17 weeks fetal stage. This finding is in accordance with Schumacher's (1962) report that at birth this muscle presents the most complex system of aponeuroses of all masticatory muscles.

Based on the literature and on the present findings, it appears that in humans muscle fibres are arranged in a complex, pennate pattern from the early fetal stages, and that they may differ between individuals. Muscle fibres seem to be initially attached at both ends to loose connective tissue; this tissue presumably differentiates into tendinous layers as functional demands increase. Since it is known that in pigs the proportion of muscle length and aponeurosis length remains constant during growth (Richter and Herring, 1993), and that changes in masseter orientation in rabbits (Langenbach, 1992) and humans (Burdi and Spyropoulos, 1978) are minimal, it is further suggested that the arrangement of muscle fibre in the human masseter does not change drastically with growth. Thus, despite some changes in the pennation angles with the increase in muscle fibre length and jaw growth, the pennation pattern probably remains fairly unchanged throughout life.

In animal experiments, muscle fibres belonging to a single motor unit (MU) can be quite easily followed through several histological sections if the fibres have been glycogen-depleted by stimulating their functionally-isolated axons (Herring *et al*, 1989; Ounjian *et al*, 1991). Two-dimensional outlines of the MU fibres can then be digitized at a number of levels along the longitudinal axis of the muscle for subsequent 3D reconstruction (Ounjian *et al*, 1991). The glycogen-depletion method cannot, however, be employed in human experimentation, and it is clear that alternative techniques of following nerve pathways and their associated muscle fibres in human material have not yet been fully developed. Furthermore, as shown in this study, it is difficult to follow MU fibre contours in different histological sections of fetal human muscles, and very difficult

to classify their orientation reliably and objectively. The muscle fibres are relatively immature, compounding the problem of analysis, and serial cross-sections of the whole fetal muscle offer a poor basis for muscle reconstruction, because the microtome knife frequently intersects the fibres at odd angles, and fibre architecture can be extremely difficult to interpret. It is possible that careful dissection of fetal muscles may prove to be a better way to indicate fibre placement and muscle subdivisions.

In summary, the identification of peripheral nerve pathways and of complex muscle fibre arrangements suggest that the fetal masseter muscle can be divided into four neuromuscular compartments, which present fairly developed pennation patterns. Since major structural boundaries were not found in early fetal life, and the measurement of fibre angulation proved difficult, it was not possible to compare regional organization of the human fetus directly with the adult counterpart.

3.1.2 Adult Masseter Anatomy

The performance of a muscle is determined by its internal architecture (Edgerton, Roy and Apor, 1986), which is characterized by fibre length and angle and the division of muscle mass by tendons (Bodine *et al*, 1982). Muscle fibre and tendon lengths should be considered separately, in a functioning muscle, for tendon compliance can affect internal mechanics and force output (Zajac, 1989).

Although the architectural design and the biomechanical properties of a skeletal muscle are highly correlated with its physiological characteristics, little is known about how the architectural features affect the physiological properties of motor units (Edgerton *et al*, 1987; Gans, 1982; Muhl, 1982; Ounjian *et al*, 1991). Numerous reports on muscle fibre lengths indicate that these may vary among and within muscles, within as well as across species (Huber, 1916; Sacks and Roy, 1982; Loeb *et al*, 1987; Schumacher, 1961c; Van Eijden and Raadsheer, 1992). Huber (1916) reported that in the rabbit gastrocnemius, a pennate muscle, the majority of the muscle fibres extended between tendinous insertions, on both sides. In contrast, it has been demonstrated that in long, parallel-fibred muscles, fibres may terminate in the middle of a fascicle and may taper at either their proximal or distal end, or both (Loeb *et al*, 1987). Ounjian *et al* (1991) also showed that within the cat tibialis anterior muscle, single MUs of the fast type did not extend the entire distance between musculotendinous planes of origin and insertion. Their fibres had slightly different lengths, although in some cases where fibres shared an origin at one end of a fascicle, they tended to be of similar lengths. Intrafascicular fibre endings were tapered. In contrast, fibres from slow units extended

the entire distance between both musculotendinous planes, and terminated at the tendon as blunt endings (Ounjian *et al*, 1991). Yet another type of ending (partial tapering) was found for slow units in the tibialis anterior, indicating another mode for MU force relay to tendon (Eldred *et al*, 1993). Finally, despite the fact that fibres had varied lengths, subgroups of fibres of a unit tended to end at about the same level whether the endings were midfascicular or at a tendon (Ounjian *et al*, 1991). Although muscle fibre architecture is important in the transfer of muscle force to tendon and bone, especially in a powerful muscle like the masseter, the fibre orientation, MU architecture and location relative to tendons and type of fibre endings are not known for this muscle.

The aims of the present study were to determine the muscles' innervation pattern relative to muscle portions, whether the muscle could be classified into anatomically discrete compartments on which physiological analyses could be performed in living subjects, and to identify the type of fibre endings present in the human masseter. These data could also be used in the future as an anatomical basis for modelling contraction mechanics.

3.1.2.1 Materials and Methods

3.1.2.1.1 Gross Anatomical Dissection

Seven adult masseter muscles (six male and one female) were obtained from the Department of Anatomy, University of British Columbia. Most of the muscles were obtained from partially-dentate cadavers. One muscle was obtained from a fully-dentate, while another from an edentulous cadaver. Ages varied between 50 and 70 years. The

muscles were excised from their attachments by separating the periosteum from the mandibular ramus and by cutting through the origin tendons at the zygoma and through the interdigitating fibres of the temporalis. All muscles were fixed by immersion in 10% formalin. Three specimens were then placed in 20% nitric acid for 24 hours and washed in tap water before dissection. The nitric acid treatment was used to facilitate dissection by loosening connective tissues and staining muscle fibres yellow while leaving nerves and connective tissues white. From an additional masseter, small blocks of muscle were excised from representative areas, and embedded in paraffin. Twenty μm transverse sections were sampled serially every 100 μm through the entire length of each block. Alternate sections were stained for muscle fibres and connective tissue with haematoxylin and eosin and picosirius collagen stain. The histological sections were used as an aid for the conventional dissection in order to clarify regional muscle structure. An additional three muscles were washed in running tap water for 24 hours and embedded in alginate. The muscles were oriented within the alginate block, so that the superior and anterior borders were roughly aligned with the edges of the block. This block was then sliced into 3 mm sections in the frontal plane. Photographs were taken from the dissections and from each muscle slice.

3.1.2.1.2 Chemical Dissection

To evaluate muscle fibre endings, one adult human masseter muscle was chemically dissected with 30% nitric acid, which was gradually replaced with glycerol (Loeb and Gans, 1986). The masseter was dissected out with the origins and insertions

of all fibres included, it was placed into the centre of a dish, and then 30% nitric acid in saline poured over it. The dish was covered and the specimen was initially checked every hour for the first 8 hours. Thereafter the specimen was checked every 12 hours. After 4 days, fibres began to fall apart of their own accord, separating into sets of fascicles that were easily moved about. The nitric acid was then replaced with a 50% glycerin/30% nitric acid mixture for two days, to slow down the digestion. After this, the mixture was finally replaced by 50% glycerin in water, to arrest further breakdown. Once the major portions had been separated, fascicles were gently transferred into a Petri dish, and portions of the specimen were removed until only a few undamaged fibres remained. This process was checked under a dissecting microscope. Selected, undamaged fibres were then gently floated onto a standard microscope slide onto which a coverslip was mounted with glycerin and sealed with nail polish. The fibres were then examined under a light microscope.

3.1.2.2 Results

In one specimen, the nerve trunk divided into three primary branches, while in the other specimens it divided into only two. The superior and middle primary branches in the first specimen, and the superior primary branch in the other specimens, innervated the deep masseter region. They entered the muscle through the mandibular notch just anterior to the condylar region, and extended anteriorly running parallel to the zygomatic arch, just medially to Aponeurosis IV. The inferior primary branch in all specimens appeared to be the continuation of the main trunk and started fairly parallel

to the other primary branches. It initially divided into two intramuscular branches, the offspring continuing to run parallel to the two primary branches, innervating the deep masseter muscle. The main trunk continued its path laterally, running obliquely from the supero-posterior corner towards the anterior, superficial masseter. Several smaller intramuscular branches spread off the main trunk, innervating the intermediate masseter. The nerve distribution supplied the more lateral regions by running along the aponeuroses and crossing through the muscular layers. The "Nervenknotten" described by Lau (1972) was observed in all specimens.

Most muscle fibres and aponeuroses extended into a thick periosteum layer which covered a wide area of the mandibular angle and ramus. This periosteum layer extended approximately three-quarters of the length and three-quarters of the height of the muscle, measured from the mandibular angle. Other muscle fibres and tendons inserted into a thinner periosteum layer (anterior region), and directly into bone (deep posterior masseter portion).

The findings from the dissections performed for this thesis (Figure 10) are consistent with Gaspard *et al's* (1973) and Baron and Debussy's (1979) reports. The masseter was found to be formed by four incompletely separate muscle sheets: masseter superficialis (lamina prima and lamina secunda), masseter intermedius and masseter profundus (pars anterior and pars posterior). The simple, parallel-fibred anterior portion described by Ebert (1939) was also identified in all specimens, being most prominent in the edentulous individual.

It has been observed in this study, as well as by others, that the deepest part

Figure 10 Masseter-muscle dissection showing the superficial and intermediate muscle layers. Parasagittal view of the lateral side of a left adult human masseter. Anterior is to the left, and superior is to the top. The lamina prima (left) and lamina secunda (right) of the Masseter superficialis are shown reflected. The Masseter intermedius is shown to the right, below the lamina secunda of the Masseter superficialis.

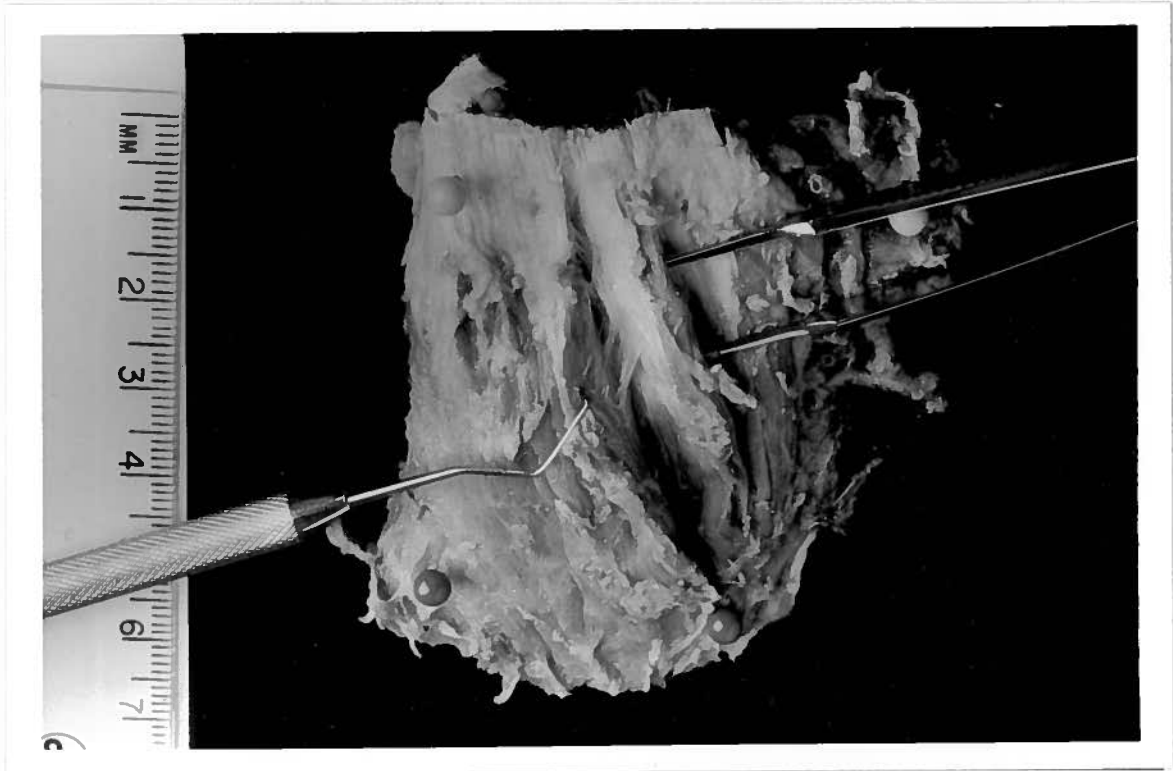


Figure 11 Masseter-muscle dissection showing its layered arrangement posteriorly and the ascending attachment sites of muscle fibres as the layers become deeper. Parasagittal view of the lateral side of a left adult human masseter. Anterior is to the left and superior is to the top. Masseter superficialis and Masseter intermedius are reflected. Masseter profundus fibres are seen at the top right, including their aponeurotic attachment, which is somewhat like that of the temporalis muscle.



of the masseter is often inseparably fused with the most superficial fibres of the temporal muscle. This group of muscle fibres has been previously described as a separate muscle unit, termed the zygomaticomandibular muscle. It has been reported that identifying the distinction of this muscle unit in many animals is easier than in man (Sicher, 1960; Lau, 1972). In the present study, a separate portion of the deep masseter, situated medially to Aponeurosis V (Figure 12), originated from the lower border and medial surface of the zygomatic arch and inserted into the basal part of the coronoid process and the adjacent parts of the mandibular ramus. This deep masseter portion could also be described as the zygomaticomandibular muscle. The fibres of both the deep masseter and of the zygomaticomandibular muscle were arranged in a fan shape, resembling the temporalis when viewed laterally (Figure 11).

Initially, an attempt was made to identify the intramuscular aponeuroses according to Schumacher's (1961c) classification. Although the masseters all had numerous aponeuroses, they were not continuous through the muscles, and did not divide the muscles into distinct compartments. Interleaving aponeuroses started either at the muscle origin or at the insertion, extending into the muscle mass downwards or upwards. In most cases, during dissection, aponeuroses started near bone with thick cross-sectional area, tapering towards the other extremity. Numerous differences were found between subjects in terms of quantity, thickness and distribution of aponeuroses, and it was not possible to identify Schumacher's aponeuroses in all specimens. The masseter from the female edentulous cadaver had the smallest cross-sectional size of the sample, and the smallest number of aponeuroses, which were thicker than these of other

Figure 12 Masseter-muscle cross-section showing its internal aponeuroses. The level of cross-section is approximately halfway through the muscle in both figures. (a) In this specimen, five aponeuroses similar to those described by Schumacher (1961c) can be depicted. Here, superficial (between Ap I and II), intermediate (between Ap II and III), and deep masseters can be seen. Vascularization and innervation are parallel to the medial aspect of Aponeurosis IV (*). (b) In this specimen, aponeuroses II, IV and V can be seen. Additional tendon sheets are also present. In both figures, the main aponeuroses are indicated by numbers. Medial is to the left.

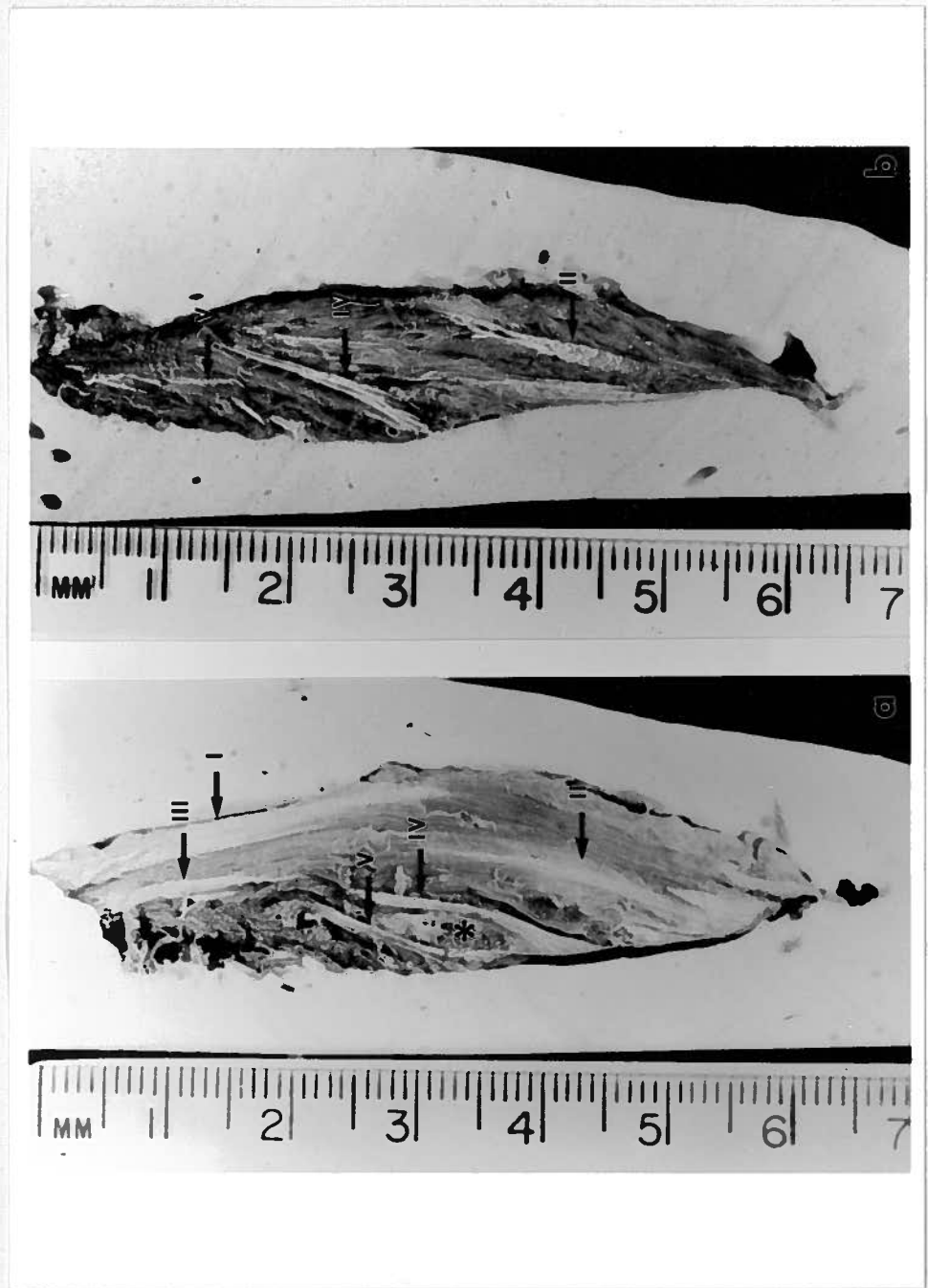
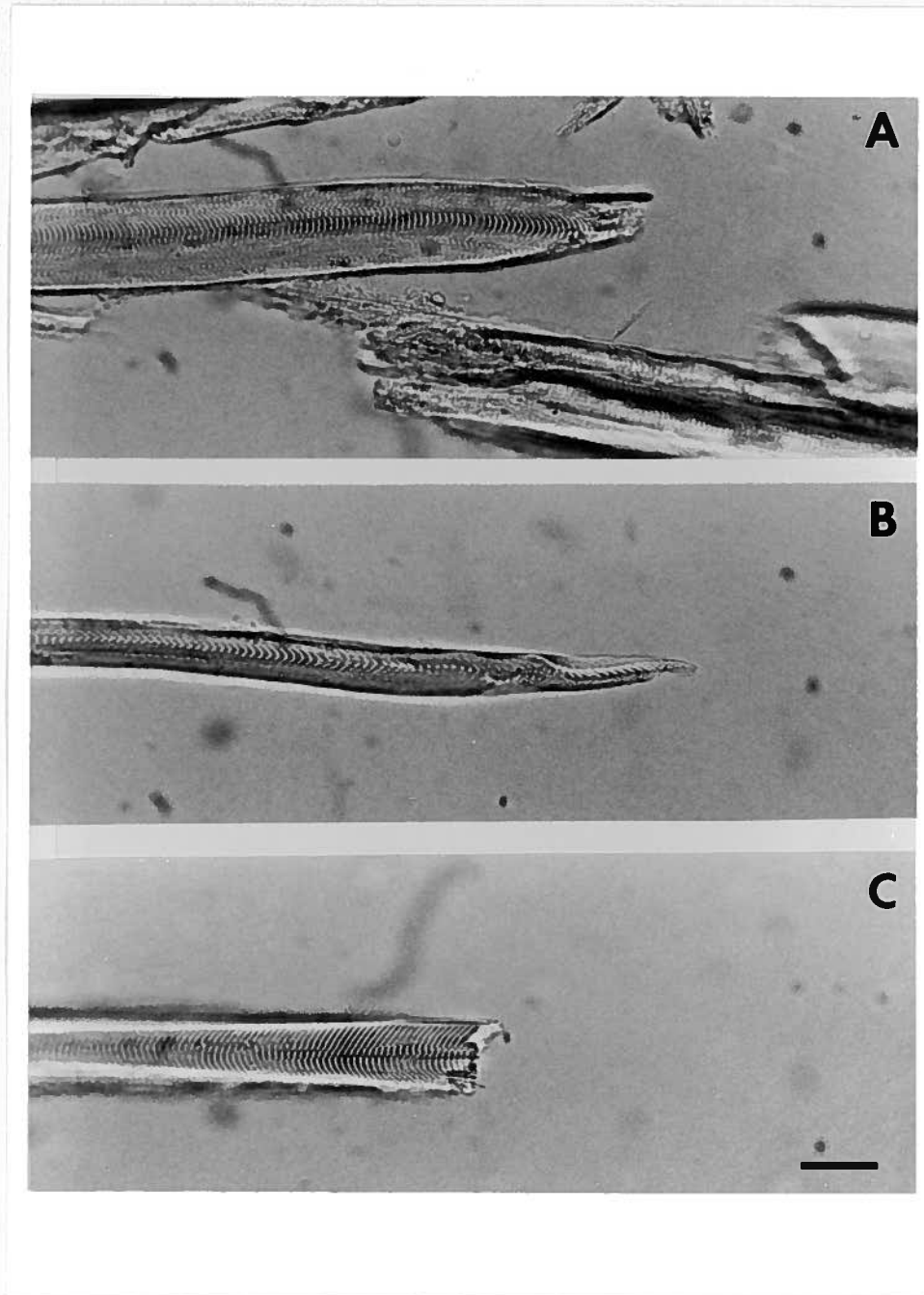


Figure 13 Masseter-muscle fibre endings. Both, blunt (A) and partial tapered (B) fibre endings are found. A group of fibres were intentionally damaged, and their ends shown for comparison (C). The calibration bar represents 25 μm .



specimens from partially dentate individuals. In this case, only three aponeuroses were identified, namely Aponeurosis I, II and III. One partially-dentate individual had the largest number of aponeuroses. These were thin, and in many cases would disappear in the next 3 mm slice, or after two slices. Basically, this muscle possessed all five aponeuroses as described by Schumacher (1961c), and a few other tendon sheets situated predominantly in the posterior two thirds of the muscle (Figure 12B). The largest muscle of all was found in the fully dentate individual. This muscle showed the thickest aponeuroses, and was almost identical to Schumacher's (1961c) description. The only exception was Aponeurosis V, which inserted into the mandibular ramus, rather than originating from the zygomatic arch. No additional aponeurosis was found in this case (Figure 12A). The aponeuroses were qualitatively longer in the superficial muscle region than in the deep muscle region. A slight antero-posterior size difference was also noted. In some cases, the aponeuroses presented an antero-posterior "zig-zagged" edge within the muscle mass. This pattern was predominantly found in Aponeurosis I, and has been illustrated before by Ebert (1939), Schumacher (1961c) and Lam (1991). Although they were not measured, relative tendon length to muscle size did not seem to vary between individual specimens.

Chemical dissection revealed that fibres from the masseter muscle had two types of endings, blunt and partially tapered (Figure 13). The fibres could be divided into three groups. In one group fibres had both ends tapered, in another, fibres had blunt ends at both poles, and in the third group, fibres were blunt at one end, and tapered at the other end.

The present description of the masseteric nerve agrees with that illustrated by Lau (1972) and Xiguang *et al* (1986). The general pattern of the first primary branch supplying the deep masseter and the main branch innervating the entire muscle while running in a lateral, forwards and downwards direction is similar to that found in pig (Herring *et al*, 1989), sheep and dog (Lau, 1972). As previously discussed by Herring *et al* (1989), although the nerve trunks may be common to several muscles, and in this case may be common to several muscle anatomical compartments, individual axons are probably not, innervating motor unit territories which may be confined to tendinous boundaries.

The results of the present study, showing that tendon lengths vary with muscle region, are in accordance with Van Eijden and Raadsheer's (1992) report. The inter-individual variation in number of aponeuroses might be explained by differences in functional demands on the masseter between different individuals. This notion would be consistent with Schumacher's (1962) report on increased internal tendinous complexity with increased functional demand. This individual variance in aponeurotic design may also account for the lack of consistency in the description of the masseter in the literature.

Eldred *et al* (1993) observed that even fibres which had blunt ends at both poles were not strictly uniform in calibre throughout their lengths, and had their shape described as a tenuous spindle with truncated ends. In these MUs, the mean values for areas along the poles were 16% smaller than areas along the central segment. The

functional consequence of this finding is that along an individual fibre of varying calibre the production of force should be greatest where the cross-sectional area is maximal, and along a tapering termination the capacity for production of force decreases until it is finally lost at the fibre tip. A concomitant premise is that along each of these fibres, the force production is larger at the fibre's wide segment than at its thinner endings. The excess of force produced at the wide segment must therefore be transmitted to the fibre surroundings, otherwise it may stretch the tapered fibre terminals (Street, 1983).

During the contraction of a MU, the produced force is transferred to the tendon via the connective tissue (Schmalbruch, 1974; Swatland, 1975; Rowe, 1981) and neighbouring, passive muscle fibres (Demiéville and Partridge, 1980). If we assume that in the masseter muscle all muscle fibres end on tendons, most of the unit's force should be directly transferred to the tendon via the specialized surface features (Tidball and Daniel, 1986) of the blunt type of ending. However, in the case of fibres with the partially tapered ends, force should be still relayed via the surrounding tissue (Street, 1983). In the masseter, where both blunt and partially tapered fibres apparently project onto a tendinous insertion, both types of force transfer, direct and indirect, can be expected.

In an analysis of three-dimensional tendon plane orientation, Lam *et al* (1991) suggested that muscle fibre orientations between tendon planes may not have equal pennation angles at their proximal and distal ends, since the tendons are not parallel to each other. It is possible that the partially tapered muscle fibre endings observed in the present study play a role in compensating for the non-parallelism between aponeuroses,

ensuring that the angle of pennation is equivalent on either side of the fibre, and/or on either side of the resultant force applied to the tendon.

3.1.3 Morphological Reconstruction in Living Subjects

To study muscle biomechanics and function relative to internal architecture, anatomical and physiological investigations of muscle structures should ideally be performed in living subjects. This obviates sole reliance on gross anatomical and histological studies of cadaver material, which may have different dispositions of internal structures. In addition, non-invasive methods enable the evaluation of muscle mechanics during natural tasks. For this purpose, Magnetic Resonance (MR) imaging offers a significant tool in the visualization of internal muscle architecture, and efforts were made to determine whether it could be applied to the human masseter.

3.1.3.1 Methods

3.1.3.1.1 Magnetic-Resonance Imaging

Because of the importance of MR imaging in living-subject studies, a brief review on the technique will be presented. Proton MR imaging is a noninvasive resonance measurement technique, which utilizes a high strength static magnetic field, pulsed radiowaves, and switched gradient magnetic fields to generate images of both hard and soft tissues (Lam *et al*, 1989). This imaging system probes the nuclear magnetic properties of the hydrogen atom to generate the MR signal (Selzer, 1986; Nixon, 1987). A hydrogen atom has a nucleus consisting of one proton. This has a minuscule amount of intrinsic magnetism, which is proportional to another intrinsic entity of elementary particles called "spin". In this case, spin does not represent a physical rotation, but it means that a proton may be likened to a tiny bar magnet (Young, 1984). These magnetic

dipoles are randomly oriented within a tissue (Harms and Kramer, 1985). Magnets used in MR imaging possess stationary magnetic field strengths from 0.15-2.25 Tesla. When a tissue is placed into one of these magnetic fields, the randomly oriented magnetic dipoles respond to the force of the field by trying to orient parallel to it. Under these conditions, each proton begins to precess at the same rate, but at a random phase. Together these individual magnetic moments create a net magnetic moment, pointing along the axis of the external magnetic field. Once this is achieved, a radiofrequency (rf) field is activated, acting in a direction perpendicular to the main field. When the rf is in phase with the precessing spins, it induces rotation of the net magnetic moment by 90 degrees. This transition into transverse magnetization is called resonance, where the nuclear magnets tend to spin inphase with one another. Without the creation of resonance there would be no detectable signal to create an image. After the rf field has been turned off, the magnetic moment can induce voltage in the receiver coil, situated in the transverse plane. Once the rf field is removed the transverse magnetization gradually decays; the resulting loss of signal intensity as a function of time is known as a "free induction decay" (FID). The processes involved with signal loss are generally called "relaxation". Spin-lattice relaxation or " T_1 " refers to the return of the nuclear magnets to their original alignment with the static magnetic field. Spin-spin relaxation or " T_2 " refers to the loss of the inphase spinning of the nuclear magnets (Harms and Kramer, 1985; Fullerton, 1982). Because the initial signal amplitude is proportional to the transverse magnetization, which is itself proportional to the number of nuclei excited in a particular voxel of tissue, differences in hydrogen density become discernible in the

MR image.

Contrast between areas of differing proton density can be enhanced if a MR scan is biased towards T_1 or T_2 characteristics. This effect can be achieved by using rf pulse sequences such as "inversion recovery" or "spin-echo"; the latter being the most versatile sequence producing an image biased towards T_2 (Thornton, 1987). The contrast in a spin-echo image is determined by the relative decay of MR signal emitted from different tissues at the time of sampling. Signal intensities of musculoskeletal tissues at a given time vary considerably, being of highest intensity for muscle and medullary bone, of intermediate intensity for fat and of low intensity for blood vessels, tendons and cortical bone (Thornton, 1987; Berquest, 1987; Scholz *et al*, 1989).

Materials which contain significant amounts of iron, cobalt, nickel, and chromium may exhibit ferromagnetic properties due to their high magnetic permeabilities (Lam *et al*, 1989). These materials are commonly used in metallic implants, dental fillings, appliances and surgical prosthesis, producing artifacts on MR images, which usually appear as low-intensity, black regions (Lam *et al*, 1989; Fache *et al*, 1987; Seltzer and Wang, 1987).

3.1.3.1.2 Imaging

Six subjects were imaged; muscles and internal tendons were traced, digitized and reconstructed according to the method described below. The muscle reconstructions were then used for subsequent studies in this thesis.

To permit merging the MR images of the orofacial region with other datasets

in future experiments, an L-shaped fiducial reference grid, consisting of thermoplastic material filled with 5 mM copper sulphate at each corner, was attached rigidly to a plastic eyeglass frame, so that it was positioned just posterior to the right masseter muscle. This concentration of aqueous copper-sulphate solution was chosen from an imaging trial, in which several different concentrations were tested. The 5 mM solution yielded the best image of the reference grid, that is it yielded high-intensity signal with the smallest amount of "blur". Silicone liners were used to custom-fit the frame to the nose and ears for stability and reproducibility of placement (Figure 14). Each subject wore this device during imaging, and later, during EMG recording sessions.

A MR 1.5-Tesla system (Signa; General Electric Medical Systems, Milwaukee, WI) was used to obtain conventional T2-weighted images of the muscle. Each subject was asked to lie in a supine position on the unit's gantry bed, and a 5 cm surface receiving-coil was placed over the grid and the masseter muscle. The subject's head was then aligned with the Frankfort horizontal plane at a right angle to the gantry's bed with the aid of a laser-light referencing system. During imaging, each subject was asked to bite lightly at the intercuspal position, while a series of contiguous, 3 mm sections in the coronal plane were obtained. This plane was chosen according to previous recommendations by Lam (1991) and Koolstra *et al* (1990).

Signal averaging hinders tendon plane visualization in the sagittal plane, and does not permit the differentiation between the deep masseter and the temporalis muscle in the axial plane. Therefore, coronal sectioning was carried out to resolve the internal architecture of the masseter muscle optimally. To obtain the best MR signal

Figure 14 Reference L-shaped grid attached to a plastic eyeglass frame. Right lateral view showing the eyeglass lenses (right) and the silicone-lined earpieces (left). The reference grid is built of thermoplastic material and filled with copper-sulphate, which resonates during imaging.

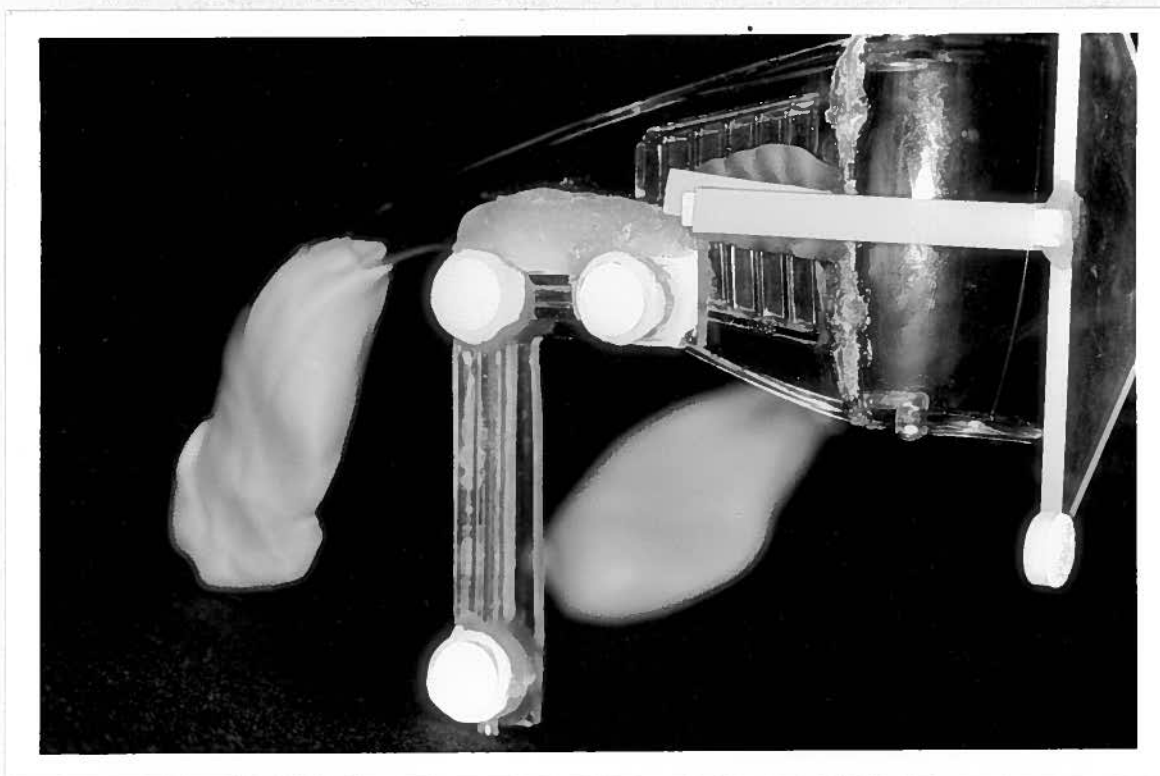
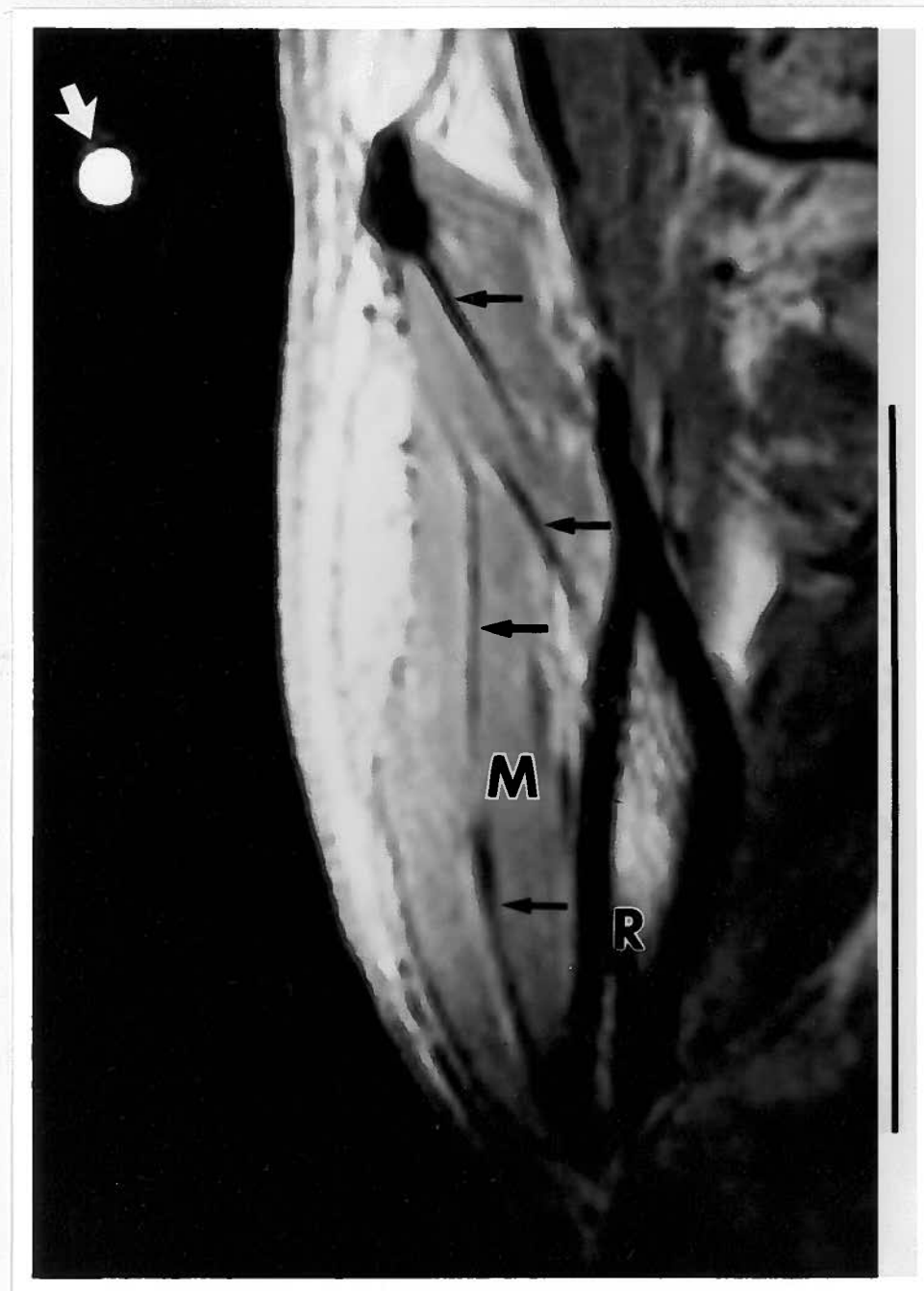


Figure 15 Coronal spin-echo Magnetic Resonance image. The masseter muscle (M), internal tendons (thin arrows), mandibular ramus (R), and reference marker (arrow) are depicted. The image was obtained with a 5 cm surface coil (TR: 2000 ms, TE: 25 ms). The scale bar is 5 cm.



contrast between muscle and tendon, without the interference of adipose tissue, spin-echo sequences with a repetition time (TR) of 2000 ms and with echo times (TE) of 25 and 80 ms were used. Two excitations were utilized with a 12 cm field of view and a 256 x 192 matrix (Figure 15). With this pulse sequence, the external reference marker produced the highest intensity signal, seen in the image as white structures. In contrast, cortical bone and the internal tendons produced low-intensity signals, appearing black against the intermediate light-grey image of the muscular tissue. Although higher tissue differentiation is expected from longer TE images, higher contrast between tissue was obtained from the 25 ms TE, which produced a more anatomically defined image. Hard copies of all coronal sections were then produced, and a 5 cm scale bar was included on each image.

3.1.3.1.3 Reconstruction

Sectional outlines of the muscle, its internal tendons, bone and the copper sulphate markers were traced onto acetate overlays and digitized, (Model HP9874A Digitizer and HP350 computer, Hewlett Packard Canada, Vancouver, B.C.). Calibration bars on each section were used to scale and reference these sections to a common origin. Profile coordinates at every 0.3 mm were stored, and each section was assigned its appropriate coronal depth (Hannam and Wood, 1989). From the individual profile data, 50 equally-spaced points were selected to describe the boundary of each tissue outline. This number of points has previously been found to be adequate in rendering satisfactory representation of complex shapes such as intramuscular tendon contours (Lam, 1991).

Three-dimensional reconstruction of the data was then carried out with an engineering solid-object modelling package (I-DEAS version 6.0, SDRC, Milford, Ohio) and a graphics workstation (HP Turbo SRX, Hewlett-Packard, Canada). Each group of 50 profile coordinates was transformed into closed third-order splines⁶, forming a "wireframe"⁷ (Figure 16). Several contiguous planar outlines were then "skinned" by the connection between corresponding points of adjacent profiles to create 3D surfaces or solids (Figure 17). Since the equally-spaced 50 points in each profile had been arranged in a clock-wise sequence starting from the top-most position, minimal surface distortion (twist) was observed in the final objects. Accentuated twists were only found in the condylar region of the mandibular reconstruction of two subjects, due to the sudden change in shape from one contiguous profile to the next. Similar distortions have been also previously reported in solid models constructed using different approaches (Sinclair *et al*, 1989; Koriath, 1992). To improve one of the reconstructions of the mandible, which presented accentuated twists in the condylar area, an alternative approach was tried. This method treated the outlines' raw data as a matrix, consisting of 50 points per outline times the number of contiguous sections of the given tissue. The matrix was then fitted with a surface skin by interpolation (Koriath, 1992). However this did not render better results; on the contrary, the twists were even more accentuated. Since little or no twist was present at the areas of interest; that is, at the tendons and at the area of attachment

⁶ A *spline* is a closed or open curve whose shape is defined by a higher order polynomial.

⁷ A *wireframe* is a collection of points and curves.

Figure 16 Antero-lateral view of the sectional outlines of a reference grid and right masseter muscle with its internal tendons. Masseter muscle contours are plotted with stippled lines. These outlines are closed third-order splines, which form a "wireframe" in I-DEASTM.

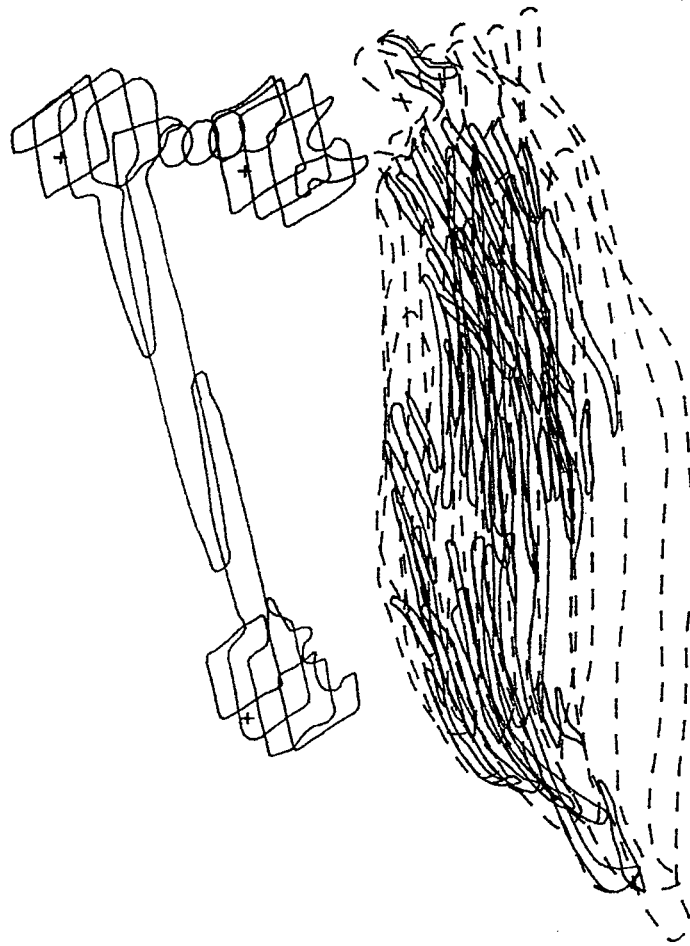


Figure 17 Three-dimensional reconstruction of the reference grid, masseter muscle and internal tendons. Antero-lateral view of the solid objects in I-DEAS.



of the masseter into the mandibular ramus no further alternative reconstruction technique was pursued.

3.1.3.1.4 Error of Method

To determine geometrical differences between the original structures and the reconstructed model, three linear dimensions, and an angle of the "true" L-shaped reference grid, were compared against their modelled counterparts. Spatial coordinates of the centroids on the lateral surfaces of the fiducial-grid-corner cylinders were recorded with an optical three-dimensional measuring system (Reflex Metrograph, HF Ross, Salisbury, Wilts, U.K.). Linear distances between the centroids and the angle between two of these lines were then calculated (Figure 18A). In addition, the thickness of the cylinders were measured with calipers (Figure 18B). Distances were then compared against measurements taken from homologous locations on the grid's reconstructed model. Measurements were made for each custom L-shaped fiducial grid. The linear and angular values for both "true" and "MR-derived reconstructions" of the grids are shown in Table II. The error is defined as the length or angular difference, expressed as a percentage of the true value. From this table, most cases had estimated errors below 3%, with the exception of one case along the vertical bar (7.3%), and two cases along the horizontal bar (19.6% and 3.5%).

3.1.3.2 Results

In all subjects, a high-intensity signal (white) was observed running diagonally

Figure 18 Linear and angular measures used to compare the reconstructed against the true reference grid. (A) Sagittal view of two linear distances measured between the centroids on the lateral surface of the L-shaped grid cylinders, representing the horizontal (H) and the vertical (V) bar dimensions. Between the intersecting lines the angle (α) is calculated. (B) represents the thickness of the corner cylinder, which is measured along the medio-lateral direction.

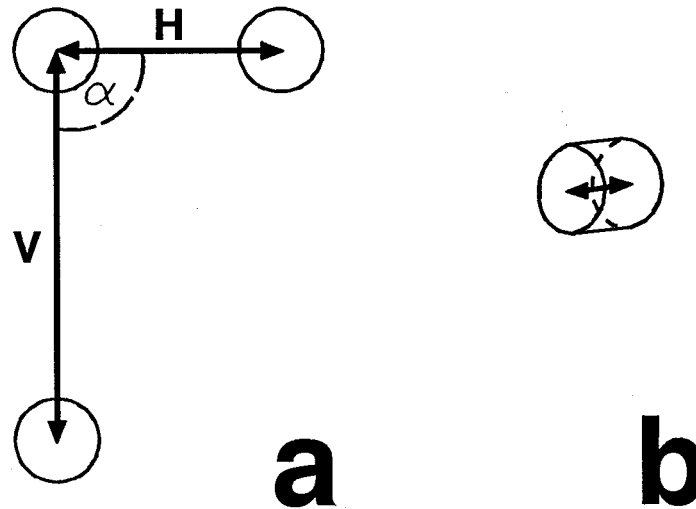


Table II Linear and angular dimensions measured from homologous points on the reference grids of six subjects and their reconstructed counterparts. The distances are given in millimetres and the angles in degrees. Differences are expressed in percentages relative to the true grids. Representation of the linear and angular measures are shown in Figure 18.

SUBJECTS	ANGLE			VERTICAL BAR			HORIZONTAL BAR			THICKNESS		
	True	MRI	Error	True	MRI	Error	True	MRI	Error	True	MRI	Error
	[Metro Data]	[I-DEAS]	[%]	[Metro Data]	[I-DEAS]	[%]	[Metro Data]	[I-DEAS]	[%]	[Calipers]	[I-DEAS]	[%]
1	90.35	91.57	-1.35	54.37	53.15	2.24	24.30	24.37	-0.29	7.65	7.76	-1.44
2	91.01	90.00	1.11	59.08	54.78	7.28	22.91	18.43	19.55	6.55	6.42	1.98
3	90.15	90.22	-0.07	54.74	53.75	1.81	23.03	22.69	1.50	6.90	7.00	-1.45
4	87.36	87.35	0.01	52.61	52.04	1.08	25.87	24.96	3.52	7.90	7.89	0.13
5	88.58	88.55	0.04	56.11	54.63	2.63	26.06	25.52	2.06	6.90	7.06	-2.32
6	90.50	90.26	0.26	54.70	54.36	0.61	23.23	23.16	0.32	8.05	8.01	0.50

from the lateral aspect of the muscle to the mandibular ramus, separating the superficial portion from the deep posterior portion of the masseter (Figure 19A). This is the image of the connective-tissue layer, which surrounds nerves and blood vessels (seen on the image slice, close to the mandibular ramus, as small dark structures) which is present inside the posterior muscle "pocket", frequently cited in anatomical reports of the masseter. The delineation between the masseter and temporal muscles was arbitrary in all cases, since no space nor tendon exists between these two muscles. In reality they form an anatomic unit (Sicher, 1960).

In all imaged individuals, the five aponeuroses described by Schumacher (1961c) were present. In three individuals, the muscle structure was simple, with only a few small additional tendinous layers. Examples of two individuals are shown in Figure 15 and Figure 19A. However, in the remainder of the subjects, internal architecture was more complex. In these, the basic five aponeuroses could be depicted, but several additional layers added to the internal architectural complexity. Figure 19B shows an MR coronal section in one of these individuals, while Figure 20 shows the entire muscle reconstruction of another subject.

Similar to the findings from the muscle dissections, aponeuroses thickness and number varied according to subject. The three subjects having the largest masseter cross-sectional sizes presented an increased number of aponeuroses, which were thicker than in other individuals. The subject with the narrowest muscle, however, had slightly thicker aponeuroses than another subject with also small muscle cross-sectional size.

Figure 19 MR coronal sections of two subjects showing differences in internal muscle architecture. (a) This image slice shows the connective tissue separating the superficial and deep masseter portions, blood vessels (*), and Aponeuroses I, II, III, IV and V. (b) Image from a second subject with a more complex internal muscle architecture. Aponeuroses I, II, III, IV and V are seen with additional others. Calibration bars represent 5 cm. (R) Mandibular ramus; (Z) Zygomatic arch.

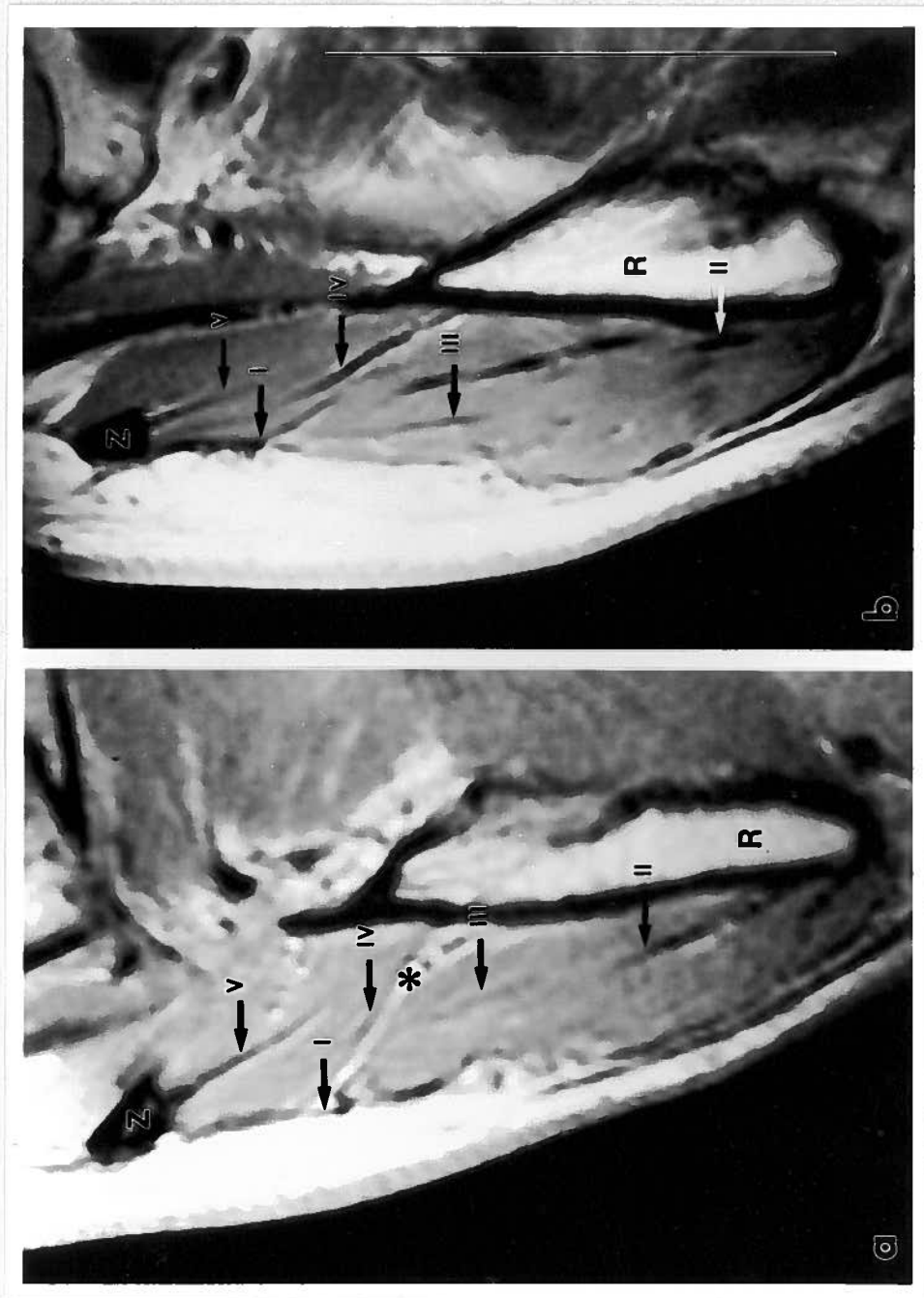
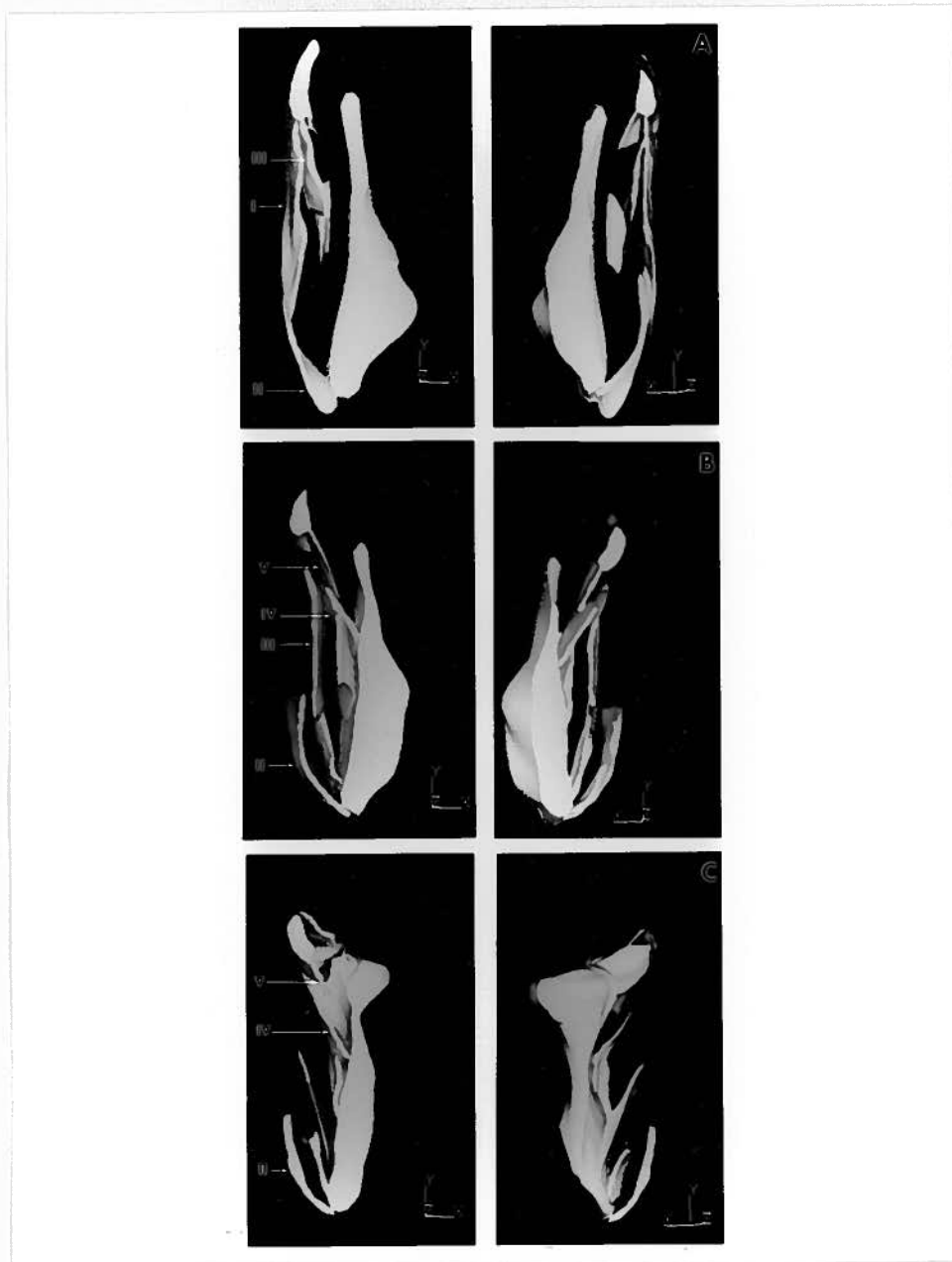


Figure 20 Computer reconstruction of interstitial tissues in the right masseter muscle, viewed frontally. Frontal MR-images were digitized, stacked, and "skinned" to represent solid objects. Frontal software cuts divided the muscle and mandibular ramus and zygoma in three segments, shown here separately. (A) Anterior; (B) central; and (C) posterior segments. On the left side of each picture, the tissues are seen from the front, while on the right side they are seen from the back. As in the anatomical specimen (Figure 12B), the classical aponeuroses [labelled according to Schumacher's (1961c) definition] can be seen together with additional ones. In (A), Aponeuroses I and II appear to be continuous when seen from the front. Note that when seen from the back, it is clear that they are separate structures.



3.1.3.3 Discussion

In vitro studies have shown that T2 relaxation times depend on collagen fibres orientation in the magnetic field. When the fibres are oriented at 0°, 90° and 180° in relation to the constant magnetic induction field, the echo nearly disappears, primarily due to the structural anisotropy of collagen (Berendsen, 1962; Migchelsen and Berendsen, 1973). An increase in tendinous signal intensity is however observed at the "magic angle" of 55° (Fullerton *et al*, 1985). In the masseter muscle, the tendons are aligned along the long axis of the body, thus are oriented at small angles relative to the magnet. Fullerton *et al* (1985) argued that in such cases, tendons would be rarely observed in clinical MR imaging, on the one hand because the "magic angle" would be seldom encountered, and on the other, due to the relative long TEs which are used clinically. Therefore, there should be a lack of echogeneity from the tendons, which should appear black in all spin-echo images, yielding high contrast against the proton-rich background of the surrounding muscle. More recent reports have shown however, that although angle-dependent signal intensity should be most prominent at short TEs of 10 msec, it is still sometimes observed at TEs of 25 msec. This is in part due to the improved signal-to-noise ratio of stronger (1.5T) magnets, partly because parts of tendons may be oriented at 55° in relation to the magnetic field and partly because of the blending of the tendon with muscle fibres at the musculotendinous insertion (Erickson *et al*, 1991). It is assumed that the "magic angle" effect is quite rare during imaging of the masseter, due to the 15° angulation (Schumacher, 1961c) of the internal tendons relative to the medial plane. Furthermore, the internal anatomy of our

reconstructions is consistent with anatomical reports.

In the creation of a MR image, the magnetic field is mapped in such a manner that it becomes position-dependent. Signals from contiguous, predefined tissue volumes (voxels) are detected simultaneously, and then converted into a two-dimensional (pixel) image. Since spatial accuracy is essential for most imaging purposes, MR systems have been previously examined for inherent non-linearities caused by inhomogeneities in the static magnetic and radiofrequency fields. It has been established that in a large volume at the center of the magnet coil, no distortions occur, producing linear images (Stewart, 1987). In addition, the use of a fixed receiver coil, previously used in the orofacial region (Seltzer and Wang, 1987; van Spronsen *et al*, 1987; Hannam and Wood, 1989; Koolstra *et al*, 1990; Schellhas, 1989) produces signals of even distribution throughout an entire slice. The signal-to-noise ratio of these signals are further improved with a surface coil and the number of repetitive signal acquisitions. The latter, the spatial resolution along one axis of the specimen, and the TR determine the length of imaging time (Lam, 1991). Since it is required that subjects remain motionless during the imaging sessions to avoid movement artifacts, the need to keep imaging time short becomes evident. Therefore, the image matrix was reduced to 256 x 192 and only two signal averages were chosen throughout image acquisition. The pixel dimension of the images obtained can be deduced by dividing the field of view by the number of pixels in the matrix (Price *et al*, 1992). In the present study, the resolution of the plane of image was 0.5 x 0.6 mm, with a slice thickness of 3 mm. While it is possible to obtain images with thinner slices, disadvantages include reduction in the signal-to-noise ratio, and requirement of greater

acquisition time.

Three-dimensional morphological reconstructions are commonly achieved from two-dimensional planar images (Hannam and Wood, 1989; Koolstra *et al*, 1990; Lam, 1991; Koriath, 1992). The fidelity of these reconstructions depend on minimum head movement during image acquisition, slice thickness and tracing accuracy (Koolstra *et al*, 1990). Minor head movements from breathing and swallowing are common during the image acquisition process, and they may distort or blur tissue boundaries (Lam, 1991). Slice thickness may affect the images similarly, especially where the amount of a given tissue for signal averaging is minimal; for example at musculotendinous junctions. Additionally, slice thickness is of great concern when a surface skin between sectional, planar contours is to be produced. Here, the problem of approximating surfaces between successive slice contours is greatly reduced when their separation approaches zero, particularly when adjacent contours are irregular or dissimilar in shape (Sinclair *et al*, 1989). Lam (1991) expressed some concern regarding the surface generation between adjacent tendon contours obtained from 5 mm MR images. Surface formation from thinner, 3 mm MR slices have, however, greatly improved. As previously discussed by Koolstra *et al* (1990) and Lam (1991), muscle outlines were not always clearly distinguishable. The interdigitation of fibres from the deep masseter and temporalis muscles does not permit the boundary between these two muscles to be sharply defined. In addition, a low-intensity signal depicting the masseter fascia, which is tightly attached to the superficial tendon of the masseter (Sicher, 1960), made the distinction in certain regions between fascia and the superficial-masseter Aponeurosis I difficult.

It is also possible to generate volumetric images. That is, from such a data set, transverse, sagittal and coronal images across any point within the imaged volume can be displayed (Chakeres *et al*, 1992). Usually the MR information is directly transferred into computer-reconstruction programs avoiding the need for tracing and digitizing. Software can be written to assign boundaries automatically between tissues, by detecting differences in the grey-shade scale. This approach has produced quite successful results in the reconstruction of bony structures. However, in the case of the masseteric region, operator interpretation of the obtained image is still necessary, since muscle tissue boundaries are less well-defined.

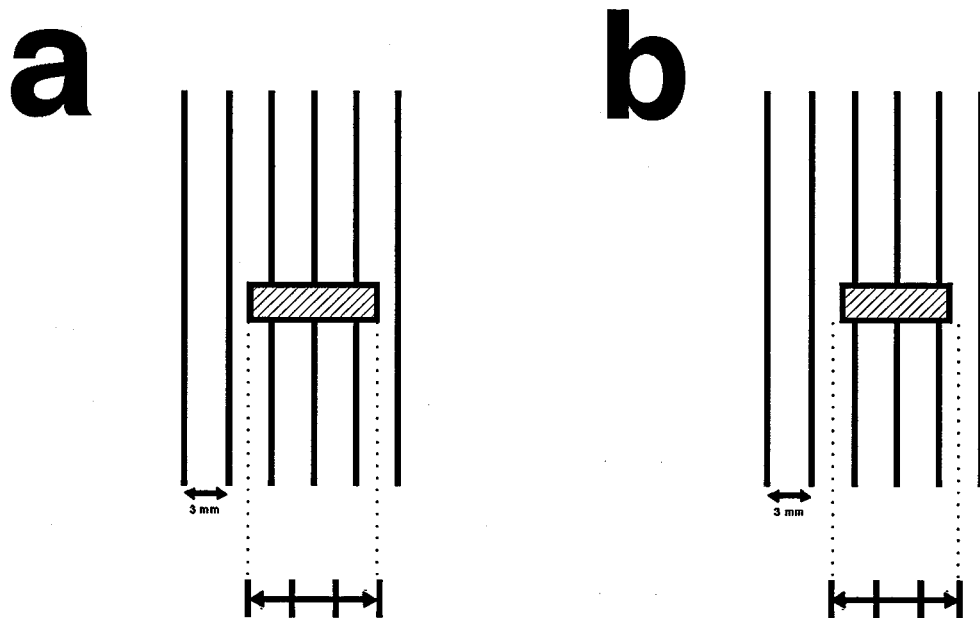
The quantification of the error between a complex three-dimensional form and its reconstruction is not trivial, since it is difficult to obtain homologous points in both structures. The criterion for homology is that points must be consistently and reliably located with a measurable degree of accuracy on both considered forms (Lele and Richtsmeier, 1991). Form of an object involves both size and shape. Landmark and outline data are two types of data commonly used to compare distinct forms (Lele, 1991). With this purpose, several different morphometric analyses have been developed, which involve rigorous statistical methodologies and which are based on the description of outline or landmark data in two- (Rohlf and Bookstein, 1990) or three dimensions (Lele, 1991; Lele and Richtsmeier, 1991).

Since landmarks on the biological object were non-existent and a series of measurements made up of external dimensions such as maximum breadth and length of the structure proved to be difficult, homologous points on the external reference grid in

this study, were used to assess the error between the "true" object and its reconstruction. In this assessment, any errors which occurred during all steps of the methodology were combined.

The relatively large errors found in the horizontal-bar reconstructions, that is in the antero-posterior direction, may be explained as the result of a combination of two factors: the image-plane of section, and the averaging process by which the MR slices were obtained. Theoretically, a well-defined line should be pictured at the interface of the high-intensity signal from the copper-sulphate-filled cylinder against the dark background. This should be observed medio-laterally with a resolution of 0.5 mm (as discussed above) and supero-inferiorly with a resolution of 0.6 mm, in the coronal plane of section. This decreased resolution in the supero-inferior axis explains the larger errors found in this dimension. In the antero-posterior direction, each slice is the result of signal averages through 3 mm of tissue. Let us assume that the copper-sulphate-filled cylinder ended half-way through the 3 mm depth on both sides. In this case, only half of the signal intensity (intermediate grey) would be depicted in the first and last image sections in which the copper sulphate appears, when compared against an image section right across the grid. Despite this apparent loss in signal, the true length of the cylinder is detected. In another example, consider that the cylinder ended at only one quarter of the 3 mm depth, on both sides. Here, the detected signal is even weaker on both extremes, but the sections are still included in the reconstruction. In this situation, an antero-posterior "shift" of the boundaries occurs (Figure 21). Here, the potential for overestimating the sizes of structures is apparent, again explaining the results.

Figure 21 Schematic illustration of MR data acquisition. Examples of data acquisition from copper-sulphate-filled horizontal bars placed at different positions relative to the planes of section. Contiguous 3 mm MR slices are taken in the coronal plane (illustrated by solid lines). Stippled lines represent averaged data, which form the image. Short vertical lines (below) represent traced contours of the imaged bars viewed from the sagittal aspect. Arrows indicate the reconstructed length of the imaged object. In (a) the horizontal bar ends half way through each 3 mm averaged section. The true dimension of the bar is reproduced from the images. In (b) the horizontal bar ends at both sides, at one quarter of the thickness of the respective slices. Error of overestimating the bar's length in this case is possible.



In a study of the validation of three-dimensional reconstructions of the knee anatomy, measurements between external reference markers and biological loci were taken from milled slices of a cadaveric specimen, and from the MR-based reconstructions. It was found that the accuracies of intermarker distances and of the knee-condylar dimensional measurements on the reconstructions averaged 97.5% and 93% of the milled slices, respectively (Smith *et al*, 1989). Therefore, it is expected that the error of the reconstruction of the masseter muscle is also slightly larger than the error of the reconstruction of the fiducial grid. This assumption is based on the fact that signal average processes are more complex on the biological tissue than on the copper-sulphate - air interface, contributing to interpretation errors during tracing.

Though it may be desirable to validate muscle reconstruction in living individuals against their true muscle morphology, it is impractical. Validation could not be carried out in the present study, and it was assumed that the muscle reconstructions accurately represented true individual muscle morphology in accordance with previous MR studies of the masseter in fresh human cadavers (Lam, 1991) and rabbits (Ralph *et al*, 1991), and the knowledge obtained from direct muscle dissections. Similar to the findings in one dissected cadaver (Figure 12B), all reconstructed muscles had the basic aponeuroses described by Schumacher (1961c) as well as other smaller tendinous sheets. The internal architecture varied among individuals. Some muscles had more internal tendinous sheets than others, perhaps due to the different functional strategies used by each individual. The findings suggest that it is important to study morphology and function in the same individual, and to compare the results only against matched

anatomical and physiological data obtained similarly from other subjects.

3.2 Movement of Masseter Insertions at different Jaw Positions

A complex system of internal aponeurotic septa separating groups of muscle fibres with varying lines of action is common in many mammalian jaw muscles (Hiiemae and Houston, 1971; Herring *et al*, 1979; Weijs and Dantuma, 1981; English, 1985; Weijs *et al*, 1987). The human masseter is typical, since it contains wide anteroposterior aponeurotic septa which extend into the muscle mass alternately from the zygomatic arch and from the lateral surface of the mandible (Ebert, 1939; Schumacher, 1961c; Lam *et al*, 1991). Interleaving aponeuroses enable muscle fibres to be packed into a multipennate arrangement (Gans and Bock, 1965; Herring, 1980; Wineski and Gans, 1984), allowing the fibres to attach either to an insertion tendon or directly to periosteum. As a result, masseter origin and insertion sites cover broad areas of the zygomatic arch and mandibular ramus (Schumacher, 1961c; Gaspard, 1987).

To characterize the functional capabilities of a muscle, knowledge of its three-dimensional (3D) architectural design is necessary (Gans and deVree, 1987). Within the human masseter, 3D orientation of muscle fibres and tendons have been estimated (Baron and Debussy, 1979; Lam *et al*, 1991), as well as the size and placement of sarcomeres (Van Eijden and Raadsheer, 1992). Sarcomere length vary in separate muscle regions and are known to be affected differentially with computer simulations of simplified, arbitrary jaw displacements (Van Eijden and Raadsheer, 1992). Since the displacement of the adult human jaw is complex, involving a combination of rotations and translations about instantaneous centres of rotation (Grant, 1973; Brown, 1975), it is expected that the movement of the masseter insertion area is of equal complexity. It

is also expected that insertion site displacements vary according to region.

The aims of the present study were to determine how masseter muscle insertions are affected three-dimensionally by jaw movements, and to relate the findings to regional muscle function.

3.2.1 Simulated Function in Dry Skulls

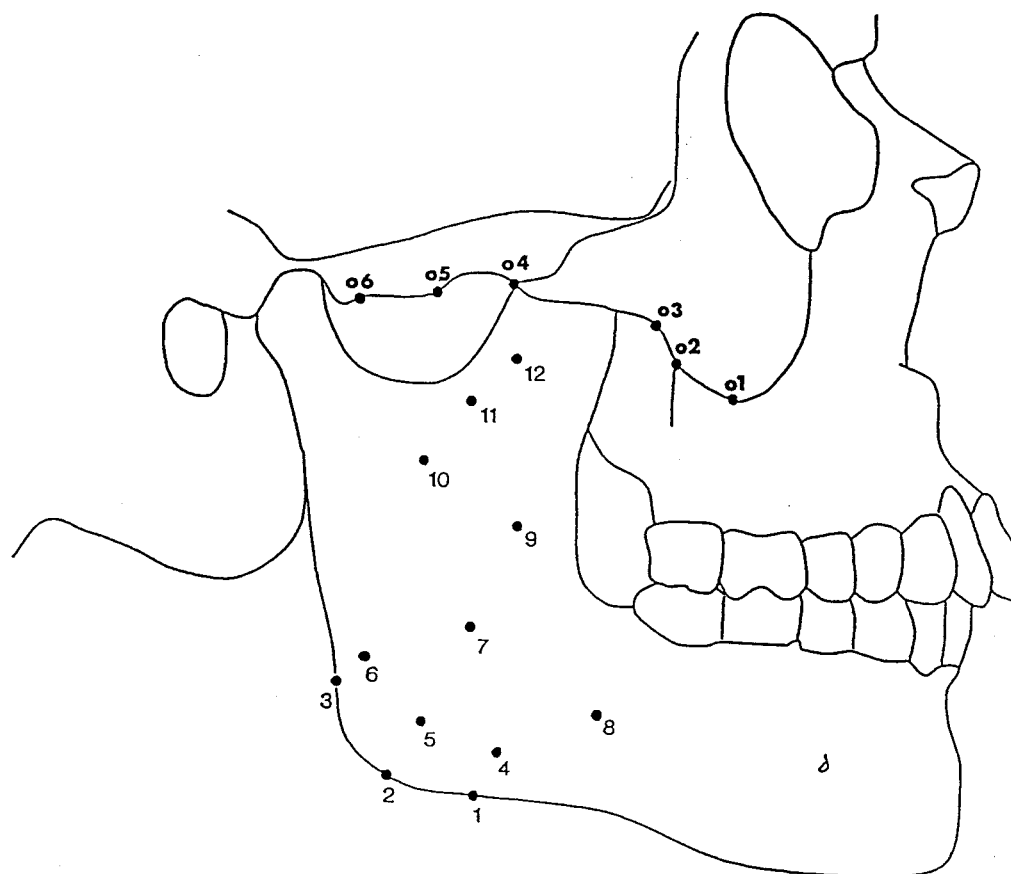
3.2.1.1 Methods

Fourteen adult human East Indian skulls (seven female and seven male), from the collection of the Department of Anatomy at the University of British Columbia were used. To describe the sample, and to reveal any differences in the craniofacial dimensions, a lateral cephalometric radiograph was taken of each specimen at a tube-film distance of 165 cm and an object-film distance of 14 cm. Thirteen selected conventional linear and angular cephalometric variables were then measured according to criteria and definitions described by Lowe (1980). In conformity with his abbreviations, the anterior position of the maxilla was defined by the angle SNA, occlusal plane by the angle SN-OP, palatal plane by the lines ANS-PNS and SN, maxillary length by the linear distance from the midcondylar point to the inferior point of the anterior maxilla, anterior position of the mandible by the angle SNB, mandibular plane angle by the lower border of the mandible and the line SN, gonial angle by the lower border of the mandible and the posterior border of the ramus, mandibular length by the linear distance from the midcondylar point to pogonion, relative mandibular prognathism by the angle ANB, maxillary-mandibular length difference calculated from

the mandibular length minus the maxillary length, upper face height by the linear distance between nasion and a projection from ANS along a perpendicular to the nasion-menton line, and the same projection of ANS, and ramus height by the distance from the superior condylar point to gonion measured perpendicular to the line SN. In addition, transverse distances were measured directly on the skull by means of calipers. Bizygomatic width was measured as the largest distance between the zygomatic arches; intercondylar width as the distance between the lateral poles of the condyles; and bigonial width as the distance between the gonions.

The masseter muscle attachment sites were represented by six origin and twelve insertion points. The locations of these followed osteological criteria reported previously (Baron and Debussy, 1979; Gaspard, 1987), but were also guided by known muscle morphology (Ebert, 1939; Schumacher, 1961c; Gaspard, 1987). The location of these attachment points (Figure 22) are as follows: *o1*) is the most anterior point of the masseteric attachment, and occupies the top of an eminence immediately anterior to the zygomaticomaxillary suture; *o2*) is the top of an eminence which is the Paturet's sub-jugal eminence to which Zlabek's tendon attaches (Paturet, 1951); *o3*) is situated at the junction of the anterior and middle thirds of the inferior border of the zygomatic bone, and is located at the top of an eminence posteriorly to the Paturet's sub-jugal eminence; *o4*) is at the small bony spur just anterior to the squamoso-zygomatic suture at the posterior border of the superficial masseter; *o5*) is at the geometric centre of the longitudinal fossa of the inferior border of the zygomatic process of the squama; *o6*) is the most posterior point of the masseteric attachment, just anterior to the articular

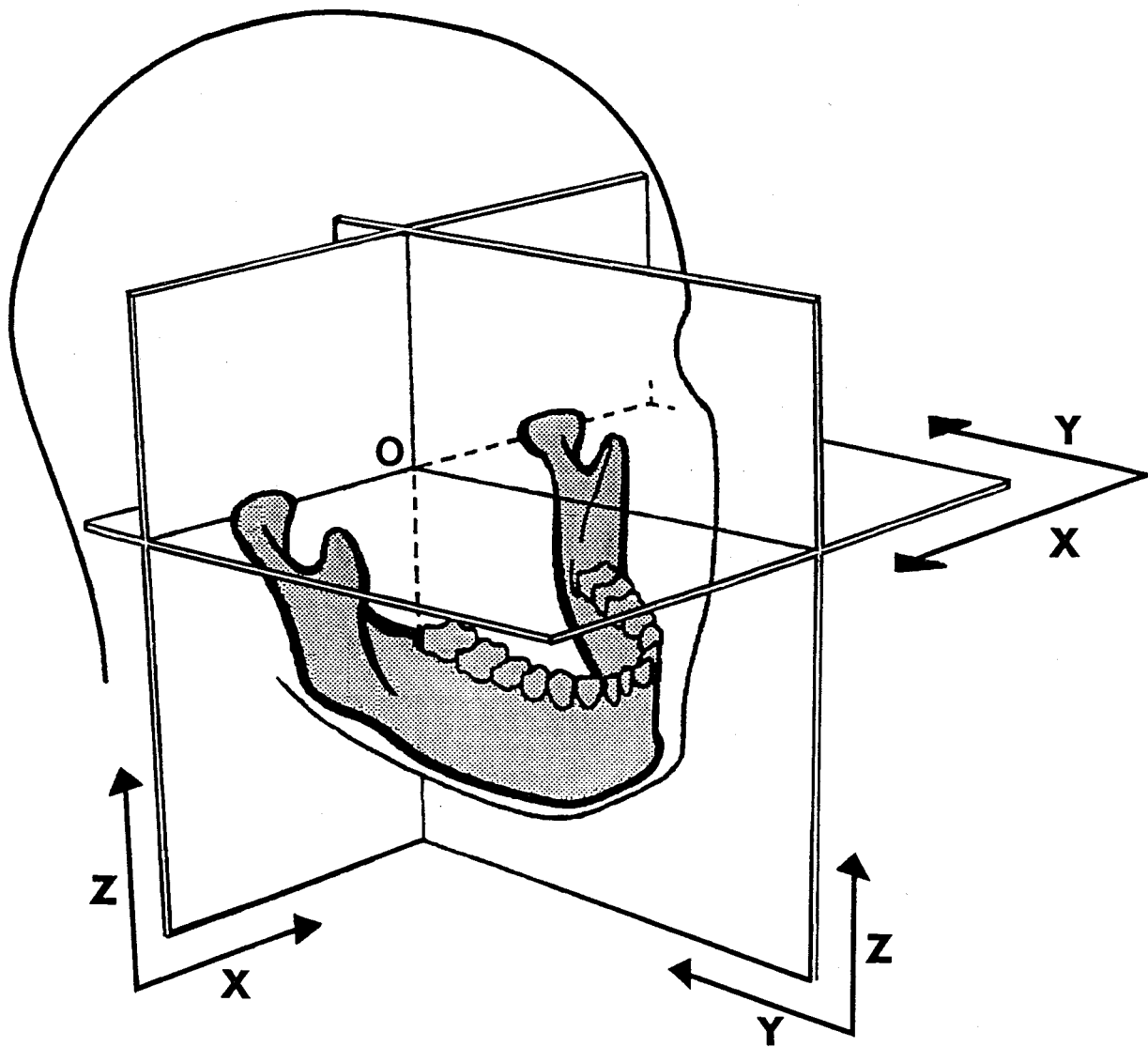
Figure 22 Masseter attachment points represented by six origin and twelve insertion points. Points 1-8 represent the superficial masseter attachment area, and points 9-12 the deep masseter insertion. Similarly, o1-o4 represent superficial, and o4-o6 deep-masseter origins.



eminence; (1) is at the pre-angular bony projection which corresponds to the anterior limit of Cihak and Vlcek's masseteric tuberosity (1962); (2) is at the centre of the angular bony projection; (3) is at the post-angular bony projection which corresponds to the posterior limit of Cihak and Vlcek's masseteric tuberosity (1962); (4) is the anterior border of the attachment of "Sehnenspiegel 2"; (5) is the middle part of the attachment of "Sehnenspiegel 2"; (6) is the posterior part of the attachment of "Sehnenspiegel 2"; (7) is at the geometric centre of a rhomboidal area corresponding to Weidenreich's masseteric fossa; (8) is the most anterior point of the crista to which the anterior border of the superficial masseter attaches; (9) is at the Lenhossék's crista ectocondyloidea; (10) is at the tuberculum musculi zygomaticomandibularis, which is the inferior limit of the fovea musculi zygomaticomandibularis, situated between the coronoid process and the condylar process (Cihak and Vlcek's, 1962); (11) is at the geometric centre of the "V" shaped crista musculi zygomaticomandibularis; (12) is at the geometric centre of a pentagon centred on the body of the coronoid process. Insertion sites 1-3, 4-6, 7-8, 9-10 and 11-12 were selected to represent the muscle layers I and II of the superficial, III of the intermediate, and IV and V of the deep masseter, respectively.

For each skull, all anatomical reference landmarks and attachment points were digitized three-dimensionally at different jaw positions with an optical system (Reflex Metrograph, HF Ross, England) capable of 0.1 mm resolution (Takada *et al*, 1983). The metrograph coordinates of the muscle attachment sites were transformed into skull-referenced coordinates by translating the metrograph origin to a skull origin, then by mathematically rotating the data. The skull's references were defined as follows: origin:

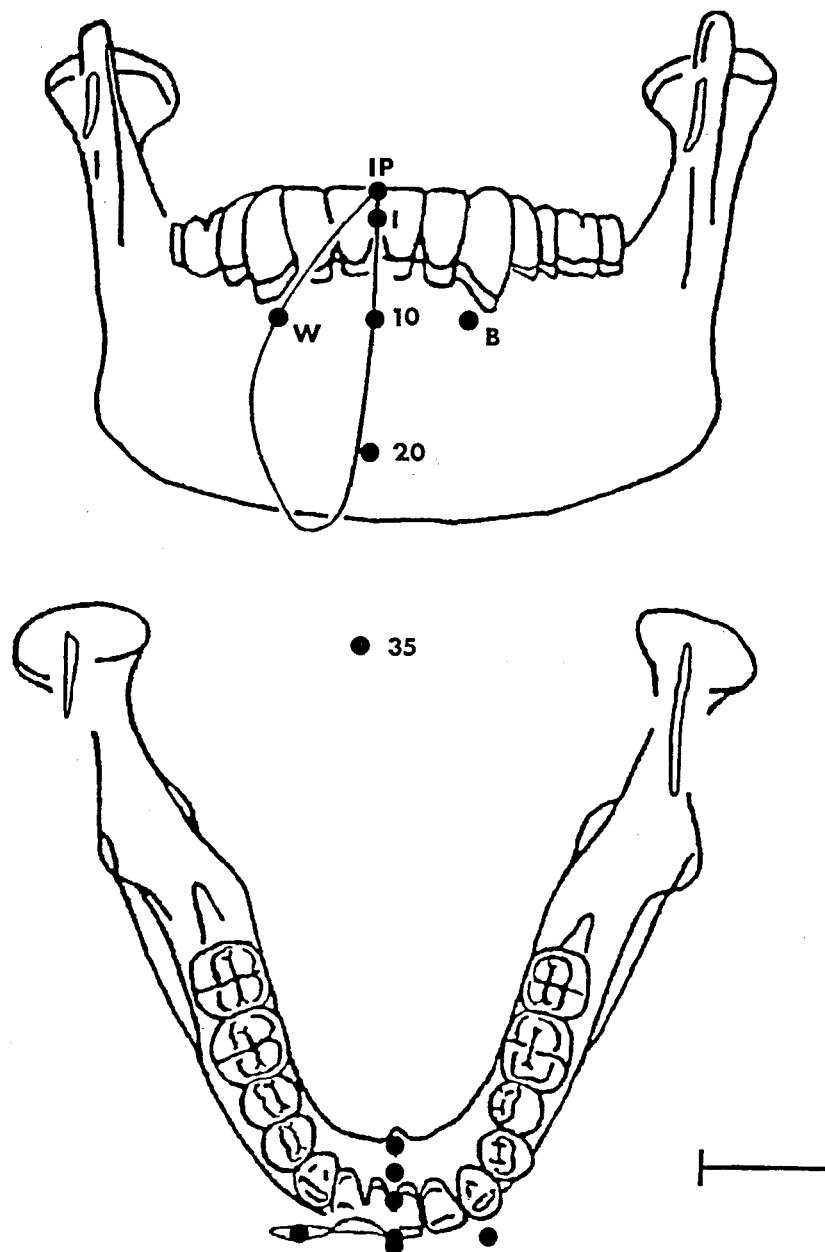
Figure 23 Orientation of the three planes of the skull's coordinate system. Origin (O); Frankfort horizontal (XY); mid-sagittal (YZ); and coronal (XZ) planes.



a point halfway between the centre of the two external auditory meati; yz plane: the mid-sagittal plane; xz plane: the coronal plane; and xy plane: a plane parallel to the Frankfort horizontal plane (Figure 23).

In order to analyze the degree of movement that the muscle attachments underwent during simulated functional jaw movements, seven representative jaw positions were selected (Figure 24). They included the intercuspal position (IP), midline jaw openings at three gapes (10, 20 and 35 mm measured between the incisors), simulated masticatory positions on the working and balancing sides (10 mm incisal opening with 5 mm incisal lateral deviation to the respective side), and incisal edge-to-edge contact. With the exception of the intercuspal position, these positions were maintained by silicon bite blocks placed between the incisors and molars. The simulated masticatory positions were obtained by moving the mandibles from the maximum intercuspation to the various functional jaw positions, which were determined by dental and condylar guidance coupled with the predetermined jaw openings, based on previous reports on chewing cycles by Lundeen and Gibbs (1982) and Hannam *et al* (1977). The average thicknesses of the articular soft tissue layers and disks were simulated with wax inserts according to data published by Hansson *et al* (1977) and Christiansen *et al* (1987). Vertical lines drawn on the upper and lower arches at the central incisors, and at the temporomandibular joints with the teeth in maximal intercuspation were used as a guide to measure the amount of distance moved by the mandible. All vertical, transverse and antero-posterior distances were measured on or between these lines with calipers to confirm the deviation of the mandible from the intercuspal position.

Figure 24 Illustration of the seven representative jaw positions. Frontal and horizontal views of the mandible indicating the five midline gapes, and two simulated masticatory positions. Positions include intercuspal position (IP); incisal contact (I); three different jaw openings at (10); (20); and (35) mm; working (W); and balancing sides (B). Mandibular movements were controlled by dental- and articular-guidance paths. Calibration bar represents 10 mm.



The orthogonal distances that the muscle attachment landmarks moved were then calculated from the coordinates of each landmark for each jaw position, and expressed relative to their common coordinates at maximal tooth intercuspation.

To test for any statistically significant difference between female and male cephalometric measures, and to express the differences between the various distances travelled by each insertion at different jaw positions, multiple one-way analysis of variance followed by Tukey tests were used. In the latter case, jaw position was considered as the factor and the three orthogonal directions (x, y, z distances) as dependent variables. Here, the tests were not used to determine whether the insertion points had significantly different movement patterns with varying jaw positions on individual specimens, because all insertion points were located on the same rigid bone (mandible), and their displacements were dependent and predictably different from each other. However, the differences between the various distances travelled by each insertion at different jaw positions were used as descriptors of sample behaviour, since this was not readily predictable given the anatomical variations in the specimens.

3.2.1.2 Results

3.2.1.2.1 Cephalometric Analysis of the Skull Sample

Comparisons between female and male skeletal data showed that sex differences were negligible for most measures ($p > 0.05$). Exceptions were the mandibular and maxillary length, upper face height and bigonial width, which had slightly larger values in males (see Table III). Because the variation in craniofacial dimensions were

Table III Facial dimensions of female and male skulls. Means and standard deviations are expressed in mm¹.

Measure ²	Female (f)	Male(m)	f/m * 100%
Length			
Mandibular	111.5 ± 4.7	119.1 ± 5.2	93.6
Maxillary	89.2 ± 3.4	93.0 ± 3.3	95.9
Difference btw Mand. and Max.	22.2 ± 3.1	26.1 ± 3.1	85.1
Height			
Face (total)	116.3 ± 6.4	124.8 ± 8.0	93.2
Upper face	48.6 ± 2.5	52.9 ± 3.9	91.9
Width			
Bigonial	88.9 ± 6.5	99.3 ± 3.9	89.5

¹No. of observations: 7 in each group

²For definitions, see text.

Table IV Craniometric measurements in fourteen skulls. Units are expressed in mm and degrees. Coefficients of variation (CV) are reported in percentages (SD/Mean *100%).

Relationship	Measurement	Mean	SD	Maximum	Minimum	CV (%)
Maxilla to cranium	Anterior position of maxilla (SNA)	85.5	4.3	92.2	78.6	-
	Occlusal plane (SN-OP)	15.1	4.0	20.5	4.7	-
	Palatal plane (SN-PP)	8.0	1.9	11.5	5.7	-
	Maxillary length	91.1	3.8	97.6	83.0	4.1
Mandible to cranium	Anterior position of mandible (SNB)	78.6	3.7	85.6	73.1	-
	Mandibular plane (SN-MP)	35.2	4.7	44.9	26.5	-
	Gonial angle	126.3	4.3	133.5	118.7	-
	Mandibular length	115.3	6.2	126.0	107.0	5.4
Maxilla to mandible	Relative mandibular prognathism (ANB)	6.9	3.0	11.8	2.6	-
	Maxillary-mandibular length difference	24.2	3.6	29.5	17.2	14.8
Vertical Proportions	Upper face height	50.8	3.9	59.5	45.4	7.6
	Lower face height	69.8	5.2	77.7	63.7	7.5
	Ramus height	60.1	5.7	68.1	50.0	9.5
Transverse Proportions	Bizygomatic width	120.1	4.8	127.0	113.0	4.0
	Bicondylar width	109.9	4.4	117.0	104.0	4.0
	Bigonial width	94.1	7.5	104.0	77.0	8.0

small, no further gender distinction was made in subsequent analysis. The group means, standard deviations, ranges and coefficient of variations derived from the cephalometric radiography, as well as mean bizygomatic, bigonial and intercondylar width, are shown in Table IV. The cephalometric characteristics of our sample appeared to be typical of a modern population and fairly comparable to the subjects from other studies (Weijs and Hillen, 1986; Hannam and Wood, 1989; van Spronsen *et al*, 1991; Lam *et al*, 1991). A few variables, however, differed from those in the previous studies. Mandibular plane angle, mandibular length and relative mandibular prognathism were larger, while bizygomatic and bigonial widths were smaller. These differences are probably explained by race and perhaps gender differences between this sample and those previously studied.

3.2.1.2.2 Sample Variation in Insertion Site Location during Dental Intercuspatation

Variations in the location of the twelve insertion sites are presented in Table V. Mean values of the coordinate points and their standard deviations are shown for the fourteen skulls, with their mandibles in the intercuspal position. The largest variations in the sample occurred in the superficial masseter insertion sites, especially in the vertical dimension (z), reflecting differences in size and shape of the lower jaws.

3.2.1.2.3 Effect of Jaw Position on Insertion Site Location

Table VI describes the amount of displacement of masseter insertions at the

Table V **Mean location of putative muscle insertion sites for 14 skulls.**

Insertion	x	y	z
1	43.2 \pm 4.5	21.1 \pm 4.0	59.8 \pm 5.9
2	45.3 \pm 5.2	14.6 \pm 3.5	54.9 \pm 6.2
3	44.9 \pm 4.5	10.1 \pm 2.9	46.3 \pm 5.5
4	43.1 \pm 3.5	24.5 \pm 4.3	56.1 \pm 5.4
5	44.7 \pm 3.9	18.1 \pm 3.7	51.4 \pm 5.3
6	45.1 \pm 3.8	14.3 \pm 3.2	44.0 \pm 4.9
7	43.9 \pm 2.8	24.7 \pm 2.6	43.5 \pm 4.0
8	39.8 \pm 2.9	35.4 \pm 2.8	54.8 \pm 4.6
9	43.2 \pm 2.3	31.5 \pm 3.5	32.7 \pm 4.5
10	45.6 \pm 2.2	25.4 \pm 2.9	24.2 \pm 2.8
11	45.0 \pm 2.5	30.8 \pm 2.9	18.9 \pm 2.7
12	45.2 \pm 2.7	37.8 \pm 3.6	14.2 \pm 3.0

Note: Means and standard deviations of the coordinate points are in mm.
All measurements are made in the intercuspal position.
For descriptions of insertion codes, axes and origins, see Figs. 22, 23 and text.

Table VI Effect of jaw position on displacement of insertions expressed by mean orthogonal distances. All displacements are relative to the intercuspal position. Mean and standard deviations are expressed in mm¹.

Insertion ²	Jaw position								
	Working side			Balancing side			Incisal bite		
	x	y	z	x	y	z	x	y	z
1	-2.1 ± 0.8	7.2 ± 1.3	-0.8 ± 0.6	2.0 ± 1.0	4.3 ± 1.1	-3.2 ± 1.1	-0.3 ± 0.6	-1.8 ± 1.3	-1.9 ± 0.7
2	-1.5 ± 0.7	6.5 ± 0.9	0.0 ± 0.7	2.0 ± 0.8	3.8 ± 1.2	-3.2 ± 1.0	-0.1 ± 0.8	-1.7 ± 1.0	-1.8 ± 0.7
3	-1.1 ± 0.5	5.3 ± 1.1	0.4 ± 0.5	1.6 ± 0.9	2.8 ± 1.2	-2.1 ± 0.9	0.0 ± 0.8	-1.9 ± 1.1	-1.7 ± 0.7
4	-2.1 ± 0.8	6.7 ± 1.1	-1.1 ± 0.8	2.2 ± 1.3	4.2 ± 1.2	-3.6 ± 1.0	-0.2 ± 0.8	-1.6 ± 1.4	-1.8 ± 0.8
5	-1.5 ± 0.9	6.2 ± 1.2	-0.4 ± 0.7	2.1 ± 0.8	3.4 ± 1.2	-2.7 ± 1.3	0.1 ± 0.8	-1.6 ± 1.1	-1.6 ± 0.7
6	-1.4 ± 0.6	5.6 ± 1.1	-0.1 ± 0.5	1.6 ± 0.8	2.6 ± 1.1	-2.4 ± 1.1	0.0 ± 0.8	-1.6 ± 1.1	-1.7 ± 0.8
7	-1.7 ± 0.7	5.4 ± 1.2	-1.2 ± 0.4	2.1 ± 0.6	2.6 ± 1.2	-3.6 ± 1.1	-0.1 ± 0.9	-1.6 ± 1.0	-1.7 ± 0.8
8	-2.3 ± 0.6	6.7 ± 0.9	-2.6 ± 0.5	2.8 ± 1.1	4.1 ± 1.2	-5.0 ± 0.8	0.1 ± 0.9	-1.7 ± 1.1	-2.1 ± 0.9
9	-2.1 ± 0.6	4.1 ± 1.2	-2.3 ± 0.6	1.6 ± 0.7	1.3 ± 1.1	-4.6 ± 1.1	-0.4 ± 0.8	-1.6 ± 1.2	-1.7 ± 0.8
10	-1.5 ± 0.5	3.2 ± 0.7	-1.6 ± 0.5	1.5 ± 0.8	0.4 ± 1.0	-3.9 ± 0.7	-0.3 ± 0.7	-1.6 ± 0.9	-1.6 ± 0.8
11	-1.5 ± 0.5	2.4 ± 0.6	-2.4 ± 0.5	1.6 ± 0.7	-0.4 ± 1.2	-4.8 ± 1.0	-0.1 ± 0.6	-1.9 ± 1.0	-1.7 ± 0.9
12	-1.4 ± 0.6	1.6 ± 0.7	-3.1 ± 0.5	1.8 ± 1.0	-1.1 ± 1.1	-5.5 ± 1.2	0.0 ± 0.9	-1.9 ± 1.1	-1.6 ± 1.0

¹ No. of observations: 14 in each case.

² For insertion site descriptions (1-12) see text.

Note: Positive direction of the x-, y- and z- axes are to the left, posteriorly and upwards, respectively.

Table VI Continuation.

Insertion	10 mm open			20 mm open			35 mm open		
	x	y	z	x	y	z	x	y	z
1	-0.2 ± 0.9	4.9 ± 1.3	-2.6 ± 0.7	0.0 ± 1.0	12.0 ± 1.2	-2.6 ± 0.7	0.1 ± 1.2	22.9 ± 2.9	-1.4 ± 1.6
2	-0.1 ± 0.8	4.3 ± 1.5	-1.9 ± 0.7	0.2 ± 0.9	10.6 ± 1.3	-1.6 ± 1.1	0.5 ± 1.2	20.4 ± 2.7	1.0 ± 1.4
3	0.0 ± 0.9	3.2 ± 1.3	-1.2 ± 0.9	0.2 ± 0.9	8.4 ± 1.3	-0.8 ± 0.8	0.4 ± 0.8	16.4 ± 2.8	2.0 ± 1.5
4	-0.1 ± 0.8	4.7 ± 1.2	-2.9 ± 0.8	0.1 ± 1.1	11.2 ± 1.1	-3.7 ± 1.0	0.2 ± 1.1	21.7 ± 2.4	-2.9 ± 1.9
5	0.0 ± 1.0	4.1 ± 1.3	-2.3 ± 0.9	0.3 ± 1.1	10.1 ± 1.1	-2.3 ± 1.1	0.4 ± 1.2	19.4 ± 2.3	-0.7 ± 1.7
6	-0.1 ± 0.9	3.1 ± 1.2	-1.9 ± 0.8	0.1 ± 1.2	8.4 ± 1.4	-1.7 ± 0.8	0.4 ± 1.2	16.0 ± 2.3	0.1 ± 1.2
7	0.0 ± 0.9	3.3 ± 1.0	-3.1 ± 0.5	0.1 ± 0.9	8.3 ± 1.2	-4.1 ± 0.8	0.2 ± 1.1	16.8 ± 2.1	-4.1 ± 1.2
8	0.2 ± 1.0	4.6 ± 1.6	-4.4 ± 0.5	0.2 ± 1.3	11.5 ± 1.5	-6.7 ± 1.0	0.4 ± 1.2	22.4 ± 2.6	-7.7 ± 1.4
9	-0.1 ± 0.7	1.9 ± 1.3	-4.0 ± 0.8	-0.2 ± 1.0	5.9 ± 1.5	-6.2 ± 1.0	0.3 ± 1.0	13.0 ± 2.3	-7.9 ± 1.1
10	-0.1 ± 0.9	1.0 ± 1.1	-3.4 ± 0.5	0.1 ± 0.9	3.9 ± 0.9	-5.2 ± 1.0	0.1 ± 0.9	8.9 ± 1.4	-6.3 ± 1.3
11	-0.1 ± 0.5	0.1 ± 1.2	-4.1 ± 0.8	-0.1 ± 0.8	2.5 ± 1.0	-6.6 ± 0.9	0.3 ± 0.8	7.1 ± 1.0	-9.0 ± 1.2
12	0.0 ± 0.7	-0.4 ± 0.9	-4.7 ± 0.6	0.1 ± 1.1	1.4 ± 1.2	-8.4 ± 0.8	0.4 ± 1.0	5.5 ± 1.0	-12.1 ± 1.4

different jaw positions. These data are expressed as means and standard deviations for distances between the maximum intercuspation and the different jaw positions in the three orthogonal directions.

Deviations from sample means were generally less than 1 mm, except for mean displacements in the anteroposterior (y) direction. The deviation was most noticeable on the balancing side and during midline tasks, and probably reflects both differences in the size of the ramus and in the variables responsible for anterior movement during lateral excursion and jaw opening.

For every insertion site, as expected, the one-way analysis of variance revealed significant differences in transverse, antero-posterior and vertical muscle insertion displacement as the jaw positions changed ($p < 0.001$). To test for the effects of jaw displacement on the movement of putative muscle layers, five representative muscle insertions were chosen. These represented the center of the attachment of the aponeurotic sheet I (2), of aponeurotic sheet II (5), and of the muscular attachment to the mandible of aponeurotic sheet III (7), as well as the deep posterior (10) and deep anterior muscle portions (11). Multiple comparisons were made between the 3D distances travelled by these insertions at the working- and balancing-side positions, and at a 10 mm midline jaw opening. Midline incisal edge-to-edge, 20 mm and 35 mm jaw openings were not included in this analysis, because for these tasks all insertion sites predictably move in a single plane by increasing amounts, relative to the increasing jaw opening.

When the working side position was compared against the balancing side, and

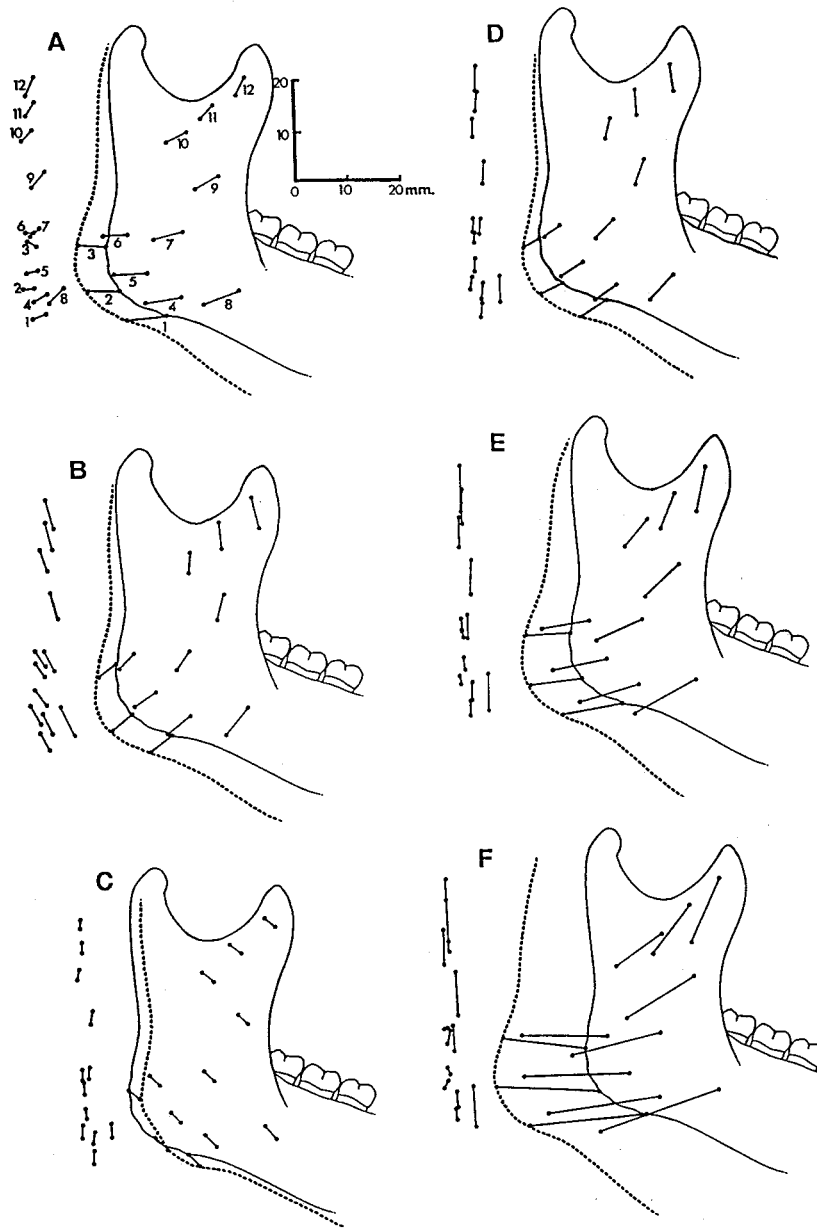
against a 10 mm jaw opening, the analysis of variance revealed statistically-significant different amounts of movement for insertion 2 ($p < 0.05$). Significantly different distances were also found for the displacement of insertion 5, when the working side was compared against a 10 mm jaw opening ($p < 0.01$). Finally, when the balancing and working sides were compared, significant differences in displacement were found for insertion 11 ($p < 0.01$).

3.2.1.2.4 Differences within Putative Muscle Layers

In order to analyze the displacement that the various muscle layers are subjected to during normal mandibular movements, the different insertion sites were grouped into layers I (1-2-3), II (4-5-6), III (7-8), IV (9-10) and V (11-12). A qualitative displacement analysis was performed within the individual muscle layers by comparing anterior against posterior insertions. Each jaw position was considered separately.

Generally, anterior insertion sites moved consistently longer distances relative to posterior insertions, showing differences in displacement ranging from 0.1 to 7.4 mm within the same layer. If incisal bite and a 35 mm jaw opening are not taken into the analysis, displacement differences ranged from 0.5 to 4.2 mm. For the incisal bite however, all insertions displaced by equal amounts, maintaining the same direction of movement (Figure 25).

Figure 25 Mean displacements of the twelve insertion points at six different jaw positions. These include working (A) and balancing sides (B), and the four midline gapes: incisal bite (C), 10 mm (D), 20 mm (E) and 35 mm (F) jaw openings. For each jaw position, the coronal projection of attachment side movements is shown on the left, and the corresponding sagittal projection is shown on the right. Continuous-mandible outlines illustrate the jaw at the intercuspal position. Stippled outlines illustrate the jaw at the various gapes and eccentric jaw positions. All insertion displacements are shown as lines connecting the location of each insertion point at the different jaw positions relative to the location of the same insertion point at the intercuspal position (topmost point of each line). The 12 insertion points are indicated by numbers in (A), and are also illustrated for the other jaw positions (B-F).



3.2.1.2.5 Differences between Putative Muscle Layers

Comparisons between the various muscle layers and between the corresponding anterior and posterior insertions of a single layer were also made qualitatively for each jaw position. Considered three dimensionally, the displacements covered a wide range. The shortest mean distance was 2.5 mm for the deep-posterior (10) portion at the incisal contact position, while the longest distance was 23.8 mm for the superficial-anterior (8) muscle at maximum gape. Collectively, the more superficial layers moved longer distances than did the deeper layers for all jaw positions, except for the incisal edge-to-edge bite. Variations in the amount of insertion displacement between the different skulls were more prominent in symmetric than in asymmetric jaw positions. In the asymmetric jaw positions, they were smaller for the balancing than for the working side (Table VII).

Sagittal and coronal projections of attachment site movements are shown in Figure 25, and infer fascicle lengthening and rotation. They reveal that for the superficial-anterior (8), superficial-posterior (3), and deep-posterior (10) masseter, the balancing-side masticatory position and the incisal contact position provided the most advantageous lines of action, for muscle fibres which contribute mostly to jaw displacement by changing their length. For the deep-anterior (9) masseter, the working-side task was most advantageous in this respect. Superficial-anterior and superficial-posterior masseter had also an advantageous line of action at 10 mm jaw opening, while the deep-posterior and deep-anterior masseters were well aligned at 20 and 35 mm jaw openings.

Table VII **Effect of jaw position on displacement of insertions expressed by mean linear distances.** All displacements are relative to the intercuspal position and are expressed as three-dimensional resultants. Mean and standard deviations are expressed in mm¹.

Insertion ²	Jaw position					
	Working side	Balancing side	Incisal bite	10 mm open	20 mm open	35 mm open
1	7.6 ± 1.2	5.9 ± 0.8	2.9 ± 1.0	5.7 ± 1.0	12.5 ± 1.3	23.0 ± 2.9
2	6.7 ± 0.9	5.1 ± 0.8	2.7 ± 0.9	4.9 ± 1.1	10.8 ± 1.2	20.5 ± 2.7
3	5.5 ± 1.1	4.1 ± 1.1	2.8 ± 1.0	3.7 ± 0.8	8.5 ± 1.3	16.6 ± 2.8
4	7.2 ± 1.0	6.2 ± 0.9	2.7 ± 1.2	5.7 ± 0.8	11.9 ± 1.0	22.0 ± 2.4
5	6.5 ± 1.1	5.1 ± 0.9	2.6 ± 0.9	4.9 ± 1.0	10.4 ± 1.1	19.6 ± 2.3
6	5.6 ± 1.1	4.3 ± 0.8	2.4 ± 1.0	3.9 ± 0.7	8.5 ± 1.2	16.0 ± 2.3
7	5.8 ± 1.0	5.2 ± 0.8	2.7 ± 1.0	4.7 ± 0.6	9.4 ± 1.0	17.4 ± 1.9
8	7.6 ± 0.7	7.2 ± 0.8	3.0 ± 0.9	6.6 ± 0.9	13.4 ± 1.2	23.8 ± 2.5
9	5.2 ± 1.0	5.3 ± 1.0	2.7 ± 1.1	4.7 ± 0.7	8.7 ± 0.8	15.3 ± 2.1
10	4.0 ± 0.5	4.4 ± 0.8	2.5 ± 1.0	3.8 ± 0.6	6.6 ± 0.7	11.0 ± 1.2
11	3.7 ± 0.4	5.2 ± 1.1	2.7 ± 1.1	4.3 ± 0.8	7.2 ± 0.9	11.6 ± 1.0
12	3.9 ± 0.6	6.0 ± 1.3	2.7 ± 1.2	4.8 ± 0.6	8.6 ± 0.8	13.4 ± 1.2

¹ No. of observations: 14 in each case.

² For insertion site descriptions (1-12) see text.

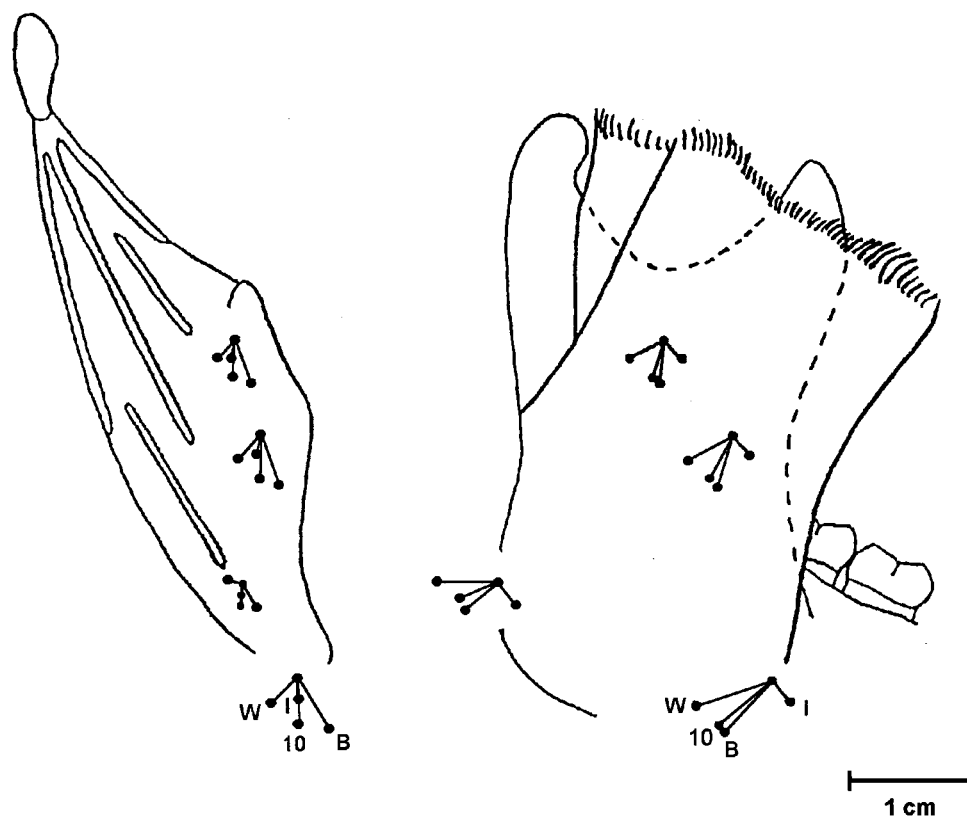
When the three jaw openings (10, 20 and 35 mm; Figure 25 D-F) were compared, a striking feature was the change in direction of movement of insertions belonging to the superficial and deep muscle portions. It is suggested that the fibres of the superficial masseter (1-6) are well-aligned to contribute to closing movements at small gapes (around 10 mm; Figure 25 D) but less well-aligned to contribute to movements at large gapes (35 mm; Figure 25 F), where fibres in the deep part (9-12) of the muscle may have a better line of action. As expected, from the incisal contact position (Figure 25 C) all insertions displaced similarly.

For the simulated functional jaw movements, there are considerable differences in the movements of attachment sites in both projections when the working side (Figure 25 A) is compared with the balancing side (Figure 25 B). On the working side, all attachment sites tend to move upwards, forwards, and medially. The superficial sites (1-6) move much more horizontally than do the deep sites (9-12) in both projections. These movement patterns are not consistent with the probable orientations of the muscle fibres in either part of the muscle. When insertions are moved towards the balancing side the majority of points move upwards, forwards, and laterally. In contrast, these directions are more consistent with probable muscle fibre orientations (Figure 26).

3.2.1.2.6 Orientation of Masseter Insertion relative to Origin

To evaluate the orientations of masseter muscle attachment sites relative to each other when the teeth were in the intercuspal position, both origin and insertion points of the superficial and deep muscle portions were plotted in the (horizontal) XY

Figure 26 **Mean functional displacements of four putative muscle attachment sites in the human masseter.** Movements between four jaw positions are simulated. The positions include incisal, edge-to-edge tooth contact (I); 10 mm jaw opening (10); the turnaround between opening and closing for a chewing stroke on the ipsilateral working side (W); and on the balancing side (B). The apices of the movement vectors represent the dental intercuspital position. Data are shown in both frontal and lateral projection, and are derived from simulations in 14 adult skulls. Calibration bar represents 10 mm.



plane. Origin points o1-o4 and insertion points 1-3 and 8 were used to represent the superficial masseter attachment areas, while points o4-o6 and 9-11 were used to represent attachment areas of the deep-masseter portion (Figure 27). For each skull, linear-regression lines were fitted through individual sets of points, and their intercept, slope and R-values recorded. Mean and standard deviations were subsequently calculated for the intercepts and slopes of regressions that had R-values larger than 0.45 (Table VIII). The resultant four mean regression lines were then plotted, and their angles measured relative to the midsagittal axis. For the superficial and deep masseter portions, the origin and insertion attachment sites were angled at 25° , 15° , -4° and 19° relative to the midsagittal plane, respectively. During working-side-mandibular movements, the insertion lines of the deep masseter approached parallelism with their respective origin attachment sites. However, the insertion lines of the superficial portion deviated even further from parallelism relative to their origin. During balancing-side movements, the inverse was true. The attachment sites of the superficial portions approached parallelism, while the attachment sites of the deep masseter deviated even further from each other (Figure 28).

3.2.1.2.7 Discussion

Ideally, the displacement of muscle attachment areas should be measured during normal jaw function. This requires muscles to be imaged in living subjects, computer reconstruction of attachment landmarks, and recordings of movements of identified sites to be made in three dimensions with a transducer system having six

Figure 27 Orientation of origin and insertion sites. Insertion points are plotted in the XY-plane relative to their origin counterparts. The jaw is at the intercusp position in both graphs. Superficial (A), and deep (B) masseter insertions (filled symbols) are shown relative to their origins (open symbols) for six skulls. Each skull is represented by a different symbol.

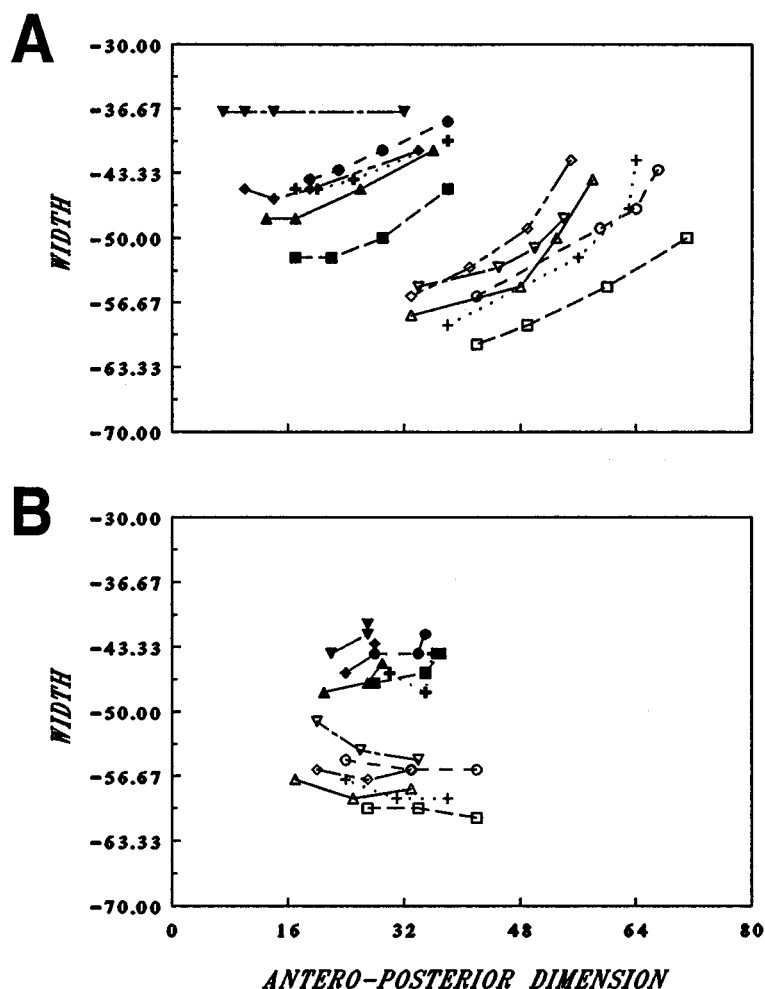
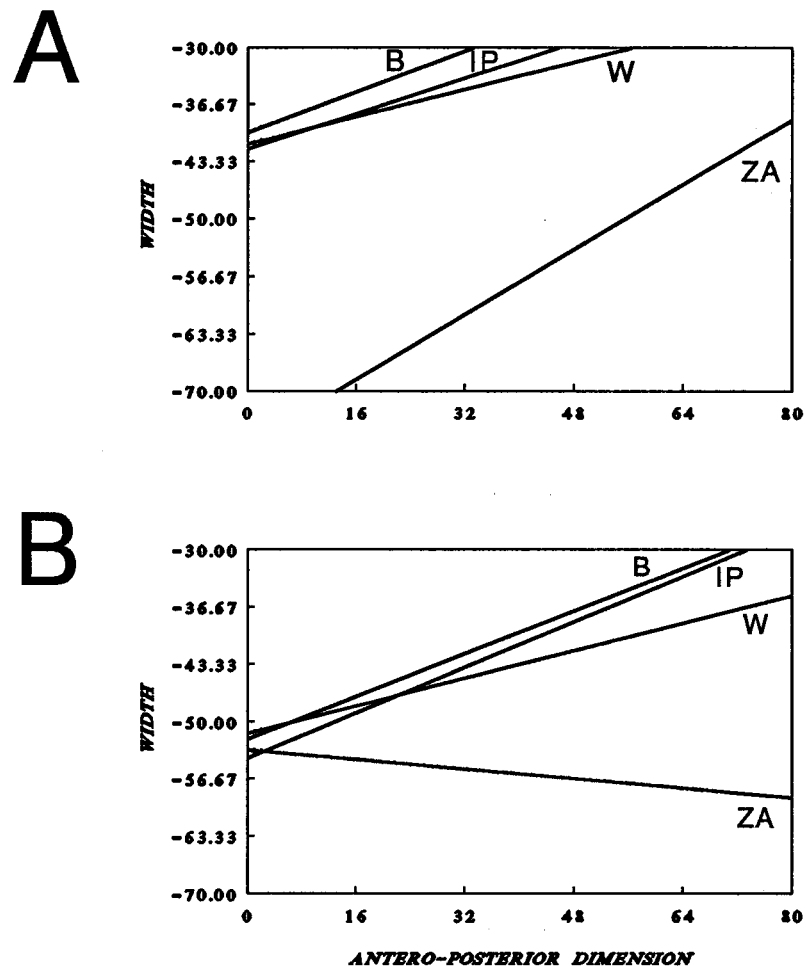


Table VIII Linear regression analyses for points representing attachment sites. Linear regression through the points at the origin (O) and insertion (I) of the superficial and deep masseter muscles are expressed in mm. Mean and standard deviations of the intercepts and slopes were calculated only for linear regressions with R-values greater than 0.45.

Skull	Superficial portion						Deep portion					
	Zygomatic arch (O)			Mandible (I)			Zygomatic arch (O)			Mandible (I)		
	Intercept	Slope	R-val	Intercept	Slope	R-val	Intercept	Slope	R-val	Intercept	Slope	R-val
1	-76.4	0.51	0.91	-52.8	0.32	0.98	-56.4	-0.06	0.50	-55.1	0.33	0.89
2	-76.4	0.48	0.98	-50.2	0.32	1.00	-53.8	-0.06	0.87	-49.3	0.19	0.61
3	-77.4	0.38	1.00	-58.8	0.34	0.95	-58.0	-0.07	0.88	-55.1	0.28	0.88
4	-81.4	0.57	0.94	-49.8	0.25	0.98	-54.0	-0.14	0.87	-55.0	0.50	0.94
5	-66.7	0.33	0.94	-37.0	0.00	1.00	-45.9	-0.28	0.93	-61.0	0.63	0.94
6	-77.2	0.61	0.97	-47.0	0.19	0.92	-50.0	-0.27	0.88	-61.5	0.42	0.92
7	-77.7	0.43	0.83	-51.0	0.27	1.00	-58.0	0.06	0.47	-53.3	0.27	0.91
8	-83.5	0.56	0.99	-49.5	0.19	0.92	-53.4	-0.08	0.50	-52.9	0.30	0.87
9	-73.1	0.43	0.91	-46.7	0.22	0.96	-57.0	-0.13	0.85	-53.2	0.29	0.65
10	-72.4	0.39	0.95	-54.1	0.36	1.00	-44.7	0.34	0.99	-47.0	0.29	0.65
11	-76.0	0.51	0.94	-50.6	0.33	0.98	-53.9	-0.06	0.53	-52.9	0.28	0.85
12	-82.8	0.48	0.95	52.3	0.33	0.97	-56.2	0.00	0.04	-54.3	0.39	0.79
13	-65.1	0.33	0.82	-44.7	0.31	0.99	-60.3	0.00	0.03	-49.3	0.10	0.16
14	-79.2	0.54	0.99	-47.2	0.27	1.00	-57.3	0.00	0.00	-47.0	0.00	0.00
Mean	-76.1	0.47		-41.9	0.26		-53.2	-0.07		-54.2	0.35	
SD	5.4	0.09		27.6	0.09		4.6	0.17		4.1	0.12	
n	14	14		14	14		11	11		12	12	

Figure 28 Orientation of origin and insertion sites at three jaw positions. In (A), the superficial-masseter insertion is illustrated in the balancing side (B), intercuspipal position (IP) and working side (W), represented by linear-regression lines in the XY-plane relative to their origin in the zygomatic arch (ZA). In (B), the deep-masseter insertion is illustrated in the same jaw positions relative to its origin. Regression lines were fitted through insertion and origin points of all 14 skulls.



degrees of freedom. While theoretically possible, such an experiment poses formidable technical problems.

A second approach could have been to use a computer model to predict multiple trajectories, at multiple sites, for simulated jaw movements made for many different craniofacial configurations. As the mandible is a rigid body, the displacements of all points on it are predictable provided the displacement of any three are known. Thus, a computer model could be used to predict the displacement of attachment sites for any combinations of skeletal and of movement variables, provided that these are known. Such a model could have provided multiple predictive curves, but it would be difficult to decide which parts of the displacement curves should be considered important unless specific morphological dimensions and related movement patterns were available. Even having accomplished this, one would be left with the problem of specifying which combinations best represent those likely to be found in a sample of living human subjects.

The third approach, which was the method of choice here, involved the measurement of putative muscle attachment sites on mandibles which were subjected to movements simulated according to the condylar and dental guidances likely to be present in a series of differently-shaped, dry human skulls. Using this approach it was possible to investigate a larger number of specimens (as opposed to a study in living subjects, in which the number of participants is even more restricted). It had, however, some limitations. Although the landmark locations were directly visualized based on osteological criteria, they were arbitrary and only approximated the "true" attachment

locations in each skull since muscles were not present. Also, the assumption of tasks with common dental arch positions may not have been correct for the different craniofacial shapes used in the sample, and the simulation of articular movements with published records and artificial articular disks may not have duplicated the real jaw movement that occurred for each specimen in life. Although these errors were present, the data were reasonably homogeneous and indicated the probable order of displacement expected in a living sample with comparable skeletal morphology. They also provided a realistic estimate of the demands placed upon the average masseter muscle. In addition, these data may be used in future models of the masseter and encourage further experiments to reveal individual differences in living human subjects.

It is known that the human masseter muscle has a complex internal architecture. Its muscle fibres are arranged on a multipennate pattern between ample aponeurotic sheets, and together with their sarcomeres show moderate length differences anteroposteriorly (30%) and mediolaterally (5%), (Ebert, 1939; Schumacher, 1961c; Van Eijden and Raadsheer, 1992). Lam *et al* (1991) also suggested that the muscle fibre orientations between aponeurotic sheets may have different pennation angles at their proximal and distal ends. This, added to regional variation of sarcomere length, suggests a substrate for differential contraction according to task, and suggest that differential tension may be produced within the muscle.

Despite the possibility of dissimilar contraction patterns of the muscle masses on either side of the aponeurotic sheets, it may be assumed that these muscle fibres mostly co-activate, and that for any degree of activation, the resultant line of action

would be along the planes of orientation of the aponeurosis (Gans and Bock, 1965; Otten, 1988). If so, the orientation of aponeuroses and the displacement of any of their mandibular attachment sites during function have an extreme impact on suitability for participation in a particular task. On the other hand, the line of contraction followed by masseter muscle fibres may or may not coincide with the direction of movement of their attachment to the mandible, since the latter is determined by the combined action of several muscles. It is therefore possible that particular groups of fibres are more efficiently aligned for some tasks than for others, independent of the fibre's line of action.

In this study, the extent and direction of movement of the various aponeurotic attachment sites were evaluated, and the relationships between the various insertion movement trajectories and the probable orientation of the aponeurotic sheet planes were analyzed. The results suggest that contraction of muscle fibres in the masseter would best contribute to displacement of the mandible when jaw closing takes place in the midline and when the muscle is on the balancing side at the beginning of the closing stroke during chewing. In these cases, fibre alignment approximates the lines of movement of the attachment sites. However masseter fibres are poorly aligned to shorten with jaw displacement during movement from an edge-to-edge incisal position towards full intercuspation in incision and on the working side during chewing, (note Figure 26-(I) in the sagittal projection and Figure 26-(W) in the coronal projection). Here the actions of the fibres are actually perpendicular to the movement of the attachments. Because the masseter muscle is known to be active during these functions, it is assumed that the

produced forces are not used for generating jaw movement, but are used for developing forward and lateral compression between the teeth when the jaw moves into the intercuspal position.

The analysis is in agreement with physiological findings. It has been known for years that the deep and superficial masseters are capable of differential contraction according to task. Recently, it has been suggested that it can be even further divided into at least three parts: anterior deep, posterior deep and superficial (Blanksma *et al*, 1992), although the results of her study were obtained under isometric conditions. During lateral, posterolateral and posterior directed tooth-clenching the deep portion is more active than the superficial portion of the muscle. The same activity pattern is present during ipsilateral tooth-clenching at eccentric jaw position. Distinctions however must be made between static and dynamic acts with regard to the muscle's internal behaviour. During chewing at the ipsilateral side, both muscle portions were equally active, while during contralateral chewing the deep portion was more active than the superficial muscle portion. Furthermore, during the act of incision the masseter muscle is as active as during chewing (Hylander and Johnson, 1985), which is not the case during static incisal biting (Belser and Hannam, 1986).

This study also shows that there can be considerable differences between subjects. Even though this sample was small and from a single ethnic group, the skeletal differences were sufficient to show quite large differences in the movement of attachment sites when similar functional acts were simulated. This implies different mechanical and functional activation strategies, which could explain the great inter-

subject variability known to exist in muscle activation patterns and frequently demonstrated in electromyographic studies. This variability makes pooling of functional data difficult.

Recently, Van Eijden and Raadsheer (1992) have provided a comprehensive description of regional muscle fibre, tendon and sarcomere length in the human masseter. In their study, parameters were initially measured with the mandible in a closed position, then changes in length were calculated with a computer model simulating a series of tasks similar to those used in the present study. Sarcomere excursions were estimated to be relatively small in the deep-posterior region and large in the superficial-anterior part when the jaw was rotated open and closed about a transverse axis, but the reverse was true when the jaw was rotated contralaterally about a vertical axis. In this situation, sarcomere lengths shortened initially, but started to lengthen as the movement continued. The angle at which this transition between sarcomere lengthening and shortening occurred was determined by the tilt of the muscle's line of action relative to the vertical axis. It was argued that a correlation exists between the muscle fibre tilt and the jaw-deviation angle at which this transition occurs (i.e. the larger the tilt, the larger is the angle), and that insertions were displaced from a posterior to a anterior location relative to their point of origin. In the skull sample, however, this situation occurred only 14% of the time. In the remaining cases, the insertion remained posterior to the origin, suggesting that in this skull sample the transition of sarcomere shortening to lengthening would occur only at large balancing-side mandibular deviations. Although the location of insertion points varied in both

studies, that is, in the present sample the mandibles were shorter and narrower, both studies complement each other in the sense that while the former provides anatomical information of fibre, sarcomere and tendon lengths, the skull sample provides information on the full, natural range of attachment movement.

In conclusion, the human masseter is clearly not a simple muscle. It consists of different structural compartments with varying fibre, tendon and sarcomere lengths, which are also angled differently in 3D. These structural characteristics and functional demands place very different constraints upon regional displacement of different parts of the muscle, and probably vary significantly between individuals. This leads to the suggestion that intramuscular morphology, electromyographic activity and attachment displacement in 3D during functional movements should probably be studied together in individual living subjects. In this way, the functional role of separate muscle portions could be better assessed.

3.2.2 Function in Living Subjects

Measurements of the displacement of the human mandible during function are common and are referred to as jaw tracking (Lundeen and Gibbs, 1982; Jemt, 1984; Mohl *et al*, 1990; Hannam, 1992). This measurement is obtained by recording the trajectory of movement of sensors (magnetic, light-emitting or reflective) attached to specific points of interest, normally anatomical. Most jaw tracking devices measure only three degrees of freedom, usually expressing motion of the incisor point. The limitation of these types of devices is that they are only capable of tracking the displacement patterns of the region where the sensor is attached. Whenever there is the interest of recording any other site remote from the moving sensor, a tracking device with six degrees of freedom must be used. This type of tracking device allows an investigator to measure simultaneous motion of other anatomical or reference points based on the assumption that the mandible and attachments are a rigid unit, and mathematical data conversion. These more elaborate sensing systems have been used to quantify the three-dimensional motion of distant condylar and tooth cusp points (Lundeen and Gibbs, 1982; Merlini and Palla, 1988; Hagiwara *et al*, 1993b), and could be used to measure the motion of any other site including the attachment areas of the masticatory muscles. Thus, the availability of this new type of jaw-tracking system enables the recording of the displacement of masticatory muscles' insertions during natural jaw movements. Improvements in MR imaging techniques enable the visualization of internal muscle architecture, and therefore, the determination of the actual location of the attachment sites. In addition, modern engineering software (i.e. solid-object modelling techniques)

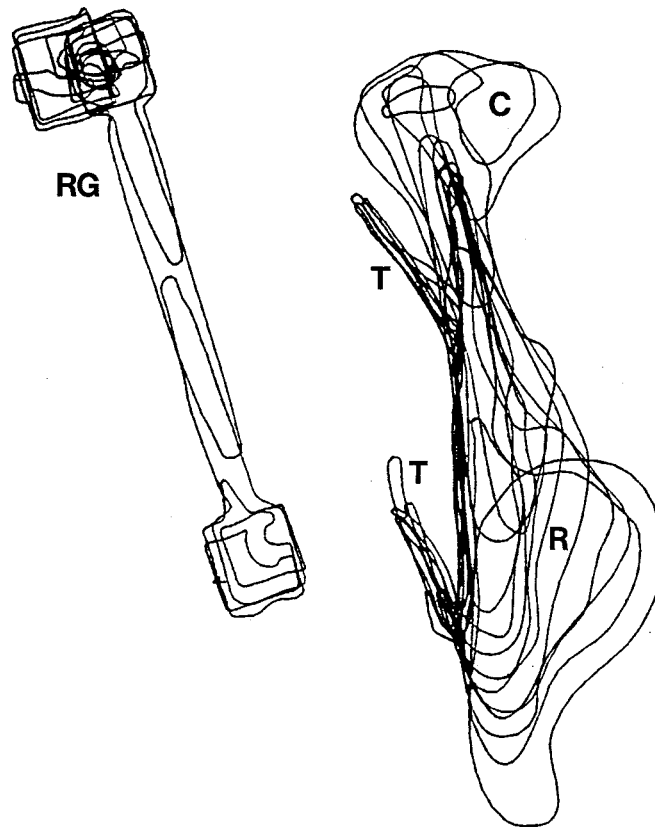
facilitates the three-dimensional reconstruction of the muscle architecture. The availability of these techniques inspired the development of a method which combines the muscle reconstructions and jaw-tracking records through a common reference system, and allows the measurement of the actual displacements of the masseter muscle insertions in four living subjects. Thus the goal in this part of the study was to develop an experimental approach that might be useful in future studies of muscle mechanics, and to determine whether estimates of attachment site displacement made previously in dry skulls were representative of those in living subjects.

3.2.2.1 Methods

During each jaw movement recording session a customized plastic eyeglass frame was worn by the subject to provide a fixed spatial reference (details on page 103). Each subject wore this device during a separate imaging session in which a 1.5 Tesla unit (Signa, GE Medical Systems, Milwaukee) was used to obtain T2-weighted images of the muscle and the reference grid. Spin-echo sequences with TR of 2000 ms and TE of 25 and 80 ms were used to obtain a series of contiguous, 3 mm sections in the coronal plane. From each coronal section, outlines from the muscle, internal tendons, bones and copper-sulphate markers were traced and digitized (Model HP9874A Digitizer, Hewlett-Packard, Canada). The profile coordinates were then used in an engineering solid-object modelling package (I-DEAS, SDRC, Milford) to reconstruct the muscle and its internal structures in 3D, as shown in Figure 29.

An optical motion-analysis device (MacReflex System, Qualisys AB, Partille,

Figure 29 Anterior view of the sectional outlines of a reference grid, right mandibular ramus and condyle, and selected right-masseter-tendinous insertions. These outlines are closed third-order splines, which form a "wireframe" in I-DEASTM. (C) Condyle; (R) Mandibular ramus; (RG) Reference grid; (T) Tendinous insertions.

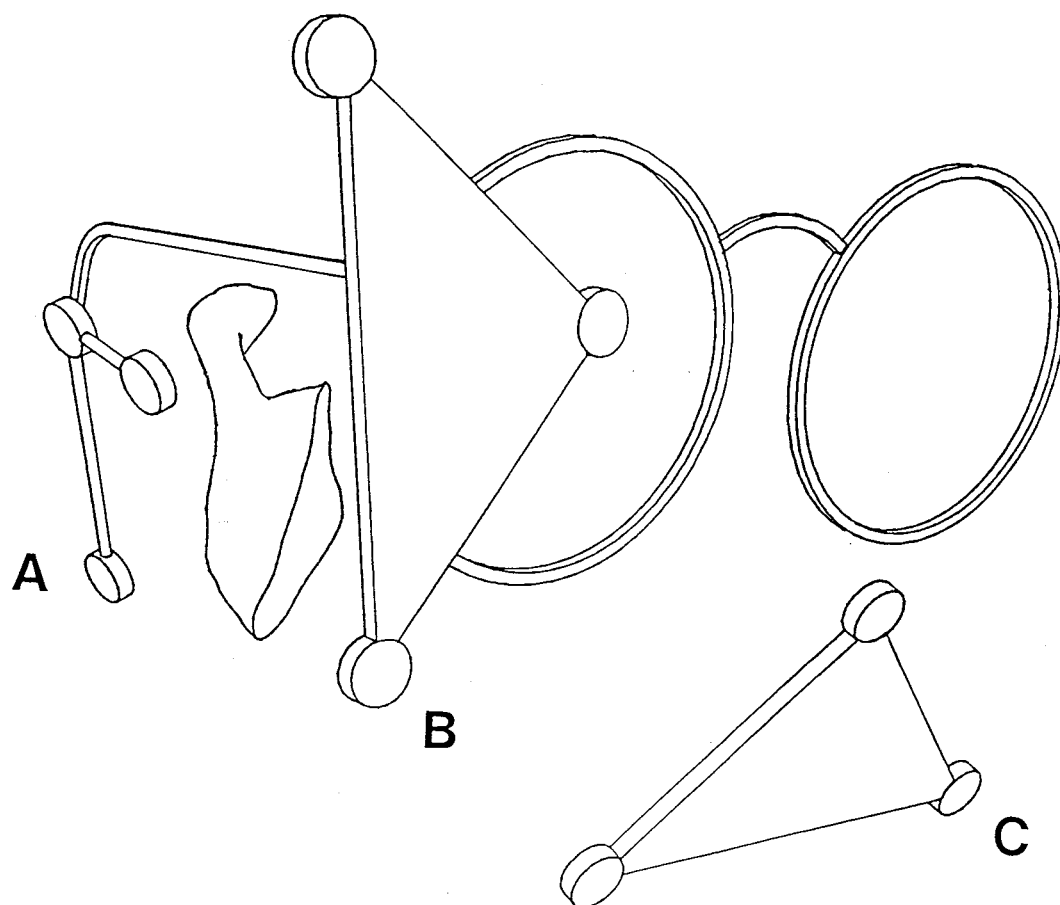


Sweden) and two marker triads were used to record the 3D movement of the mandible. One triad was fixed to the front of the eyeglass frame, while the other was attached to a dental clutch cemented to the labial surfaces of the mandibular front teeth (canine to canine). Each triad consisted of three reflective markers. The optical system was used to measure the 3D coordinates of the mandible's triangle relative to the reflective markers on the front of the frame (Figure 30). The tracking system was calibrated so that markers could be detected within a cube of 130 mm (x axis), by 150 mm (y axis), by 100 mm (z axis), with a static resolution better than 0.1 mm in any dimension (Hagiwara *et al*, 1993a).

Each subject was asked to perform four separate gentle, static biting tasks. These included biting at the intercuspal position, with the jaw in left and right laterotrusion, and incisal biting. All biting tasks were performed on a plastic suction tip with a diameter of 10 mm. To estimate reproducibility, one subject was asked to repeat these tasks five times. For each jaw position, the coordinates were sampled by two video cameras every 20 ms for 0.5 s, then stored and converted into 3D spatial coordinates in a microcomputer (Macintosh IIsi, Apple, Cupertino, California, and MacReflex software, Qualysis AB, Partille, Sweden). The reflective-markers' coordinates were sampled 25 times and averaged for further analysis.

In addition to the biting tasks, all subjects were asked to chew gum unilaterally, on both the right and left sides. For chewing, the coordinates were sampled every 20 ms for 15 s. With this sampling rate, at least 13 complete envelopes were recorded for each unilateral chew of each subject. To simplify analysis, only one "typical"

Figure 30 Schematic illustration of the global setup for a jaw tracking run. A copper-sulphate-filled, L-shaped grid attached to an eyeglass frame (A). Three reflective markers are mounted on the front of the frame (B) and three on a triangle cemented to the anterior teeth (C).



chewing envelope of each task was selected from those available.

To express attachment site displacement relative to the same coordinate system used in the skull study, a modified dental earbow with reflective markers on each earbar and on an infraorbital pointer, was used. Each subject was instructed to bite gently in the intercuspal position, while the location of the mandibular-clutch-marker triangle was recorded relative to the earbow. These data were then used in I-DEAS to orientate the reference grid, masseter muscle and bone reconstructions to the desired coordinate system, that is, relative to the Frankfort Horizontal plane, with the origin situated halfway between the meatal landmarks (Hagiwara *et al*, 1993a).

To relate the jaw-motion data to the MR images, a separate optical measuring system (Reflex Metrograph, HF Ross, Salisbury, UK) was used to measure the 3D coordinates of the markers on the front of the frame relative to those of the L-shaped grid visualized during imaging. All data were then transferred to the solid-object modelling package (I-DEAS, SDRC Corp. software), in which coordinate conversions were performed. Conversions involved superimposition of like markers by a series of translations and triaxial rotations.

Four muscle attachment points were selected for each subject. These were defined as the most anterior and posterior points of the mandibular insertions of aponeuroses II and IV, as described by Schumacher (1961c) and Lam (1991). The orthogonal distances that these landmarks had to move were then calculated from the jaw-motion data at each jaw position. For the chewing data, only four selected data points per envelope were analyzed. These were defined as the most left lateral, right

lateral, inferior and superior points of the representative chewing cycle. Displacements of the attachment points were then calculated relative to their common coordinates at maximal tooth intercuspation.

Due to the small sample size, and for reasons discussed above, no statistical test to determine the significance of differences between the various distances travelled by each insertion at different jaw positions were used.

3.2.2.2 Results

Distances between the anterior and posterior insertion points of both aponeurosis (II and IV) are shown in Table IX. The antero-posterior length of aponeurosis II varied greatly between subjects, but tended to be larger than aponeurosis IV, which showed small inter-subject variability. The standard error of the measurement was estimated to be 0.07 mm. This was obtained by sampling the position of one insertion site, with the teeth in the intercuspal position, on three separate occasions.

When the subject repeated the static tasks five times, the largest variation was found to occur in the supero-inferior (y) direction (Table X). It was also observed that during the working side task, insertion displacement in the lateral (x) direction was smaller than expected, and in two cases it deviated to the opposite side (medially). A possible explanation for this finding is the presence of a cross-bite in the right canine region of this subject.

Table XI shows, for all four subjects, the mean and standard deviation values of the four insertion points, namely, posterior (1) and anterior (2) insertions of

Table IX Anteroposterior dimensions of the mandibular insertions of Aponeuroses II and IV in four subjects. All values are expressed in mm.

Aponeurosis	Subject				Mean \pm SD
	I	II	III	IV	
II	26.01	12.50	15.23	10.94	16.17 \pm 5.88
IV	11.64	13.19	9.27	11.43	11.38 \pm 1.40

Table X Displacements of one insertion point of one subject at different jaw positions. Each position was repeated five times. Displacements are expressed as orthogonal distances (in mm) calculated from the insertion's coordinate point at maximum intercuspation.

Task	Repeats					Mean \pm SD
	I	II	III	IV	V	
Working Side	x	0.46	-1.10	-0.17	0.04	-0.19 \pm 0.51
	y	-2.45	1.69	-0.04	-1.82	-0.86 \pm 1.51
	z	-7.46	-9.72	-9.35	-7.35	-8.41 \pm 0.97
Balancing Side	x	2.03	0.73	0.62	0.62	1.07 \pm 0.55
	y	-4.28	-1.06	-0.53	-0.75	-1.78 \pm 1.39
	z	-4.93	-6.95	-6.69	-7.33	-6.48 \pm 0.82
Open	x	0.31	-0.15	0.32	-0.50	-0.07 \pm 0.33
	y	-3.39	-1.07	-1.97	-1.51	-2.08 \pm 0.80
	z	-6.76	-5.61	-5.98	-5.96	-6.11 \pm 0.38

Table XI Mean displacements and standard deviations of four insertion points of four subjects at different jaw positions. Displacements are expressed as orthogonal distances (in mm) calculated from the insertion's coordinate point at maximum intercuspation.

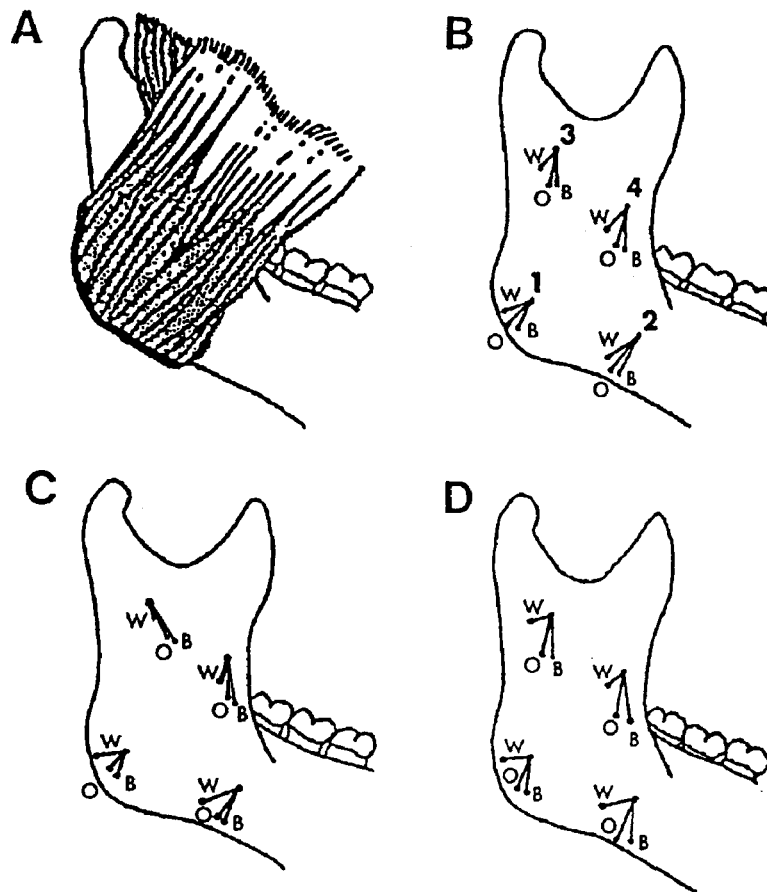
Task	Insertion Points				
	1	2	3	4	
Working Side	x	-0.80 ± 0.75	-0.94 ± 0.92	-0.57 ± 0.68	-0.67 ± 0.73
	y	-1.88 ± 1.28	-3.28 ± 1.39	-2.96 ± 1.10	-3.90 ± 1.16
	z	-4.79 ± 0.81	-5.76 ± 0.58	-2.27 ± 1.79	-3.10 ± 1.10
Balancing Side	x	1.54 ± 0.32	1.95 ± 0.50	1.51 ± 0.30	1.78 ± 0.48
	y	-4.34 ± 0.69	-5.63 ± 0.34	-5.37 ± 0.53	-6.25 ± 0.38
	z	-2.07 ± 1.90	-3.07 ± 1.64	0.49 ± 2.18	-0.40 ± 1.90
Open	x	0.41 ± 0.38	0.35 ± 0.39	0.60 ± 0.33	0.45 ± 0.27
	y	-3.99 ± 1.04	-5.44 ± 0.64	-5.12 ± 0.40	-6.13 ± 0.48
	z	-3.44 ± 1.43	-4.47 ± 1.30	-0.79 ± 2.21	-1.62 ± 1.80

aponeurosis II, and posterior (3) and anterior (4) insertions of aponeurosis IV, during the working, balancing and incisal bites with jaw opening. As in the skull study, displacement of the insertions in the antero-posterior (z) direction varied the most, reflecting differences in mandibular ramus lengths. Additionally, when compared with the skull data, the living subjects showed a tendency to displace the insertions over smaller distances in the medio-lateral direction during the working side bite. Larger mean distances were observed, however, in the supero-inferior direction at all three tasks and in the medio-lateral direction at the incisal bite.

When the displacements of the anterior and posterior insertions were compared, there was a tendency for the anteriorly located insertions to displace larger distances than their posterior counterparts. The exception to this pattern was the insertion displacements of aponeurosis IV during the balancing side bite. The mean value of the posterior insertion (3), antero-posterior (z) movement was larger than that of the anterior attachment, and in addition it was oppositely directed (anteriorly), [Table XI, Figure 31]. When the data for each subject were individually analyzed (see Appendix), it was found that for subject III (Figure 31 C), insertion 3 moved anteriorly during all three tasks, while insertion 4 moved anteriorly during balancing and incisal bite. In addition, for these two tasks insertion 4 moved smaller antero-posterior (z) distances than 3. For subject IV (Figure 31 D), the insertions of aponeurosis IV moved anteriorly only during the balancing side bite. In this subject insertion 3 moved larger distances in the antero-posterior direction during the working and incisal bite tasks.

When the static-bite-tasks were compared against the chewing data, it was

Figure 31 Diagram illustrating the displacement trajectories of insertions of aponeuroses II and IV in living subjects. Diagram in (A) illustrates masseter muscle orientation. (B) illustrates displacements of the anterior (2) and posterior (1) insertion points of aponeurosis II, and anterior (4) and posterior (3) points of aponeurosis IV. The average trajectory movements of the insertions in four subjects are represented by two-dimensional vectors in the parasagittal plane. Displacements of insertions of subject III (C), and of subject IV (D) are shown separately. All trajectories are relative to the intercusp position (point of convergence), and represent working (W), balancing (B) and incisal bites (O) with the jaw opened by 10 mm.



found that all insertions had similar displacements at both incisal bite and at maximum opening in the chewing cycle. In contrast, at the maximum medial and lateral deviations of the mandible in the chewing cycle displacements were smaller than during static bites. During chewing, similar findings of the deep masseter (aponeurosis IV) insertion displacements were found (Tables XII and XIII). When compared against the skull data it was found that jaw movements in living subjects displaced greater distances in the supero-inferior direction and smaller distances medio-laterally.

3.2.2.3 Discussion

Although MR imaging has been used previously for muscle visualization (Koolstra *et al*, 1990; Lam *et al*, 1991; Ralph *et al*, 1991) and tracking devices have been used to measure jaw movements (Lundeen and Gibbs, 1982; Merlini and Palla, 1988; Hagiwara *et al*, 1993b), there have been no attempts to combine these techniques to study structure and function. Despite some limitations in the visualization of internal structures, especially muscle fibre orientation as discussed in an earlier section of this thesis, the method presented here should be useful for future work where the structure and function of muscles in individual subjects are to be evaluated. It could also prove to be extremely valuable in experiments in which regional electromyographic activity is simultaneously recorded, and the electrodes located relative to the internal muscle structure.

A limitation of the method, however, is that it does not take tissue (bone and muscle) deformation into account. It is known that the mandible deforms by different

Table XII Mean displacements and standard deviations of four insertion points of four subjects during right-sided chewing. Representative points were chosen from one typical chewing stroke from each subject. That is, the most lateral, medial and inferior points of the envelope. Displacements are measured relative to the intercuspal position and are expressed as orthogonal distances (in mm).

Task	Insertion Points				
	1	2	3	4	
Medial	x	-0.80 ± 0.95	-0.84 ± 1.12	-0.65 ± 0.82	-0.68 ± 0.89
	y	-2.59 ± 2.25	-3.45 ± 2.56	-3.23 ± 2.22	-3.73 ± 2.46
	z	-1.39 ± 1.46	-1.88 ± 1.42	-0.04 ± 0.70	-0.41 ± 0.66
Lateral	x	-0.91 ± 0.70	-1.04 ± 0.71	-0.78 ± 0.65	-0.84 ± 0.65
	y	-1.49 ± 1.48	-2.30 ± 1.96	-2.08 ± 1.72	-2.50 ± 1.90
	z	-2.11 ± 1.12	-2.69 ± 2.00	-1.08 ± 0.97	-1.42 ± 1.46
Open	x	-1.11 ± 0.98	-1.37 ± 1.12	-1.08 ± 0.79	-1.19 ± 0.73
	y	-4.02 ± 2.45	-5.81 ± 3.41	-5.51 ± 3.11	-6.51 ± 3.39
	z	-3.52 ± 1.30	-4.77 ± 2.22	-0.87 ± 0.61	-1.68 ± 1.34

Table XIII Mean displacements and standard deviations of four insertion points of four subjects during left-sided chewing. Representative points were chosen from one typical chewing stroke from each subject. That is, the most lateral, medial and inferior points of the envelope. Displacements are measured relative to the intercuspal position and are expressed as orthogonal distances (in mm).

Task		Insertion Points			
		1	2	3	4
Medial	x	0.97 ± 0.96	1.26 ± 1.08	0.89 ± 0.84	1.06 ± 0.93
	y	-1.97 ± 1.19	-2.52 ± 1.71	-2.42 ± 1.59	-2.67 ± 1.75
	z	-0.74 ± 0.72	-1.28 ± 1.55	-0.06 ± 0.86	-0.39 ± 1.10
Lateral	x	0.73 ± 1.28	0.96 ± 1.53	0.74 ± 1.19	0.91 ± 1.25
	y	-2.99 ± 2.23	-3.68 ± 2.51	-3.55 ± 2.31	-3.93 ± 2.47
	z	-0.49 ± 1.05	-0.99 ± 0.91	0.61 ± 1.02	0.25 ± 0.77
Open	x	0.65 ± 1.22	1.08 ± 1.73	0.78 ± 1.27	1.01 ± 1.43
	y	-4.79 ± 3.22	-6.70 ± 4.36	-6.47 ± 4.16	-7.52 ± 4.45
	z	-3.18 ± 1.20	-4.80 ± 1.17	-0.34 ± 1.67	-1.33 ± 1.03

amounts during maximum isometric clenching, depending on the task performed (Korioth, 1992). The method presented in this segment of the thesis, however, is based on the assumption that the mandible is a rigid structure, and does not correct for mandibular deformations that might occur during function. Mandibular deformations are, however, small relative to movements (approximately 1 mm at the gonial angle during unilateral maximum clenching at the molar teeth region; i.e. approximately one fifth of the attachment movement). Although it is possible that the reduced amount of insertion displacement observed during chewing is the result of an estimation error rather than a different strategy used by the subjects to perform the different tasks, it is not likely. In addition, it can be argued that muscle activity seldom achieves maximum levels during gum chewing, and that deformations at submaximum levels should be minimal (less than 1 mm at the mandibular angle).

During function, it is possible that the intramuscular structures are deformed differently according to task. A possible approach to test for this potential deformation would be to image each subject repeatedly with the mandible at different positions. The drawbacks to this approach are the length of imaging time, which precludes imaging the muscle at sustained maximum contraction, and imaging costs. An alternative approach might be to image the muscle at different jaw positions with ultrasound. Here it remains to be seen whether the resolution is adequate for the recognition of internal muscle structures.

When compared against the skull data, there was a tendency for the insertion sites to displace greater distances in the infero-superior direction and smaller distances

medio-laterally. This might be explained by the need for more vertical-directed, bite-force vectors during natural acts performed by living subjects than during those simulated in the skull sample. An alternative explanation for these differences could be the sample populations (i.e. East Indian skulls versus the Mongoloid morphology of the living subjects, who were Japanese). Additionally, if a distinct "bolus hardness" had been used instead of the chewing gum, the dimensions of the chewing envelope could have been different, possibly approaching those in the skull study.

As previously discussed by Van Eijden and Raadsheer (1992) and consistent with the skull study, the deep masseter insertion sites behave differently from the other muscle attachment areas. When the mean data from the living subjects are analyzed (Table XI), it can be noted that while the posterior insertion point of the deep masseter moves forwards, the anterior insertion displaces backwards. If the fibres in this muscle portion are arranged parallel to each other in the sagittal view, it would seem that this muscle portion might twist longitudinally during function. It is known, however, from anatomical dissections (Figure 11) that this portion of the muscle is fan-shaped. It could be argued therefore that insertion displacement runs parallel to muscle fibre orientation, which differs from the anterior to the posterior portion of the deep masseter. It could be also proposed that the deep muscle portion is structurally and functionally compartmentalized into anterior and posterior regions. Additionally, when individual subjects are analyzed (see Appendix), muscle fibre orientation may vary between subjects, being more vertical in some subjects than others. These propositions however, cannot be proven with the present technology, since imaging methods with sufficient

resolution to identify muscle fibres are unavailable.

In conclusion, the data obtained from the skull sample generally match the insertion displacement measured in the small sample of living subjects. While they are only an approximation, they offer the advantage of estimating probable insertion movements from a large sample. On the other hand, measurement of attachment movement in living subjects as demonstrated in this thesis opens up the possibility of evaluating "true" insertion displacements relative to regional muscle activity. From both studies, it can be suggested that the masseter is a multifunctional muscle having regions which are best suited to certain tasks. For example, it is proposed that the masseter contributes mostly to jaw movement when the muscle is on the balancing side during chewing, while it generates interocclusal, crushing forces when it is on the working side. In addition, the deep masseter has different lines of action, varying biomechanically antero-posteriorly. Finally, the study also confirms the feasibility of making high-resolution muscle reconstructions and of locating the tendinous insertion sites on the mandible which can then be tracked with six degrees of freedom. This method could be used to estimate insertion displacements in other muscles and in any motor control studies where it is important to measure insertion displacement and muscle activity simultaneously.

3.3 Evaluation of the Masseter's Functional Performance

3.3.1 Electromyographic Recording Techniques

Electromyography (EMG) is a method commonly used to study the electrical activity of skeletal muscles arising from voluntary or involuntary contractions. The myoelectric signal originates in the depolarization of the muscle-cell membrane to the threshold level resulting in an action potential (AP), which is generated and propagated along the muscle fibre.

Conventional needle EMG techniques do not record single-muscle-fibre APs, but rather potentials generated by the near synchronous depolarization of many muscle fibres in a single-motor unit (MU) which summate to form a compound AP. The characteristics of the compound APs may vary significantly depending on the anatomical and physiological properties of the MU muscle fibres, the control scheme of the peripheral nervous system, the temperature of the muscle, the age of the subject, the distance between the active muscle fibre and the recording sites, the chemical properties of the metal-electrolyte interface, as well as the characteristics of the instrumentation that it is used to detect and observe them (Daube, 1978; Gath and Stålberg, 1975; Lenman and Ritchie, 1987; Stålberg and Trontelj, 1979). Various characteristics of the MU compound AP can be described both qualitatively or quantitatively. These include peak-to-peak amplitude, number of phases, duration, number of turns, area, and pattern of firing (Nandedkar and Sanders, 1989; Stålberg and Trontelj, 1979), and are useful in the diagnosis of a number of muscle disorders (Daube, 1978; Stålberg and Trontelj, 1979).

When several MUs are firing, the random temporal and spatial superposition of their APs produce a complex myoelectric signal, known as interference pattern EMG. This type of myoelectric activity is commonly recorded in kinesiological studies which have utilized surface or bipolar fine-wire electrodes based on the original design described by Basmajian and Stecko (1962). To evaluate these complex signals, various analytical techniques are available. These include integration, frequency analyses, turns counting, zero-crossing analysis and analyses of the degree of superimposition (Richfield *et al*, 1981).

3.3.2 Preliminary Experiments using Single-Wire EMG Recording Technique

Since the human masseter muscle can be divided into at least four anatomical compartments innervated by separate main branches of the masseteric nerve (the anterior and posterior regions of the superficial masseter, and the anterior and posterior regions of the deep masseter), it is possible that at least some functional differentiation occurs between them. It has long been known that selective contraction of fibre groups is found in the masseter muscles of pig (Herring *et al*, 1979), rabbit (Weijs and Dantuma, 1981) and to a certain extent in man (Belser and Hannam, 1986). Although surface electrodes are commonly used to record activity in human masticatory muscles, they are not selective enough to sample regions within a muscle. Concentric-needle electrodes or bipolar-wire electrodes are more appropriate for this purpose but have their limitations. Needle electrodes are impractical in mobile jaw muscles which are activated during mastication and tooth grinding, and paired-wire electrodes rarely maintain a consistent

spacing between the bared electrode tips (Jonsson and Bagge, 1968; Loeb and Gans, 1986). It has been suggested that offset twist hooks are suitable for pennate muscles, reducing the possibility that the contacts will short and providing a more predictable interelectrode distance (Loeb and Gans, 1986). However, the insertion of bipolar wire electrodes in a muscle does not always guarantee an interference signal of predictable quality or range of pick-up, and variations in the sample volume from which electrical activity is recorded may result in poor reproducibility (Kadaba *et al*, 1985; Komi and Buskirk, 1970; Perry *et al*, 1981). This has led to the proposal that unipolar wire electrodes should be considered as an alternative (Kadaba *et al*, 1985).

The aim of this study was to provide focal multiunit EMG at data collection rates which would be manageable for data storage, and which would be reliable for the future investigation of functional masseter subdivisions. The long-term goal was to test the hypothesis that the human masseter muscle is divided into at least three neuromuscular compartments, based upon the assumption that differences between the anterior and posterior portions of the superficial masseter were unlikely due to their common fibre orientations.

3.3.2.1 Materials and Methods

Each single-wire electrode was constructed from Teflon-coated stainless-steel wire, 0.075 mm in diameter (Medwire Corp, Mount Vernon, NY). The recording area was obtained by carefully stripping the Teflon coat off the tip of the wire strands to avoid nicking the wire, then warming the remaining teflon against a soldering iron to

produce a smooth, continuous border between the bared tip and the insulated part of the wire, and cutting off the bared tip so that it was 1 mm long (Loeb and Gans, 1986). This end was then bent to form a 2 mm hook, which should anchor the wire in position. The wire was inserted percutaneously into the muscle with the aid of a 27 gauge hypodermic needle. The electrode is designed to combine symmetrical, omni-directional properties with a decreased shunting effect (due to its large tip size) in order to record high-amplitude, high-frequency, intramuscular signals. A conventional skin-patch electrode, 30 x 15 mm (Lec Tec Corp, Minnetonka, MN) was fixed to the skin overlying the muscle and was used as the indifferent. The signals from both electrodes were differentially amplified using a bandpass filter with -3 dB roll-offs at 300 and 3000 Hz. At maximal muscle contraction, the spectral peak of surface EMG recorded from the masseter muscle is about 78 Hz, although with lesser degrees of activation a second peak may appear around 130 Hz (Palla and Ash, 1987). These components are, therefore, removed by bandpass filtering. The myoelectric signals are then sampled digitally.

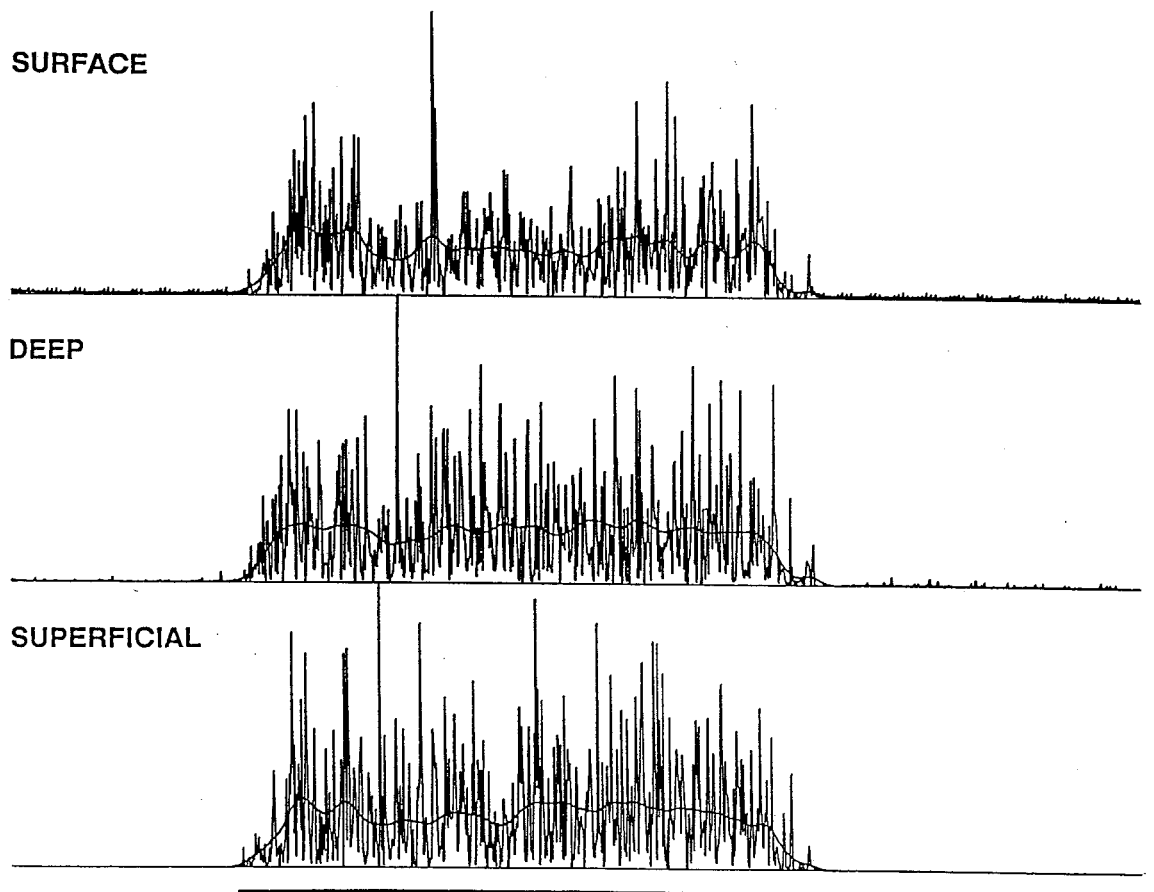
To evaluate whether this system would be useful for quantifying regional activity in the jaw muscles, the following protocol was used. Two single-wire electrodes were inserted into a subject's right masseter muscle. One was placed approximately 10 mm into the superficial body of the muscle and the other about 12 mm into the preauricular trigonum to reach the muscle's deeper, posterior fibres. The determination of the wire location was based on known differences in the anatomical sites of superficial and deep parts of the masseter muscle and direct palpation. Individual patch surface electrodes were placed on the overlying skin in each case. Although a common

indifferent surface electrode could have been used, it was found that separate electrodes yielded improved signal to noise ratios. For comparative purposes, a pair of silver surface electrodes (Grass Instrument Co, Quincy, MA) were placed 20 mm apart over the centre of the muscle. A ground electrode was fixed to the back of the neck. All signals were amplified differentially (AI 2130 amplifiers, Axon Instruments Inc, Burlingame, CA) using bandpasses from 300-3000 Hz (wire electrodes) and 30-1000 Hz (surface electrodes).

The subject was asked to carry out a series of brief tooth-clenching tasks designed to differentially activate the two regions of the muscle. These tasks consisted of maximum clenching with the teeth in full intercuspation, with efforts directed vertically (perpendicular) to the plane of dental occlusion, anteriorly (protrusively) and towards the left and right sides.

The signals were sampled every 0.1 msec by a data acquisition system and microcomputer (HP 3852 A and HP 350, Hewlett-Packard Canada, Vancouver, Canada) over manually triggered sampling periods of 2 seconds. For each electrode, the data recorded for each task carried out were rectified and smoothed with a low-pass Butterworth digital filter at 10 Hz cut-off frequency as shown in Figure 32 (Scott *et al*, 1983). These data were then normalized to the maximum value recordable from that electrode irrespective of task. One hundred data values representing the task epoch (between 400 and 1500 msec of the sampling period) were downloaded to a microcomputer for graphical display and statistical analysis. Data from the three different muscle sites were displayed in an X,Y plot in order to test their relationship

Figure 32 Rectified, digitized data from three muscle sites, obtained during a vertically oriented maximum tooth clench. Smoothed waveforms resulting from a 10 Hz digital Butterworth filter have been superimposed in each case. The task epoch is defined by the horizontal bar. The horizontal calibration bar represents 200 msec, and the vertical bar represents 360 μ V, 510 μ V and 500 μ V for surface, deep and superficial muscle regions respectively.

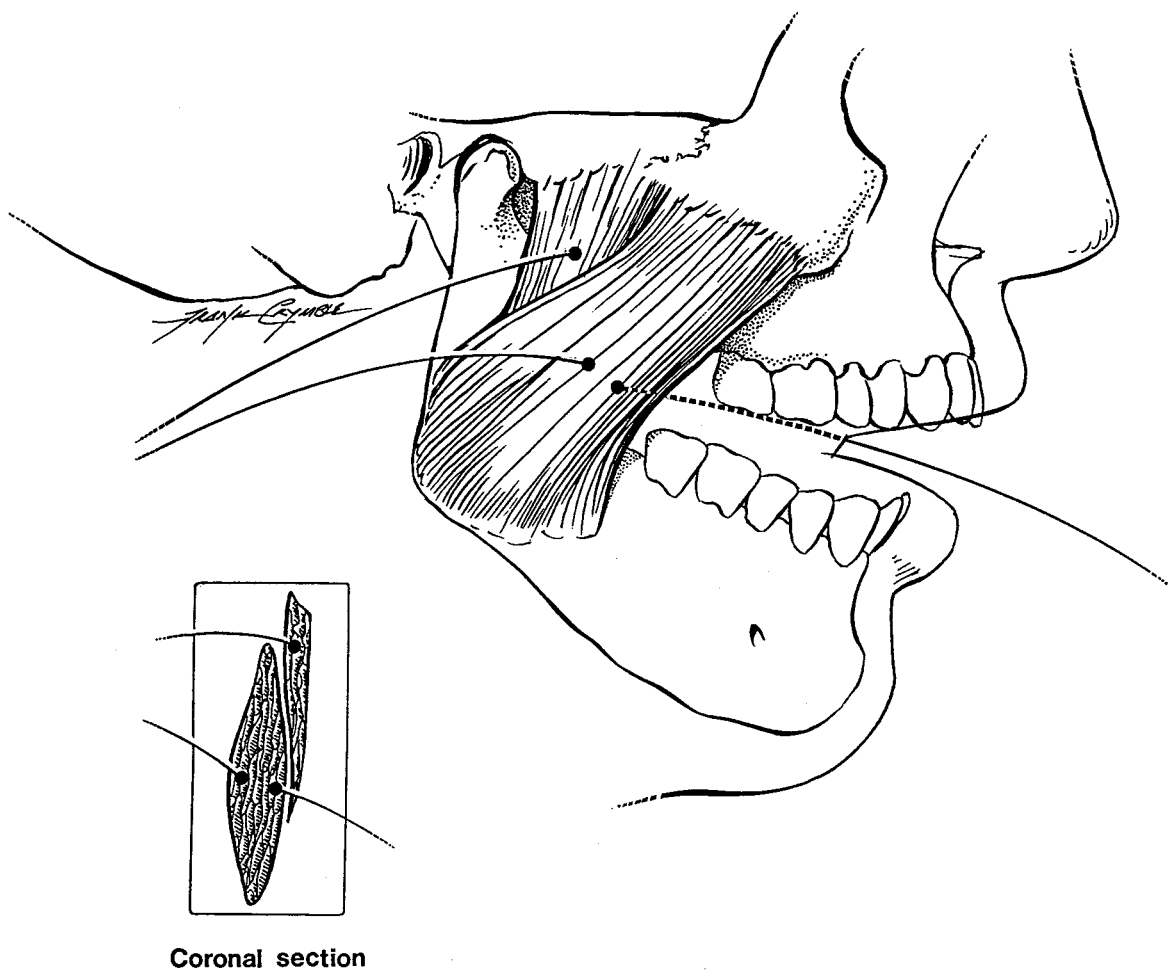


by means of linear regression. This test was chosen since regions of the muscle which behaved identically would be expected to show linearly related responses for the same task, and a regression line with a zero intercept and a slope of unity.

To test the hypothesis that the human masseter is divided into at least three functionally separate regions, three single-wire electrodes were inserted into the subject's right masseter muscle during a separate recording session. One was placed approximately 5 mm into the deep portion of the muscle via an intra-oral approach. The loose end of the wire was then fixed against the upper canine tooth to avoid the possibility of the subject biting on it. The second wire was placed approximately 12 mm into the preauricular trigonum to reach the muscle's deep posterior portion, while the third wire was placed about 10 mm into the centre of the inferior bulge of the superficial masseter (Figure 33). Individual reference patch surface electrodes were placed on the overlying skin, and a ground electrode was fixed to the back of the neck. Surface electrodes were placed 20 mm apart over the centre of the muscle. All signals were amplified and bandpass-filtered in the same fashion as described above.

The subject was again asked to carry out a series of brief tooth-clenching tasks designed to differentially activate the three regions of the muscle. These tasks consisted of maximum clenching with the teeth in full intercuspation, and with efforts directed vertically to the occlusal plane, posteriorly, anteriorly, towards the left and right sides, and towards the right antero-lateral side. In addition, the subject was asked to grind the teeth from the right canine edge-to-edge position, past the intercuspal position, all the way to the left canine edge-to-edge position, and then to grind again in the opposite

Figure 33 Illustration of the right masseter muscle in the lateral and frontal views, showing wire electrode location.



direction. Recorded signals were sampled and stored as previously described.

3.3.2.2 Results

Rectified, digitized data from the first test are shown in Figure 34 for all three electrodes both during rest and during three clenching tasks. Each record represents a single clench. The greatest amount of activity for both wire and surface electrodes was recorded when clenching was carried out perpendicular to the dental occlusal plane. A marked separation between superficial and deep masseter intramuscular responses was seen when efforts were directed towards the left and right sides. These responses were consistent with previous reports of masseter muscle behaviour (Belser and Hannam, 1986).

In Figure 35, X,Y plots of normalized muscle activity are shown. Although the deep and superficial muscle portions behaved similarly during the intercuspal tooth clench, the deep masseter muscle was almost exclusively active during a right-directed clench (on the ipsilateral side) while it was less active during a left canine tooth clench. The surface electrode preferentially selected activity from the superficial fibres of the muscle at low levels of contraction, but appeared to reflect activity from another source as contraction efforts increased (Figure 35), (Guld *et al*, 1973).

Figure 36 shows oscilloscope traces of muscle activity recorded from the anterior deep, posterior deep and superficial masseter regions, as well as activity recorded with a surface electrode during static clenches. As shown before, the greatest amount of activity for the wire and surface electrodes was recorded when clenching was

Figure 34 Rectified, digitized data from three electrode sites. The superficial and deep recordings were obtained from single-wire electrodes, and the surface record from bipolar silver discs. Rest activity 1) and maximum clenches were directed towards the right side 2), anteriorly 3) and vertically 4). Responses recorded from the skin surface and superficial parts of the masseter muscle have an increasing pattern of activity from 1-4, while the deep masseter muscle behaves differently. The horizontal calibration bar represents 400 msec, and the vertical bar represents 720 μV , 1030 μV and 1000 μV for surface, deep and superficial regions respectively.

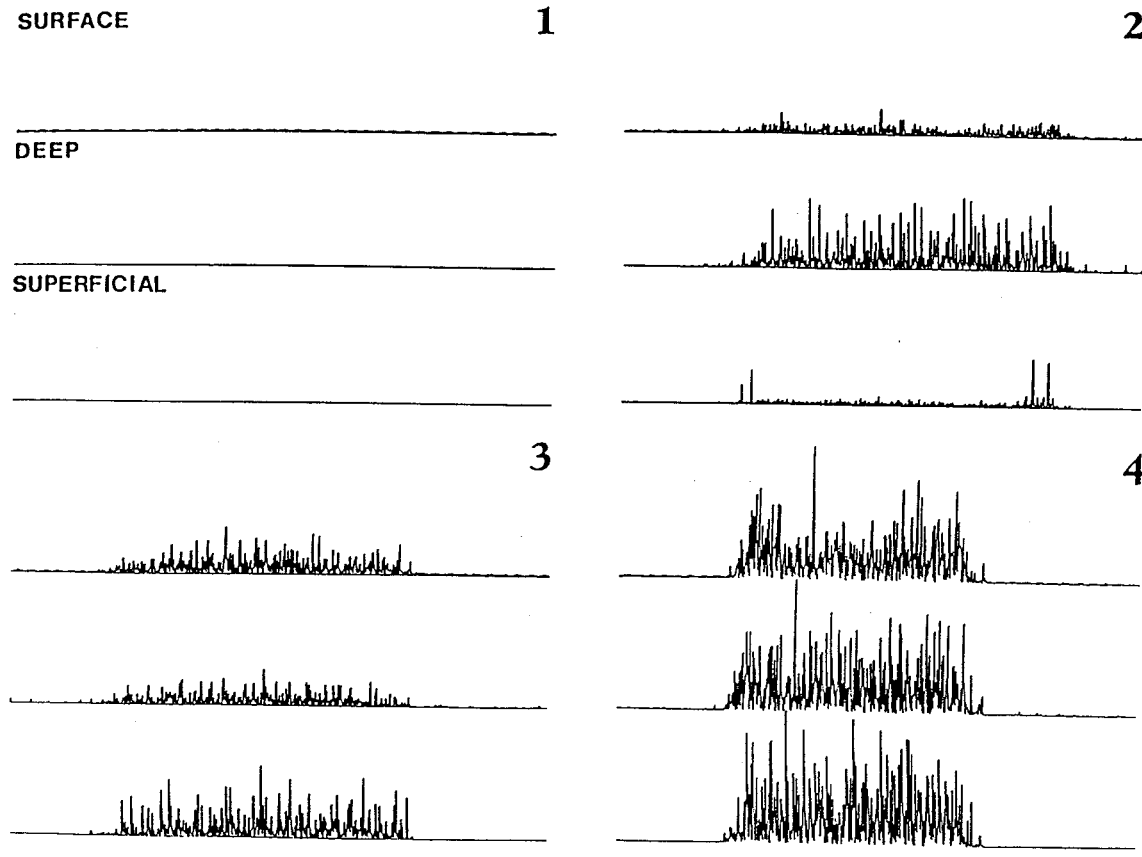


Figure 35 Smoothed, normalized data from three electrode sites plotted against each other for three representative tasks. In each case, the stippled line represents the ideal relationship between the two variables, assuming that they behave identically. The solid line represents a regression line fitted through 100 data points ($p < 0.001$). The graph in 4 represents the relationship between surface EMG activity and superficial masseter activity. Spm: superficial masseter; Dmm: deep masseter muscle; Sfm: surface masseter.

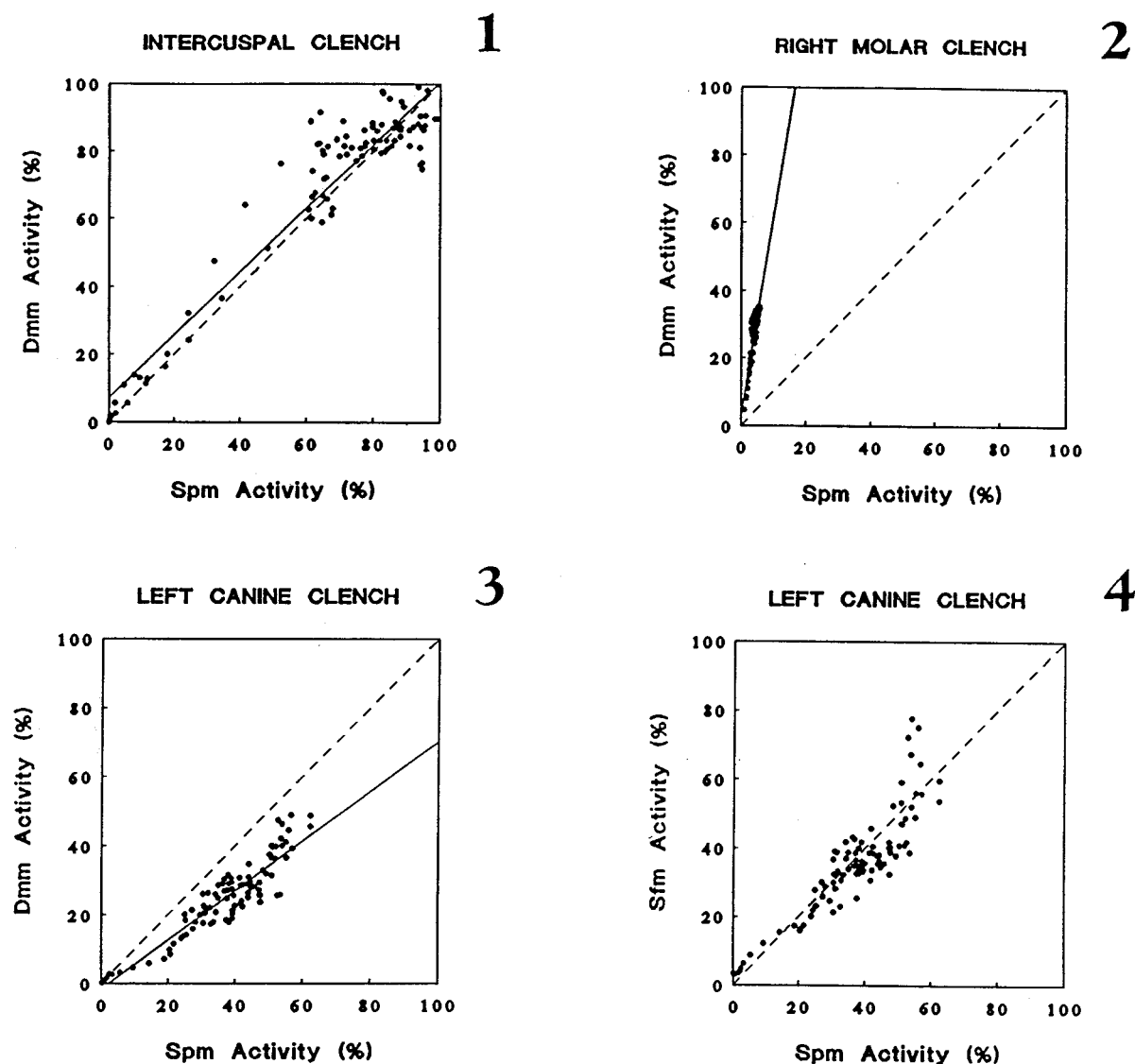
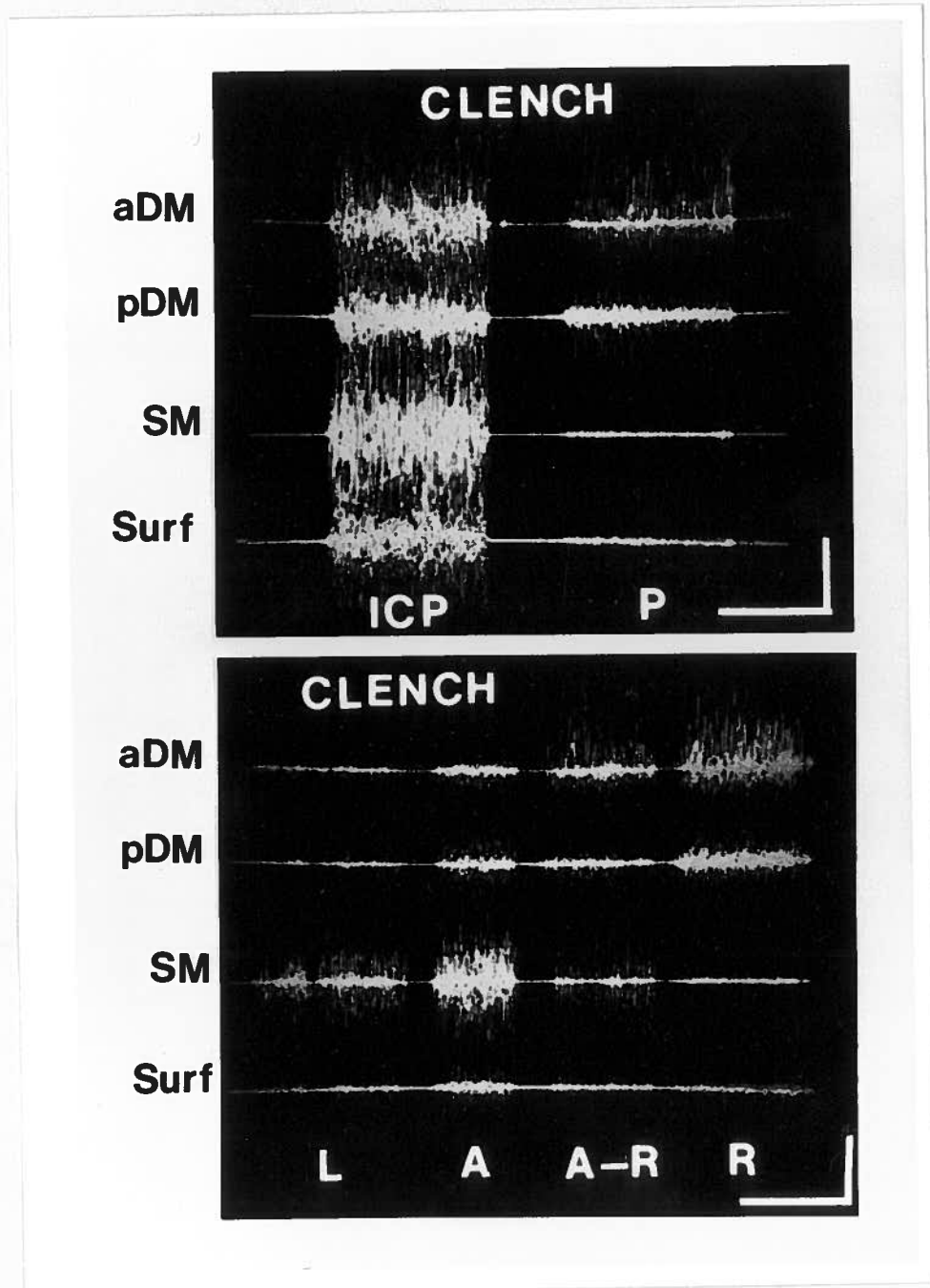


Figure 36 Raw data from four muscle sites, obtained during different clenching tasks. The horizontal calibration bar represents 200 msec, and the vertical bar represents 500 μ V. Tasks are intercuspal position (ICP), posterior (P), left (L), anterior (A), antero-right (A-R), and right (R) clenches. aDM: anterior deep masseter; pDM: posterior deep masseter; SM: superficial masseter; Surf: surface electrode recording.



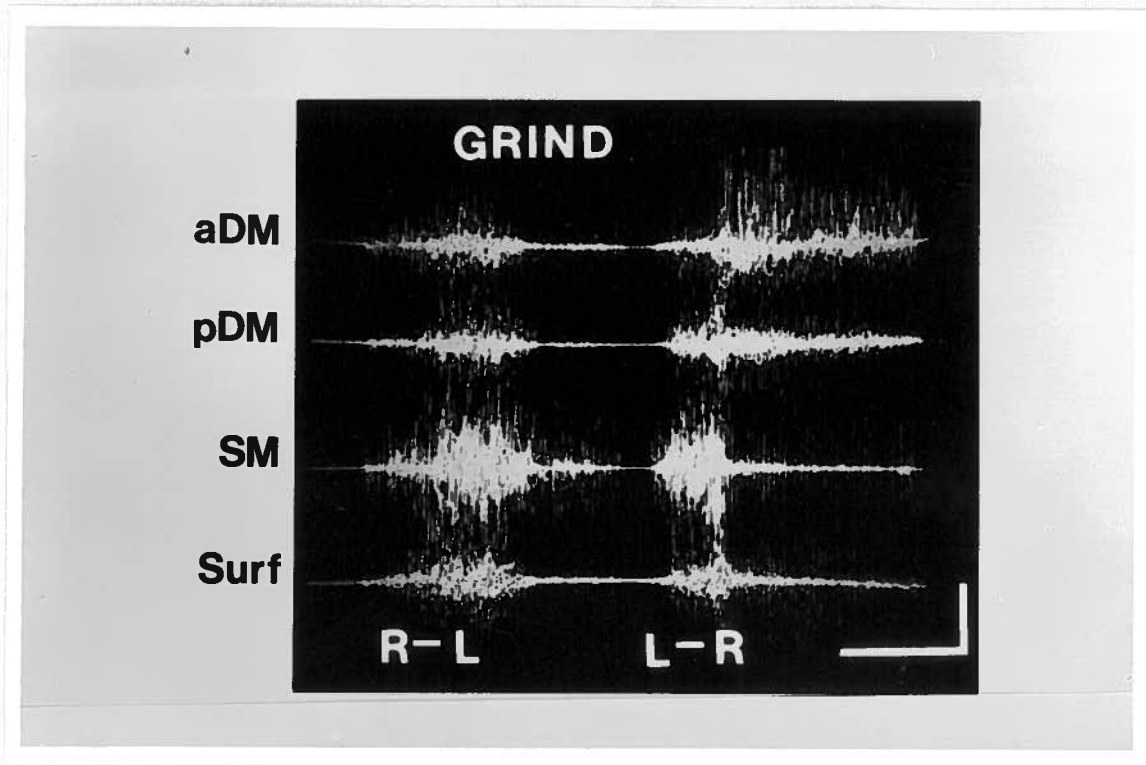
carried out in the intercuspal position. Both anterior and posterior deep masseter regions were active during posterior- and right- directed clenching, while the superficial masseter was almost silent. In contrast, during left- and anteriorly- directed clenching, the superficial masseter was more active than the other regions. During the right antero-lateral clench, the distinction between muscle regions was not so obvious. During this task, and to a lesser extent during the right lateral clench, the anterior deep region was more active than the posterior deep masseter.

Figure 37 shows oscilloscope traces of muscle activity recorded with all three wire and surface electrodes during two dynamic tasks. Maximum myoelectrical activity is obtained at the centre of each burst, approximately when the teeth are in the intercuspal position. At the beginning and end of a left- directed grind, the superficial masseter is more active than the other muscle portions, especially when the teeth approach the contralateral (left) canine edge-to-edge position. Initially during the right-directed grind, rapidly increasing muscle activity is observed in the superficial masseter. At the interocclusal position, slightly more activity is seen in the posterior than in the anterior deep masseter. Towards the end of the grind (ipsilateral side), the myoelectric activity pattern reverses. The posterior deep masseter shows the highest level of activity followed by the anterior deep portion. Almost no muscle activity can be seen in the superficial masseter at this point in the movement.

3.3.2.3 Discussion

The single-wire approach for recording jaw muscle activity avoids the

Figure 37 Raw data from four muscle sites, obtained during two distinct grinding movements. The horizontal calibration bar represents 200 msec, and the vertical bar represents 500 μ V. Tasks are two grinding strokes from the right canine edge-to-edge position to the left canine edge-to-edge position, and from the left canine edge-to-edge position to the right canine edge-to-edge position. Abbreviations are the same as in Figure 36.



reproducibility problem posed by variable interelectrode distances commonly associated with conventional bipolar wire electrodes. While the regional selectivity here demonstrated is theoretically less than that for paired-wire systems, it seems to be sufficiently focal to distinguish major muscle subgroups. The signals consist mainly of multiunit interference patterns, although single MUs can occasionally be identified. The peculiarity of the technique permits several different analytical procedures, e.g. turn analyses and estimations of integrated activity, in addition to the low-pass digital filter demonstrated here. Although the approach described produces interference signals not unlike those of surface electromyograms and can be analyzed in a similar fashion, it does not share their wide-field sampling characteristics, and the signal-to-noise ratio obtained is consistently good due in part to the low-frequency cut-off. At low levels of muscle contraction however, single-wire electrodes, like bipolar indwelling electrodes, tend to produce the clumped discharges of a few MUs and sometimes single MU spikes. Bursts with high frequency components and large interdischarge intervals are difficult to quantify reliably by the filtering and integrative techniques commonly used in interference EMG.

It has been often assumed that when bipolar fine-wire electrodes are selectively placed and closely spaced, APs are recorded from only a small population of active muscle fibres. In addition, when recordings are made differentially with high quality amplifiers, it is expected that the EMG records do not contain significant electrical activity from other sources, such as surrounding muscles (Loeb and Gans, 1986). It is known, however, that when muscle fibres contract, they produce action

currents which spread by volume conduction (resistive and capacitive) through all adjacent tissues (Gydikow *et al*, 1982; Loeb and Gans, 1986). Therefore, any indwelling EMG electrode may record APs from muscle regions other than the region under study. Although such "cross-talk" has been found to be minimal in some studies (Fetz and Cheney, 1980) recently it has been suggested that it could be quite significant, especially when records are made from small muscles or from small animals (Mangun *et al*, 1986; O'Donovan *et al*, 1985; Bawa *et al*, 1986). In an attempt to examine the extent of cross-talk in the cat lateral gastrocnemius, English and Weeks (1989) found that when a neuromuscular compartment was stimulated, small potentials resulting from passive conduction could be recorded in adjacent muscle compartments. Sometimes, the amplitude of the cross-talk signals recorded from the activation of large MUs could be as large as small units present in the compartment of residence. In addition, when electrodes were placed at compartment boundaries, no clear compartment selectivity was found.

In humans, it is very difficult to evaluate the extent of signal contamination by cross-talk. While direct neural stimulation of the masseteric nerve (Dao *et al*, 1988) and concomitant recording of different muscle regions are theoretically possible, it is presently difficult to stimulate a nerve branch which clearly innervates a single muscle compartment. Another approach could be to stimulate a group of muscle fibres directly, and record from different muscle areas in order to demonstrate "cross-talk". In this thesis, however, such lines of investigation were not pursued.

In conclusion, even though fine-wire electrodes may be extremely useful in

kinesiological studies, they have limitations. Their advantages include the fact that these electrodes are extremely fine and therefore almost painless, they remain in place during jaw movements and strong muscle contractions, and their electrode tip can be adapted for broad or focal pick-up area (i.e. interference-pattern or single-MU EMG studies) within a specific muscle region. In addition, if Teflon-coated silver wires are used they could be located three-dimensionally when detected by a combination of frontal and lateral radiographs. However, precautions need to be taken in the design of experiments in which wire electrodes are used to study various masseter regions simultaneously, due to the potential for cross-talk.

During the course of this investigation, an extensive interference EMG study of regional activity in the human masseter was published by Blanksma *et al* (1992). These workers used multiple paired-wire electrodes inserted into six regions of the muscle, and concluded that the masseter can certainly be divided functionally into superficial, anterior deep and posterior deep parts, and possibly additional ones. The limitations of the paired-wire approach and its analysis however have already been discussed. Similar limitations disclosed by the present study argue for the use of a more discriminatory approach for recording focal muscle activity in the masseter. Since the single MU represents the most discrete functional entity within the muscle, it was decided to pursue further physiological studies at this level, and to avoid the quantitative problems associated with the analysis of multiunit discharges.

3.3.3 Motor-Unit Behaviour

The goals of these investigations were to develop methods for recording MU activity associated with different voluntary oral tasks, and to establish the reproducibility of the measurements under controlled experimental conditions. Since the long-term aim was to compare the behaviour of a population of units selected from different parts of the masseter during the performance of various physiological tasks, it was considered important to confirm that stable measurements of MU performance were possible.

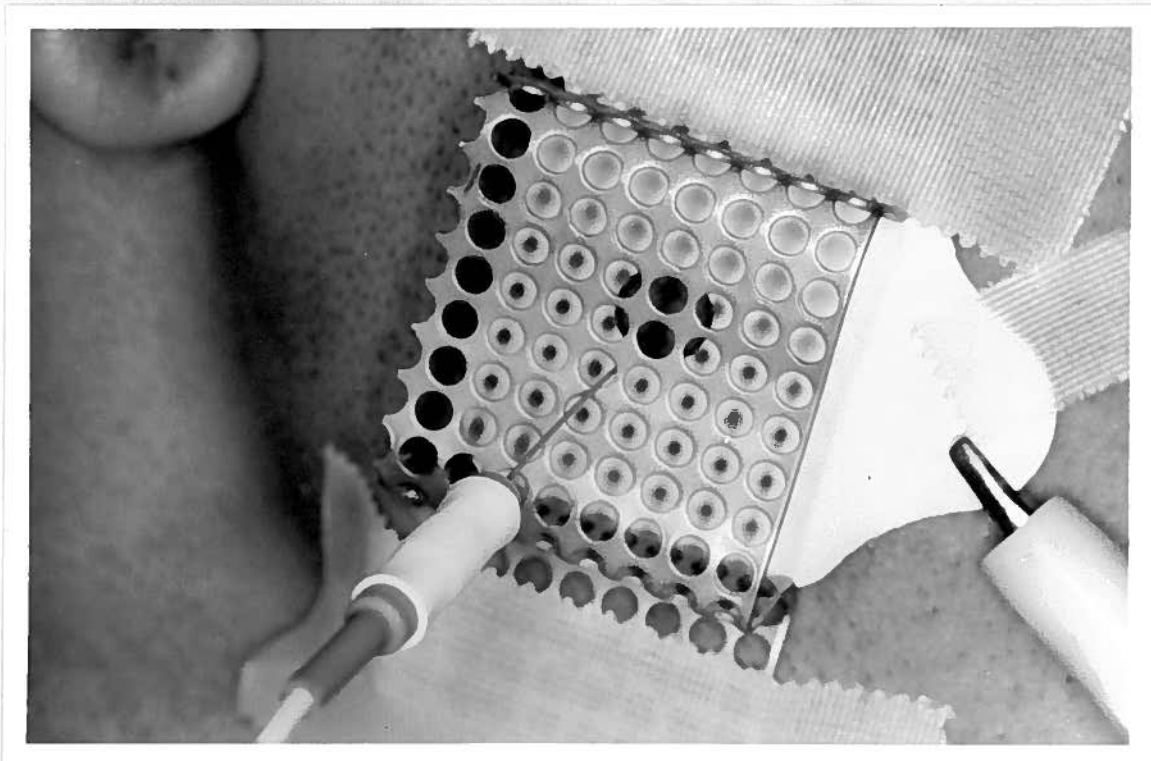
3.3.3.1 General Methods

3.3.3.1.1 Motor-Unit Recording

Activity from multiple low-threshold motor units (MUs) located in the central part of the superficial right masseter muscle was recorded with monopolar needle electrodes (MF37, TECA Corp, Pleasantville, NY) from eight healthy adults. These needles were made of stainless steel, measuring 0.35 mm in diameter (28 gauge) and 37 mm in length. With the exception of the electrode's conically-sharpened recording tip (area = 0.12 mm²), the needle was insulated with Teflon. A surface reference electrode (SynCor, Lec Tec Corp, Minnetonka, MN) was placed over the masseter muscle. A second surface patch-electrode was fixed to the back of the neck to act as a ground.

During each session, the needle was inserted percutaneously at right angles to the skin surface, and its hub supported by an extraoral framework to stabilize the electrode's position (Figure 38). Subjects were asked to lightly activate the masseter (less than 10% of maximum voluntary contraction), while the needle was gently moved

Figure 38 Motor-unit recording technique in the masseter muscle. A surface patch-electrode with a hole in its centre is attached to the skin overlying the right masseter muscle to act as a reference. A perforated metal platform is positioned over the patch-electrode and fixed to the skin by adhesive tape. A monopolar needle is then inserted into the muscle through the reference electrode's perforation, and stabilized *in situ* by the platform.

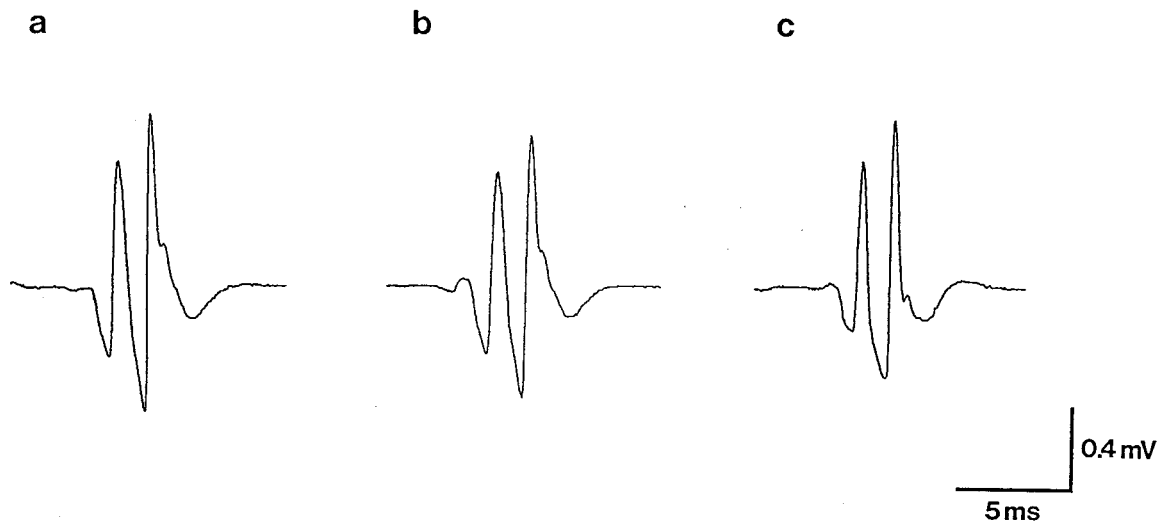


inwards and outwards along a medio-lateral trajectory until an action potential was obtained. These were amplified and bandpass-filtered between 300 Hz and 5 kHz (Model A1 2010, Axon Instruments, Burlingame, CA). Furthermore, the signals were modulated with a variable gain control to allow continuous adjustment of spike amplitude prior to high-speed sampling.

Although it has been postulated that physiological signals may have high-frequency components up to 30 kHz, spectrum analysis of the action potential generated when a single cell depolarizes indicates that essentially all of the signal is produced within the frequency domain from DC to 10 kHz. Since compound-action potentials (CAPs) are the sum of several single-cell action potentials, the frequency domain of extra-cellular physiological signals should be equal or less than the frequency domain of the single-cell action potential. Hence, monitoring CAPs with amplifiers at the bandwidth of DC to 10 kHz should be adequate. The signal components of a single MU CAP is also determined by the type of EMG electrode being used to record them, by the distance between the recording area and the active muscle fibres, and by volume conduction. Because of this latter property, slow-frequency components on an EMG record may have in fact been originated in quite distant regions (Stålberg and Trontelj, 1979). For this reason, low-cut filters have been successfully used to improve the selectivity of EMG recordings, while still preserving important waveform components of the CAPs (Gath and Stålberg, 1976; Stålberg and Trontelj, 1979).

In the masseter muscle, an amplifier bandwidth of 300 Hz to 10 kHz has been considered potentially useful when monopolar needle electrodes are used in experiments

Figure 39 Effects of different bandpass-filters on a single MU waveform shape. CAPs of a masseter muscle unit were averaged ($n = 16$) for the display of waveform changes due to different amplifier bandpass-filter settings. In (a) the bandwidth was 10 Hz - 10 kHz, in (b) 10 Hz - 5 kHz, and in (c) 300 Hz - 5 kHz.



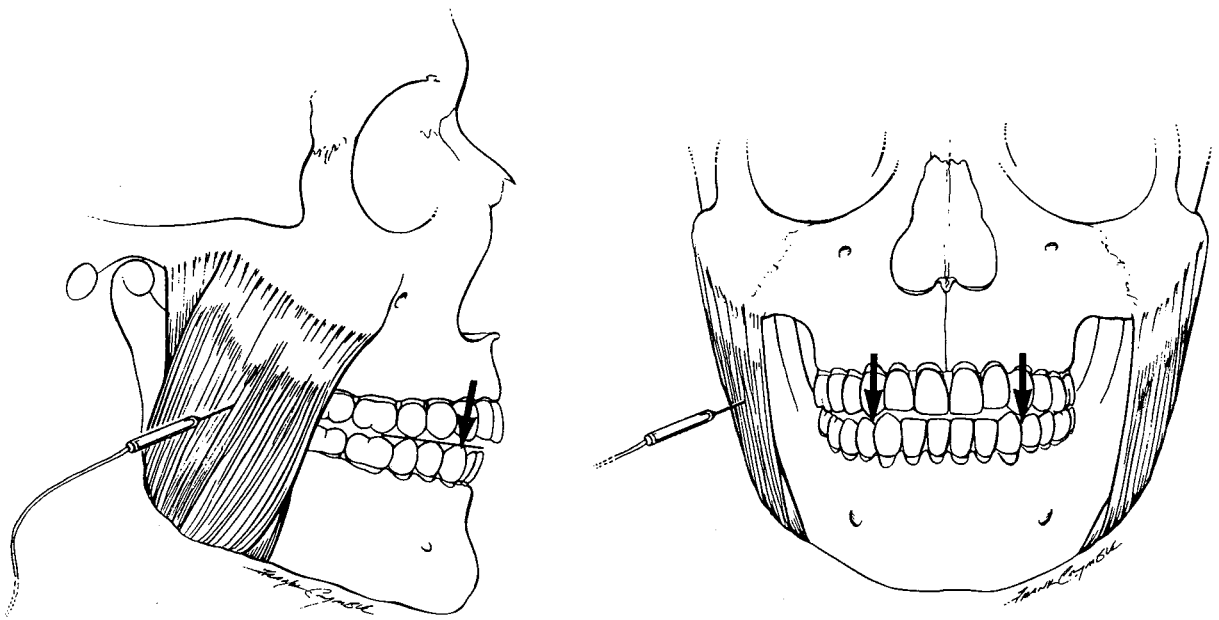
requiring quantification of unit firing patterns (McMillan, 1989). This filtering procedure yields a good signal-to-noise ratio and preserves an adequate definition of waveform singularities for spike interval analysis. In the present work, digital sampling rates were restricted to a maximum of 12 kHz. Hence, the high-cut filters were lowered to 5 kHz to avoid the problem of aliasing during sampling.

Changes in the waveform shape of a CAP, recorded from a continuously firing masseter single MU in a normal subject when the filter settings were changed, are shown in Figure 39. When the high-cut filter setting was altered from 10 kHz to 5 kHz with the low-cut filter remaining constant at 10 Hz, the amplitude of the signal did not lower substantially, nor did high frequency components change dramatically. When the low-cut filter was changed from 10 Hz to 300 Hz, while the high-cut filter was maintained at 5 kHz, almost no change in signal amplitude was observed although slower frequency components were reduced. These findings are in agreement with previous reports (Stålberg and Trontelj, 1979; McMillan, 1989), and the change to a lower high-cut filter was not considered to affect either the signal-to-noise ratio or the signal waveform seriously.

3.3.3.1.2 Bite-Force Measurement

Study casts were obtained for each subject and mounted on a Denar Mark II semi-adjustable articulator (Denar Corporation, Anaheim, CA). These were used to construct a bite force device which could be inserted between the teeth with minimum jaw separation. The device included a strain-gauge transducer, which fitted a slide-in

Figure 40 Sagittal and frontal profiles of the skull showing location and orientation of bite force measurements. The MU recording site is indicated by the monopolar needle electrode inserted into the right masseter muscle, portrayed in the sagittal and frontal views. The functional occlusal plane is illustrated as a straight line in the sagittal view, and the location and orientation of the force measurements are pictured in arrows. Note that the mandible is rotated in a minimal jaw opening at the midline, and that the biting forces are applied perpendicular to the functional occlusal plane.



acrylic housing cemented to the mandibular canine tooth, and an opposing acrylic platform cemented to the maxillary canine. The device was customized to each subject, so that isometric biting forces could be recorded perpendicular to the occlusal plane at the right and left canine teeth with the jaw positioned in the midline (Figure 40).

The strain-gauge transducer was built with two parallel stainless steel bars, measuring 1.5 mm in thickness and 13 mm in width. An overload stopper was incorporated between the bars, separating them by 3 mm and creating a 30 mm long cantilever. Two strain-gauges with 120 Ohm resistance were mounted on opposite sides of one of the bars (beam) at the portion that is subject to bending strain. Under these conditions, when force is applied, one strain gauge is subjected to tensile strain while the other experiences compressive strain. Since both gauges are affected by intra-oral temperatures in the same way, the bridge remains balanced for temperature variations and the gauges provide twice the sensitivity of one gauge for beam deflections.

To ensure a uni-directional force application through a constant point on the transducer, a spherical load point was permanently fixed to the sensor. Calibration studies were performed to determine the reproducibility and linearity of the transducer. A bench-mounted calibration system permitted various loads to be applied to the transducer (Universal Testing Machine, Instron Model 4301, Canton, Mass). The transducer was capable to record forces up to at least 30 N, although the working range of canine bite forces sufficient to activate single MUs was consistently less than 10 N (Figure 41).

All forces were recorded with the strain-gauge transducer, which could be

Figure 41 Calibration of the force transducer. Force in Newtons (N) plotted against voltage (V) for a series of loads applied perpendicular to the force transducer. A linear regression line was fitted through the plotted values.

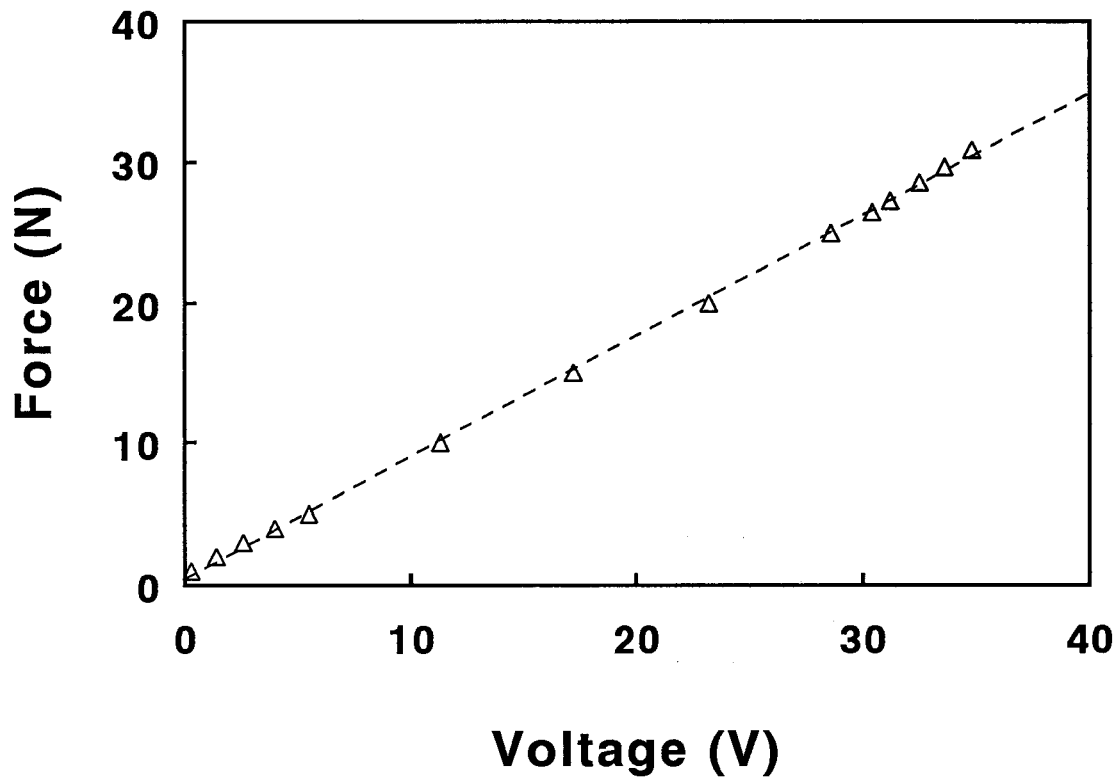
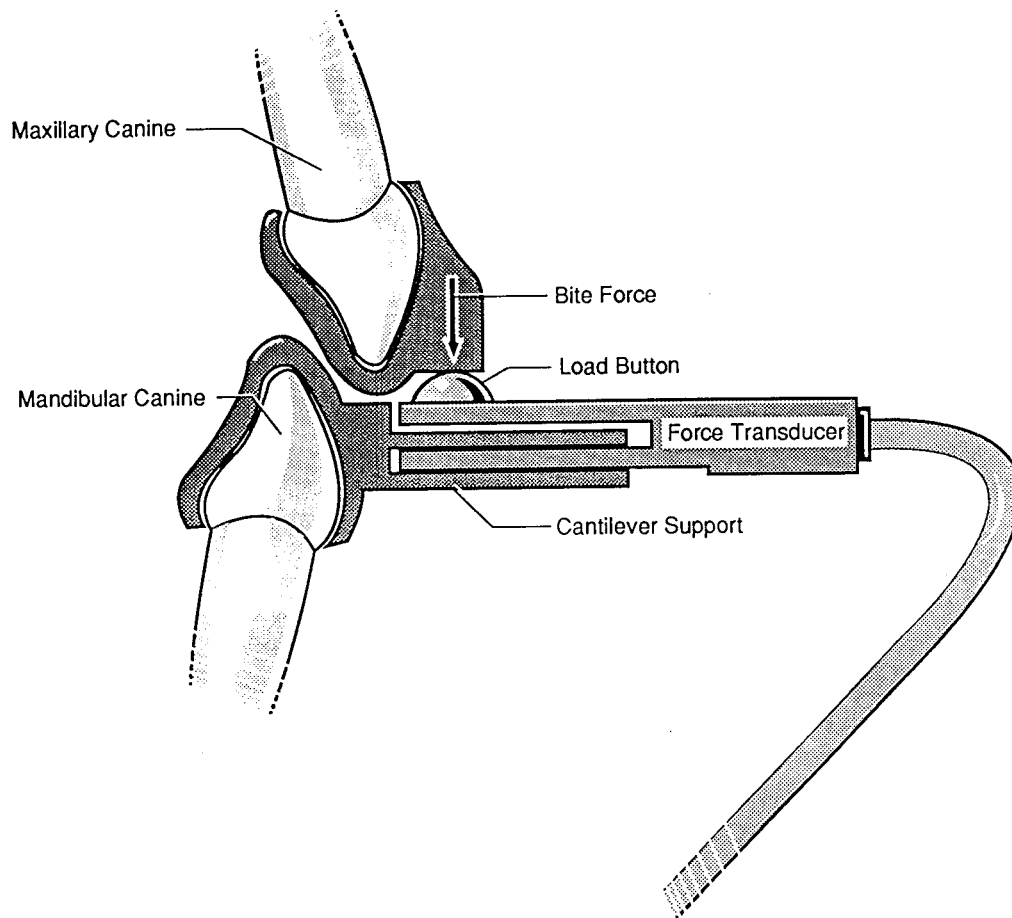


Figure 42 Illustration of the Bite Force Transducer in situ. The device was slid into a metal sleeve within the cantilevered support of the mandibular canine tooth housing. The position of the load button was constant with respect to the opposing maxillary housing. Matched copings were made for the canine teeth on the right and left sides.



housed in either of two customized, labially-cantilevered supports temporarily cemented bilaterally on the mandibular canine teeth at minimum occlusal separation (5 mm measured at the incisors). Its spherical load point opposed a flat platform on matching supports on the respective opposing teeth (Figure 42). Thus it was possible to change the laterality of contact while still using the same sensor. Force signals were amplified with a carrier amplifier (Tektronix Inc, Beaverton, Ore) and bandpass-filtered between DC and 300 Hz.

3.3.3.1.3 Sampling and Data Analysis

MU activity and bite force were initially sampled simultaneously onto tape (Unitrade, Data Acquisition and Storage System) at 48 kHz, and then sampled off-line at 12 and 1 kHz, respectively, by a data acquisition and microcomputer system designed for this purpose (Discovery, Brainwave Systems Corp, Denver, Co). Individual records were analyzed off-line to determine the firing pattern, recruitment threshold and sustained force levels of all the single units recorded during the separate tasks. For this purpose a combination of commercial software (Discovery, Brainwave Systems Corp, Denver, Co) and custom-written software was used. Motor-unit CAPs in each record were discriminated by the identification and discrimination of waveforms with different shapes. The method is based on extracting waveform parameters (i.e. peak amplitude, valley amplitude, spike height and width, template match, etc.) for each waveform. These can then be used to describe the difference between various groups of waveforms by displaying various combinations of waveform parameters in X/Y point plots. Waveforms

which share similar features form "clusters" of points on these X/Y point plots. These clusters are then assigned into different groups (or MUs) for further analysis. Spike trains were then examined visually for reliability. Data were rejected if more than 5 spikes were unclassified due to recognition errors. Additionally, for each unit, interspike intervals (ISIs) smaller than 20 ms and exceeding 200 ms were excluded from the calculation of the mean ISI and standard deviation, to avoid the inclusion of false positive spikes, or errors of spike recognition. This last procedure minimized the effect of recognition errors on the firing rate statistics (Eriksson *et al*, 1984; Nordstrom and Miles, 1991a). In single MU records, this method allowed reliable recognition of the unit's waveforms with only occasional discrimination errors. In multiple unit records, however, some additional spikes were missed due to occasional waveform superimposition of synchronous CAPs of different units.

For each unit, the mean ISI and standard deviation were calculated from 200 intervals obtained from 201 consecutively occurring CAPs in the middle of each EMG record (McMillan and Hannam, 1992). The mean bite force and standard deviation were also calculated over this period of time.

3.3.3.2 Effect of Bite Side on MU Behaviour

The complexity of the masseter muscle, and the bilateral tasks to which it contributes suggest that MU properties such as recruitment threshold and the regularity of sustained rates of firing might alter according to task. In previous studies, it has been assumed that the twitch tension produced by a motor unit (MU) in the masseter muscle

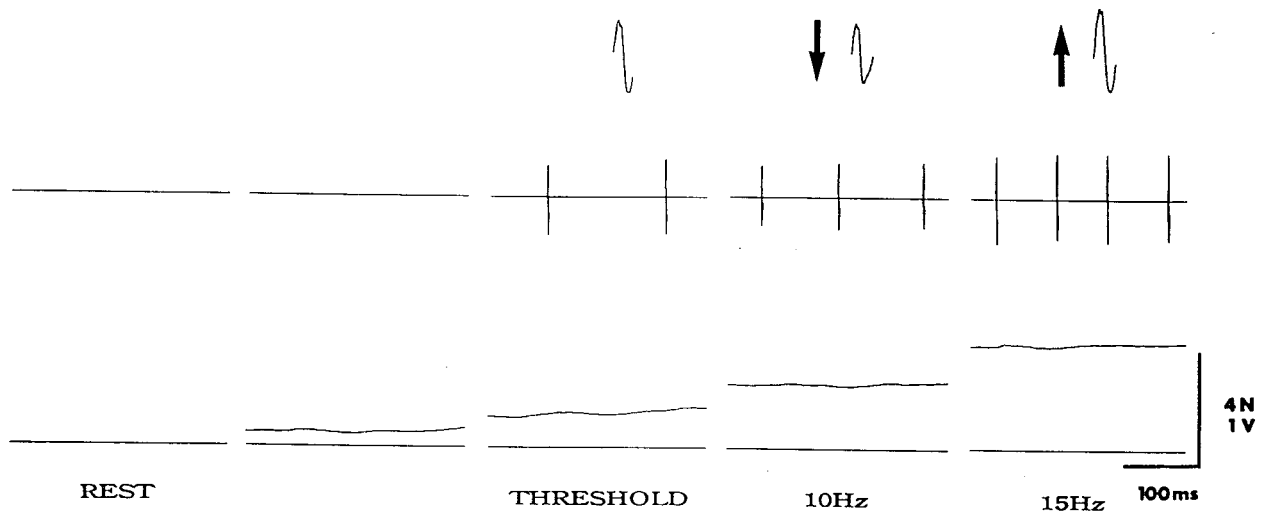
is directly transferred to the teeth (Nordstrom *et al*, 1989). Based on this assumption, when a MU in the right masseter activates, its tension should be identically transferred to the right or left canine teeth, provided that the location and angulation of the recorded bite force are the same when viewed sagittally. However, for tasks which are carried out by more than one muscle, and for muscles which are compartmentalized, differences in the activation of separate muscles and in regional activation of the masseter may severely affect this coupling from unit through intramuscular aponeuroses to the endpoint at the tooth. For example, reduced or no forces may be produced at the teeth during coactivation of elevators and depressors even though elevator MUs are active; and in the case of regional muscle activation, the transfer of MU twitch tension could be affected by differential intramuscular forces produced by nearby compartments. Thus, heterogeneity may result in different forces produced at the level of the teeth as bite strategy changes. If this is the case, the contribution of a given unit to bite force may differ due to any muscle length change (Miles *et al*, 1986), a change in location of the bite point with respect to the unit (due to different lever arms), and as a consequence of altered inter- and intra- muscular mechanics upon differential muscle activation. In an experimental situation in which bite-force-lever arms are identical in the parasagittal plane, it is possible that during slow increasing followed by sustained MU firing, recruitment thresholds and sustained bite forces may differ, because of dissimilar intramuscular unit recruitment patterns which change with task. In the present study, this possibility was addressed by analyzing the functional performance of a sample of low-threshold MUs in the superficial region of the masseter muscle when they contributed

to two different, symmetrical, unilateral biting tasks. Of special interest was the quantification of the effect of sidedness, as well as the reproducibility of MU behaviour when the same task was repeated. The study required a more rigorous analysis of jaw muscle MU behaviour than has been usual in previous investigations.

3.3.3.2.1 Methods

To test for the effect of bite side on MU behaviour, the subjects were instructed to carry out three tasks: two separate sustained biting tasks with the transducer placed on the right side, and one sustained biting task with the transducer on the left side. The order in which tasks were performed was changed randomly. For each task, the subject was asked to alter the force of his or her bite slowly through MU recruitment threshold, and then with the aid of auditory and visual feedback, to attempt steady MU firing for approximately 30 s first at 10 Hz, then at 15 Hz (Figure 43). The visual feedback target consisted of triggering the spikes on an oscilloscope and instructing the subject to maintain the MU firing at such a rate, that spikes would fall within a marked bandwidth on the monitor (100 ± 10 ms; 67 ± 7 ms). During multi-unit recordings, a window discriminator was used to separate the "target unit" from the background units. During changeovers, the maxilla-jaw relationship was kept unchanged with the aid of a bite block and the MU was driven without significant pauses. On a few occasions, the needle was gently repositioned to retain maximum amplitude of the CAP. To ensure that tasks were performed by the same unit, the waveform shapes of the CAPs were always compared.

Figure 43 Recruitment and firing pattern of a masseter MU at different bite force levels. Recruitment of a masseter MU, (centre traces). Five levels of bite force measured on the right side of one subject are shown, (lower traces). These increase from left to right, passing from rest, through the recruitment threshold, and include efforts to maintain unit firing at 10 Hz and 15 Hz. Variable gain was used to modulate spike amplitude (arrows) and facilitate MU discrimination, (centre and upper traces). The spike components shown were discriminated by cluster-cutting mixed-unit responses.



For each task, five functional properties of the MUs were assessed: recruitment threshold, coefficient of variation of the firing rate, accuracy index (i.e. difference between the target ISI and the performed mean ISI), mean sustained bite force, and a sensitivity index (i.e. defined as the slope of the curve describing the relationship between mean ISI and bite force).

To test for the reproducibility between both right-sided bites, and to test for the difference between right and left-sided bites, repeated measures analyses of variance were carried out for the entire data sample of the following measures: recruitment thresholds, mean sustained bite forces, coefficient of variation of the firing rate, and the sensitivity index. Linear regression analysis was also performed to test for significant relationships between the variables.

Although subjects were instructed to control the mean ISI of the feedback units at 100 ms, their ability to control the MU firing was not precise. To compare the variability of MU discharge for different tasks, it is therefore necessary to normalize the variance measure to a mean ISI of 100 ms for each unit performing each task. To achieve this, an adaptation of a previous method suggested by Eriksson *et al* (1984) and Nordstrom and Miles (1991a) was employed. For each unit, all three datasets containing 200 intervals were used. Mean and standard deviation (SD) were calculated for a sliding data window defined at a width of 11 intervals and a slide increment of 1 interval. Resulting mean values were then grouped into equally sized bins (5 ms each). The mean value of the SD values in each of these classes was then calculated. The median values of each bin and the mean SD values were plotted against each other, and a linear

regression performed. The equation of the linear regression was then used to estimate the value of the SD at a mean ISI of 100 ms. Provided that the 100 ms was within the range of mean ISI values used in the calculation of the linear regression, this final measure of variability of the unit, the estimated SD, was considered reliable. This was the case for 23 units which were included in the analysis. The estimated SDs from all units were grouped by task and linear regression analysis performed to test for the relationship between MU firing variability in the different tasks.

To compare MU firing rates between tasks, separate one-way analyses of variance were used. Since it is known that the distribution of ISIs in a slow firing unit is skewed to the right (Person and Kudina, 1972; Derfler and Goldberg, 1978), the database was normalized by natural logarithmic transformations (McMillan and Hannam, 1992). Each unit was initially tested for the reproducibility of MU characteristics during right-sided biting (which were presumed to be identical), and for differences between the right and left-sided biting by analysis of variance followed by Tukey's test. Statistically significant differences were then analyzed for their practical implications. For this purpose, the differences between the median values of the ISIs of the tasks were calculated for each unit. A difference of ± 10 ms (i.e. between 9 and 11 Hz) and of ± 7 ms (i.e. between 14 and 17 Hz) was not considered important (Samuels, 1989). In addition, the median value of the ISI of each unit was subtracted from the "target value" (i.e. from 100 ms [10 Hz], and from 67 ms [15 Hz]) for all tasks. Again, differences of ± 10 ms and ± 7 ms were considered practically insignificant.

3.3.3.2.2 Results

Fifty-one MUs were included in the analysis. Figure 43 shows the typical contribution of a MU to bite force. It was recruited at 1.2 N and as its firing rate was increased, a proportional increase in bite force was obtained. In most experiments the MUs clearly participated in the different tasks, but their behaviour could not always be assessed due to non-discriminable summation between units. In some experiments completely different units became active when the bite side was changed; and in five cases, units unequivocally fired on one side only. Therefore, the total number of units varied in the different population samples.

During right- and left- sided bites, the recruitment thresholds of 29% and 44% of the units, respectively, were too low to measure (i.e. these units did not contribute directly to these particular bite forces). Recorded threshold values ranged from 0.3 N to 12 N, and were neither reproducible between the right-side bite repetitions nor showed consistent task-related differences when the right- and left- side bites were compared (Figures 44 and 45). This was confirmed by statistical analysis of the entire data sample. Repeated-measures analysis of variance did not reveal significant differences between the mean recruitment thresholds for each task ($p=0.5$), and regression analysis revealed that the highest correlation occurred between the two right-sided tasks ($R=0.73$; $R^2=0.53$; $p<0.0001$), accounting for the reproducibility in only 53% of the sample. Between the recruitment thresholds of the right and left sided bites, the Pearson regression analysis revealed a lower correlation ($R=0.67$; $R^2=0.45$; $p<0.0001$).

Similar to the behaviour of recruitment thresholds, repeated-measures analysis

Figure 44 Distribution of recruitment thresholds by task. The data are shown as box plots. In each case, the centre horizontal line represents the median of the measured thresholds. The central box spans the interquartile range. The whiskers include values which fall within 1.5 times of this range. Outside values are plotted as asterisks and empty circles. The numbers below each box indicate the sample sizes for the respective tasks, which include two right-sided biting acts (R1 and its repeated version, R2), and a left-sided one (L).

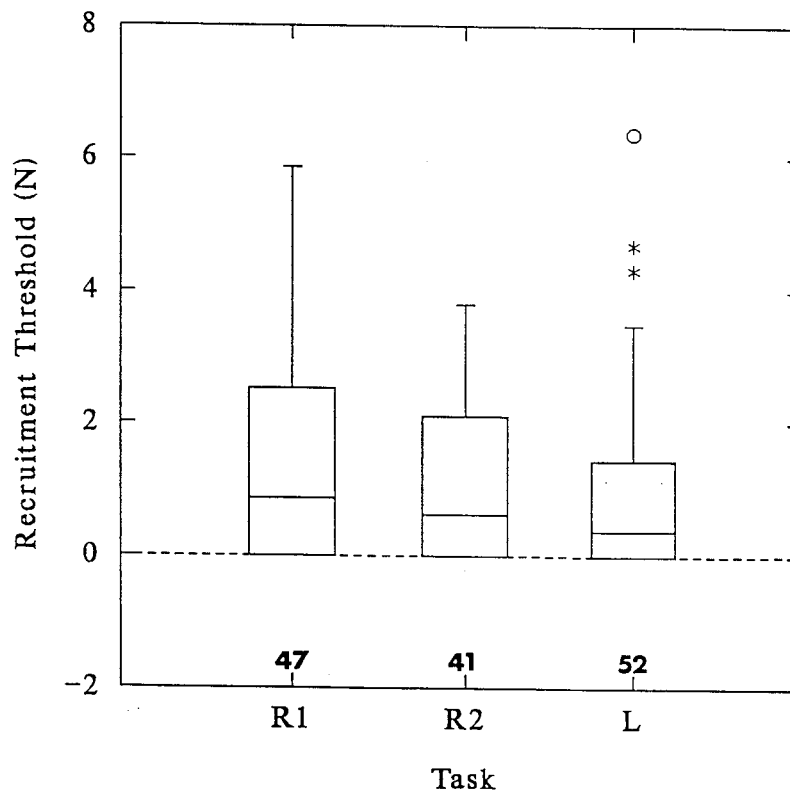
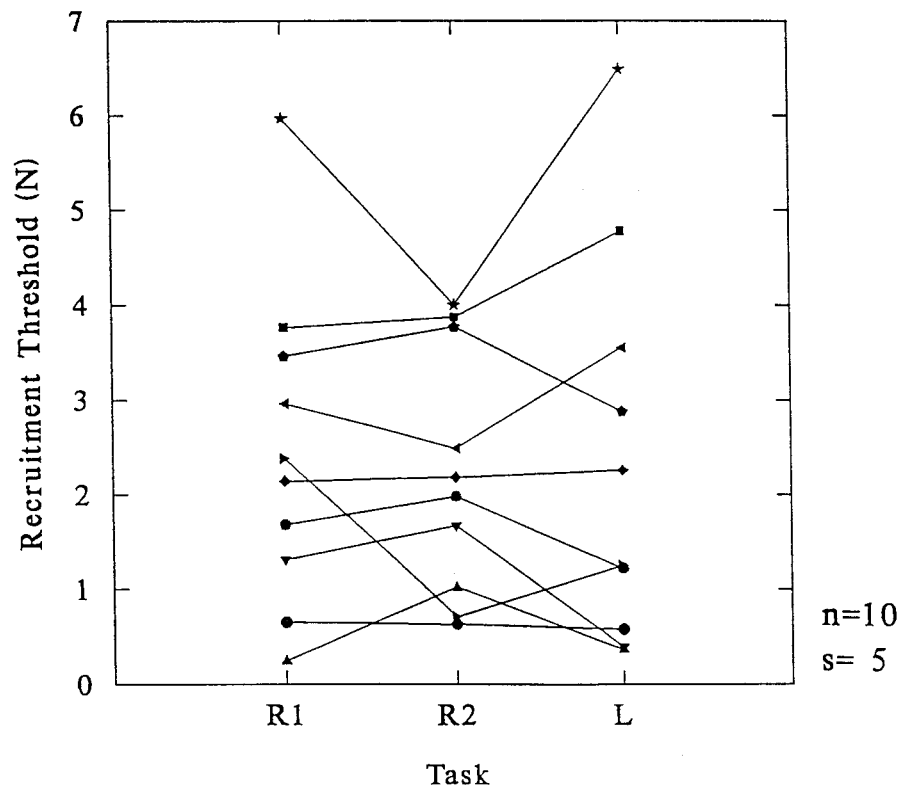


Figure 45 Recruitment thresholds arranged according to task for 10 MUs from five subjects. Abbreviations as for Figure 44. No consistent trend is evident as the task changes.



of variance did not reveal significant differences in mean bite forces with task for units driven at 10 Hz ($p=0.49$) and at 15 Hz ($p=0.80$). Regression analysis revealed that when the right side bite was repeated with units firing at 10 Hz and 15 Hz, mean sustained bite forces were correlated at $R=0.59$ ($R^2 = 0.34$; $p < 0.0001$) and $R=0.42$ ($R^2 = 0.18$; $p < 0.01$), respectively. When the right bite was compared with the left bite, it was found that at 10 Hz the data was correlated with $R=0.39$ ($R^2 = 0.15$; $p=0.03$), and at 15 Hz the mean bite forces were not correlated ($R=0.22$; $R^2 = 0.05$; $p=0.23$). The relationship between mean bite force and mean ISI when the target rate for one task changed from 10 Hz to 15 Hz, is shown in Figure 46. Here, 14 MUs were selected from one subject who was biting on the left side. In most cases, bite force increased as the ISIs shortened, i.e. as the firing rate increased, but in two units there was an actual decrease in bite force. The majority of units made a positive and roughly similar contribution to bite force, irrespective of task. The overall mean sensitivity index (slope) was 60 mN/ms. The highest number of small, unmeasurable changes in bite force occurred on the left side.

Variations in the patterns of discharge (expressed by the coefficient of variation, and arranged according to task) are shown in Figure 47. Consistently, the ISIs varied less for tasks performed at 15 Hz than for those at 10 Hz. Repeated-measures analysis of variance of the entire data sample failed to reveal significant differences between the mean coefficient of variations of the three tasks when attempts were made at either target rate ($p > 0.05$). Regression analysis revealed that the discharge variability in a unit performing different tasks was correlated. When the right side repeats and the left versus right side variability were plotted against each other, correlation coefficients

Figure 46 Changes in bite force when attempted MU firing at 10 Hz is increased to 15 Hz. Data are shown for 14 units from the same subject. The horizontal axis represents the duration of the inter-spike interval (ISI) which is the reciprocal of the instantaneous firing rate. The open and closed circles are paired measurements from the same units. In each case, the lines connecting them show the relationship between the change in bite force and the change in ISI.

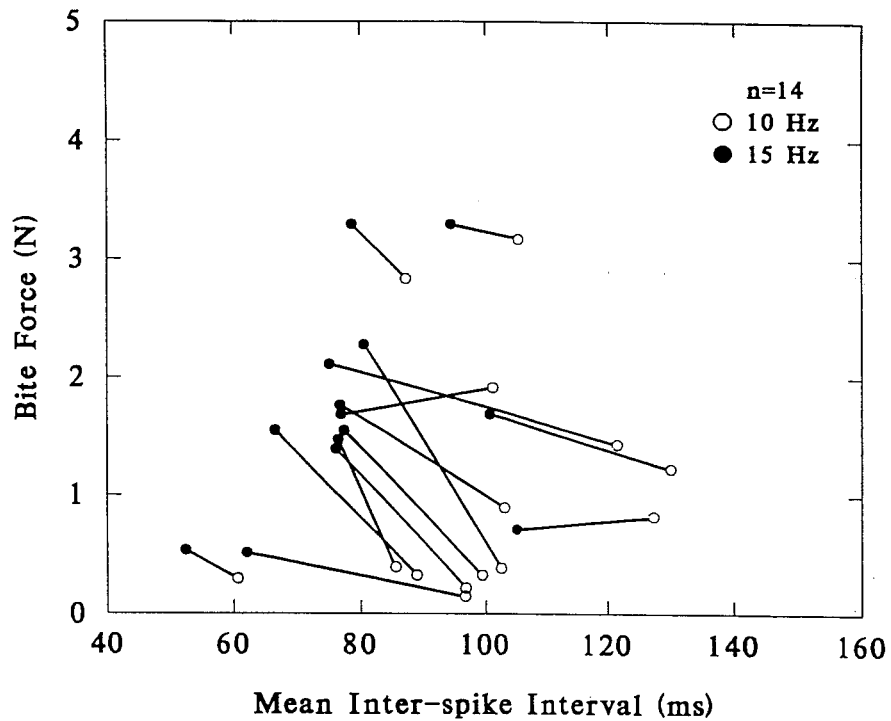


Figure 47 Distribution of Coefficients of Variation arranged by task for attempted MU firing rates of 10 Hz and 15 Hz. All abbreviations and conventions for box plots as for Figure 44.

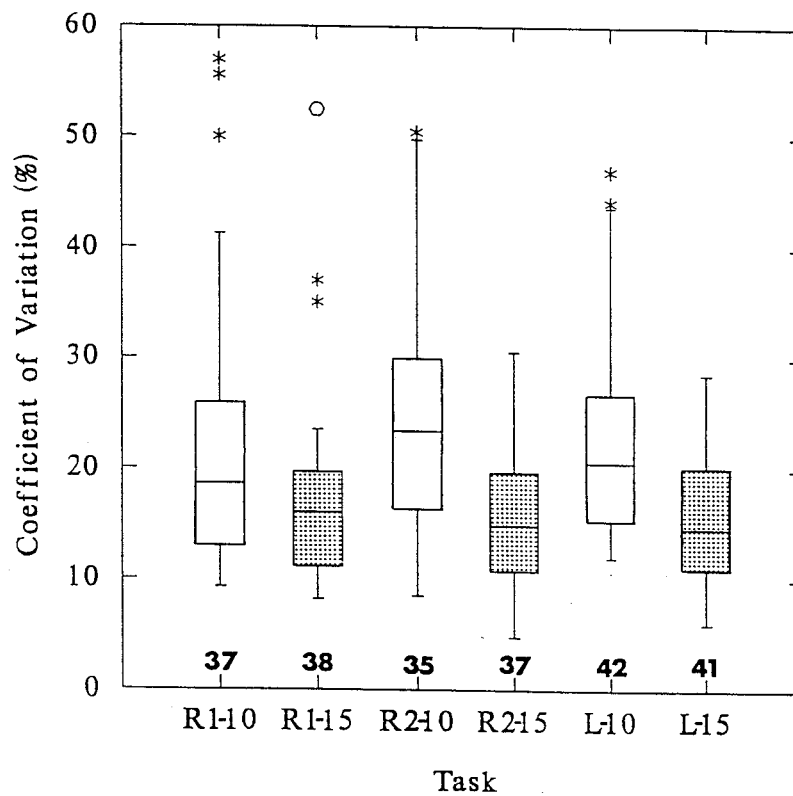
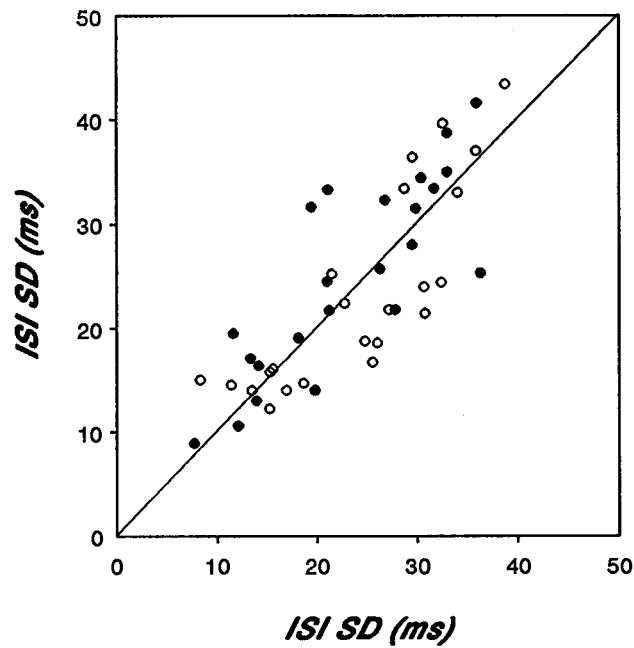


Figure 48 Two-dimensional plot of the ISI standard deviations of the first against the second right-sided biting task, and against the left side. The data for the right side comparison is presented by filled circles, and data for the right-left side comparison by open circles. The straight line represents the optimum linear relationship if tasks were to be identical.

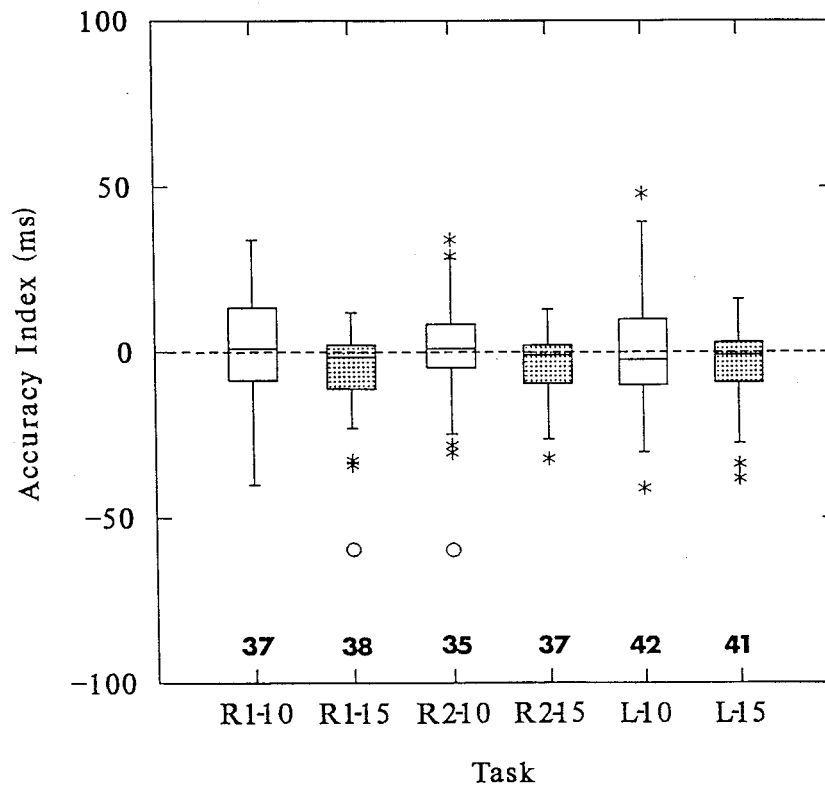


were $R=0.82$ ($R^2 = 0.68$; $p < 0.0001$) and $R=0.83$ ($R^2 = 0.69$; $p < 0.0001$), respectively (see also Figure 48).

When individual units were tested for reproducibility of firing ($n=37$), the analysis of variance revealed statistically significant differences between both right-sided bites for all units activated while the subjects attempted to drive them at 10 Hz ($p < 0.05$). When the difference between the median firing rates were compared, 45% of the units were reproducible. From these reproducible units, 64% were driven at the same firing rate during both, left- and right- sided tasks, while 23% were faster and 12% were slower on the left-sided task than on the right bite. When the difference between the median firing rates of units being driven at approximately 15 Hz were compared, 80% of the units were reproducible during both right-side bites. From these, 84% of the units had the same firing rate at the left and right bites, while 16% were faster at the left side. No unit fired at lower rates at the left side. In addition, EMG records during left-sided clenching frequently included more units than their right-sided counterpart.

When the subjects attempted to drive the units at the two target rates, there was an equal distribution of mean ISIs above and below the target rates (Figure 49). Subjects frequently reported that it was difficult to drive MUs steadily at 10 Hz, and two subjects could only maintain steady firing at 13 Hz. The evaluation of unit accuracy index by task (difference between observed median firing rate and "target"), revealed that subjects asked to activate the units at 15 Hz did so more accurately (i.e. with less variation) than at 10 Hz. When the subjects were asked to activate their units at 10 Hz, only 29% of the units were accurate irrespective of task, while when they were activating

Figure 49 Distribution of "Accuracy Indices" arranged by task for attempts at two different rates of MU firing. The data are presented as box plots. The open boxes represent attempted firing at 10 Hz, while the filled boxes represent attempted firing at 15 Hz. All other abbreviations as for Figure 44.



units at 15 Hz, 60% and 72% of the units were accurate on the left- and right- sided tasks, respectively.

3.3.3.2.3 Discussion

As for the limb, it is believed that the size principle provides a general description of MU recruitment in the masseter muscle (Goldberg and Derfler, 1977). If the muscle length is kept constant and if the rate of increase in isometric contraction is controlled (Miles *et al*, 1986), the threshold force for activation of a unit is assumed to be reproducible. On rare occasions, however, alterations in recruitment order occur (Desmedt and Godaux, 1979). The general acceptance that MU recruitment thresholds in the limb muscles are quite reproducible when measured under controlled conditions (Freund, 1983) has been questioned. For example, it has been reported that they may vary with the complexity of the motor task (ter Haar Romeny *et al*, 1982), and the experimental situation (Romaiguère *et al*, 1989). Variability in recruitment threshold is commonly found between different tasks performed by a multifunctional muscle (ter Haar Romeny *et al*, 1982), especially when other muscles also contribute to the produced force (Thomas *et al*, 1986). Recruitment threshold has been shown to vary with the direction of application of bite force (Hattori *et al*, 1991), and coactivation of other jaw muscles have been shown to alter masseter MU spike-triggered bite force (McMillan *et al*, 1990). The present findings that MU recruitment thresholds were neither reproducible, nor varied consistently with task, are therefore similar to the observations by Romaiguère *et al* (1989) regarding fluctuations in MU recruitment thresholds. These

authors suggested that motoneuron pool excitability was greatly influenced by the subject's emotional, attentional and physiological state. It is also possible that the present findings are the result of co-activation of other jaw muscles. It has been reported that the increase of isometric force, controlled by conventional methods of the kind used in the present study, is never a completely smooth ramp, but incorporate small, rapid fluctuations which are significant determinants of the variation of recruitment threshold (Miles *et al*, 1986). This assumption might be especially critical for jaw muscles which are known to be less developed for pursuit-tracking experiments than for limb muscles (Van Steenberghe *et al*, 1991), possibly because the jaw muscles are not designed for long sustained bite force tasks during natural function. Hence, the input to the various motoneuron pools may fluctuate, so that units belonging to different muscles and to different groups within a muscle may together achieve the proposed task. It is theoretically possible that the transducer system itself contributed to recruitment threshold variability, but this is unlikely. Care was taken to ensure that only one sensor was used, and that it always sensed forces at the same load point. The device's location and orientation were fixed relative to the opposing teeth, and ensured by its assembly on articulated dental casts.

The majority of units made a positive and roughly similar contribution to bite force, irrespective of task. It is known that recruitment of MUs is not the sole mechanism contributing to the total force production by a muscle, but that increase in MU firing rate also contributes to force increase. Similar mechanisms are used by MUs in the masseter muscle, where there is the tendency for MUs with the lowest recruitment

thresholds to show the largest rate changes per kilogram of interocclusal force change (Derfler and Goldberg, 1978). Thus, during small inter-occlusal force production, it is expected that several MUs are recruited simultaneously to achieve significant force increases. The present study showed that the highest number of small changes in recruitment threshold and sustained bite force, the largest number of MU recruitment, and the largest tendency for MUs to be driven faster occurred during left-sided clenching. Provided that the original assumption is correct (that the lever arms for both bite force points are identical), it is proposed that a common strategy to achieve left-sided bite forces is to recruit a larger number of units. Concurrently, small units will show larger increases in firing rate because of the increased excitatory input onto the motoneuron pool. That is, in this task the excitatory drive, responsible for the recruitment and frequency coding of MUs in the right superficial masseter muscle, has a different weighting factor than when a subject performs a right-sided bite. This suggestion is in accordance with Ter Haar Romeny's *et al* (1982) report for the biceps muscle.

The majority of MUs studied were polymodal, whereas a few units were selectively activated depending on the task being carried out. This finding concurs with previous reports on multitask units in limbs (Thomas *et al*, 1986; 1987; Ter Haar Romeny *et al*, 1982) and in the human masseter (Eriksson *et al*, 1984; McMillan and Hannam, 1992). However, the presence of task-specific units, while also reported by Eriksson *et al* (1984), was not confirmed by McMillan and Hannam (1992). This lack of agreement might be explained by the fact that while in the present study subjects were

able to activate units at two very specific bite points, in the latter work they were encouraged to attempt an array of intraoral tasks until MU firing was resumed.

The lowest steady firing rate (LSFR) at which subjects are able to drive masseter MUs seems to be greater than the LSFR at which subjects commonly drive their units in limb muscles (Petajan, 1981). It has been indicated that it is difficult to drive MUs consistently, without significant pauses below 8 Hz (Nordstrom *et al*, 1989; Eriksson *et al*, 1984), and that the LSFR may also vary with intraoral task (McMillan and Hannam, 1992). Better maintenance of consistent ISIs is thus expected at higher rates of firing, since the variability of spike discharge increases exponentially when the rate demanded falls below a critical value (Freund, 1983). For these reasons, the target firing frequencies of 10 and 15 Hz were chosen to increase the likelihood of discharge reproducibility, and because they were similar to those often used in jaw muscle MU studies (Miles and Türker, 1986; McMillan and Hannam, 1989b). In the present population of MUs, the firing rate of units for most subjects was actually 10 Hz or less, whereas for two subjects it was reported to be 13 Hz or more. The lack of any systematic change in the ability of subjects to drive MUs at either rate when the bite side alters suggests that most low threshold units in the superficial region of the muscle contribute roughly equally to right and left-sided biting, at least at the low firing rates tested.

The regularity and rate of MU firing are determined by the intrinsic properties of the motoneuron and by the excitatory drive to the motoneuron pool, which changes with variations in central and peripheral inputs (Henneman and Mandell, 1981). In the trigeminal system, peripheral sensory receptors include muscle spindles, cutaneous, joint

and periodontal mechanoreceptors, and free nerve endings (Dubner *et al*, 1978). Periodontal receptors have been located in higher numbers in the anterior region of the dental arch, and are known to be directionally sensitive (Hannam, 1982). They appear to be involved in inhibitory feedback mechanisms to jaw closing muscles (Kidokoro *et al*, 1968), and therefore are likely to have played a role in the input modulation to the studied motoneuron pool.

There are several possible outcomes for MU firing behaviour during the performance of different biting tasks. A given MU may fire for one task but not another; its recruitment threshold may be different from one task to another; the firing rate at a controlled frequency may vary more for one task than another; and the MU may contribute more vigorously to one task than to another. Properties like these require some form of quantifiable measurement if comparisons of MU behaviour between tasks, or between regions during the performance of a standard task, are needed. In addition, the results suggest that when muscle regions are surveyed for task specificity, MUs should be driven at 15 Hz instead of 10 Hz, and tested for firing reproducibility. Presently, conventional physiological measures of MU behaviour, while perhaps useful for qualitative comparisons, are so variable that useful comparisons are impossible once the task is changed.

In conclusion, very large sample sizes may be necessary to establish any effect of sidedness (or for that matter, task), at least for low threshold MUs. The results also suggest that care should be exercised when recruitment threshold or lower rate limit are used as dependent variables to classify jaw muscle low threshold MUs. Examples here

include jaw MU recruitment thresholds, putative unit twitch tensions, and task comparisons. The study infers that not only a change in task, but also the repetition of the same task after an interval, could produce very different results than those reported in many previous studies. These conclusions however do not necessarily apply to medium or high threshold MUs in the masseter muscle, which may have different functional properties and which remain relatively unstudied.

3.3.3.3 Effect of Experimental Paradigm

Since it has been shown that the experimental paradigm itself can affect recruitment threshold of MUs in the wrist extensor muscles (Romaiguère *et al*, 1989), it was hypothesized that MU firing properties and resultant bite force might have been affected by the kind of feedback available to the subjects. The extent to which the experimental paradigm might have affected the measurements reported above was investigated in the following manner.

3.3.3.3.1 Methods

All subjects were instructed to activate a single MU and maintain a steady firing rate for approximately 30 s while biting on the force transducer placed between the right canines. Subjects repeated this task four times. The first time, subjects were instructed to maintain steady MU firing at 10 Hz with the aid of auditory and visual feedback (as described in section 3.3.3.2.1). During this segment of the experiment, the

mean bite-force value was evaluated on-line with the aid of a digital voltmeter. After a short pause, during which the jaw relationship was maintained, the subject was again asked to reactivate the unit. The second time, instead of auditory and visual MU feedback, the force record was displayed on the oscilloscope in a fast trace so that only a horizontal line crossed the entire screen. The subjects were requested to maintain a vertical level bite-force based on the previous voltmeter reading. After another short pause, the subjects were asked to repeat the same task for a third time, with no feedback whatsoever. Here, the subjects could only rely on memory. Finally, the subjects were asked to repeat the task once more, again with visual and auditory MU feedback. With the exception of the first run, the order at which subsequent tasks were carried out was random. In addition, CAP shapes were always compared for all four tasks to ensure that the same unit was retained throughout the experiment.

Motor-unit mean firing frequencies and their "target" accuracy were estimated for each trial as before. Differences smaller than 10 ms were considered insignificant. Discharge variability per task was assessed by adding the standard deviations of ISIs of each unit into a population sample and then comparing them by repeated-measures analysis of variance, followed by Tukey's test.

Since it was expected that the amplitude of sustained bite forces between tasks might vary, the mean bite force values over the 20 s recording period, during which each unit's ISIs were analyzed, were also compared. Here, in each case, the mean bite force for the first task was normalized to unity, and bite forces for the other tasks were then expressed relative to this value. To test for differences in sustained bite-force values

between tasks, repeated-measures analysis of variance was carried out for the entire data sample, followed by Tukey's test. All normalized values were then averaged according to group, and compared as a population. Differences less than 0.10 were considered insignificant.

3.3.3.3.2 Results

The responses of 38 units were analyzed. Although most were active for all four tasks, occasionally some units stopped firing, or could not be reliably discriminated. Therefore, the total number of units in a given sample varied according to task.

The subjects had little difficulty performing the task when visual and auditory unit feedback was given. When force feedback was provided instead of unit feedback, 20% of the MUs under investigation were silent, although bite-force levels were adequately maintained. In these cases, the experimental run was interrupted, unit feedback was provided, then withdrawn, and force feedback given for another 30 s. When no feedback of any kind was provided, force levels were usually slightly higher and additional MUs were activated.

When the difference between the median firing rates (i.e. ISIs) of units firing with visual and auditory feedback, and with force feedback were compared ($n=28$), 43% of the MUs had reproducible firing rates. When the difference between the median firing rates of units firing with visual and auditory feedback, and with no feedback were compared ($n=27$), 26% of the units had reproducible responses. Finally, when the difference between the median ISI values of units firing between both runs with visual

and auditory feedback were compared ($n=32$), it was found that 54% of units had reproducible firing rates.

Variations in the patterns of discharge are shown in Table XIV. Although differences in discharge variability between tasks were found to be statistically insignificant ($p>0.5$), there was a tendency for freely firing MUs (without feedback) to have lower SDs, as opposed to when subjects were target-tracking.

When the unit-accuracy index (difference between observed median firing rate and 100 ms) was investigated for both tasks in which subjects were given auditory and visual feedback, 61% and 62% of the units, respectively, were driven at accurate rates. In contrast, 39% and 38% of the units, respectively, were driven faster than the suggested target rate. When the subjects were given force feedback, 36% of the units fired accurately, while 57% were driven faster. When no feedback was provided, subjects activated only 33% of the units at 10 Hz, while 63% were driven above that rate.

Mean sustained-bite forces ranged from 1.4 N to 17.7 N. For all tasks, the mean bite-force values and standard deviations, and their normalized values and standard deviations are shown in Table XIV. When bite-force levels were compared between the initial visual and auditory feedback and force feedback, it was found that only 30% of bite-force levels of the entire sample were reproducible (i.e. varied less than 0.1 of the control value). From these units, 50% had reproducible bite-force levels when also compared with the task where no feedback was provided. The vast majority of units, however, did not show reproducible bite-force levels when different types of feedback were provided.

Table XIV Discharge patterns and sustained-bite force levels of MUs activated during four tasks. Discharge patterns are expressed in ISIs and in coefficients of variation (CV). Force levels are expressed in Newtons and in normalized values. Sample sizes (n) are reported in the text.

Feedback Type	MU Discharge Pattern	
	Mean \pm SD	CV (%)
Visual and Auditory	96 \pm 29	30
Force	90 \pm 28	31
None	81 \pm 25	31
Visual and Auditory	97 \pm 30	31

Feedback Type	Bite-Force Level	
	Mean \pm SD	Norm \pm SD
Visual and Auditory	6.9 \pm 3.7	1.00 \pm 0.00
Force	6.2 \pm 3.6	1.07 \pm 0.47
None	6.9 \pm 4.0	1.11 \pm 0.55
Visual and Auditory	7.1 \pm 4.7	1.14 \pm 0.58

Thus the main finding in the present study was that although auditory and unit feedback ensured the highest reproducibility of MU firing pattern, the mean firing rates of 46% of active MUs in the superficial portion of the human masseter muscle were not similar when the same task was performed twice. Although there was a tendency for the firing variance to improve when the task was performed freely (with no feedback), this could not be confirmed statistically. As expected, the unit-firing "accuracy" was the highest when unit feedback was used, while units were driven at faster rates during the force-tracking run, and were especially fast when no feedback was provided. On several occasions units would stop firing when bite-force feedback was used. Finally, the mean sustained bite forces were not reproducible, but fluctuated between tasks.

3.3.3.3 Discussion

Fluctuation of MU firing within a motoneuron pool has been reported by Nordstrom and Miles (1991b), who found that 58% of active background units changed their mean firing rate with time, when a "feedback unit" was driven at a fixed frequency. These observations, and the present study, imply that even within a small region of muscle, the behaviour of MUs during the performance of a constant task is not stable over time. The non-reproducibility of many units' mean firing rates when a task is repeated indicates that there is a differential change in the net excitation of a proportion of MUs in the muscle with prolonged activity.

It is commonly accepted that features such as size-related recruitment order, proportional increase in firing frequency of active units as the force increases (Milner-

Brown *et al.*, 1973; Monster and Chan, 1977; Goldberg and Derfler, 1977), and the common modulation of firing of simultaneously active units during a constant-force isometric contraction is brought about by the uniform descending signal to the motoneurons which receive a large number of common inputs. However, if input signals are unequally distributed amongst motoneurons in a pool, they would mediate differential changes in MU firing pattern. An additional physiological mechanism which has been implicated in the maintenance of consistent firing patterns of spinal motoneurons is recurrent inhibition (Freund, 1983). However, no Renshaw-type recurrent collaterals have been identified in the jaw muscles (Derfler and Goldberg, 1978).

A single classically defined motoneuron pool and its associated MUs are, however, rarely activated independently during a contraction. Rather, a contraction may involve a group of synergists (for example the temporalis, masseter and medial pterygoid muscles) acting as a unit, or it may involve only a part of a complex muscle. The group of MUs activated for a particular task is defined as a "task group" (Loeb, 1985). Since the essence of the size principle is to increase force smoothly and minimize fatigue (Henneman and Olson, 1965), then the orderly recruitment should hold within every task group, which could comprise a group of synergists, a single muscle, or only a part of a muscle (Riek and Bawa, 1992). If it is assumed that during the chosen biting task the motoneuron task group was activated according to the notions of the size principle, no variability would have been expected. However, most fibres in the human masseter are homogeneous in terms of size and type (Eriksson and Thornell, 1983). Therefore, it is

possible that fluctuations in the excitatory input of the MU pool caused the variability of the physiological features. Similarly, it has been argued that it is excessive to expect a perfect recruitment order of hundreds of units, and that occasional errors may be either imperceptible or inconsequential (Cope and Clark, 1991). An alternative notion to this variability is that MU recordings were made from a group of MUs, which was not the principal task group responsible for force production. Rather, it was in the fringe of where the main activity was occurring therefore explaining the variability in MU firing.

In summary, regardless of the source of differential changes in MU activity with task repetition, the present results demonstrate that jaw muscle MU firing patterns may be modified by facilitation or suppression of some units during a continuous isometric contraction.

It seems clear that even when the source of feedback for an individual attempting to drive MUs in the masseter is optimized, approximately half the units will show behavioural characteristics which preclude the statistical confirmation of reproducibility in performance when the same task is repeated. When these results are taken together with those of MU behaviour in the previous study, it is concluded that conventional measurements of behaviour in low-threshold masseteric MUs are unsuited for quantitative comparisons between MUs in different parts of this muscle.

3.4 Motor-Unit Territory Relative to the Masseter's Internal Architecture

The relationship between human masseter MU territories and the muscle's internal anatomy is unknown. In experimental animals it is possible to use glycogen depletion to map MU territories, as has been done in several skeletal muscles (English and Letbetter, 1982a; English and Weeks, 1984; Richmond *et al*, 1985), including the pig masseter (Herring *et al*, 1989). However, this method is impossible in humans, and electrophysiological techniques which scan muscles cross-sectionally are used instead to determine the volume in which fibres of a MU are distributed (Buchthal and Schmalbruch, 1970; Stålberg *et al*, 1976).

Two physiological techniques have been used to measure MU territories in the human masseter. In one, scanning electromyography with a roving needle disclosed the temporal and spatial distribution of electrical activity along a uniaxial cross-section of the MU (Stålberg and Antoni, 1980; Stålberg and Eriksson, 1987). In the other, single MU activity was sampled from two muscle sites simultaneously. Here, the recording tips of two stationary needle electrodes were located stereotaxically, and the three-dimensional distance between the recording sites was calculated (McMillan and Hannam, 1989a). Both techniques have limitations. Scanning EMG does not measure the anteroposterior nor the superior-inferior dimensions of the territory, although it does reveal quite accurately the limits of MU activity in the axis of the scan. The twin-needle method has the advantage of providing a three-dimensional estimate of the territory's dimension, but it can systematically underestimate the limits of unit activity because both needles are required to record discernible action potentials.

Recently, a different approach, which included the stereotactic location of electrode recording sites within the human masseter, has been used (McMillan and Hannam, 1989a). This technique utilized MR imaging, which has become a useful technique for the three-dimensional reconstruction of human anatomical structures (Hannam and Wood, 1989; Schellhas, 1989; Sasaki *et al*, 1989). However, in the McMillan and Hannam study the recording sites were located stereotactically in whole-muscle reconstructions, and their position relative to internal aponeurotic boundaries was unknown. An experimental approach with the ability to image internal aponeurotic boundaries would permit the question of anatomical compartmentalization of MUs to be addressed.

Improvements in MR imaging now enable the visualisation of internal muscle architecture, and solid-object modelling techniques make three dimensional reconstruction of muscle architecture feasible in living subjects (Lam *et al*, 1991). In addition, the development of new, highly accurate, three-dimensional tracking devices makes it possible to monitor the orientation and translational displacement of the jaw and any other object, including needle electrodes, in real time during recording sessions. These improvements encouraged the development of a method for mapping MU territory in relation to internal muscle anatomy in order to gain insight into functional compartmentalization in the human masseter.

In this part of the study, the aim was to test the hypothesis that MU territories are small and confined to aponeurotic boundaries, and that any large territories are located in the anterior, fused part of the muscle. Support for this hypothesis would imply that the human masseter is capable of differential contraction exerting internal force

vectors with different directions.

3.4.1 Methods

3.4.1.1 Stereotactic Location of EMG Needle Electrode Scans

To map MU territory in relation to the internal aponeurotic network of the human masseter a method was developed that combined data from three separate sources: magnetic resonance imaging of the muscle, three-dimensional tracking of the needle electrode, and EMG scanning technique. For clarity, each component of the method will be described in separate sections.

3.4.1.1.1 Morphologic Reconstruction

During the imaging session, each subject wore a customized eyeglass frame, lined with silicone impression material to fit to the nose and ears of each subject and ensure stability and reproducibility during placement. Each frame incorporated a fiducial L-shaped reference grid filled with 5 mM copper sulphate, rigidly fixed to a position just posterior to the right masseter muscle. A 1.5 Tesla MR unit (Signa, GE Medical Systems, Milwaukee) was used to obtain T2-weighted images of the muscle and the reference grid. Spin-echo sequences with repetition time (TR) of 2000 ms and echo times (TE) of 25 and 80 ms were used to obtain a series of contiguous, 3 mm sections in the coronal plane. As described in more detail in an earlier section of this thesis, outlines from the muscle, internal aponeuroses and copper-sulphate markers were traced and digitized from each coronal section (Model HP9874A Digitizer, Hewlett Packard,

Canada). The profile coordinates were then used in an engineering solid-object modelling package (I-DEAS, SDRC, Milford) to reconstruct the muscle and its internal structures in three dimensions.

3.4.1.1.2 Motor-Unit Recording

During each recording session, the customized plastic eyeglass frame was worn by the subject to provide a fixed spatial reference. In each case, an insulated, monopolar needle electrode (MF-37, TECA, Pleasantville, NY) with a surface reference electrode overlying the muscle recorded activity from a MU. This method was selected because the smaller diameter of the monopolar needle causes less discomfort during insertion (an advantage during multiple recording sessions, especially with facial muscles) and has been shown to be sufficiently selective for macro MU recording if combined with bandpass-filtering to remove low frequency components of the EMG signal (Gath and Stålberg, 1976; McMillan and Hannam, 1989a; McMillan and Hannam, 1991). The needle was introduced percutaneously, perpendicular to the skin surface. Muscle fibre activity was amplified (Model Al 2130, Axon Instruments, Burlingame, CA), and bandpass-filtered between 300 Hz and 10 kHz (Gath and Stålberg, 1976). A separate surface electrode was attached to the back of the neck as a ground. The needle electrode was attached to a needle holder carrying three reflective markers 10 mm in diameter, which were arranged in a triangle when viewed coronally.

The subject was asked to activate the MU by gently biting with the teeth together in the dental intercuspal position, and to maintain a continuous low rate of

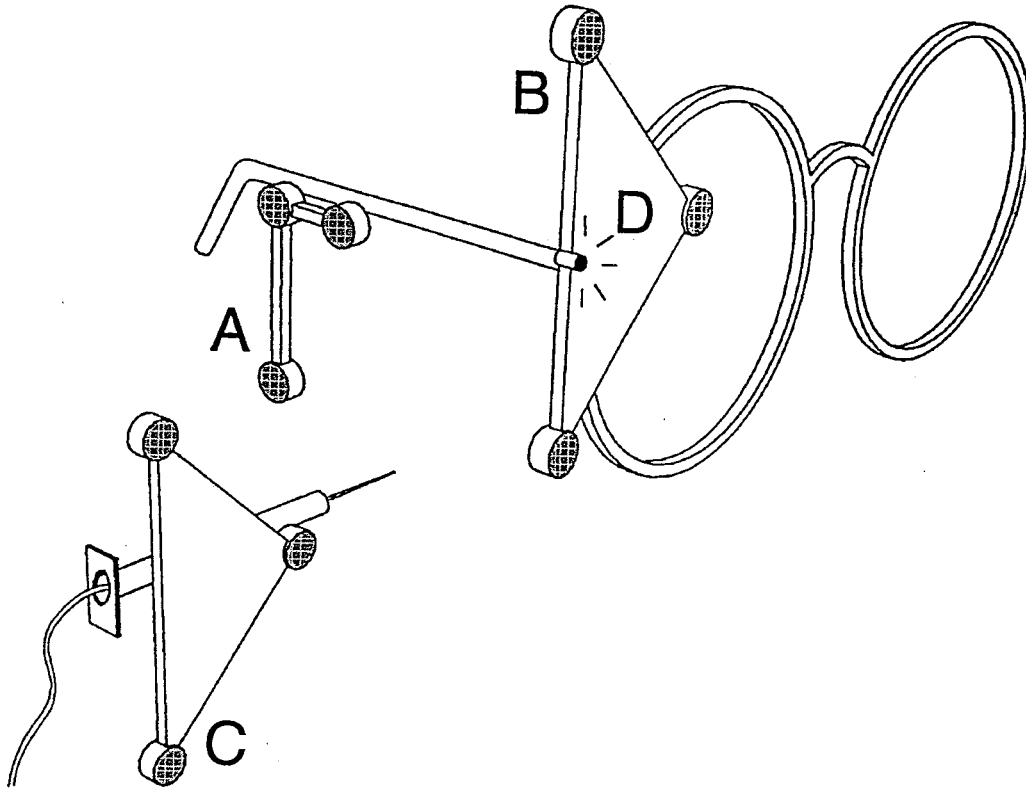
firing (12-15 Hz) with the aid of auditory feedback. The compound action potentials (APs) obtained from the MU were monitored on a digital storage oscilloscope (Model 2232, Tektronix Canada, Vancouver, BC). When a clearly defined AP was obtained, the subject was asked to maintain a constant effort. The needle electrode was advanced slowly into the muscle until the activity disappeared, then withdrawn gently along a mediolateral trajectory so that steady unit activity reappeared, increased in amplitude, decreased again, and was finally lost. Each complete electromyographic scan was sampled on digital tape at 48 kHz (DAS System, Unitrade, Minneapolis, MN).

3.4.1.1.3 Needle Location

The three dimensional movement of the roving needle was recorded continuously with an optical motion analysis device (MacReflex System, Qualisys AB, Partille, Sweden). This had a precision of 0.03 mm and dynamic accuracy of 0.3 mm, and it was used to measure the three-dimensional (3D) coordinates of the centroids of the needle's markers with respect to three markers located on the front of the frame (Figure 50). The coordinates recorded by the two video cameras were sampled every 20 ms over a period of 15 s, stored into a microcomputer (Macintosh IIsi, Vancouver, B.C.) and converted into 3D spatial coordinates by means of the optical system's software (MacReflex, Qualisys AB, Partille, Sweden).

At the end of each recording session, while the needle electrode was still attached to its holder, a separate optical system (Reflex Metrograph, HF Ross, Salisbury, Wilts, U.K.) with a resolution of 0.1 mm (Takada *et al*, 1983) was used to measure the

Figure 50 **Schematic illustration of the global setup for a needle tracking run.** A copper-sulphate-filled L-shaped Grid attached to an eyeglass frame (A). Three reflective markers are mounted on the front of the frame (B) and three on the needle electrode holder (C). The LED used for timing is also fixed to the front of the frame (D).



3D coordinates of the centroids of the needle holder's markers and the needle's tip. The coordinates of the centroids on all markers on the front of the frame and those of the L-shaped grid were also measured with the same instrument.

The location of the needle tip relative to the anatomical landmarks was calculated in I-DEAS with an algorithm that permitted coordinate rotation and superimposition. Initially, the three centroids of the L-shaped grid were determined from the solid object model. Then, sequential superimpositions of the locations of markers determined from the MacReflex and Metrograph systems were performed. In this way, the needle electrode tip position was calculated relative to the solid object origin (Figure 51) and displayed graphically within the reconstructed muscle (Figure 52).

3.4.1.1.4 Scan Location

To synchronize the time bases of the MU recording with the needle tip's location, an infrared light emitting diode (LED) one mm in diameter was fixed to the frame (Figure 50). At the beginning of the MacReflex sample, a single LED flash (1 ms duration, and synchronous with the camera sample onset) was hand-triggered. Simultaneously, a 1 ms square wave pulse was embedded onto the digital tape. After the recording session, the electromyographic record was replayed, sampled at 32 kHz and stored with the aid of commercially available software (BrainWave Systems Corp, Thornton, Colorado) for off-line analysis in a microcomputer (Premium, AST Research, Inc, Irvine, California). Sequential spike-by-spike visual analysis of the regularly firing MU ensured that the same unit was sampled as its amplitude and fibre content changed

Figure 51 Schematic representation of the merge of the three datasets. (I) represents the reconstructed muscle and the reference L-shaped grid obtained from the MR images. (II) represents the spatial relationship between the same reference grid and the reflective-marker triangle on the eyeglass frame. Their 3D coordinates were measured with the Reflex Metrograph. (III) represents the same eyeglass frame triangle (right), and the needle-holder triangle with the attached electrode (left). Data from one triangle relative to the other was obtained with the MacReflex system, while the relationship of the electrode to the triangle was obtained with the Reflex Metrograph. Data superimposition of the same triangles from these separate datasets is performed in I-DEAS, to enable the display of the needle tip location relative to the muscle as shown on the far right.

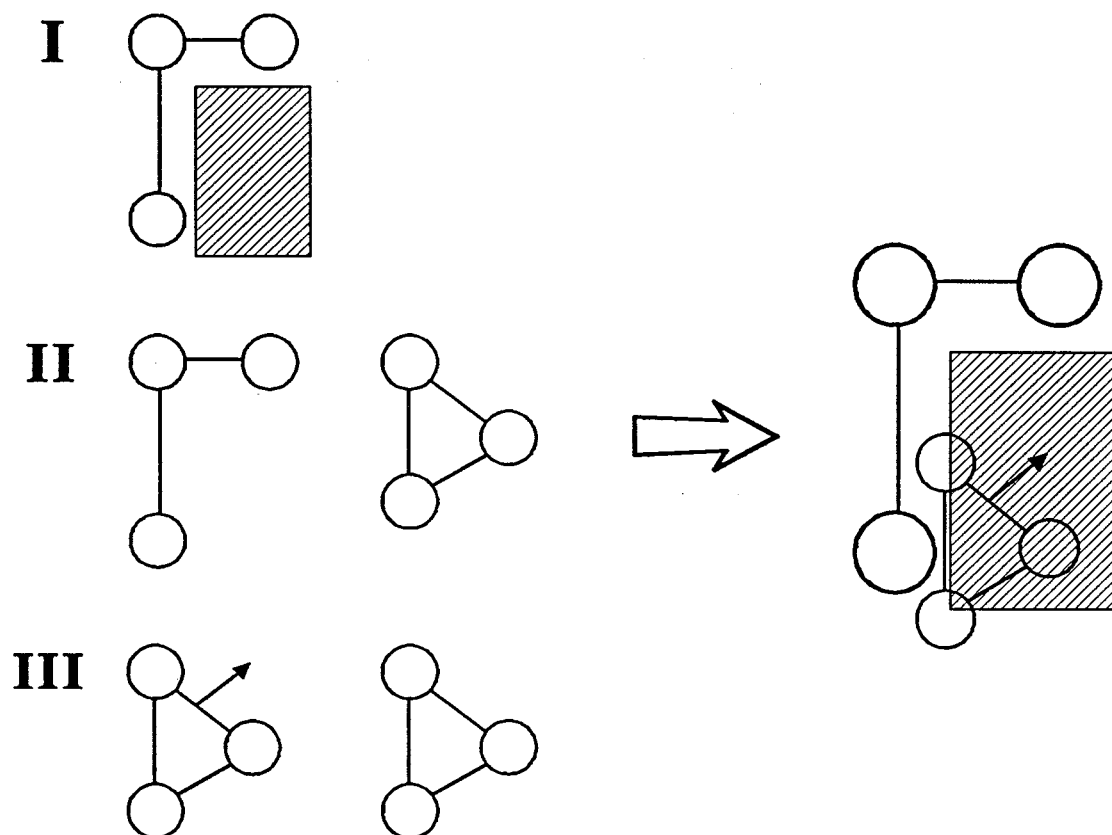
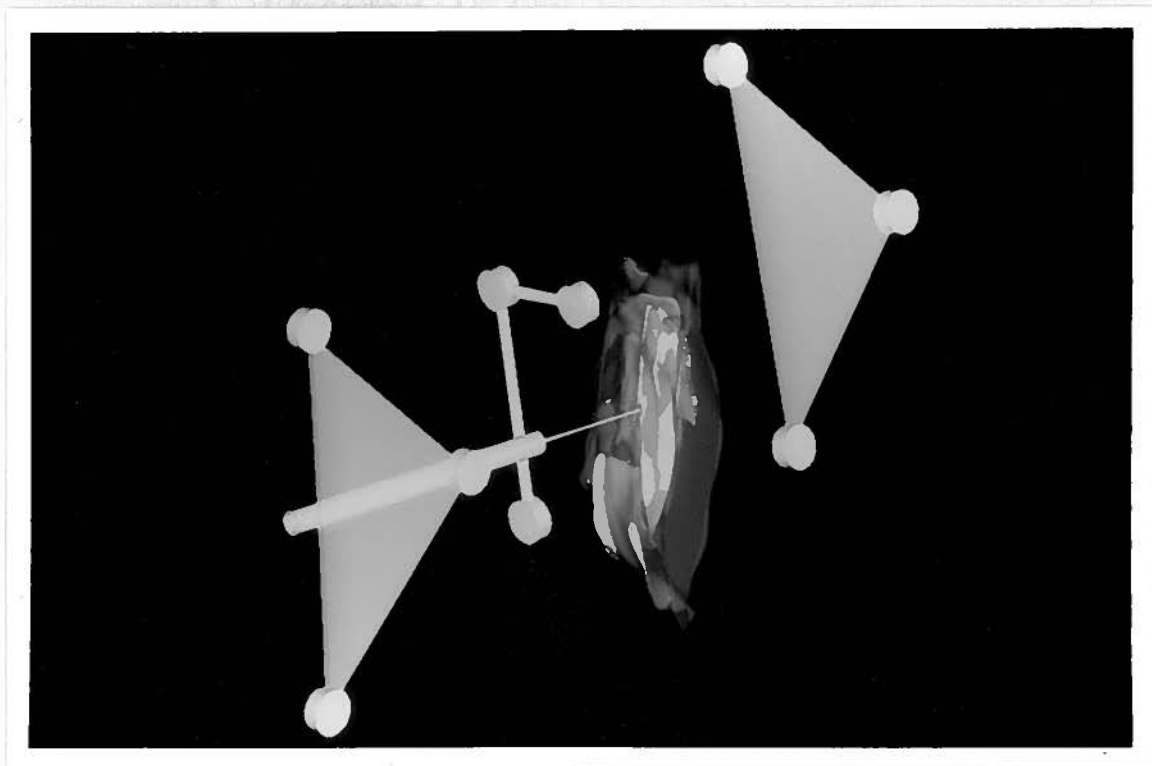


Figure 52 **Right antero-lateral view of the final reconstruction.** The right masseter muscle, eyeglass frame triangle, needle-holder triangle and needle electrode are graphically displayed. Similar data of electrode tip position are available for every 20 msec of a needle scan through the muscle.



uniformly during electrode movement (Figure 53A, top), and determined the beginning and end of MU activity (Figure 53A, bottom). Time stamps were used to mark the limits of the recorded spike train, when the spike amplitude became so small that the differentiation of the MU from the background activity was no longer possible. The scanning record was rejected when the start or end of the unit activity was uncertain due to contamination by other units or baseline noise. The time stamps were referenced to the calculated needle tip locations at corresponding times in the tracking record. The linear distances between the limits of recordable single MU activity for each subject were then displayed graphically as bars within the reconstructed masseter muscle. For example, typical mediolateral electromyographic scans for two MUs are shown in Figure 53A (center) and 53B. These had linear scans of 3.2 mm and 4.3 mm respectively, and are illustrated in Figure 54. Together, they provide examples of an average-sized MU which lies well within identified aponeurotic boundaries, and a larger MU which clearly crosses a tendinous sheet.

3.4.1.1.5 Methodological Errors

To assess the reproducibility with which the frame could be repositioned, we attached a plastic reference triangle, with three reflective markers, to an indented acrylic bite-fork held firmly between the teeth. The frame, with its three markers, was then placed on the subject, and the three-dimensional location of all six markers were recorded with the MacReflex system. Three linear distances were calculated between corresponding pairs of reference and frame markers. The frame was then removed, and

Figure 53 Typical EMG records obtained during two separate needle scans. In (A) the middle trace shows the response of a single MU as the needle is moved through the muscle. The unit increases in amplitude, then decreases again, as the needle is moved. An expanded version of selected spikes of the unit (not consecutive, for reasons of clarity) is shown in the top trace. The bottom trace diagrammatically represents the needle movement, recorded with the tracking system. S and E indicate the start and end of MU activity. The square wave pulse and LED flash are illustrated on each trace on the left. In (B) the response of a second MU is shown for comparison as the needle is moved through the muscle.

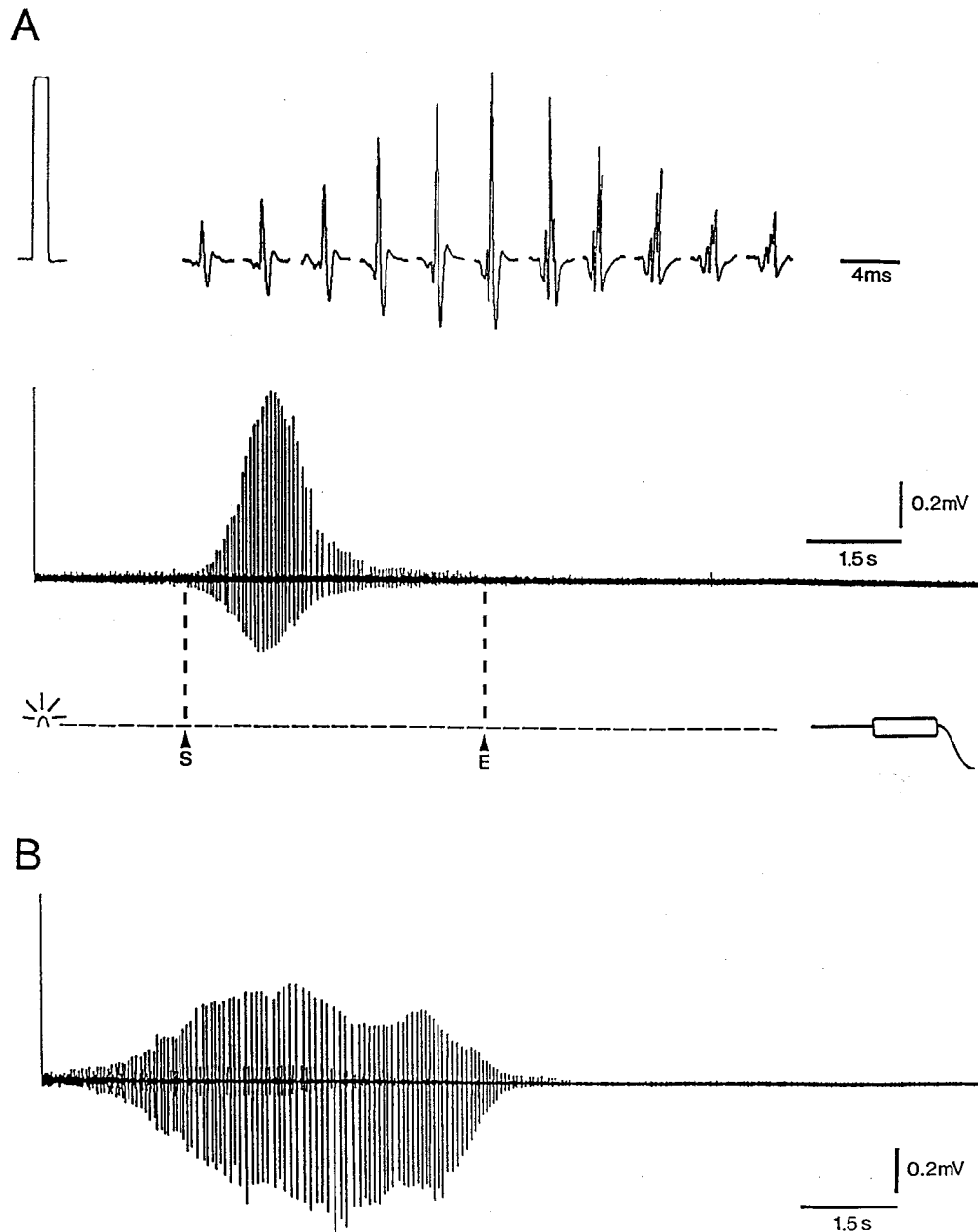
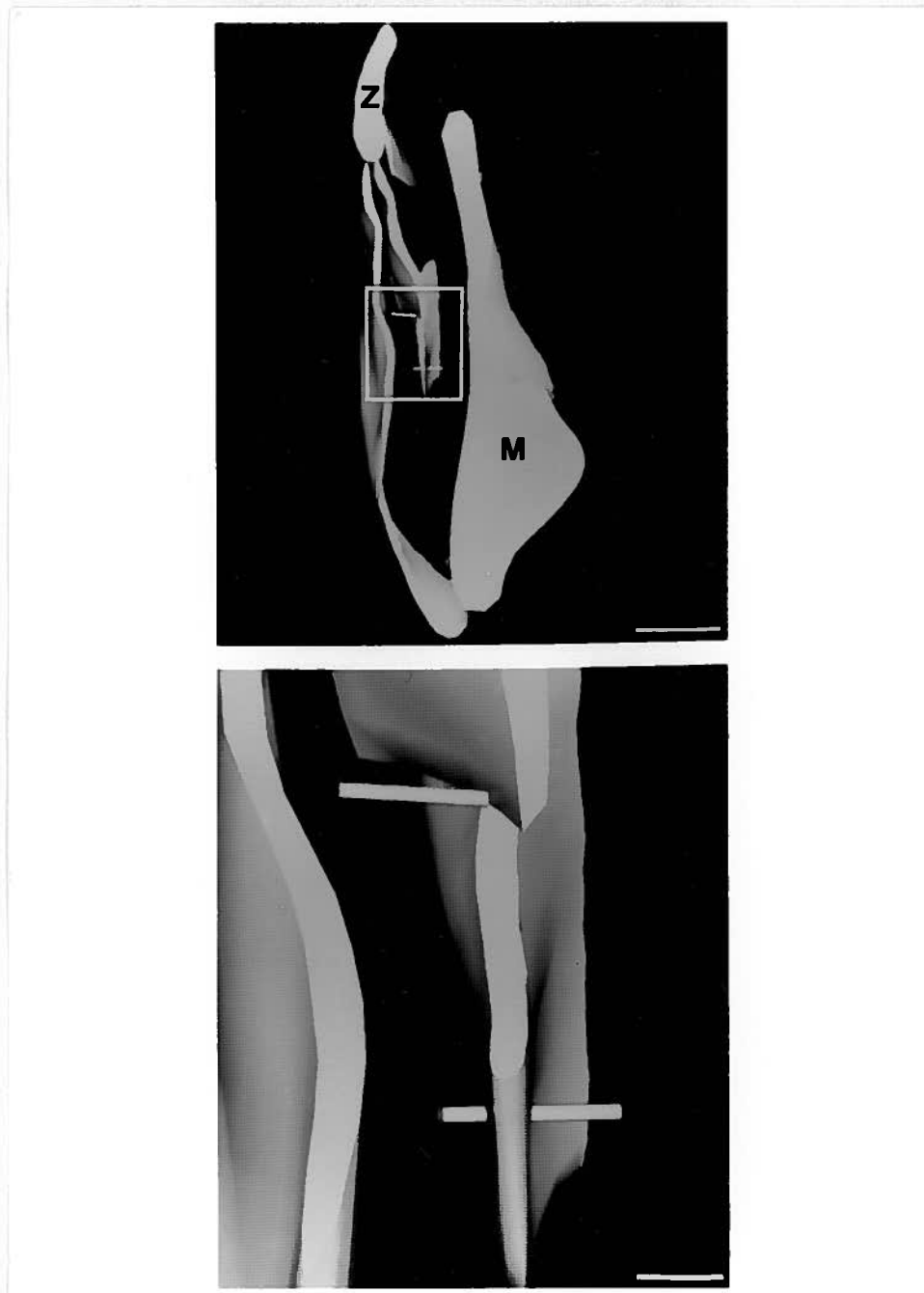


Figure 54 Coronal view of the 3D reconstruction of part of the right masseter muscle. The mediolateral territorial dimensions of two different MUs are represented by bars. The top one lies between two aponeuroses (Ap.I [left] and Ap.III), and the bottom one passes through an additional tendon sheet (insert above and magnification below). Only part of the reconstruction is shown for clarity. (Z=zygomatic arch; M=ramus of the mandible) Scale bars represent 1 cm (top) and 1.8 mm (bottom).



the procedure repeated five times. Since the average linear distances between the two triangles were estimated to be 113.70, 76.45 and 68.23 mm, and their standard deviations were 0.52, 0.53 and 0.41 mm, respectively, the coefficients of variation were 0.5%, 0.7% and 0.6%, respectively.

The accuracy with which the needle tip position could be predicted was tested in the following manner. A subject was imaged according to the protocol described above, and the MR images were traced, digitized, and reconstructed. The centroids of the L-shaped grid were determined and the frame markers added to the reconstruction. In a separate recording session, the tip of a needle electrode was placed against the marked centroid of the lateral surface of the copper-sulphate-filled marker at the corner of the L-shaped grid, instead of inside the muscle. This location was also recorded with the MacReflex system. Both the needle tip and needle holder markers' centroids were then measured with the Metrograph, permitting the location of the needle tip to be calculated and compared with the corresponding position in the grid reconstruction. This procedure incorporated all inherent errors in the system, including those incurred during the imaging, digitizing and reconstruction procedures, the use of the MacReflex and Metrograph, and operator error. The difference between the two positions was estimated to be 0.07 mm in the mediolateral dimension, 1.02 mm in the vertical dimension, and 0.45 mm in the anteroposterior dimension. Mediolaterally, the error of the method is minimal in relation to the average tendon sheet thickness of approximately 1 mm and the average MU territory width of approximately 3.5 mm.

The method employed to estimate MU territory size is based on the

measurement of the distance between the beginning and end of unit activity, which should represent the diameter of the MU. The error of this measurement is however difficult to determine in humans. MU territory size can be underestimated if the trajectory of movement of the needle electrode is through the periphery of the unit's three-dimensional volume. Alternatively, it can be overestimated depending on the volume conduction of the unit's action potentials, and/or depending on the electrode's uptake radius. Considering the electrode used in the present study, an error of up to 1 mm at both ends of the unit's cross-section could be expected. Since the average thickness of an aponeurosis is 1 mm, only a territory overestimation greater than 1 mm at one end of the mediolateral dimension (the end closest to an aponeurosis) would have been sufficient to erroneously affect the relationship of a unit's territory for crossing a boundary.

3.4.1.2 Motor-Unit Territory

Experiments were carried out on four adult male subjects. Their ages ranged from 29-36 years, and all had a complete natural dentition and no history of jaw dysfunction. The subjects were selected because of their skill in activating single MUs. The experiment was approved by the Human Experimentation Committee at the University of British Columbia, and each subject gave informed consent.

In each case, a monopolar needle electrode (MF-37, TECA, Pleasantville, NY) was inserted into the right masseter muscle and referenced to a surface patch electrode attached to the overlying skin. In some cases, two monopolar electrodes were inserted

simultaneously to record synchronous activity. An additional surface electrode was attached to the back of the neck and used as a ground. At the beginning of each recording session, the subject was asked to activate a single MU by gently biting with the teeth in full dental intercuspation, thus producing a continuous low rate of firing (12-15 Hz) with the aid of auditory feedback. MU activity was amplified, band-pass-filtered, and sampled according to the previous description. Scanning recordings were randomly obtained from different parts of the right masseter muscle on all subjects. Multiple recording sessions were used to enable different parts of each muscle to be searched systematically.

Following the analysis of each spike train, time stamps representing the limits of MU activity were referenced to the calculated needle tip locations at corresponding times in the needle movement record, and subsequently located relative to its corresponding internal muscle architecture. Graphical representations of the mediolateral scans were then produced and their relationship to aponeuroses was classified into two groups, one where the mediolateral territorial dimension was confined to tendinous boundaries, and the second where it passed through an aponeurosis by more than 0.5 mm. This paradigm was chosen to minimize the influence of any technical error in the determination of MU territory location, thereby enabling territory classification to be ascertained. Mean mediolateral dimensions for both groups were compared statistically, by means of an independent t-test, to determine whether the mediolateral territorial dimensions of MUs that extended across an aponeurosis were larger. Then, their spatial distribution relative to gross anatomical portions was

investigated. Each muscle was divided into three antero-posterior and two medio-lateral regions on the basis of gross anatomical subdivisions (Ebert, 1939; Schumacher, 1961c).

The width of the muscle was also assessed for each subject. The mean value was obtained by measuring the distance along a transverse axis between the most lateral point and the medial contour of the five widest, contiguous muscle coronal outlines. To test for the dependence of the mediolateral territorial dimension on the muscle's width in each subject, both analysis of variance and regression analysis were used.

3.4.2 Results

Single-MU recordings were obtained for 162 units. In most recordings the electrical activity increased and decreased quite smoothly during the electrode scan, as found in previous studies (Stålberg and Antoni, 1980; Stålberg and Eriksson, 1987). No abrupt changes in amplitude due to the passage of the electrode through a tendon were observed, although the shape of the spike train in a scan was not always symmetrical. In a few cases, a reduction in spike amplitude was observed at the centre of a scan, with subsequent increase as the electrode moved further through the unit territory, and in other cases the amplitude slowly increased to maximum and then rapidly declined, until activity was lost. The formation of these complex patterns suggested that they could have been the result of a change in velocity, or even a change in the direction of the electrode movement during the particular scan. To determine whether this assumption was correct, plots of the needle movement velocity were made for two asymmetrical scans. These are shown in Figure 55, in which time stamps at every 180 ms within the start and end of the

respective MU activities are plotted against the linear distances of electrode displacement which occurred between consecutive time intervals. Contrary to what was expected, in both cases the velocity of the needle movement was constant throughout the scan. An alternative explanation for this type of appearance is that as the recording tip moves across the unit territory it samples a different combination of action potentials from the scattered muscle fibres belonging to the same MU. This assumption is however very difficult to prove, requiring complex computer simulations of the number and of the distribution of active muscle fibres relative to the electrode's field of pick-up, and of other variables, such as volume conduction and filtering systems.

The mediolateral territorial dimensions of the single MUs varied between 0.4 and 13.1 mm. Seven units in three muscles showed values between 9.1 and 13.1 mm, and are comparable to the larger units reported by Stålberg and Eriksson (1987). The average width and standard deviation for 162 units from the four muscles was 3.7 ± 2.3 mm. Their distribution is shown in Figure 56.

Most MU territories (145/162) were confined to subvolumes within tendinous sheets (Figure 57). A small number of these spanned the entire muscle layer, reaching the tendon sheets on either side of the layer. Only 17 territories (approximately 10% of the sample) crossed aponeuroses. These MUs ranged in width from 3.0 to 13.1 mm and did not include any of the smaller MU sizes (<3 mm) found in the aponeurosis-confined group. The relative distributions of confined and extended territories are shown in Figure 57. A one-tailed t-test performed on logarithmic transformations of the data revealed that the mean sizes of extended MUs were greater than those of confined MUs

Figure 55 Needle movement velocity during two separate needle scans. In (A) the top trace shows an asymmetric response of a single MU as the needle is moved through the muscle. The bottom diagram represents the needle movement velocity plot. In (B) the response of a second MU as the needle is moved through the muscle is shown with the record's needle movement velocity. This is an example of a spike train in which the amplitude decreased and increased again in the centre of the MU territory. Note that in both diagrams the velocity of the needle scan is constant, indicated by the slopes of the two graphs.

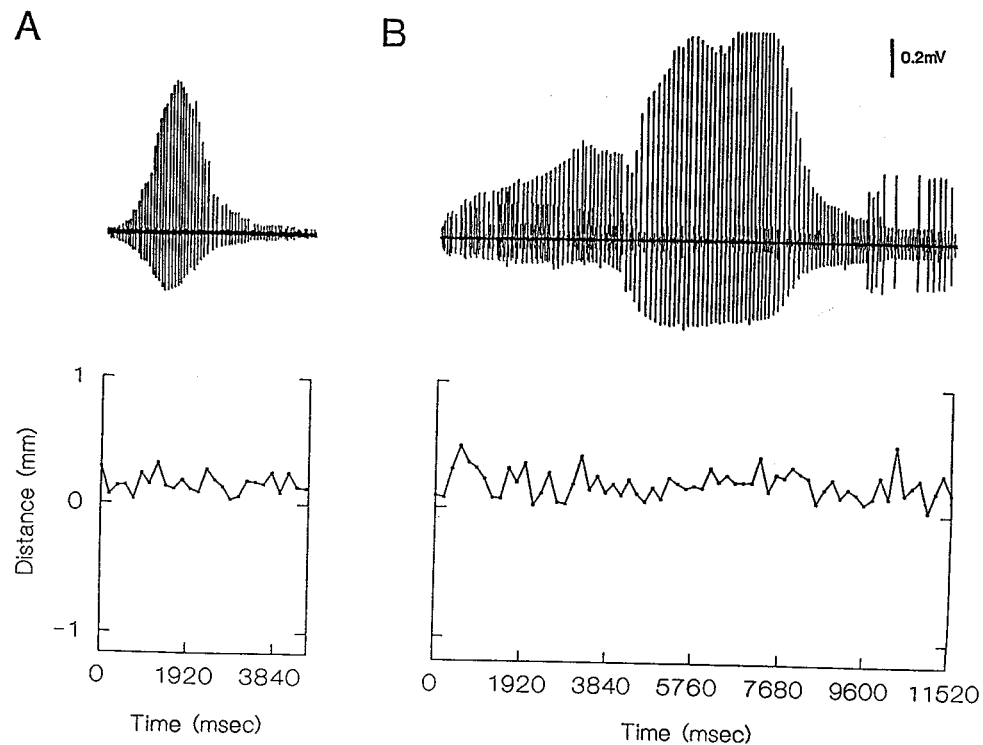


Figure 56 **Distribution histogram of the territorial widths of 162 single MUs in the right masseter muscle.** MU territories are grouped into classes with individual widths of 1 mm. Every second bin has been labelled at the center of the class boundary. The mean value for this distribution is 3.7 mm.

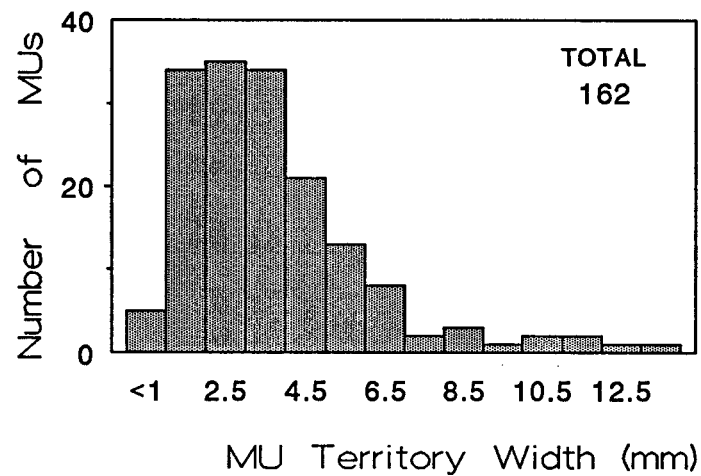
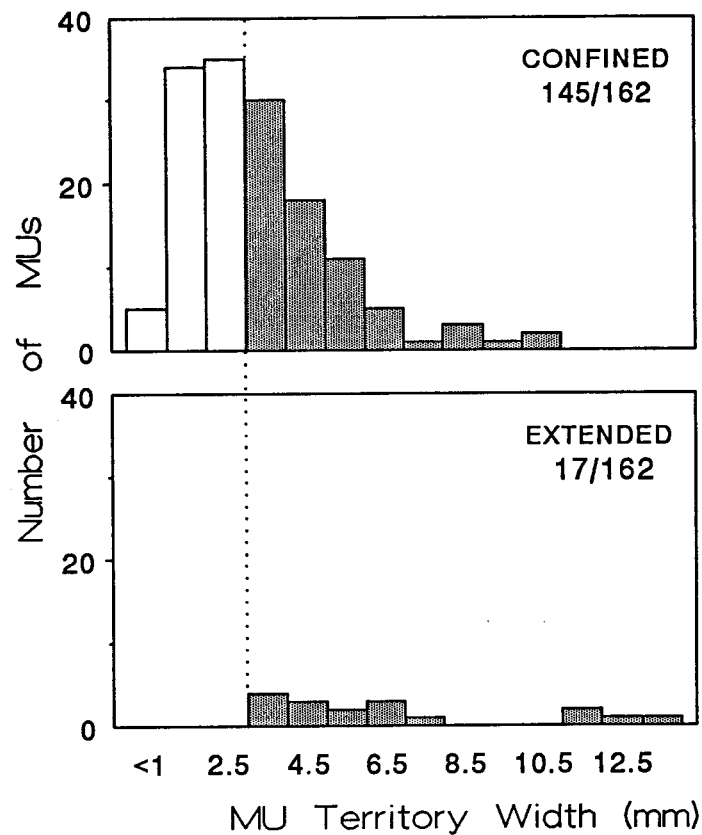


Figure 57 **Relative sizes and frequencies of confined and extended MU territories.**
 Distribution histogram of territorial widths of MUs which are confined by tendinous boundaries (above), and those which extend across tendon sheets (below). MU territories with widths greater than 3 mm are shown to the right of the dotted line (shaded bins). Numbers indicate relative sample sizes.



($p < 0.001$).

The distribution by region of 88 MUs with dimensions larger than 3 mm is shown in Figure 58. The location of the territories which extended across aponeurotic layers did not appear to be specific to any muscle region, although there was a tendency for them to be found in the middle region in the para-sagittal plane and in the centre and deep regions in the coronal plane (Figure 58).

Analysis of variance revealed that the mean mediolateral territorial dimensions between subjects were significantly different at the 99% confidence limit ($p < 0.01$). Additionally, the individual mediolateral dimensions were shown to depend on that individual's muscle width (Linear regression: $r = 0.98$). The subject with the smallest muscle had the smallest territories, while larger individuals had larger territories (Table XV).

3.4.3 Discussion

Magnetic resonance imaging reliably visualizes the intramuscular tendons, which anatomically subdivide the masseter muscle in rabbit (Ralph *et al*, 1991) and in humans (Lam *et al*, 1991). Because few mobile protons are available in tendons, they produce a low intensity MR signal, and are seen as black structures adjacent to the surrounding proton-rich muscle (Berendsen, 1962; Migchelsen and Berendsen, 1973). On occasion, normal tendons may demonstrate increased tendinous signal intensity. This occurs when tendons are oriented at approximately 55° relative to the magnetic field (Fullerton *et al*, 1985) and is most prominent on T1-weighted, imaging sequences

Figure 58 Distribution of MU territories with widths greater than 3 mm, according to muscle region. (A) Lateral and frontal diagrams of the masseter showing the six different regions. (P=posterior, Mi=middle, A=anterior, S=superficial, C=central and D=deep) (B) Distribution of MUs with territories confined to aponeuroses (above), and extended across tendon sheets (below).

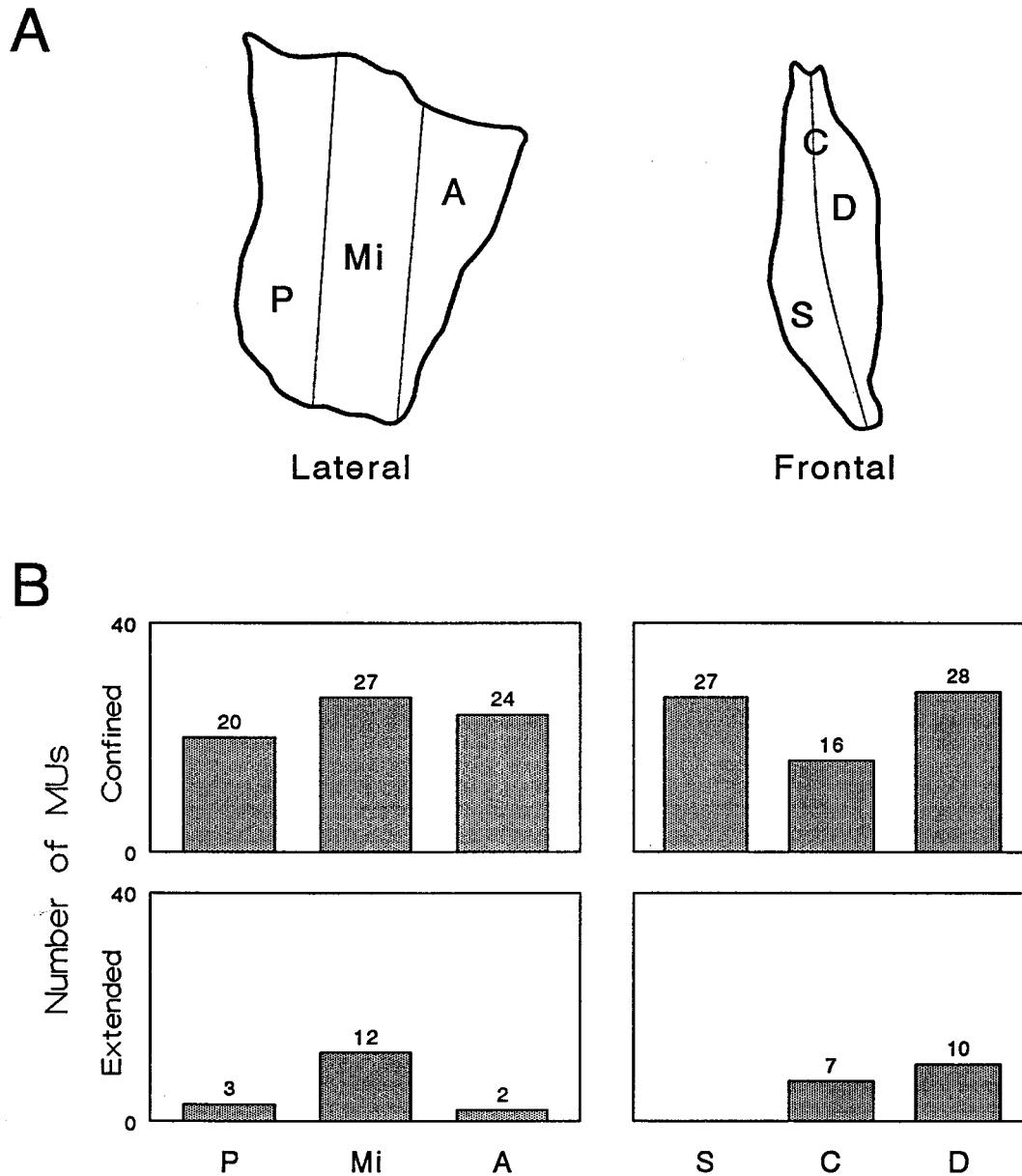


Table XV Muscle width and mediolateral territorial dimensions from MUs in the right masseter muscle of four subjects. All values are expressed in mm.

Subjects	Muscle Width (mm)		MU Territory Width (mm)				
	Mean	SD	Mean	SD	Min.	Max.	n
1	21.5	1.2	4.4	2.4	1.1	11.2	40
2	19.7	1.6	3.8	2.8	0.6	13.1	48
3	16.4	1.3	3.4	2.2	0.4	11.6	40
4	14.8	1.1	2.9	1.2	0.9	5.3	34

(Erickson *et al*, 1991). In the present study, coronal sections through the masseter were obtained. In this plane, low intensity signals from the tendinous sheets were expected because of their orientation of 15° relative to the midsagittal axis (Schumacher, 1961c). To further ensure high contrast differentiation between the tendinous structures and the muscle, we selected T2-weighted images. Using this imaging sequence, the possibility of obtaining higher angle-dependent signals from tendons was reduced. Reliable internal anatomy identification was then confirmed from our reconstructions, which are consistent with previous anatomical reports.

Electromyographic scanning does not indicate the total territory of a MU, but only its extent along the recorded cross-sectional area. The scan, on occasions, may well be at the periphery of the MU territory. Other factors that have to be taken into consideration when evaluating MU territory are the pickup area of the recording electrode and its possible bending, especially when a fine needle is used. The uptake radius has been estimated previously to be about 1 mm for a concentric needle electrode (Thiele and Boehle, 1975), and should be approximately the same for the electrode used in this study given the similarity of the intramuscular recording surface areas, and the filtering procedure used (Ekstedt and Stålberg, 1973; Gath and Stålberg, 1976; Stålberg and Trontelj, 1979). Theoretically, a 10 degree deflection of the shaft at the needle hub could result in a 6 mm deflection of the needle tip in the anteroposterior or superior-inferior direction relative to the recording cameras. However, this would only result in a 0.6 mm error in the estimation of needle tip location along the mediolateral axis in the muscle. Thus the error in locating MU territories relative to the tendon sheets is

minimal in the coronal plane of interest used in this study.

The transverse width of MU territories measured with this method correspond closely with previously published figures for the human masseter muscle (Stålberg and Eriksson, 1987; McMillan and Hannam, 1991). With the present technique however, observations can be made of both the number of territories which are large enough to cross tendinous boundaries and those which are restricted to small muscle subvolumes.

The study shows that the identification of regional morphology by MR may be correlated with electromyographic assessments of muscle function in human subjects. This method can be used to estimate the relationship between neuromuscular partitioning and intramuscular architecture in the different orofacial muscles, and it can be easily adapted to verify unit locations in studies of human motor control.

The recording method was a modification of the EMG scanning technique introduced by Stålberg and Antoni (1980). Originally, the technique employed two needle electrodes. One, a single-fibre EMG electrode, was stabilized in a muscle site to record a single-fibre action potential which acted as a trigger. A second concentric electrode was then moved through the muscle to record motor-unit activity, synchronous with the single-fibre action potentials. In the present study, however, a single monopolar needle was used because it is more comfortable in the facial region, especially during multiple insertions at repeated recording sessions. This type of electrode, when used in conjunction with a high lowcut-filter, has a similar selectivity to that of a concentric electrode. If the radius of electrical pick-up had been wide, the results would have revealed large MU territories for most units. In contrast, the mean territorial width (3.7

± 2.3 mm) in the experiment was highly consistent with previous reports. Stålberg and Eriksson (1987) reported the mean scan length for 32 single motor-units in the inferior part of the masseter to be 3.7 ± 0.6 mm, and McMillan and Hannam (1991) reported the mean distances measured along a medio-lateral axis for 32 paired recording sites to be 3.2 ± 2.3 mm. Confirmation of the selectivity of the single-needle approach was also obtained by the preliminary experiments in which two needles recorded activity from the same MU, one stationary electrode being used to trigger the display of activity recorded from a second, roving electrode in a manner comparable to that described by Stålberg and Antoni (1980). When the width of the MU was estimated from the triggered recordings and also from the roving needle alone (as was done in this experiment), the results were identical.

In Stålberg and Eriksson's (1987) work, the twin needle technique was also believed to reduce the potential error of overestimating territory size that might occur should the electrode be moved obliquely to the muscle-fibre direction. Their means of detecting a skewed scan was to observe a continuous change in latency between the triggering-action potential and the recorded motor-unit potential. In the present experimental design, any such error in orientation could be easily detected on the graphical display of the reconstruction.

The human masseter muscle can be divided into three anteroposterior groups based on fibre length (Schumacher, 1961c), which varies from 25-39 mm. Medio-laterally, the muscle fibres are equally long within a given anteroposterior group (Ebert, 1939). The muscle fibres which comprise a MU are considered to be of uniform length and

histochemical type (Zajac, 1989; Brandstater and Lambert, 1973). From the present experiment, it seems reasonable to assume that typical MU territories in the human masseter occupy volumes whose boundaries are defined supero-inferiorly by the length of the muscle fibres and by the internal tendon sheets. In the horizontal plane, their mediolateral dimensions are about 3-4 mm. Since the muscle is arranged in strips of fibres arranged anteroposteriorly, masseter MU territories are most likely arranged in strips of varying lengths, and have elliptical cross sections with their long axes oriented anteroposteriorly. This organization has been previously suggested by Herring *et al* (1991) for the pig masseter, in which MUs are restricted to small volumes of a muscle fascicle.

Earlier studies have suggested that most MUs are small, occupying discrete muscle volumes, while few units are large, occupying larger volumes (Stålberg and Eriksson, 1987; McMillan and Hannam, 1991). In glycogen-depletion studies in the pig masseter, depleted fibres, belonging to small MUs, have been found occasionally occupying large volumes in several discontinuous, widely-separated muscle regions, separated by aponeuroses (Herring *et al*, 1989). Theoretically, this broad innervation areas may result from axon branching. If an axon divides into two nerve branches, multiple muscle areas can be innervated (Pfeifer and Friede, 1985; Herring *et al*, 1989; English, 1990). This possibility however has been considered unlikely, and the presence of widely-distributed, depleted fibres was attributed to the technical difficulty in isolating a single axon for electrical stimulation (Herring *et al*, 1989). Similar patterns of discontinuous MU territories were not found in scanning EMG studies, however, large

units were found to cross aponeuroses. This finding may be interpreted as the result of the technical procedure itself. For example, wide-field electrode pick-up as a consequence of volume conduction may occur within the muscle (Stålberg and Trontelj, 1979). While this is a possible explanation for the results seen in the present study, it is unlikely, and although not proven, axon branching, is another possible explanation for this type of structural arrangement.

The correlation between MU territory size and overall muscle width is also relevant here. The same tendency was observed in the infant pig by Herring *et al* (1991), who reported the two largest territories in the masseters of older (and larger) piglets. Stålberg and Eriksson (1987) postulated that these units belonged to especially wide compartments. If their interpretation is correct, the largest units should be found in the superficial, anterior part of the muscle, where the deep and superficial portions fuse. This idea is only partially supported in the present study, for while a few large, confined units (± 9 mm) were encountered in the wide superficial muscle region, some large territories were found in other muscle regions, where they passed through aponeuroses. In the masseter, units with the lowest thresholds are located preferentially in the deep, medial part of the muscle, while higher threshold units seem to predominate in the superficial posterior region (Eriksson, 1982). Since the recordings were mostly from low-threshold MUs, they probably represent the type-I fibre population. This might explain the relatively larger number of MUs recorded in the middle and deep regions of the muscle.

The functional significance of widely-dispersed innervation territories is

uncertain. Stålberg and Eriksson (1987) suggested that large MU territories might be advantageous in motor tasks where there is less need for finely-graded control of jaw movements, and where the recruitment of such units may favour force development in static contraction, as for example in biting in the intercuspal position. It is also possible that these territories ensure internal tendon stiffness in situations where only one compartment is active, avoiding extreme internal tendon deformation and permitting fine vector gradations. The regional restriction of most MUs provides the basis for the idea that the central nervous system might control the contraction of discrete muscle regions independently, as has been previously proposed for the human masseter (Stålberg and Eriksson, 1987). This arrangement would allow differential contraction of MUs on either side of a tendon sheet to develop forces in several directions, and thereby explain the functional heterogeneity frequently reported in this muscle (Belser and Hannam, 1986; Tonndorf *et al*, 1989; Blanksma *et al*, 1992). Alternatively, these units could be simply available for developmental plasticity, when muscle adaptation to new conditions such as change or loss of dentition is required.

In conclusion, the human masseter seems to have a highly compartmentalized neuromuscular organization. The presence of territories between intramuscular tendons suggests that differential contraction may be possible on either side of central tendons provided the nervous system utilizes this structural substrate. The presence of a few large territories which extend across aponeuroses suggests that in these units, tensions must always be produced on either side of the aponeurosis whenever these units are active. The findings are thus generally consistent with the idea that there is at least some form

of mechanical heterogeneity in the masseter. The study also confirms the feasibility of making high-resolution reconstructions and of locating either stationary or roving EMG needles stereotactically relative to internal muscle compartments. This method could be used to estimate territories in other muscles and also be used in motor-control studies when it is important to locate recording sites.

4. GENERAL DISCUSSION AND CONCLUSIONS

The present studies of anatomical, biomechanical and physiological behaviour in the human masseter aimed to extend the knowledge of the functional organization of this muscle. The primary goal was to establish the presence of neuromuscular compartments within the muscle, their behaviour relative to intraoral tasks, and their relationship with the muscle's internal architecture. For many years, it has been assumed that the motor system would control the various jaw muscles as simple, whole structures, which would contract differentially to grade inter-occlusal forces and jaw movements during natural function. However, now it seems clear that in fact (at least in the masseter) a more refined foundation for the coordination of intramuscular activity exists.

Anatomical and physiological findings indicate that the human masseter muscle may be divided into at least three (possibly four) neuromuscular compartments. These form a multipennate muscle, which may vary in internal structural complexity between individuals, both in fetal and adult specimens. In an attempt to perform a detailed quantification of muscle fibre orientation in humans, it was found, however, that there are some major technical difficulties. Human specimens are not readily available, and the large sizes of human specimens complicate a thorough investigation with current histological methods. In addition, muscle fibres in young fetuses are not totally developed, which contribute to the difficulty in measuring fibre angulation and in identifying internal tendinous structures.

In contrast, the development of a Magnetic-Resonance imaging and three-

dimensional modelling technique used in the present experiments permitted the reconstruction of the complex internal structure of the human masseter muscle and mandible. Although the orientation of muscle fibres could not be visualized, the technique was found to be reliable, as confirmed by comparisons between the reconstructed muscles and the conventional anatomical dissections. An additional value of this technique is that it permits the investigation of the internal tendinous muscle structure in living subjects.

During jaw movements, insertions of muscle fibres in distinct regions of the human masseter displace by different amounts and directions, which suggests that its muscle fascicles lengthen and rotate differentially. Regional differences in these physical attributes vary with task being performed, and suggest that some muscle portions have more advantageous lines of action for certain tasks than for others, and that they vary between individuals. In this study, the ability to measure jaw movements with six degrees of freedom, added to the method for combining the orofacial tissue reconstruction with jaw-movement records, allowed the three-dimensional measurement of masseter-insertion displacement in living subjects. This has not been possible, previously.

During function, recruitment and rate-coding of motor units (MUs) in the human masseter by the central nervous system seem to follow the general principles regarding "size" and "common-drive" found in the motoneuron pools of other skeletal muscles (De Luca and Mambrito, 1987). Recruitment thresholds are however not stable, and the order of recruitment can change. Both are influenced by the type of task

performed, the manner in which it is approached, and its duration. Masseter MUs are usually polymodal, in that they can contribute to more than one intra-oral task, and they are difficult to drive at rates below 10 Hz. To produce bite forces, most MUs are recruited quite early in the performance of a task. The motor system relies mainly upon rate-coding over a wide range of voluntary contraction, although later recruitment of additional higher-threshold units does also contribute to the increase in bite force to reach the maximum level (Derfler and Goldberg, 1978). Since most masseter MUs are of similar size and type (Eriksson and Thornell, 1983) and since they are recruited concomitantly during light bite forces, it is possible that random fluctuations in the membrane potentials of motoneurons may affect the mechanism by which synaptic current is converted into spike trains (Calvin and Stevens, 1968). Thus, it is suggested that non-static behaviour of low-threshold masseter MU firing patterns is the result of a constant modification of the properties of some units by facilitation or suppression during a continuous isometric contraction. The modified low-threshold MU behaviour is further complicated by the effects of task, which may affect the interaction between descending, corticobulbar drive and peripheral input from orofacial and muscle receptors.

The present results support the notion that coactivation within and between the jaw muscles is a possible factor influencing the fluctuations in recruitment threshold, sustained-bite force and MU firing properties. In addition, there is enough circumstantial evidence to suggest that regional differences in MU behaviour also exist. However, no direct links between MU behaviour and internal muscle structure have

been established so far. It is important to emphasize that this, and most other, studies have been restricted to low-threshold MUs, which may behave differently than their high-threshold counterparts. The present results suggest that efforts to demonstrate regional differences in low-threshold MU behaviour with changes in task are difficult to validate statistically. Thus caution should be exercised when variables similar to these are used to classify MU type in human jaw muscles.

Previous electromyographic investigations of motor-unit (MU) sizes (Stålberg and Eriksson, 1987; McMillan and Hannam, 1991) in the human masseter have failed to correlate them with the muscle's internal architecture. The development of a method to locate electromyographic-needle-electrode scans stereotactically relative to internal tendinous boundaries, enabled the investigation of MU territories within the human masseter. Masseter MU mapping revealed that the mean territorial width was 3.7 ± 2.3 mm and varied between 0.4 mm and 13.1 mm. The widths were comparable to those of previous reports (Stålberg and Eriksson, 1987; McMillan and Hannam, 1991), and were related to the subject's muscle size as also noted in pig (Herring *et al*, 1991). The fact that most territories were distributed within discrete tendon-bounded compartments in the masseter provides an anatomical basis for selective activation of the muscle. However, it is also possible that this arrangement provides a flexible means for ensuring tendon stiffness and mechanical adaptation of the multipennate masseter during growth and development, whether or not the muscle is activated selectively. Since the majority of MU territories are dispersed within tendinous boundaries, motoneurons may be organized into separate task groups, which alter their contribution to bite force

depending on the intraoral task and experimental paradigm.

Collectively, the findings of the present study underline the complexity of the human stomatognathic system. The unique structural, MU-territorial organization, and task-related functional properties of the MUs in the masseter apparently provide a peripheral system which can be constantly adjusted by descending control and peripheral inputs to shade muscle activity to perform the intended task. Inter-individual variability with respect to anatomical, biomechanical and functional properties suggest that in future studies, it will be important to combine morphological and physiological information within a given human subject, and that care should be exercised when interpreting data from pooled samples.

5. FUTURE DIRECTIONS

It is known that there are considerable changes in human jaw movements associated with the different dentitions that appear during postnatal growth. It is possible that these variations in masticatory envelopes are due to a change in relative muscle fibre growth, by the utilization of different contraction strategies, or a combination of both. Whereas it seems that shifts in the human masseter fibres' angulation occur during growth, detailed data on such alterations are not available. It would be therefore useful to determine the angulations of masseter fibres in humans at different ages, and correlate these with functional jaw movements.

Alternatively, it is possible that these changes are due to muscle contraction patterns which simply become more refined with age. This assumption would be consistent with the view that ontogenetic changes in oral behaviour are caused by the development of a different motor pattern (presumably on a suitable anatomical substrate), and not by a major change in morphology other than size. Whether motor-unit (MU) territories are also restricted to small muscle portions, and whether differential contraction of the masseter muscle also occurs in young humans still remains to be confirmed. If it is assumed that in young humans MU territories are restricted to tendinous boundaries and that the contraction pattern is homogeneous, the stimulus for adoption of complex regional motor contraction patterns might be the result of learning. That is, after experimenting with various contraction patterns, the growing individual with a more complex dentition might select a group of muscle fibres which work most efficiently for the given task.

Given the variability in length and type of fibre terminations in the adult muscle, and their implication in muscle force production, a more detailed evaluation of the distribution of different types of fibre endings within the muscle and within the MU would be useful. Since it is not easy, at present, to study detailed MU anatomy in humans, an animal model would be indicated, which would follow the methods described by Ounjian *et al* (1991) and Eldred *et al* (1993). Briefly, if it is assumed that muscle fibres belonging to a MU taper towards their ends forming an elliptic shape, the sum of fibre areas measured on a single section through the approximate midlength of the MU, would not represent the true physiological cross-sectional area (CSA) of the unit. The suggested, more adequate method consist of measuring the CSA of a single MU, defined as the sum of the maximal areas to be found anywhere along the length of each of the MU fibres. The presence of MU territories of distinct shapes would infer that production of muscle tension varies within the muscle.

The use of MR imaging facilities enables an individualized assessment of muscle cross-sectional size, of internal muscle structure, and of craniofacial architecture in living subjects, which could be used for longitudinal or cross-sectional studies of craniofacial development or jaw biomechanics. With the development of software designed to reconstruct three-dimensional shapes directly from grey density values obtained from three-dimensional imaging techniques, the development of individualized reconstructions of human anatomy will be extremely simplified.

The ability to combine MR images with jaw movement data, measured with six degrees of freedom, is an advanced technology, useful in the study of masseter

attachment movement. This method could also be used to study masseter attachment displacement combined with electromyographic recording of different muscle regions, and in many other studies of attachment displacement, in which mandibular motion is subjected to different situations, such as by using bite splints of different designs, or chewing on different food consistencies. This type of experiments could prove to be useful in the evaluation of masticatory dysfunctions.

Muscle mechanics studies have commonly suggested that in a pennate structure, muscle fibre contraction promote parallel sliding of the central aponeurosis relative to the attachment tendons. Since MU territories were found to be mostly confined within tendinous boundaries, it is possible that differential contraction could approximate the central aponeurosis to one of the attachment tendons, changing in that way the orientation of the resultant muscle-force vector. While it is theoretically possible to investigate this supposition with MR imaging of the muscle when the jaw is kept at different relationships relative to the maxilla, the required long imaging sessions makes it impractical. In recent years, ultrasound imaging has been increasingly used in clinical and experimental investigations in living subjects. Its non-invasiveness, availability and ease of usage makes it a useful and more practical tool to investigate internal aponeuroses movement during natural function.

It is possible that high threshold MUs in the human masseter have more robust firing properties than the low threshold units studied in this thesis. If this is so, data collection of the functional behaviour of MUs, with known locations relative to internal muscle structures, would provide additional valuable data for the development

of a model of the internal mechanics of the masseter. Ultimately, such information would add to our understanding of motor control patterns in the orofacial region.

The stereotaxic technique developed in this thesis could be utilized in a variety of functional studies. The size and location of high threshold MU territories could be studied in the masseter, to confirm whether they are also restricted to tendinous boundaries, or if they extend over a large volume passing across tendons. If the latter assumption proves correct, it would mean that only low threshold units are capable of differential contraction. In addition, motor control studies, in which it is important to locate the electromyographic recording sites relative to internal muscle structure, could be performed.

Finally, the relationship between form and function in the masticatory system could be further explored to include other muscles and bone. With the same techniques utilized in this thesis, anatomical variations of other muscles and bones could be explored between individuals of similar or of different age groups. The displacement of different jaw muscles' attachment sites, and the motion of the mandible and condyle could be also analyzed. The behaviour of MUs in other jaw muscles and their territory size and location could be investigated, and compared against the masseter muscle.

Collectively, these data could be used to generate individualized computer models, which could be animated to perform static and dynamic mandibular tasks, and which could be manipulated to predict treatment outcomes in the fields of orthodontics, prosthodontics (including craniomandibular disorders) and surgery.

6. BIBLIOGRAPHY

Altman J, Bayer SA (1982) Development of the cranial nerve ganglia and related nuclei in the rat. *Adv Anat Embryol Cell Biol* 74:1-89.

An KN, Takahashi K, Harrigan TP, Chao EY (1984) Determination of muscle orientations and moment arms. *J Biomech Engng* 106:280-282.

Armstrong JB, Rose PK, Vanner S, Bakker GJ, Richmond FJR (1988) Compartmentalization of motor units in the cat neck muscle, biventer cervicis. *J Neurophysiol* 60:30-45.

Bagust J, Lewis DM, Westerman RA (1973) Polyneural innervation of kitten skeletal muscle. *J Physiol* 229:241-255.

Barnard RJ, Edgerton VR, Furukawa T, Peter JB (1971) Histochemical, biochemical and contractile properties of red, white and intermediate fibers. *Am J Physiol* 220:767-770.

Baron P, Debussy T (1979) A biomechanical functional analysis of the masticatory muscles in man. *Archs oral Biol* 24:547-553.

Basmajian JV, Stecko GA (1962) A new bipolar indwelling electrode for electromyography. *J Appl Physiol* 17:849.

Bawa P, Binder MD, Reunzel P, Henneman E (1986) Recruitment order of motoneurons in stretch reflexes is highly correlated with their axonal conduction velocity. *J Neurophysiol* 52:410-420.

Becht G (1954) Comparative biologic-anatomical researches on mastication in some mammals. I & II. *Proc K ned Akad Wet (Series C)* 56:508-527.

Belser UC, Hannam AG (1986) The contribution of the deep fibers of the masseter muscle to selected tooth-clenching and chewing tasks. *J Prosthet Dent* 56:629-636.

Bennett MR, Lavidis NA (1984) Development of the topographical projection of motor neurons to a rat muscle accompanies loss of polyneural innervation. *J Neurosci* 4:2204-2212.

Bennett MR, Davies AM, Everett AW (1988) The development of topographical maps and fiber types in toad (*Bufo marinus*) gluteus muscle during synapse elimination. *J Physiol* 396:371-496.

Benninghoff A, Rollhäuser H (1952) Zur inneren Mechanik des gefiederten Muskels.

Pflügers Arch ges Physiol 254:527-548.

Berendsen HJC (1962) Nuclear magnetic resonance study of collagen hydration. J Chem Phys 36:3297-3305.

Berquest TH (1987) Technical consideration. In Magnetic Resonance of the Musculoskeletal System. Berquist TH (editor), Raven Press, New York, pp 65.

Binder MD, Stuart DG (1980) Responses of Ia and spindle group II afferents to single motor-unit contractions. J Neurophysiol 43:621-629.

Blanksma NG, Van Eijden TMGJ (1990) Electromyographic heterogeneity in the human temporalis muscle. J Dent Res 69:1686-1690.

Blanksma NG, Van Eijden TM, Weijs WA (1992) Electromyographic heterogeneity in the human masseter muscle. J Dent Res 71:47-52.

Bodine SC, Roy RR, Meadows DA, Zernicke RF, Sacks RD, Fournier M, Edgerton VR (1982) Architectural, histochemical, and contractile characteristics of a unique biarticular muscle: the cat semitendinosus. J Neurophysiol 48(1):192-201.

Borg TK, Caulfield JB (1980) Morphology of connective tissue in skeletal muscle. Tissue & Cell 12:197-207.

Brändle K (1989) A new method for aligning histological serial sections for three-dimensional reconstruction. Comput Biomed Res 22:52-62.

Brandstater ME, Lambert EH (1973) Motor unit anatomy. Type and spatial arrangement of muscle fibers. In New Developments in Electromyography and Clinical Neurophysiology. Desmedt JE (editor), Karger, Basel, vol 1, pp 14-22.

Bredman JJ, Wessels A, Weijs WA, Korfage JAM, Soffers CAS, Moorman AFM (1991) Demonstration of 'cardiac-specific' myosin heavy chain in masticatory muscles of human and rabbit. Histochem J 23:160-170.

Brooke MH, Kaiser KK (1970) Three "myosin adenosine triphosphatase" systems: The nature of their pH and sulfhydryl dependence. J Histochem Cytochem 18:670-672.

Brown MC, Booth CM (1983) Postnatal development of the adult pattern of motor axon distribution in rat muscle. Nature 304:741-742.

Brown T (1975) Mandibular movements. Monographs of Oral Science 4:126-150.

Buchthal F, Schmalbruch H (1970) Contraction times and fibre types in intact human muscle. *Acta Physiol Scand* 79:435-452.

Buchthal F, Schmalbruch H (1980) Motor unit of mammalian muscle. *Physiol Revs* 60:90-142.

Büdingen H-J, Freund H-J (1976) The relationship between the rate of rise of isometric tension and motor unit recruitment in a human forearm muscle. *Pflügers Arch* 362:61-67.

Burdi AR, Spyropoulos MN (1978) Prenatal growth patterns of the human mandible and masseter muscle complex. *Am J Orthod* 74(4):380-387.

Burke RE (1981) Motor units: Anatomy, physiology, and functional organization. In *Handbook of Physiology, The Nervous System, Motor Control, Part 2*. Brookhart JM, Mountcastle VB, Brooks VB and Geiger SR (eds), Williams and Wilkins, Baltimore, pp 345-422.

Burke RE, Levine DN, Zajac FE, Tsairis P, Engel WK (1971) Mammalian motor units: physiological-histochemical correlation in three types in cat gastrocnemius. *Science* 174:709-712.

Burke RE, Tsairis P (1973) Anatomy and innervation ratios in motor unit of cat gastrocnemius. *J Physiol* 234:749-765.

Butler-Browne GS, Eriksson P-O, Laurent C, Thornell L-E (1988) Adult human masseter muscle fibres express myosin isozymes characteristic of development. *Muscle & Nerve* 11:610-620.

Cachel S (1984) Growth and allometry in primate masticatory muscles. *Arch oral Biol* 29:287-293.

Calvin WH, Stephens CF (1968) Synaptic noise and other sources of randomness in motoneuron interspike intervals. *J Neurophysiol* 31:574-587.

Cameron WE, Binder MD, Botterman BR, Reinking RM, Stuart DG (1981) "Sensory partitioning" of cat medial gastrocnemius muscle by its muscle spindles and tendon organs. *J Neurophysiol* 46:32-47.

Carew TJ, Ghez C (1985) Muscles and muscle receptors. In *Principles of Neural Science*. Kandell ER, Schwartz JH (eds), Elsevier, New York, pp 443-456.

Carlsöö S (1952) Nervous coordination and mechanical function of the mandibular elevators. An electromyographic study of the activity, and an anatomic analysis of the

mechanics of the muscles. *Acta odont scand suppl* 11(10):1-132.

Carlsöö S (1958) Motor units and action potentials in masticatory muscles. *Acta Morphol Neerl Scand* 2:13-19.

Carpentier P, Yung JP, Marguelles-Bonnet R, Meunissier M (1988) Insertions of the lateral pterygoid muscle: an anatomic study of the human temporomandibular joint. *J Oral & Maxillofac Surg* 46:477-482.

Chakeres DW, Caudill J, Schmalbrock P (1992) Multidimensional Fourier Transformation Imaging. In *Fundamentals of Magnetic Resonance Imaging*. Chakeres DW, Schmalbrock P (eds), Williams & Wilkins, Baltimore, Maryland, pp 81-100.

Christiansen EL, Thompson JR, Zimmerman G, Roberts D, Hasso AN, Hinshaw DB Jr, Kopp S (1987) Computed tomography of condylar and articular disk positions within the temporomandibular joint. *Oral Surg Oral Med Oral Path* 64(6):757-767.

Cihak O, Vlcek O (1962) Crista et fossa musculi zygomatico-mandibularis. *Anthropologie* 66:503-525.

Clamann HP (1970) Activity of single motor units during isometric tension. *Neurology* 20:254-260.

Clark RW, Luschei ES (1981) Histochemical characteristics of mandibular muscles of monkeys. *Exp Neurol* 74:654-672.

Clark RW, Luschei ES, Hoffman DS (1978) Recruitment order, contractile characteristics and firing patterns of motor units in the temporalis muscle of monkeys. *Exp Neurol* 61:31-52.

Close R (1973) Properties of motor units in fast and slow skeletal muscle of the rat. *J Physiol (London)* 234:723-748.

Cooper S, Daniel PM (1963) Muscle spindles in man; their morphology in the lumbricals and the deep muscles of the neck. *Brain* 86:563-586.

Cope TC, Clark BD (1991) Motor-unit recruitment in the decerebrate cat: several unit properties are equally good predictors of order. *J Neurophysiol* 66(4):1127-1138.

Covell DA, Herring SW (1993) Mandibular periosteal migration in the growing guinea pig. *Annu Meet Northwest Sect AADR, Abstr* 3.

Covell DA, Noden DM (1989) Embryonic development of the chick primary trigeminal sensory-motor complex. *J Comp Neurol* 286:488-503.

- Cuajunco F (1940) Development of the neuromuscular spindle in human fetuses. Carnegie Inst Wash Publ 518, Contributions to Embryology 28(173):95-128.
- Cuajunco F (1942) Development of the human motor end plate. Carnegie Inst Wash Publ 541, Contributions to Embryology 30(195):127-152.
- Culling CFA (1963) Handbook of histopathological techniques. Butterworths & Co., 2nd edition.
- D'Amico-Martel A, Noden DM (1983) Contributions of placodal and neural crest cells to avian cranial peripheral ganglia. Am J Anat 166:445-468.
- Dao TTT, Feine JS, Lund JP (1988) Can electrical stimulation be used to establish a physiologic occlusal position? J Prosthet Dent 60(4):509-514.
- Daube JR (1978) The description of motor unit potentials in electromyography. J Neurol 28(7):623-625.
- De Luca CJ (1985) Control properties of motor units. J exp Biol 115:125-136.
- De Luca CJ, Mambrito B (1987) Voluntary control of motor units in human antagonist muscles: coactivation and reciprocal activation. J Neurophysiol 58(3):525-542.
- Dechow PC, Carlson DS (1990) Occlusal force and craniofacial biomechanics during growth in rhesus monkey. Am J Phys Anthropol 83:219-237.
- Demiéville HN, Partridge LD (1980) Probability of peripheral interaction between motor units and implications for motor control. Am J Physiol 238:119-137.
- Derfler B, Goldberg LJ (1978) Spike train characteristics of single motor units in the human masseter muscle. Exp Neurol 61:592-608.
- Desmedt JE (1980) Patterns of motor commands during various types of voluntary movement in man. Trends Neurosci 3:265-268.
- Desmedt JE, Godaux E (1975) Vibration-induced discharge patterns of single motor units in the masseter muscle of man. J Physiol 253:429-442.
- Desmedt JE, Godaux E (1979) Recruitment patterns of single motor units in the human masseter muscle during brisk jaw clenching. Archs oral Biol 24:171-178.
- Desmedt JE, Godaux E (1981) Spinal motoneuron recruitment in man: rank deordering with direction but not with speed of voluntary movement. Science

214:933-936.

Diewert VM, Maeda S, Lozanoff S (1991) Analysis of human fetal craniofacial growth between 12 and 20 weeks with finite element modeling. In IV. International Conference on "Fundamentals of bone growth: methodology and applications" (3rd: 1990, Los Angeles, Calif). Dixon AD, Sarnat BG, Hoyte DAN (eds), CRC Press, Boca Raton, Florida, pp 565-578.

Donahue AP, English AW, Roden RL, Schwartz GA (1991) Tenotomy delays both synapse elimination and myogenesis in rat lateral gastrocnemius. *Neurosci* 42(1):275-282.

Donahue AP, English AW (1989) Selective elimination of cross-compartmental innervation in rat lateral gastrocnemius muscle. *J Neurosci* 9(5):1621-1627.

Drury RAB, Wallington EA (1980) Connective tissue fibres. In Carleton's *Histological Technique*. Oxford University Press, 5th edition.

Du Brul EL (1980) *Sicher's Oral Anatomy*, St Louis, CV Mosby Co. 7th edition.

Dubner R, Sessle BJ, Storey AT (1978) *The neural basis of oral and facial function*. Plenum Press, New York.

Dullemeijer P (1974) *Concepts and approaches in animal morphology*. Van Gorcum, Assen.

Ebert H (1939) Morphologische and Funktionelle Analyse des Musculus masseter. *Z anat EntwGesch* 109:790-802.

Edgerton VR, Roy RR and Apor P (1986) Specific tension of human elbow flexor muscles. In *International Series on Sports Sciences. Volume 16: Biochemistry of Exercise VI*. Saltin B (editor) Human Kinetics Publishers, Champaign, Illinois, pp 487-500.

Edgerton VR, Bodine SC, Roy RR (1987) Muscle architecture and performance. Stress and strain relationships in a muscle with two compartments in series. *Med Sport Sci* 26:12-23.

Edström L, Kugelberg E (1968) Histochemical composition, distribution of fibres and fatiguability of single motor units. *J Neurol Neurosurg Psychiat* 31:424-433.

Edström L, Grimby L (1986) Effect of exercise on the motor unit. *Muscle & Nerve* 9:104-126.

- Eisler P (1912) Die Muskeln des Stammes. In Handbuch der Anatomie des Menschen. Hrsg von K v Bardeleben Bd 2, Abt 2 Teil I, G Fischer Verlag, Jena.
- Ekstedt J (1964) Human single muscle fiber action potentials. *Acta Physiol Scand* 61, Suppl. 226:95.
- Ekstedt J, Stålberg E (1973) How the size of the needle electrode leading-off surface influences the shape of the single muscle fibre action potential in electromyography. *Comp Progr Biomed* 3:204-212.
- Eldred E, Garfinkel A, Hsu ES, Ounjian M, Roy RR, Edgerton VR (1993) The physiological cross-sectional area of motor units in the cat tibialis anterior. *J Anat Rec* 235(3):381-389.
- English AW (1984) An electromyographic analysis of compartments in cat lateral gastrocnemius during unrestrained locomotion. *J Neurophysiol* 52:114-125.
- English AW (1985) Limbs vs jaws: Can they be compared? *Amer Zool* 25:351-363.
- English AW (1990) Development of compartmentalized innervation of the rat gluteus maximus muscle. *J Comp Neurol* 301:104-113.
- English AW, Letbetter WD (1982a) Anatomy and innervation patterns of cat lateral gastrocnemius and plantaris muscles. *Am J Anat* 164:67-77.
- English AW, Letbetter WD (1982b) A histochemical analysis of identified compartments in cat lateral gastrocnemius muscle. *Anat Rec* 204:123-130.
- English AW, Timmis DP (1991) Development of compartmentalized innervation of a masticatory muscle. *J Dent Res* 70:522.
- English AW, Weeks OI (1984) Compartmentalization of single motor units in cat lateral gastrocnemius muscle. *Exp Brain Res* 56:361-368.
- English AW, Weeks OI (1987) An anatomical and functional analysis of cat biceps femoris and semitendinosus muscles. *J Morphol* 191:161-175.
- English AW, Weeks OI (1989) Electromyographic cross-talk within a compartmentalized muscle of the cat. *J Physiol* 416:327-336.
- Enoka RM, Stuart DG (1984) Henneman's 'size principle': current issues. *Trends Neurosci* 7:226-228.
- Erickson SJ, Cox IH, Hyde JS, Carrera GF, Strand JA, Estkowski LD (1991) Effect

of tendon orientation on MR imaging signal intensity: a manifestation of the "Magic Angle" phenomenon. *Radiology* 181:389-392.

Eriksson P-O (1982) Muscle-fibre composition of the human mandibular locomotor system. Enzyme-histochemical and morphological characteristics of functionally different parts. *Swed dent J suppl* 12:1-44.

Eriksson P-O, Stålberg E, Antoni L (1984) Flexibility in motor-unit firing pattern in the human temporal and masseter muscles related to type of activation and location. *Archs oral Biol* 29:707-712.

Eriksson P-O, Thornell L-E (1983) Histochemical and morphological, muscle-fibre characteristics of the human masseter, the medial pterygoid and the temporal muscles. *Archs oral Biol* 28:781-795.

Eriksson P-O, Thornell L-E (1987) Relation to extrafusal fibre-type composition in muscle-spindle structure and location in the human masseter muscle. *Archs oral Biol* 32:483-491.

Fache JS, Price C, Hawbolt EB, Li DKB (1987) MR imaging artifacts produced by dental materials. *AJNR* 8:837-840.

Farina JA, Letbetter WD (1977) Organization of primary spindle afferents with response to intramuscular branches of medial gastrocnemius nerve. *JSC Med Assoc* 73:15-16.

Faulkner MG, Hatcher DC, Hay A (1987) A three-dimensional investigation of temporomandibular joint loading. *J Biomech* 20:997-1002.

Fearnhead RW, Linder JE (1956) Observations on the silver impregnation of nerve fibres in teeth. *J Anat* 90:228-235.

Feinstein B, Lindergard B, Nyman E, Wohlfart G (1955) Morphologic studies of motor units in normal human muscles. *Acta Anat* 23:127-142.

Fenichel GM (1966) A histochemical study of developing human skeletal muscle. *Neurology (Minneap.)* 16:741.

Fetz EE, Cheney PD (1980) Postspike facilitation of forelimb muscle activity by primate corticomotoneuronal cells. *J Neurophysiol* 44:751-772.

Freimann R (1954) Untersuchungen über Zahl und Anordnung der Muskelspindeln in den Kaumuskeln des Menschen. *Anat Anz* 100:258-264.

- Freund H-J, Büdingen HJ, Dietz V (1975) Activity of single motor units from human forearm muscles during voluntary isometric contractions. *J Neurophysiol* 38:933-946.
- Freund H-J (1983) Motor unit and muscle activity in voluntary motor control. *Physiol Revs* 63:387-435.
- Fullerton GD (1982) Basic concepts for nuclear magnetic resonance imaging. *Magnetic Resonance Imaging* 1(1):39-55.
- Fullerton GD, Cameron IL, Ord VA (1985) Orientation of tendons in the magnetic field and its effect on T2 relaxation times. *Radiology* 155:433-435.
- Furstman L (1963) Early development of the human temporomandibular joint. *Am J Orthod* 49(9):672-682.
- Gagnot G, Yardin M, Delevaux F, Hernanie C (1977) Sur le développements musculo-aponevrotique du muscle masseter du lapin (*Oryctolagus cuniculus*). *Mammalia* 41:529-536.
- Gamble HJ, Fenton J, Allsopp G (1978) Electron microscope observations on human fetal striated muscle. *J Anat* 126(3):567-589.
- Gans C, Bock WJ (1965) The functional significance of muscle architecture - a theoretical analysis. *Adv Anat Embryol Cell Biol* 38:115-142.
- Gans C (1982) Fiber architecture and muscle function. *Exer Sport Sci Review* 10:160-207.
- Gans C, Loeb GE, de Vree F (1989) Architecture and consequent physiological properties of the semitendinosus muscle in domestic goats. *J Morphol* 199:287-297.
- Gans C, Gaunt AS (1991) Muscle architecture in relation to function. *J Biomech* 24(1):53-65.
- Gans C, de Vree F (1987) Functional bases of fiber length and angulation in muscle. *J Morphol* 192:63-85.
- Gaspard M, Laison F, Mailland M (1973) Organization architecturale et texture du muscle masseter chez les Primates et l'Homme. *J Biol Buccale* 1:7-20.
- Gaspard M (1987) Functional structure of the human temporal-masseter muscle complex in the fetus and the adult [Fre]. *Orthodontie Française* 58(2):549-565.
- Gasser RF (1967) The development of the facial muscles in man. *Am J Anat*

120(2):357-375.

Gath I, Stålberg EV (1975) Techniques for improving the selectivity of electromyographic recordings. Frequency- and time domain characteristics of single muscle fibre action potentials. *Electroencephalogr Clin Neurophysiol* 39:371-376.

Gath I, Stålberg E (1976) Techniques for improving the selectivity of electromyographic recordings. *IEEE Trans Biomed Eng* 23:467-472.

Gaunt WA (1971) *Microreconstruction*. Pitmans, London.

Gibbs CH, Mahan PE, Wilkinson TM, Mauderli A (1984) EMG activity of the superior belly of the lateral pterygoid muscle in relation to other jaw muscles. *J Prosth Dent* 51:691-702.

Goldberg LJ, Derfler B (1977) Relationship among recruitment order, spike amplitude, and twitch tension of single motor units in human masseter muscle. *J Neurophysiol* 40:879-890.

Goldspink G (1980) Growth of muscle. In *Development and Specialization of Skeletal Muscle*. Goldspink DF (editor), Cambridge University Press, pp 19-35.

Gollnick PD, Hodgson DR (1986) The identification of fiber types in skeletal muscle: a continual dilemma. *Exer Sport Sci Revs* 14:81-104.

Goshgarian HG (1977) A rapid silver impregnation for central and peripheral nerve fibers in paraffin and frozen sections. *Exp Neurol* 57:296-301.

Grant PG (1973) Biomechanical significance of the instantaneous center of rotation: the human temporomandibular joint. *J Biomech* 6:109-113.

Greenfield BE, Wyke BD (1956) Electromyographic studies of some muscles of mastication. *Brit Dent J* 100:129-143.

Guld C, Rosenfalck A, Willison RG (1973) Report of the committee on EMG instrumentation. Technical factors in recording electrical activity of muscle and nerve in man. *Electroencephalogr Clin Neurophysiol* 28:399-413.

Gydikov A, Gerilovsky L, Gatev P, Kostev K (1982) Volume conduction of motor unit potentials from different human muscles to long distances. *Electromyography Clin Neurophysiol* 22:105-116.

Hagiwara M, Koriath TWP, Tonndorf ML, Hannam AG (1993a) Three-dimensional motion of the mandibular condyle in human subjects. AADR Meeting, Northwest

Section.

Hagiwara M, Hannam AG, Koriath TWP, Tonndorf ML (1993b) Three-dimensional motion of the human mandibular condyle. *J Dent Res* 72, pp 267.

Hamburger V (1961) Experimental analysis of the dual origin of the trigeminal ganglion in the chick embryo. *J Exp Zool* 148:91-124.

Hamilton WJ, Boyd JD, Mossman HW (1962) *Human Embryology*. W Heffer and Sons Ltd, Cambridge, 3rd edition.

Hannam AG (1992) The measurement of jaw motion. In *Current Controversies in Temporomandibular Disorders: Proceedings of the Craniomandibular Institute's 10th Annual Squaw Valley Winter Seminar, Squaw Valley, California*. McNeill C (editor), Quintessence Publishing Co Inc, Carol Stream, Illinois, pp 130-137.

Hannam AG (1982) The innervation of the periodontal ligament. In *The Periodontal Ligament in Health and Disease*. Berkovitz BKB (editor), Pergamon Press, Oxford, pp 173-193.

Hannam AG, De Cou RE, Scott JD, Wood WW (1977) The relationship between dental occlusion, muscle activity and associated jaw movement in man. *Archs oral Biol* 22:25-32.

Hannam AG, McMillan AS (1993) Internal Organization in the Human Jaw Muscle. *CRC Critical Reviews in Oral Biology and Medicine*. In Press.

Hannam AG, Wood WW (1981) Medial pterygoid muscle activity during the closing and compressive phases of human mastication. *Amer J Phys Anthropol* 55:359-367.

Hannam AG, Wood WW (1989) Relationships between the size and spatial morphology of human masseter and medial pterygoid muscles, the craniofacial skeleton, and jaw biomechanics. *Am J Phys Anthropol* 80:429-445.

Hansson T, Öberg T, Carlsson GE, Kopp S (1977) Thickness of the soft tissue layers and the articular disk of the temporomandibular joint. *Acta Odont Scand* 35:77-83.

Harms SE, Kramer DM (1985) Fundamentals of magnetic resonance imaging. In *CRC Critical Reviews in Diagnostic Imaging*. Boca Raton, CRC Press, pp 70-111.

Hattori Y, Watanabe M, Sasaki K, Kikuchi M (1991) Motor unit behaviour in three-dimensional bite force in human masseter. *J Dent Res* 70:553.

Hatze H (1978) A general myocybernetic control model of skeletal muscle. *Biol*

Cybernetics 28:143-157.

Henneman E (1979) Functional organization of motoneuron pools: the size-principle. In *Integration in the Nervous System*. Asanuma H, Wilson VJ (eds), Tokyo, Igaku Shoin, pg 13-25.

Henneman E (1981) Recruitment of Motoneurons: The size principle. In *Motor Unit Types: Recruitment and Plasticity in Health and Disease*. Proc Clin Neurophysiol 9:26-60.

Henneman E, Clamann HP, Gillies JD, Skinner RD (1974) Rank-order of motoneurons within a pool: law of combination. J Neurophysiol 37:1338-1349.

Henneman E, Mandell LM (1981) Functional organization of motoneuron pool and its inputs. In *Handbook of Physiology. Section 1: The Nervous System, vol II. Motor Control, part 1*, pp 423-507.

Henneman E, Olson CB (1965) Relations between structure and function in the design of skeletal muscle. J Neurophysiol 28:581-598.

Herring SW (1985) The ontogeny of mammalian mastication. Am Zool 25:291-301.

Herring SW (1980) Functional design of cranial muscles: comparative and physiological studies in pigs. Am Zool 20:283-293.

Herring SW, Grimm AF, Grimm BR (1979) Functional heterogeneity in a multipinnate muscle. Am J Anat 154:563-576.

Herring SW, Wineski LE, Anapol FC (1989) Neural organization of the masseter muscle in the pig. J comp Neurol 280:563-576.

Herring SW, Anapol FC, Wineski LE (1991) Motor-unit territories in the masseter muscle of infant pigs. Archs oral Biol 36(12):867-873.

Herring SW, Muhl AF, Obrez A (1993) Bone growth and periosteal migration control masseter muscle orientation in pigs (*Sus scrofa*). Anat Rec 235:215-222.

Herring SW, Wineski LE (1986) Development of the masseter muscle and oral behavior in the pig. J Exp Zool 237:191-207.

Herring SW, Scapino RP (1973) Physiology of feeding in miniature pigs. J Morph 141:427-460.

Heslinga JW, Huijing PA (1990) Effects of growth on architecture and functional

- characteristics of adult rat gastrocnemius muscle. *J Morphol* 206(1):119-132.
- Hiiemae K (1967) Masticatory function in the mammals. *J Dent Res* 46:883-893.
- Hiiemae K, Houston WJB (1971) The structure and function of the jaw muscles in the rat (*Rattus norvegicus* L.) I. Their anatomy and internal architecture. *Zool J Linn Soc* 50:75-99.
- Hill AV (1950) The series elastic component of muscle. *Proc Roy Soc (Lond)* 38:209-230.
- Hopf G (1934) Größenunterschiede der Muskelfaserquerschnitte zwischen den einzelnen Portionen des M. masseter beim Menschen und bei einigen Säugetieren. *Z Mikroskop-Anat Forsch* 35:195-217.
- Huber GC (1916) On the form and arrangement in fasciculi of striated voluntary muscle fibers. *Anat Rec* 11:149-168.
- Huijing PA, Woittiez RD (1984) The effect of architecture on skeletal muscle performance: A simple planimetric model. *Neth J Zool* 34:21-32.
- Humphrey T (1970) Reflex activity in the oral and facial area of the human fetus. In *Second Symposium on Oral Sensation and Perception*. Bosma JF (editor), pp 195-233.
- Humphrey T (1971) Development of oral and facial motor mechanisms in human fetuses and their relation to craniofacial growth. *J Dent Res* 50(6):1428-1441.
- Hurov J, Henry-Ward W, Phillips L, German R (1988) Growth allometry of craniomandibular muscles, tendons, and bones in the laboratory rat (*Rattus norvegicus*): relationships to oromotor maturation and biomechanics of feeding. *Am J Anat* 182:381-394.
- Hylander WL, Johnson KR (1985) Temporalis and masseter muscle function during incision in macaques and humans. *Int J Primat* 6(3):289-322.
- Ishikawa H (1966) Electron microscopic observations of satellite cells with special reference to the development of mammalian skeletal muscles. *Z Anat EntwGesch* 125:43.
- Janun D, English AW (1986) Compartmentalization of single muscle units in the rat lateral gastrocnemius. *Anat Rec* 214:60A.
- Jemt T (1984) Masticatory mandibular movements. *Swed Dent J* (suppl 23).

- Johnston MC, Hazelton RD (1972) Embryonic origins of facial structures related to oral sensory and motor functions. In 3rd Symposium on Oral Sensation and Perception (The Mouth of the Infant). Bosma JF (editor), pp 76-97.
- Jonsson B, Bagge UE (1968) Displacement, deformation and fracture of wire electrodes for electromyography. *Electromyography* 8:329-347.
- Junqueira LCU, Bignolas G, Brentani RR (1979a) A simple and sensitive method for the quantitative estimation of collagen. *Anal Biochem* 94:96-99.
- Junqueira LCU, Bignolas G, Brentani RR (1979b) Picrosirius staining plus polarization microscopy, a specific method for collagen detection in tissue sections. *Histochem J* 11:447-455.
- Kadaba MP, Wootten ME, Gainey J, Cochran GVB (1985) Repeatability of phasic muscle activity; performance of surface and intramuscular wire electrodes in gait analysis. *J Orthop Res* 3(3):350-359.
- Källén B (1962) Mitotic patterning in the central nervous system of chick embryos, studied by a colchicine method. *Z Anat Entw-Gesch* 123:309-319.
- Källén B (1956) Contribution to the knowledge of the regulation of the proliferation processes in the vertebrate brain during ontogenesis. *Acta Anat* 27:351-360.
- Kanda K, Burke RE, Warmesley B (1977) Differential control of fast and slow twitch motor units in the decerebrate cat. *Exp Brain Res* 29:57-74.
- Kelly AM, Zacks SI (1969) The histogenesis of rat intercostal muscle. *J cell Biol* 42:135.
- Keynes R, Lumsden A (1990) Segmentation and the origin of regional diversity in the vertebrate central nervous system. *Neuron* 2:1-9.
- Kidokoro Y, Kubota K, Shuto S, Sumino R (1968) Reflex organization in the cat masticatory muscles. *J Neurophysiol* 13:361-364.
- Knapp TR (1992) Technical error of measurement: A methodological critique. *Am J Phys Anthropol* 87:235-236.
- Komi PV, Buskirk ER (1970) Reproducibility of electromyographic measurements with inserted wire electrodes and surface electrodes. *Electromyography* 4:357-367.
- Koolstra JH, Van Eijden TMGJ, Weijs WA, Naeije M (1988a) A three-dimensional mathematical model of the human masticatory system predicting maximum possible

bite forces. J Biomech 21:563-576.

Koolstra JH, Van Eijden TMGJ, Weijs WA (1988b) Three-dimensional performance of the human masticatory system: the influence of the orientation and physiological cross-section of the masticatory muscles. Biomechanics XI-A. Free University Press, Amsterdam, pp 101-106.

Koolstra JH, Van Eijden TMGJ, Weijs WA (1989) An iterative procedure to estimate muscle lines of action in vivo. J Biomech 22:911-920.

Koolstra JH, van Eijden TMGJ, van Spronsen PH, Weijs WA, Valk J (1990) Computer-assisted estimation of lines of action of human masticatory muscles reconstructed *in vivo* by means of magnetic resonance imaging of parallel sections. Archs oral Biol 35(7):549-556.

Korioth TWP (1992) Finite element modelling of human mandibular biomechanics. PhD Thesis, The University of British Columbia, Vancouver.

Korioth TWP, Hannam AG (1990) Effect of bilateral asymmetric tooth clenching on load distribution at the mandibular condyles. J Prosthet Dent 64:62-73.

Korioth TWP, Romilly DP, Hannam AG (1992) Three-dimensional finite element stress analysis of the dentate human mandible. Am J Phys Anthropol 88:69-96.

Kranz H, Baumgartner G (1974) Human alpha motoneurone discharge, a statistical analysis. Brain Res 67:324-329.

Kubota K, Masegi T (1977) Muscle spindle supply to the human jaw muscle. Int Dent Res 56:901-909.

Lam EWN (1991) Human masseter muscle studies by magnetic resonance. MSc Thesis, The University of British Columbia, Vancouver.

Lam EWN, Hannam AG, Wood WW, Fache JS, Watanabe M (1989) Imaging orofacial tissues by magnetic resonance imaging. Oral Surg Oral Med Oral Pathol 68:2-8.

Lam EWN, Hannam AG, Christiansen EL (1991) Estimation of tendon-plane orientation within human masseter muscle from reconstructed magnetic resonance images. Archs oral Biol 11:845-853.

Langenbach GEJ, Weijs WA (1990) Growth patterns of the rabbit masticatory muscles. J Dent Res 69(1):20-25.

Langenbach GEJ (1992) Development of form and function of the rabbit masticatory system. PhD Thesis, University of Amsterdam, Amsterdam.

Larsson L (1992) Is the motor unit uniform? *Acta Physiol Scand* 144:143-154.

Last RJ (1966) *Anatomy: regional and applied*. Churchill, J & A Ltd, London.

Lau H (1972) Innervation of the jaw muscles in representatives of various chewing types. In *Morphology of the Maxillo-mandibular Apparatus*. IX Int. Congress of Anatomists. Schumacher GH (editor), Georg Thieme, Leipzig, pp 133-137.

Lele S (1991) Some comments on coordinate-free and scale-invariant methods in morphometrics. *Am J Phys Anthropol* 85:407-417.

Lele S, Richtsmeier JT (1991) Euclidean distance matrix analysis: a coordinate-free approach for comparing biological shapes using landmark data. *Am J Phys Anthropol* 86:415-427.

Lenman JAR, Ritchie AE (1987) *Clinical electromyography*. Churchill Livingstone, Edinburgh, pp 14-24.

Lichtman JW, Purves D (1983) Activity-mediated neural change. *Nature* 301(17):563-564.

Linder JE (1978) A simple and reliable method for the silver impregnation of nerves in paraffin sections of soft and mineralized tissues. *J Anat* 127(3):543-551.

Loeb GE (1985) Motoneurone task groups: coping with kinematic heterogeneity. *J exp Biol* 115:137-146.

Loeb GE, Gans C (1986) *EMG for Experimentalists*. Univ of Chicago Press, Chicago.

Loeb GE, Pratt CA, Chanaud CM, Richmond FJR (1987) Distribution of innervation of short, interdigitated muscle fibers in parallel-fibered muscles of the cat hindlimb. *J Morphol* 191:1-15.

Lowe AA (1980) Correlations between orofacial muscle activity and craniofacial morphology in a sample of control and anterior open-bite subjects. *Am J Orthod* 78:89-98.

Lundeen HC, Gibbs CH (1982) Jaw movements and forces during chewing and swallowing and their clinical significance. In *Advances in Occlusion*. John Wright (editor), PSG Inc, Boston, pp 2-32.

Luschei ES, Goldberg LJ (1981) Neural mechanisms of mandibular control: mastication and voluntary biting. In *Handbook of Physiology. Section 1: The Nervous System*, vol II. Motor Control, part II, pp 1237-1274.

Lüscher R, Ruenzel P, Henneman E (1979) How the size of motoneurons determines their susceptibility to discharge. *Nature* 282:859-861.

MacDonald JWC, Hannam AG (1984a) Relationship between occlusal contacts and jaw-closing muscle activity during tooth clenching: Part I. *J Prosthet Dent* 52:718-729.

MacDonald JWC, Hannam AG (1984b) Relationship between occlusal contacts and jaw-closing muscle activity during tooth clenching: Part II. *J Prosthet Dent* 52:862-867.

MacDougall JD, Elder GCB, Sale DG, Moroz JR, Sutton JR (1980) Effects of strength training and immobilization on human muscle fibres. *Eur J Appl Physiol* 43:25.

Mangun GA, Mulkey RM, Young BL, Goslow GE Jr (1986) 'Cross-talk' in electromyograms: Contamination of EMGs recorded with bipolar fine-wire electrodes by volume conducted myoelectric activity from distant sources. *Electromyography Clin Neurophysiol* 26:443-461.

Mao J, Stein RB, Osborn JW (1992) The size and distribution of fiber types in jaw muscles: a review. *J Craniomandib Disord Facial Oral Pain* 6:192-201.

Mastaglia FL (1981) Growth and development of the skeletal muscles. In *Scientific Foundations of Paediatrics*. Davis JA, Dobbing J (eds), W Heinemann, pp 590-620.

Matsumoto H, Katsura S (1985) Multiple compartmentalization in the fibre architecture of rat masseter muscle. *Acta Anat Nippon* 60:90-98.

Matsumoto H, Katsura S (1987) Muscle-fibre architecture of the rat medial pterygoid muscle. *Archs oral Biol* 32:705-711.

Mauro A (1961) Satellite cells of skeletal muscle fibres. *J Biophys Biochem Cytol* 9:493.

McGeer PL, Akiyama H, Itagaki S, McGeer EG (1989) Immune system response in Alzheimer's disease. *Can J Neurol Sci* 16:516-527.

McKeon B, Burke D (1983) Muscle spindle discharge in response to contraction of single motor units. *J Neurophysiol* 49:291-302.

- McLearn D, Noden DM (1988) Ontogeny of architectural complexity in embryonic quail visceral arch muscles. *Am J Anat* 183:277-293.
- McMillan AS (1989) Human masseter motor unit behaviour. PhD Thesis, The University of British Columbia, Vancouver.
- McMillan AS, Hannam AG (1991) Motor-unit territory in the human masseter muscle. *Archs oral Biol* 36:435-441.
- McMillan AS, Hannam AG (1992) Task-related behaviour of motor units in different regions of the human masseter muscle. *Archs oral Biol* 37(10):849-857.
- McMillan AS, Sasaki K, Hannam AG (1990) The estimation of motor unit twitch tensions in the human masseter muscle by spike-triggered averaging. *Muscle & Nerve* 13:697-703.
- McMillan AS, Hannam AG (1989a) Location of needle electrode recording sites in the human masseter muscle by magnetic resonance imaging. *J Neurosci Methods* 30:85-89.
- McMillan AS, Hannam AG (1989b) Reflex inhibition in single motor units of the human lateral pterygoid muscle. *Experiment Brain Res* 76:97-102.
- Merlini L, Palla S (1988) The relationship between condylar rotation and anterior translation in healthy and clicking temporomandibular joints. *Schweiz Monatsschr Zahnmed* 98:1191-1199.
- Meyenberg K, Kubik S, Palla S (1986) Relationships of the muscles of mastication to the articular disc of the temporomandibular joint. *Schweiz Monatsschr Zahnmed* 96:815-834.
- Meyer EP, Domanico VJ (1988) Three-dimensional reconstruction: a tissue embedding method for alignment of serial sections. *J Neurosci Methods* 26:129-132.
- Migchelsen C, Berendsen HJC (1973) Proton exchange and molecular orientation of water in hydrated collagen fibers. An NMR study of H₂O and D₂O. *J Chem Phys* 59:296-305.
- Miles TS, Türker KS (1986) Does reflex inhibition of motor units follow the "size principle"? *Exp Brain Res* 62:443-445.
- Miles TS, Türker KS, Nordstrom MA (1986) Length-related changes in activation threshold and waveform of motor units in human masseter muscle. *J Physiol* 370:457-465.

- Miller AJ (1991) Craniomandibular muscles: their role in function and form. CRC Press, Boca Raton.
- Milner-Brown HS, Stein RB, Yemm R (1973) Changes in firing rate of human motor units during linearly changing voluntary contractions. *J Physiol* 239:371-390.
- Mohl ND, McCall WD, Lund JP, Plesh O (1990) Devices for the diagnosis and treatment of temporomandibular disorders. Part I. Introduction, scientific evidence, and jaw tracking. *J Prosthet Dent* 63:198-201.
- Møller E (1966) The chewing apparatus: an electromyographic study of the action of the muscles of mastication and its correlation to facial morphology. *Acta Physiol Scand* 69, Supp. 280:1-229.
- Monster AW, Chan H (1977) Isometric force production by motor units of extensor digitorum communis muscle in man. *J Neurophysiol* 40:1432-1443.
- Moore KL (1983) The ninth week to birth. In *Before we are Born. Basic Embryology and Birth Defects*. WB Saunders Company, 2nd edition, pp 68-73.
- Mosolov NN (1972) On the anatomy of human masticatory musculature. In *Morphology of the Maxillo-Mandibular Apparatus*. Schumacher G-H (editor), Thieme, Leipzig, pp 65-69.
- Muhl ZF (1982) Active length-tension relation and the effect of muscle pinnation on fibre lengthening. *J Morphol* 173:285-292.
- Munro RR (1974) Activity of the digastric muscle in swallowing and chewing. *J Dent Res* 53(3):530-537.
- Munro RR (1972) Coordination of the two bellies of the digastric muscle in basic jaw movements. *J Dent Res* 51(6):1663-1667.
- Nandedkar SD, Sanders DB (1989) Principal components analysis of the features of concentric needle EMG motor unit action potentials. *Muscle & Nerve* 12:288-293.
- Nelson GJ (1986) Three dimensional computer modelling of human mandibular biomechanics. MSc Thesis, The University of British Columbia, Vancouver.
- Nixon JR (1987) Basic principles and terminology. In *Magnetic Resonance of the Musculoskeletal System*. Berquist TH (editor), Raven Press, New York, pp 1-17.
- Noden DM (1991) Cell movements and control of patterned tissue assembly during craniofacial development. *J Craniofac Genet Dev Biol* 11:192-213.

- Noden DM (1986) Patterning of avian craniofacial muscles. *Dev Biol* 116:347-356.
- Nordstrom MA, Miles TS, Veale JL (1989) Effect of motor unit firing pattern on twitches obtained by spike-triggered averaging. *Muscle & Nerve* 12:556-567.
- Nordstrom MA, Miles TS (1990) Fatigue of single motor units in human masseter. *J Appl Physiol* 68:26-34.
- Nordstrom MA, Miles TS (1991a) Discharge variability and physiological properties of human masseter motor units. *Brain Res* 541:50-56.
- Nordstrom MA, Miles TS (1991b) Instability of motor unit firing rate during prolonged isometric contraction in human masseter. *Brain Res* 549:268-274.
- O'Donovan MJ, Pinter MJ, Dum RP, Burke RE (1985) Kinesiological studies of self- and cross-reinnervated FDL and soleus muscles in freely moving cats. *J Neurophysiol* 26:443-461.
- Ontell MA (1977) Neonatal muscle: an electron microscopic study. *Anat Rec* 189:669.
- Ontell MA and Dunn RF (1978) Neonatal muscle growth: a quantitative study. *Am J Anat* 152:539-556.
- Osborn JW, Baragar FA (1985) Predicted pattern of human muscle activity during clenching derived from a computer assisted model: symmetric vertical bite forces. *J Biomech* 18:599-612.
- Otten E (1988) Concepts and models of functional architecture in skeletal muscle. *Exer Sport Sci Review* 16:89-137.
- Ounjian M, Roy RR, Eldred E, Garfinkel A, Payne JR, Armstrong A, Toga AW, Edgerton VR (1991) Physiological and developmental implications of motor unit anatomy. *J Neurobiol* 22(5):547-559.
- Palla S, Ash MM (1987) Effect of bite force on the power spectrum of the surface electromyogram of human jaw muscles. *Archs oral Biol* 26:287-295.
- Partridge LD, Benton LA (1981) Muscle, the Motor. In *Handbook of Physiology. Sect 1: The Nervous System, vol II. Motor Control, part 1*, pp 43-106.
- Paturet G (1951) *Traité d'Anatomie Humaine*. Masson, Paris, Vol 1, pp 95, 117 and 329.
- Perry J, Easterday CS, Antonelli DJ (1981) Surface versus intramuscular electrodes

- for electromyography of superficial and deep muscles. *Physiol Ther* 61:7-15.
- Person RS (1974) Rhythmic activity of a group of human motoneurons during voluntary contraction of a muscle. *Electroencephalogr Clin Neurophysiol* 36:585-595.
- Person RS, Kudina LP (1972) Discharge frequency and pattern discharge of human motor units during voluntary contraction of muscle. *Electroenceph Neurophysiol* 32:471-483.
- Petajan JH (1981) Motor unit frequency control in man. In *Motor Unit Types, Recruitment and Plasticity in Health and Disease*. Desmedt JE (editor). *Prog clin Neurophysiol*, pp 184-200.
- Peters A (1955a) Experiments on the mechanism of silver staining. Part I. Impregnation. *Quart J micr Sci* 96:84-102.
- Peters A (1955b) Experiments on the mechanism of silver staining. Part II. Development. *Quart J Micr Sci* 96:103-115.
- Peterson JA, Benson JA, Morin JG, McFall-Ngai MJ (1984) Scaling in tensile "skeletons": Scale dependent length of the Achilles tendon in mammals. *J Zool* 202(3):361-372.
- Peterson JA, Benson JA, Ngai MM, Morin JG, Owe C (1982) Scaling in tensile "skeletons": Structures with scale-independent length dimensions. *Science* 217:1267-1270.
- Pfeiffer G, Friede RL (1985): The localization of axon branchings in two muscle nerves of the rat. *Anat Embryol (Berl)* 172:177-182.
- Price C, Connell DG, MacKay A, Tobias DL (1992) Three-dimensional reconstruction of magnetic resonance images of the temporomandibular joint by I-DEAS. *Dentomaxillofac Radiol* 21:148-153.
- Pruim GJ, de Jongh HJ, Ten Bosch JJ (1980) Forces acting on the mandible during bilateral static bite at different bite force levels. *J Biomech* 13:755-763.
- Purves D, Lichtman JW (1980) Elimination of synapses in the developing nervous system. *Science* 210:153-157.
- Radpour S, Gacek RR (1985) Anatomic organization of the cat facial nerve. *Otolaryngol Head Neck Surg* 93:591-596.
- Ralph L, Leunbach IB, Kopp S (1991) Magnetic resonance imaging of the masseter

muscle of the rabbit. *Scand J Dent Res* 99:162-165.

Ranvier L (1873) Propriétés et structures différentes des muscles rouges et des muscles blancs chez les lapins et chez les raies. *C R Acad Sci (D) (Paris)* 77:1030-1034.

Redfern PA (1970) Neuromuscular transmission in new-born rats. *J Physiol* 209:701-709.

Richfield EK, Cohen BA, Albers JW (1981) Review of quantitative and automated needle electromyographic analyses. *IEEE transactions on biomedical engineering* 28(7):506-514.

Richmond FJR, Macgillis DRR, Scott DA (1985) Muscle fibre compartmentalization in cat splenius muscle. *J Neurophysiol* 53:868-885.

Richter D, Herring SW (1993) Growth of the masseter aponeurosis in relation to muscle size. *J Dent Res* 72:724A.

Riek S, Bawa P (1992) Recruitment of motor units in human forearm extensors. *J Neurophysiol* 68(1):100-108.

Ringqvist M, Ringqvist I, Eriksson P-O, Thornell L-E (1982) Histochemical fibre-type profile in the human masseter muscle. *J Neurol Sci* 53:273-282.

Rohlf FJ, Bookstein FL (1990) Proceedings of the Michigan Morphometrics Workshop. Ann Arbor, Michigan, The University of Michigan Museum of Zoology.

Romaiguère P, Vedel JP, Pagni S (1989) Fluctuations in motor unit recruitment threshold during slow isometric contractions of wrist extensor muscles in man. *Neurosci Lett* 103:50-55.

Romer AS (1939) The vertebrate body. WB Saunders & Company, Philadelphia, 1st edition.

Rowe RW (1981) Morphology of perimysial and endomysial connective tissue in skeletal muscle. *Tissue & Cell* 13(4):681-90.

Rowlerson A, Mascarello F, Barker D, Saed H (1988) Muscle-spindle distribution in relation to the fibre-type composition of masseter in mammals. *J Anat* 161:37-60.

Rowles SL (1960) Some observations on Ungewitter's method for staining nerve fibres and nerve endings in tissue sections. *Archs oral Biol* 2:89-95.

Sacks R, Roy R (1982) Architecture of the hindlimb muscles of cats: functional significance. *J Morphol* 173:185-195.

Salmons S, Henriksson J (1981) The adaptive response of skeletal muscle to increased use. *Muscle & Nerve* 4:94-105.

Samuel EP (1953a) Impregnation and development in silver staining. *J Anat* 87:268-277.

Samuel EP (1953b) The mechanism of silver staining. *J Anat* 87:278-287.

Samuels ML (1989) Statistics for the life sciences. Dellen Publishing Company, San Francisco, California.

Sasaki K, Hannam AG, Wood WW (1989) Relationships between the size, position, and angulation of human jaw muscles and unilateral first molar bite force. *J Dent Res* 68(3):499-503.

Schellhas KP (1989) MR imaging of muscles of mastication. *AJNR* 10:829-837.

Schmalbruch H (1974) The sarcolemma of skeletal muscle fibres as demonstrated by a replica technique. *Cell & Tiss Res* 150(3):377-87.

Schmidt EM, Thomas JS (1981) Motor unit recruitment order: modification under volitional control. *Prog Clin Neurophysiol* 9:145-148.

Scholz TD, Fleagle SR, Burns TL, Skorton DJ (1989) Tissue determinants of nuclear magnetic resonance relaxation times: Effect of water and collagen content in muscle and tendon. *Invest Radiol* 24:893-898.

Schumacher G-H (1989) Innervation pattern in jaw muscles of various mammalian chewing types. *Acta Morphol Neerl-Scand* 27:139-147.

Schumacher GH (1962) Struktur- und Funktionswandel der Kaumuskulatur nach der Geburt. *Fortschr Kieferorthop* 23(1/2):135-167.

Schumacher G-H (1961a) Die Kaumuskulatur der Rodentia. In *Funktionelle Morphologie der Kaumuskulatur*. Veb Gustav Fischer Verlag, Jena, pp 189-209.

Schumacher GH (1961b) Die Kaumuskulatur der Artiodactyla. In *Funktionelle Morphologie der Kaumuskulatur*. Veb Gustav Fisher Verlag, Jena, pp 152-188.

Schumacher G-H (1961c) Die Kaumuskulatur der Menschen. In *Funktionelle Morphologie der Kaumuskulatur*. Veb Gustav Fischer Verlag, Jena, pp 13-53.

Schwartz MS, Stålberg E, Schiller HH, Thiele B (1976) The reinnervated motor unit in man. *J Neurol Sci* 27:303-312.

Scott JD, DeCou RE, Hannam AG, Wood WW (1983) The digital assessment of muscle activity during chewing, clenching and similar functions. *J Dent Res* 62:375A.

Scott SH, Thomson DB, Richmond FJR, Loeb GE (1992) Neuromuscular organization of feline anterior sartorius: II. Intramuscular length changes and complex length-tension relationships during stimulation of individual nerve branches. *J Morphol* 213:171-183.

Scott SH, Winter DA (1991) A comparison of three muscle pennation assumptions and their effect on isometric and isotonic force. *J Biomech* 24:163-167.

Seltzer SE, Wang AM (1987) Modern imaging of the masseter muscle: normal anatomy and pathosis on CT and MRI. *Oral Surg Oral Med Oral Pathol* 63:622-629.

Selzer PM (1986) Understanding NMR Imaging with the aid of a simple mechanical model. *Medical Times* 114(1):67-91.

Sherrington CS (1929) Some functional problems attaching to convergence. Ferrier Lecture. *Proc R Soc Lond Biol* 105:332-362.

Sicher H (1960) Masseter muscle. In *Oral Anatomy*. Mosby Co, pp 137.

Sinclair B, Hannam AG, Lowe AA, Wood WW (1989) Complex contour organization for surface reconstruction. *Comput & Graphics* 13:311-319.

Sjöström M, Lexell J, Downham DY (1992) Differences in fiber number and fiber type proportion within fascicles: a quantitative morphological study of whole vastus lateralis muscle from childhood to old age. *Anat Rec* 234:183-189.

Smith DK, Berquist TH, An KV, Robb RA, Chao EY (1989) Validation of three-dimensional reconstructions of knee anatomy: CT vs MR imaging. *J Comp Ass Tomography* 13(2):294-301.

Smith DM, McLachlan KR, McCall WD (1986) A numerical model of temporomandibular joint loading. *J Dent Res* 65:1046-1052.

Soussi-Yanicostas N, Barbet JP, Laurent-Winter C, Barton P, Butler-Browne GS (1990) Transition of myosin isozymes during development of human masseter muscle. *Development* 108:239-249.

Sperber GH (1989) Craniofacial Embryology. In *Dental Practitioner Handbook*

Series. Derrick DD (editor), University Press, Cambridge, 4th edition, pp 192-203.

Stålberg E (1980) Macro EMG, a new recording technique. *J Neurol Neurosurg Psychiat* 43:475-482.

Stålberg E, Antoni L (1980) Electrophysiological cross section of the motor unit. *J Neurol Neurosurg Psychiat* 43:469-474.

Stålberg E, Eriksson P-O, Antoni L, Thornell L-E (1986) Electrophysiological study of size and fibre distribution of motor units in the human masseter and temporal muscles. *Archs oral Biol* 31:521-527.

Stålberg E, Eriksson P-O (1987) A scanning electromyographic study of the topography of human masseter single motor units. *Archs oral Biol* 32:793-797.

Stålberg E, Schwartz MS, Thiele B, Shiller HH (1976) The normal motor unit in man. A single fibre EMG multielectrode investigation. *J Neurol Sci* 27:191-301.

Stålberg E, Thiele B (1975) Motor unit fibre density in the extensor digitorum communis muscle. *J Neurol Neurosurg Psychiat* 38:874-880.

Stålberg E, Trontelj JV (1979) *Single Fibre Electromyography*. Miravalle Press, Old Woking, U.K.

Stewart WA (1987) Quantitative NMR imaging and its application in vivo. MSc Thesis, The University of British Columbia, Vancouver.

Street SF (1983) Lateral transmission of tension in frog myofibers: a myofibrillar network and transverse cytoskeletal connections are possible transmitters. *J Cell Physiol* 114:346-364.

Suzuki S, Hayami A, Suzuki M, Watanabe S, Hutton RS (1990) Reductions in recruitment force thresholds in human single motor units by successive voluntary contractions. *Exp Brain Res* 82(1):227-230.

Swatland HJ (1975) Effect of fascicular arrangement on the apparent number of myofibers in the porcine longissimus muscle. *J Anim Sci* 41(3):794-798.

Takada K, Lowe AA, De Cou R (1983) Operational performance of the Reflex Metrograph and its applicability to the three-dimensional analysis of dental casts. *Am J Orthod* 83:195-199.

Tanji J, Kato M (1973a) Recruitment of motor units in voluntary contraction of a finger muscle in man. *Exp Neurol* 40:759-770.

Tanji J, Kato M (1973b) Firing rate of individual motor units in voluntary contraction of abductor digiti minimi muscle in man. *Exp Neurol* 40:771-783.

Tanji J, Kato M (1981) Activity of low- and high-threshold motor units of abductor digiti quinti in slow and fast voluntary contractions. *Prog Clin Neurophysiol* 9:137-144.

Taylor A, Cody FWJ, Bosley MA (1973) Histochemical and mechanical properties of the jaw muscles of the cat. *Exp Neurol* 38:99-109.

ter Haar Romeny BM, Denier van der Gon JJ, Gielen CCAM (1982) Changes in recruitment order of motor units in the human biceps muscle. *Exp Neurol* 78:360-368.

Thiele B, Boehle A (1975) Number of single muscle fibre action potentials contributing to the motor unit potential. 5th International Congress of EMG, Rochester, Minnesota.

Thomas CK, Ross BH, Stein RB (1986) Motor-unit recruitment in human first dorsal interosseous muscle for static contractions in three directions. *J Neurophysiol* 55:1017-1029.

Thomas CK, Ross BH, Calanchie B (1987) Human motor-unit recruitment during isometric contractions and repeated dynamic movements. *J Neurophysiol* 57:311-324.

Thomas CK, Schmidt EM, Hambrecht FT (1978) Facility of motor unit control during tasks defined directly in terms of behaviour. *Exp Neurol* 59:384-395.

Thomson DB, Scott SH, Richmond FJR (1991) Neuromuscular organization of feline anterior sartorius: I. Asymmetric distribution of motor units. *J Morphol* 210:147-162.

Thornell L-E, Billeter R, Eriksson P-O, Ringqvist M (1984) Heterogeneous distribution of myosin in human masticatory muscle fibres as shown by immunocytochemistry. *Archs oral Biol* 29:1-5.

Thornton M (1987) From NMR signal to MR image. The basic physics of MR image formation. *Radiography* 53(607):31-43.

Throckmorton GS, Throckmorton LS (1985) Quantitative calculations of temporomandibular joint reaction forces - I. The importance of the magnitude of the jaw muscle forces. *J Biomech* 18:445-452.

Tidball JG, Daniel TL (1986) Myotendinous junctions of tonic muscle cells: structure and loading. *Cell Tiss Res* 245:315-322.

Tolbert DL (1987) Intrinsically directed pruning as a mechanism regulating the

elimination of transient collateral pathways. *Dev Brain Res* 33:11-21.

Tonndorf ML, Sasaki K, Hannam AG (1989) Single-wire recording of regional activity in the human masseter muscle. *Brain Res Bull* 23:155-159.

Van der Klauuw CT (1963) Projections of deepenings and undulations of the surface of the skull in relation to the attachments of muscles. *Verh Kon Ned Akad Wetensch A/d Nat Sci* 2:1-247.

Van Eijden TMGJ, Raadsheer MC (1992) Heterogeneity of fiber and sarcomere length in the human masseter muscle. *Anat Rec* 232:78-84.

Van Eijden TMGJ, Blanksma NG, Brugman P (1993) Amplitude and firing of EMG activity in the human masseter muscle during selected motor tasks. *J Dent Res* 72(3):599-606.

Van Spronsen PH, Valk J, Weijs WA, Prahl-Andersen B (1987) Analysis of masticatory muscle orientation in adults by means of MRI. *Acta Anat* 130:96-97.

Van Spronsen PH, Weijs WA, Valk J, Prahl-Andersen B, van Ginkel FC (1991) Relationships between jaw muscle cross-sections and craniofacial morphology in normal adults, studied with magnetic resonance imaging. *Eur J Orthod* 13(5):351-61.

Van Steenberghe D, Bonte B, Schols H, Jacobs R, Schotte A (1991) The precision of motor control in human jaw and limb muscles during isometric contraction in the presence of visual feedback. *Archs oral Biol* 36(7):545-547.

Vignon C, Pellissier JF, Serratrice G (1980) Further histochemical studies on masticatory muscles. *J Neurol Sci* 45:157-176.

Vitti M, Basmajian JV (1977) Integrated actions of masticatory muscles: simultaneous EMG from eight intramuscular electrodes. *Anat Rec* 187(2):173-189.

Voss H (1935) Ein besonders reichliches Vorkommen von Muskelspindeln in der tiefen Portion des m. Masseter des Menschen und der Anthropoiden. *Anat Anz* 81:290-292.

Voss H (1971) Tabelle der absoluten und relativen Muskelspindelzahlen der menschlichen Skelettmuskulatur. *Anat Anz* 129:562-572.

Webb JN (1977) Cell death in developing skeletal muscle: histochemistry and ultrastructure. *J Path* 123:175.

Weber E (1846) Muskelbewegung. In *Handwörterbuch der Physiologie*. Wagner R

(editor). Bieweg, Brunswick, Germany, pp 1-122.

Weeks OI, English AW (1985) Compartmentalization of the cat lateral gastrocnemius motor nucleus. *J Comp Neurol* 235(2):255-267.

Weeks OI, English AW (1987) Cat triceps surae motor nuclei are organized topologically. *Exp Neurol* 96:163-177.

Weijjs WA, Brugman P, Klock EM (1987) The growth of the skull and jaw muscles and its functional consequences in the New Zealand rabbit (*Oryctolagus cuniculus*). *J Morphol* 194:143-161.

Weijjs WA, Dantuma R (1981) Functional anatomy of the masticatory apparatus in the rabbit (*oryctolagus cuniculus* L.). *Neth J Zool* 31:99-147.

Weijjs WA, Hillen B (1984a) Relationship between the physiological cross-section of the human jaw muscles and their cross-sectional area in computer tomographs. *Acta anat* 118:129-138.

Weijjs WA, Hillen B (1984b) Relationship between masticatory muscle cross-section and skull shape. *J Dent Res* 63:1154-1157.

Weijjs WA, Hillen B (1985) Cross-sectional areas and estimated intrinsic strength of the human jaw muscles. *Acta Morphol Neerl -Scand* 23:267-274.

Weijjs WA, Hillen B (1986) Correlations between the cross-sectional area of the jaw muscles and craniofacial size and shape. *Am J Phys Anthropol* 70:423-431.

Weijjs WA, Brugman P, Grimbergen CA (1989a) Jaw movements and muscle activity during mastication in growing rabbits. *Anat Rec* 224:407-416.

Weijjs WA, Korfage JA, Langenbach GJ (1989b) The functional significance of the position of the centre of rotation for jaw opening and closing in the rabbit. *J Anat* 162:133-148.

Wickwire NA, Gibbs CH, Jacobson AP, Lundeen HC (1981) Chewing patterns in normal children. *Angle Orthod* 51:48-60.

Widmalm SE, Lillie JH, Ash MM (1987a) Anatomical and electromyographic studies of the lateral pterygoid muscle. *J Oral Rehab* 14:429-446.

Widmalm SE, Lillie JH, Ash MM (1987b) Anatomical and electromyographic studies of the digastric muscle. *J Oral Rehab* 15:3-21.

Wilkinson TM (1988) The relationship between the disk and the lateral pterygoid muscle in the human temporomandibular joint. *J Prosth Dent* 60:715-724.

Willems MET, Huijing PA (1992) Effect of growth on architecture of rat semimembranosus lateralis muscle. *Anat Rec* 233:25-31.

Williams PL, Warwick R, Dyson M, Bannister LH, editors (1989) *Myology*. In Gray's Anatomy. Curchill Livingstone, London, 37th edition, pp 546-584.

Windhorst U, Hamm TM, Stuart DG (1989) On the function of muscle and reflex partitioning. *Behav Brain Sci* 12:629-681.

Wineski LE, Gans C (1984) morphological basis of the feeding mechanics in the shingle-back lizard *Trachydosaurus rugosus* (Scincidae, Reptilia). *J Morphol* 181:271-295.

Woittiez RD, Heerkens YF, Huijing PA, Rijnsburger WH, Rozendal RH (1986) Functional morphology of the m. gastrocnemius medialis of the rat during growth. *J Morphol* 187:247-258.

Woittiez RD, Huijing PA, Boom PA, Rozendal RH (1984) A three-dimensional muscle model: A quantitative relation between form and function of skeletal muscle. *J Morphol* 182:95-113.

Woittiez RD, Heerkens YF, Huijing PA, Rozendal RH (1989) Growth of medial gastrocnemius muscle and Achilles tendon in Wistar rats. *Anat Anz* 168(5):371-380.

Wood WW (1986) A functional comparison of the deep and superficial parts of the human anterior temporal muscle. *J Dent Res* 65:924-926.

Wood WW, Takada K, Hannam AG (1986) The electromyographic activity of the inferior part of the human lateral pterygoid muscle during clenching and chewing. *Archs oral Biol* 31:245-253.

Yemm R (1977) The orderly recruitment of motor units of the masseter and temporal muscles during voluntary isometric contraction in man. *J Physiol* 265:163-174.

Yoshikawa T, Suzuki T (1962) The lamination of the human masseter. The new identification of m. temporalis superficialis, m. maxillo-mandibularis and zygomatico-mandibularis in the human anatomy. [Jap] *Acta anat nippon* (Tokyo) 37:260-267.

Young SW (1984) Nuclear magnetic resonance imaging. In *Basic Principles*. Raven Press, New York, pp 11.

Xiguang L, Zhang Y, Chen Y, Chen YX (1986) Applied anatomy of the masseteric nerve. Zhonghua Kouqiangke Zozhi 21:226-227.

Zajac FE (1989) Muscle and tendon: properties, models, scaling, and application to biomechanics and motor control. Crit Rev Biomed Eng 17(4):359-411.

Zey A (1939) Funktion des Kauapparatus und Schädelgestaltung bei den Wiederkäuern. Med Inaug Diss, Frankfurt am Main.

7. APPENDIX

The orthogonal displacements of four tendinous insertion points, when the jaw is moved from tooth intercuspation to different functional positions, are presented separately for each living subject. The explanation of the methods, the anatomical location of the insertion points, and the discussion of the results are presented in section 3.2 of this thesis.

Table XVI **Displacements of four insertion points of subject I at different jaw positions.** Displacements are expressed as orthogonal distances (in mm) calculated from the insertion's coordinate point at maximum intercuspation.

		Insertion Points			
Task		1	2	3	4
Working Side	x	0.40	0.59	0.53	0.59
	y	-2.05	-4.10	-3.76	-4.39
	z	-4.14	-6.59	-2.94	-4.23
Balancing Side	x	1.61	2.32	1.88	2.15
	y	-3.94	-5.73	-5.43	-5.97
	z	-1.92	-4.19	-0.89	-2.07
Open	x	0.32	0.39	0.42	0.43
	y	-2.98	-5.08	-4.73	-5.37
	z	-3.40	-5.87	-2.16	-3.47

Table XVII Displacements of four insertion points of subject II at different jaw positions. Displacements are expressed as orthogonal distances (in mm) calculated from the insertion's coordinate point at maximum intercuspation.

		Insertion Points			
Task		1	2	3	4
Working Side	x	-0.81	-1.09	-0.66	-0.97
	y	-3.90	-5.07	-4.18	-5.28
	z	-6.16	-6.02	-3.39	-3.89
Balancing Side	x	1.45	1.42	1.36	1.36
	y	-4.17	-5.52	-4.56	-5.82
	z	-5.18	-5.06	-1.89	-2.52
Open	x	1.03	0.75	1.16	0.84
	y	-5.03	-6.31	-5.35	-6.56
	z	-5.79	-5.65	-2.74	-3.30

Table XVIII Displacements of four insertion points of subject III at different jaw positions. Displacements are expressed as orthogonal distances (in mm) calculated from the insertion's coordinate point at maximum intercuspation.

		Insertion Points			
Task		1	2	3	4
Working Side	x	-1.16	-1.38	-0.83	-1.14
	y	-0.75	-2.42	-2.54	-3.82
	z	-4.28	-5.18	0.81	-1.41
Balancing Side	x	1.99	2.56	1.68	2.35
	y	-3.73	-5.16	-5.45	-6.43
	z	-1.05	-2.13	3.86	1.41
Open	x	-0.03	-0.28	0.46	0.08
	y	-2.92	-4.63	-4.74	-6.07
	z	-2.25	-3.18	2.92	0.65

Table XIX **Displacements of four insertion points of subject IV at different jaw positions.** Displacements are expressed as orthogonal distances (in mm) calculated from the insertion's coordinate point at maximum intercuspation.

		Insertion Points			
Task		1	2	3	4
Working Side	x	-1.61	-1.87	-1.33	-1.16
	y	-0.80	-1.53	-1.36	-2.10
	z	-4.59	-5.24	-3.56	-2.87
Balancing Side	x	1.11	1.50	1.11	1.26
	y	-5.51	-6.10	-6.05	-6.77
	z	-0.13	-0.91	0.88	1.57
Open	x	0.33	0.54	0.34	0.43
	y	-5.02	-5.74	-5.66	-6.51
	z	-2.33	-3.16	-1.16	-0.37

BIOGRAPHICAL INFORMATION

NAME:

Mônica De Lorenzo Tonndorf

MAILING ADDRESS:

1983 Gainsborough Drive
Atlanta, Ga 30341
USA

PLACE AND DATE OF BIRTH:

Rio de Janeiro, RJ, Brazil

July 08, 1963

EDUCATION (Colleges and Universities attended, dates, and degrees):

Federal University of Rio de Janeiro (UFRJ), Brazil

1982 - 1986 Doctor of Dental Surgery (DDS)

POSITIONS HELD:

1983 - 1984 Teaching Assistant in Histology and Embryology - (UFRJ)

1984 - 1987 Teaching Assistant in Temporomandibular disorders (Clinics) - (UFRJ)

1985 - 1986 Teaching Assistant in Fixed Prosthodontics (Clinics) - (UFRJ)

1986 - 1987 Assistant Instructor in Prosthodontics (Clinics) - (UFRJ)

1987 - 1992 Teaching Assistant in Dental Occlusion and Temporomandibular Disorders (UBC)

1988 - 1992 Teaching Assistant in Fixed Prosthodontics (pre-clinical course) - (UBC)

PUBLICATIONS (if necessary, use a second sheet):

See attached page.

AWARDS:

1987 - 1988 Rotary International Scholarship

1988 - 1989 Government of Canada Award (WUSC)

1988 Dr. George S. Beagrie Award

1989 P.E.O. Chapter Sisterhood Award

1989 Medical Research Council of Brazil (CNPq) Fellowship - declined

1989 - 1991 Brazilian Ministry of Education Fellowship (CAPES)

1991 - 1992 University Graduate Fellowship (UBC)

Complete one biographical form for each copy of a thesis presented to the Special Collections Division, University Library.

PUBLICATIONS

Tonndorf, M.L., Sasaki, K. and Hannam, A.G. Single-wire recording of regional activity in the human masseter muscle. *Brain Res. Bull.* 23:155-159, 1989.

Tonndorf, M.L. and Hannam, A.G. Effects of bite side on human masseter motor unit behaviour. *J. Dent. Res.* 70:553, 1991.

Tonndorf, M.L. and Hannam, A.G. Masseter muscle attachment sites at different jaw positions. *J. Dent. Res.* 71:117, 1992.

Tonndorf, M.L. and Hannam, A.G. Motor unit territory in the human masseter muscle. *J. Dent. Res.* 72:371, 1993.

Tonndorf, M.L., Connell D.G. and Hannam, A.G. Stereotactic location of EMG needle electrode scans relative to tendons in the human masseter muscle. *J. Neurosci. Methods* (in press), 1993.

Tonndorf, M.L. and Hannam, A.G. Motor unit territory relative to tendon in the human masseter muscle. *Muscle & Nerve* (in press), 1993.

Hagiwara, M., Hannam, A.G., Koriath, T.W.P. and Tonndorf, M.L. Three-dimensional motion of the human mandibular condyle. *J. Dent. Res.* 72:267, 1993.